

**PROMOTING RECEPTOR CLUSTERING WITH MULTIVALENT LIGANDS AND  
IDENTIFYING LIGANDS FOR THE BETA-AMYLOID PEPTIDE**

by

Christopher W. Cairo

A dissertation submitted in partial fulfillment of the

requirements for the degree of

Doctor of Philosophy

(Chemistry)

at the

UNIVERSITY OF WISCONSIN-MADISON

2002

**Dedication**

*For Mary Ann.*

## Acknowledgments

The work described in this thesis would not have been possible without the contributions of many coworkers. Prof. Laura Kiessling has been an outstanding advisor, and has provided a unique interdisciplinary research environment. Laura has patiently indulged my intellectual wanderings, while always providing critical evaluation and direction. Prof. Regina Murphy has been an important collaborator and advisor for our studies of  $\beta$ -amyloid. Where possible, the direct contributions of individuals have been noted in each chapter. Notable among these are Jason Gestwicki, Laura Strong, Motomu Kanai, Robert Owen, Fred Boehm and Dave Mann. Many others have made less tangible, but equally important contributions: Brendan Orner, David Peal, Monica Pallitto, Jyothi Ghanta, Tao Lowe, Travis Young, Josh Kurutz, Cathy Dantzman, Michele Richards, and Faisal Syud.

I would like to thank the many people that have provided critical evaluation of this document in its many forms: Brendan Orner, Jason Gestwicki, Allison Lamanna, Robert Owen, Michele Richards, Dave Peal, Byron Griffith, and Daniel Weicherding.

The excellent facilities of the University of Wisconsin-Madison have been a great asset to much of this work, and several outstanding personnel should be acknowledged: Charles Fry (CIC), Darrell McCaslin (BIF), Gary Case (Biotech Center), Adam Steinberg (Biochemistry Media Lab), Brad Spencer (Chemistry Computing) and Martha Vestling (CIC). Additional support was been provided by Prof. Regina Murphy, Prof. Dave Nelson, Prof. Paul Friesen and Prof. Ron Raines.

**Abstract**

Progression of Alzheimer's disease is associated with the development of protein deposits in the brain composed of  $\beta$ -amyloid peptide. This peptide is known to aggregate and form amyloid fibrils, and the process of aggregation is associated with the toxicity of the peptide *in vitro*. To develop compounds that interfere with this process, a more detailed understanding of the binding of small molecules to the peptide is required. Therefore, we have developed a direct binding assay to determine the affinity of small molecules for  $\beta$ -amyloid. Additionally, the affinity of a panel of peptides related to the central hydrophobic domain of  $\beta$ -amyloid was determined. Using this assay we find that ligands with high affinity in our assay are potent inhibitors of toxicity.

Biological systems exploit multivalent presentation to enhance the affinity and specificity of many diverse interactions. Changes in apparent affinity due to multivalent presentation are responsible for the exquisite selectivity of antibodies. At the cell surface, multivalent interactions are important both for cell-cell recognition and for transfer of information to the interior of the cell. A common mechanism by which signal transduction is initiated is through alteration of the proximity of cell surface receptors. Receptor clustering is an important initiating event in diverse systems such as bacterial chemotaxis, inflammatory response, and apoptosis.

We hypothesized that synthetic multivalent ligands could provide access to new methods for systematic study of multivalent interactions. Studies to quantify a model receptor clustering event with multivalent ligands are described. Using the multivalent lectin concanavalin A (Con A), the effects of multivalent ligand structure on features of receptor

clusters such as the stoichiometry of the cluster, the rate of clustering, the proximity of the receptors and the apparent affinity of the interaction were studied. Representative ligands of several classes of organic molecules, including small molecules, dendrimers, polymers, and protein conjugates were used. Each of these classes was explored by variation of the number of binding sites for Con A. Each architectural class is shown to have distinct features and strengths. We find that linear polymers are the most efficient ligand architectures for promoting clustering of Con A.

## List of Figures

<i>Number</i>	<i>Page</i>
Figure 1.1. Amyloid inhibitor design .....	7
Figure 1.2. Specific interactions with immobilized A $\beta$ (10-35) .....	10
Figure 1.3. PM-FTIRAS spectra of CM5 surface. ....	13
Figure 1.4. Sensorgrams for compound 1.13. ....	15
Figure 1.5. Binding isotherm for 1.13. ....	16
Figure 1.6. Detailed binding isotherm for compound 1.13. ....	19
Figure 1.7. Hill plot for compound 1.13.....	22
Figure 1.8. Proposed binding model for retro-inverso peptides.....	36
Figure 1.9. Distribution of saturation values.....	41
Figure 1.10. Prevention and concentration dependence of toxicity. ....	46
Figure 1.11. Reversal of toxicity. ....	47
Figure 1.12. Correlation of affinity with <i>in vitro</i> inhibition of toxicity. ....	48
Figure 2.1. Mechanisms of multivalent binding.....	76
Figure 2.2. Monovalent ligand design.....	81
Figure 2.3. Multivalent ligand design. ....	82
Figure 2.4. Binding modes of STARFISH ligands for SLT-1. ....	92
Figure 2.5. Interplay of ligand and receptor architecture in multivalent binding. ....	95
Figure 3.1. Selected monosaccharides chemoattractants for <i>E. coli</i> . ....	101
Figure 3.2. Alternate orientations of galactose within GGBP.....	104
Figure 3.3. Autodock results for docking of galactose to GGBP.....	106
Figure 3.4. Determination of optimal linker lengths using molecular dynamics. ....	109

Figure 3.5. Structures of designed chemoattractants.....	111
Figure 3.6. Binding of ligands to GGBP. ....	115
Figure 3.7. Assays employed for studies of multivalent binding. ....	127
Figure 3.8. Measured inhibitory potency of polymers with variable binding epitope density. ....	131
Figure 3.9. Precipitation of Con A by polymers with variable binding epitope density. ....	133
Figure 3.10. Rate of Con A precipitation using variable density ROMP-derived ligands. ....	136
Figure 3.11. FRET induced by variable density ROMP-derived ligands. ....	139
Figure 3.12. Scaffolded receptor clusters. ....	143
Figure 3.13. Structures of multivalent ligands used. ....	147
Figure 3.14. Functional affinity of Con A binding to multivalent ligands.....	152
Figure 3.15. Precipitation of Con A by multivalent ligands. ....	153
Figure 3.16. Rate of precipitation of Con A by multivalent ligands. ....	154
Figure 3.17. FRET analysis of Con A complexes formed by multivalent ligands.....	155
Figure 3.18. Summary of the influence of different ligand architectures on multivalent binding. ....	156
Figure 3.19. Correlations between ligand valency and measured parameters. ....	162
Figure 3.20. Precipitation of Con A by galactose polymers. ....	169
Figure 4.1. Secondary clustering of cell surface receptors.....	186
Figure 4.2. Structures of polymers. ....	189
Figure 4.3.1. Toxicity of Con A in PC12 cells. ....	191

Figure 4.3.2. Modulation of Con A toxicity in PC12 cells in the presence of multivalent ligands. ....	191
Figure 4.4.1. Toxicity of Con A in SW837 cells. ....	195
Figure 4.4.2. Modulation of Con A toxicity in SW837 cells in the presence of multivalent ligands. ....	195
Figure 4.5.1. Toxicity of Con A in HCT15 cells. ....	198
Figure 4.5.2. Modulation of Con A toxicity in HCT15 cells in the presence of multivalent ligands. ....	198
Figure 4.6. Clustering of Con A on the surface of PC12 and SW837 cells results in apoptotic morphology. ....	199
Figure 4.7. Fas-initiated apoptotic signalling. ....	207
Figure 4.8. Crosslinking of Fas using antibodies or antibody conjugates. ....	213
Figure 4.9. Preparation of multivalent antibody conjugates. ....	216
Figure 4.10. Theoretical properties of antibody conjugates. ....	217
Figure 4.11. Activity of $\alpha$ -Fas conjugates. ....	218
Figure A.1. Compounds used for SPR studies. ....	231
Figure A.2. P-selectin binding to immobilized monomer and polymer surfaces. ....	233
Figure A.3. L-selectin binding to immobilized monomer and polymer surfaces. ....	234
Figure A.4. Jurkat cell binding to immobilized polymer A.2. ....	236
Figure A.5. Site isolation of multivalent receptors. ....	239
Figure A.6. Injections of A.3 and A.4 over Con A immobilized surfaces. ....	242
Figure A.7. Apparent affinity measurements of A.3 and A.4 on CM5 surfaces. ....	245
Figure A.8. Theoretical inter-site distance for immobilized Con A. ....	246



Figure A.9. Variation of apparent affinity on C1 surfaces. ....247

Figure A.10. Variation of apparent affinity on CM5 surfaces. ....248

## List of Tables

<i>Number</i>	<i>Page</i>
Table 1.1. Analysis of binding model for compounds 1.13-1.25. ....	21
Table 1.2. SPR results from steady state affinity determinations of pentapeptide ligands .....	27
Table 1.3. SPR results from steady state affinity determinations .....	30
Table 1.4. SPR results from steady state affinity determinations .....	32
Table 2.1. Multivalent ligands for Con A inhibition. ....	87
Table 2.2. Multivalent ligands for AB <sub>5</sub> toxins. ....	91
Table 3.1. Chemoattractant activity of synthetic galactose ligands. ....	112
Table 3.2. Binding epitope density of multivalent polymers influences the stoichiometry of Con A complexation. ....	134
Table 3.3. Correlations for density and valency of polymers produced by ROMP. ....	163
Table 3.4. Reversal of aggregation by a competitive ligand. ....	171
Table 3.5. Average distance calculations for FRET (Compounds 3.29-3.35). ....	172
Table 3.6. NMR Characterization of DP for compounds 3.29-3.35.....	178
Table 4.1. Characterized lectin toxicity.....	185
Table 4.2. Con A toxicity in PC12 and SW837 cells .....	200
Table A.1. Variable density Con A surfaces. ....	240
Table A.2. Linear fits for dissociation phase of compound A.3.....	243

**List of Abbreviations**

A $\beta$	$\beta$ -amyloid
AD	Alzheimer's Disease
ADDL	$\beta$ -amyloid derived diffusible ligands
Aha	aminohexanoic acid
AIL	<i>Artocarpus integrifolia</i> lectin
AT	anthrax toxin
ATCC	American type culture collection
ATRP	atom transfer radical polymerization
AU	absorbance unit
BCA	bicinchoninic acid
BSA	bovine serum albumin
CID	chemical inducers of dimerization
CLT	cholera toxin
Con A	Concanavalin A
DD	death domain
DISC	death-inducing signaling complex
DMF	dimethyl formamide
DMSO	dimethyl sulfoxide
DP	degree of polymerization
EC <sub>50</sub>	effective concentration, 50%

EDA	ethylene diamine
EDC	<i>N</i> -ethyl- <i>N</i> '-(dimethylaminopropyl)-carbodiimide
EDTA	ethylenediaminetetracetic acid
ELISA	enzyme-linked immuno sandwich assay
ELLA	enzyme-linked lectin assay
eq.	equation
equiv.	equivalents
Fab'	antibody fragment
FADD	Fas associated death domain
FAP	familial amyloid polyneuropathy
Fas	fatty acid synthase (CD95)
FasL	Fas ligand
Fc	fragment crystallizable
FITC	fluorescein-isothiocyanate
Fl-sCon A	fluorescein labeled succinylated Concanavalin A
FMOC	9-fluorenylmethoxycarbonyl
FRET	fluorescence resonance energy transfer
GGBP	glucose-galactose binding protein
GSA	<i>Griffonia simplicifolia</i> agglutinin
HBS	HEPES-buffered saline
HEPES	N-(2-hydroxyethyl)-piperazine-N'-(2-ethanesulfonic acid)
HIA	hemeagglutination inhibition assay
HIHS	heat inactivated horse serum

HLT	heat-labile enterotoxin
IC <sub>50</sub>	inhibitory concentration, 50%
IgG	Immunoglobulin G
IgM	Immunoglobulin M
IR	infra-red
K <sub>a</sub>	association constant
K <sub>d</sub>	dissociation constant
KINJECT	kinetic injection
LC <sub>50</sub>	lethal concentration, 50%
LCL	<i>Litchi chinensis</i> lectin
MAL	<i>Maackia amurensis</i> lectin
MALDI-TOF	matrix assisted laser desorption/ionization time-of-flight
MCP	methyl-accepting chemotaxis protein
MEM	minimum essential medium
MTT	3-(4,5-dimethylthiazol-2-yl)-2,5-diphenyltetrazolium bromide
MW <sub>A</sub>	analyte molecular weight
MW <sub>L</sub>	ligand molecular weight
NHS	<i>N</i> -hydroxy-succinimide
NMR	nuclear magnetic resonance
NPA	<i>Narcissus pseudonarcissus</i> agglutinin
PAGE	polyacrylamide gel electrophoresis
PAMAM	poly(amidoamine)
PBS	phosphate-buffered saline

PBST-Ca <sup>2+</sup>	PBS-Tween-Ca <sup>2+</sup>
PEG	polyethylene glycol
PEMA	polyethylene maleic anhydride
PHA	phytohemagglutinin
PM-FTIRRAS	polarization modulation Fourier transform infra-red reflection absorption spectroscopy
PNA	peanut agglutinin
PPL	<i>Ptilota plumosa</i> lectin
PZR	protein zero receptor
QP	quantitative precipitation
Req	equilibrium RU
Rmax	maximum RU
ROMP	ring opening metathesis polymerization
RP-HPLC	reverse phase high pressure liquid chromatography
RU	response units
SAM	self assembled monolayer
SAR	structure activity relationship
sCon A	succinylated Con A
sCon A	succinylated Concanavalin A
sFasL	soluble FasL
SDS	sodium dodecyl sulfate
SE	standard error of the mean
SLT	shiga-like toxin

SPR	surface plasmon resonance
SS	sum of the squares
STL	<i>Solanum tuberosum</i> lectin
sulfo-MBS	<i>m</i> -maleimidobenzoyl- <i>N</i> -hydroxysulfosuccinimide ester
TFA	trifluoroacetic acid
TMR	tetra-methyl rhodamine
TMS	trimethyl silyl
TNF	tumor necrosis factor
WGA	wheat-germ agglutinin

## Table of Contents

Dedication .....	i
Acknowledgments .....	ii
Abstract .....	iii
List of Figures .....	v
List of Tables.....	ix
List of Abbreviations.....	x
Table of Contents .....	xv
Forward .....	xx
Chapter 1. Affinity-Based Inhibition of $\beta$ -Amyloid Toxicity .....	1
1.1.1. Abstract .....	2
1.1.2. Protein aggregation.....	3
1.1.3. Design of direct binding assay using SPR.....	5
1.2.1. Amyloid binding studies using CM5 Surfaces.....	8
1.2.2. Amyloid binding studies using B1 surfaces .....	14
1.3. Peptide inhibitors binding to A $\beta$ (10-35) .....	17
1.4.1. Affinities of peptide ligands for A $\beta$ .....	23
1.4.2. Pentapeptide KLVxx compounds.....	24
1.4.3. Composite peptides with charged domains. ....	27
1.4.4. Alanine replacements within KLVFF. ....	31
1.4.6. D-Amino acid sequences.....	33
1.4.7. Alternative charged domains.....	37



1.4.8. Structure activity relationships for binding to A $\beta$ -derivatized surfaces. ....	38
1.5. Designing peptide inhibitors for distinct oligomerization states.....	39
1.6.1. Biological activity of peptide inhibitors.....	43
1.6.2. Ligand affinity is a predictor of toxicity inhibition.....	49
1.7. Conclusions .....	51
1.8.1. Experimental procedures.....	53
1.8.2. Binding models.....	56
1.8.3. Raw binding data from SPR experiments. ....	61
Chapter 2. Structure Based Design of Multivalent Ligands.....	69
2.1. Abstract. ....	70
2.2.1. Mechanisms of multivalent binding. ....	71
2.2.2. Variables to consider in multivalent ligand design. ....	78
2.3.1. Multivalent ligand architecture influences activity.....	83
2.3.2. Designed multivalent ligands for inhibition of Con A binding.....	83
2.3.3. Designed multivalent ligands for inhibition of AB <sub>5</sub> toxins.....	88
2.4.1. Conclusions. ....	93
Chapter 3. Influence of Ligand Structure on Multivalent Interactions .....	96
3.1. Abstract .....	97
3.2.1. Structure based design of multivalent ligands for GGBP .....	97
3.2.2. Attachment point. ....	99
3.2.3. Linker length. ....	107
3.2.4. Chemotactic activity of designed ligands.....	110
3.3.1. Assays for studying multivalent binding.....	116

3.3.1.1. Hemagglutination. ....	116
3.3.1.2. Isothermal titration calorimetry. ....	117
3.3.1.3. Quantitative precipitation. ....	119
3.3.1.4. Turbidity. ....	119
3.3.1.5. Fluorescence resonance energy transfer. ....	120
3.3.1.6. Transmission electron microscopy. ....	121
3.3.1.7. Surface plasmon resonance. ....	122
3.3.2. Multiple assays are required for study of complex interactions. ....	122
3.3.3. Multivalent binding assays to study receptor clustering. ....	124
3.3.4. Concanavalin A as a model receptor. ....	124
3.4.1. Density effects in multivalent binding. ....	128
3.4.2. Functional affinity of multivalent ligands. ....	130
3.4.3. Relative stoichiometry of Con A to ligand within the cluster. ....	132
3.4.4. Rate of cluster formation. ....	134
3.4.5. Receptor proximity. ....	137
3.4.6. Changes in binding epitope density affect multivalent binding. ....	140
3.5.1. Multivalent ligand architecture. ....	144
3.5.2.1. Low molecular weight compounds. ....	149
3.5.2.2. Dendrimers. ....	149
3.5.2.3. Globular proteins. ....	150
3.5.2.4. Linear polymers. ....	150
3.5.2.5. Polydisperse polymers. ....	151
3.5.3. The architecture of a multivalent ligand affects its binding mode(s). ....	157

3.5.4. Deciphering the rules of multivalent ligand design. ....	159
3.6. Conclusions .....	164
3.7. Experimental materials and methods .....	166
Chapter 4. Controlling Receptor Clustering <i>in vitro</i> using Synthetic Multivalent Ligands..	180
4.1. Abstract .....	181
4.2.1. Receptor clustering using multivalent lectins .....	183
4.2.2. Con A-induced apoptosis .....	183
4.2.3. Examining the toxicity of Con A in the presence of multivalent ligands .....	187
4.3.1. Con A toxicity in PC12, SW937, and HCT15 cells .....	190
4.3.2. Modulation of Con A toxicity using multivalent mannose-substituted polymers 4.1 and 4.2. ....	192
4.3.3. Polymer – Con A complexes elicit an apoptotic cell morphology.....	196
4.3.4. Clustering of cell-surface glycoproteins by Con A and multivalent ligands. ....	196
4.4.1. Synthetic multivalent ligands are effective tools for controlling receptor clustering .....	201
4.5.1. Specific cell receptors for inducing apoptosis.....	204
4.5.2. Strategies for crosslinking Fas. ....	208
4.5.3. Therapeutic utility of Fas selective ligands.....	209
4.5.4. Antibody conjugates for clustering apoptosis receptors. ....	211
4.5.5. Toxicity of multivalent Fab' conjugates. ....	214
4.6. Conclusions. ....	219
4.7. Experimental Methods. ....	221
Appendix. Surface Immobilization of Multivalent Ligands and Receptors.....	228

A.1. Immobilization of end-labeled ROMP-derived polymers.....	229
A.1.1. Introduction. ....	229
A.1.2. SPR studies of selectin binding. ....	229
A.1.3. SPR studies of cell binding.....	235
A.1.4. Conclusion. ....	235
A.2. Density-dependent multivalent binding of Con A.....	237
A.2.1. Introduction. ....	237
A.2.2. Preparation of SPR surfaces with Con A. ....	240
A.2.3. Kinetic studies of multivalent ligand binding to Con A.....	241
A.2.4. Saturable binding of ligands to Con A surface.....	243
A.2.5. Conclusions. ....	249
A.3. Experimental methods. ....	249
References .....	252

**Forward**

*It is a capital mistake to theorize before one has data.*

*Insensibly one begins to twist facts to suit theories, instead of  
theories to suit facts.*

Sherlock Holmes,

in Sir Arthur Conan Doyle's *A Scandal in Bohemia* (1891).

# Chapter 1. Affinity-Based Inhibition of $\beta$ -Amyloid Toxicity

Portions of this work are published in:

“Affinity-Based Inhibition of  $\beta$ -Amyloid Toxicity,” Cairo, C. W.; Strzelec, A.; Murphy, R. M.; Kiessling, L. L. , *Biochemistry* **2002**, *in press*.

Contributions:

Cell viability assays shown in Table 1.3 were performed by A. Strzelec.

Peptides were contributed by:

<b>1.22, 1.27-1.33, 1.41, 1.44</b>	- D. Weicherding
<b>1.34, 1.42, 1.43</b>	- A. Strzelec
<b>1.26</b>	- M. M. Pallitto
<b>1.14, 1.15</b>	- J. Ghanta

### 1.1.1. Abstract

Strategies to interfere with protein aggregation are important for elucidating and controlling the pathologies of amyloid diseases. We have previously identified compounds that block the cellular toxicity of the  $\beta$ -amyloid peptide, but the relationship between their ability to inhibit toxicity and their affinity for A $\beta$  was unknown. To elucidate this relationship, we have developed an assay capable of measuring the affinities of small molecules for  $\beta$ -amyloid peptide. Our approach employs immobilized  $\beta$ -amyloid peptide at low density to minimize the problems that arise from variability in  $\beta$ -amyloid aggregation state. We found that low molecular weight (700-1700 MW) ligands for  $\beta$ -amyloid can be identified readily by using surface plasmon resonance. The best of these bound effectively ( $K_d \sim 10 \mu\text{M}$ ) to  $\beta$ -amyloid. Several compounds with high affinity in our assay are inhibitors of amyloid toxicity. Therefore, our data support the hypothesis that ligands exhibiting greater affinity for the  $\beta$ -amyloid peptide are effective at altering its aggregation and inhibiting cell toxicity. Additionally, our assay provides a high-throughput method for the identification of new ligands capable of inhibiting amyloid toxicity.

### 1.1.2. Protein aggregation

Protein aggregation and amyloid plaque formation are implicated in the pathology of a number of disease states such as Huntington's disease, familial amyloid polyneuropathy (FAP) and Alzheimer's disease (AD) (Rochet and Lansbury, 2000; Sipe, 1992). The underlying processes that lead to aggregation in these diseases are poorly understood. In some cases, it is a matter of some controversy whether the formation of amyloid plaques plays a causative role or if it is merely symptomatic (Naslund *et al.*, 2000; Selkoe, 1997). Regardless, the development of general strategies for interfering with protein aggregation could have enormous benefits for the development of therapies and the elucidation of the etiology of these diseases.

Alzheimer's disease is a devastating neurodegenerative disorder currently affecting an estimated 4 million people in the United States (Evans *et al.*, 1989). Amyloid plaques found in AD patients contain a 39-42 residue peptide,  $\beta$ -amyloid ( $A\beta$ ), that is highly prone to aggregation under appropriate conditions (Zagorski *et al.*, 1999). The natural function of  $A\beta$  is unknown. The peptide is found in both the AD and the non-AD brain; however, in the disease state amyloid plaques containing  $A\beta$  are more abundant and are associated with neurodegeneration. A large body of evidence has suggested that the aggregation of  $A\beta$  to soluble oligomers or fibrils is important for the development of its toxic effects (Klein *et al.*, 2001; Koo *et al.*, 1999; Lansbury, Jr., 1997; Pike *et al.*, 1991; Selkoe, 1999). The findings that mutations associated with familial Alzheimer's disease influence the *in vivo* concentrations of  $A\beta$  or its propensity to form amyloid fibrils provide strong support for the significance of  $A\beta$  aggregation (Selkoe, 1997).  $A\beta$  aggregation is an excellent model system for the development



of protein anti-aggregation strategies for several reasons: 1) the aggregating species, A $\beta$ , is readily available; 2) both *in vitro* and *in vivo* model systems for toxicity of the aggregates have been developed (Annaert and De Strooper, 2000; Games *et al.*, 1995; Higuchi *et al.*, 1999; Janus *et al.*, 2000; Shearman, 1999); 3) considerable structural data have been collected on this system (Serpell, 2000). The resulting compounds can be used to investigate the role of protein aggregation in the disease. These features render A $\beta$  an excellent test case for evaluating general strategies to alter protein aggregation.

Progress in developing therapies for AD has been slow. Emerging approaches are focused on inhibiting the production of A $\beta$  in the brain (Ghosh *et al.*, 2000; Shearman *et al.*, 2000) or removing existing plaques (Bard *et al.*, 2000; Schenk *et al.*, 1999). An alternative strategy is to identify small molecules capable of binding A $\beta$ . These compounds could act by disrupting the formation of aggregates and altering aggregate structure, or by inhibiting interactions of A $\beta$  with other receptors (Harkany *et al.*, 2000; Lansbury, Jr., 1997; Moore and Wolfe, 1999; Soto, 1999; Thorsett and Latimer, 2000).

We hypothesized that compounds with high affinity for A $\beta$  would also serve as effective inhibitors of cellular toxicity. Although some inhibitors of toxicity have been shown to bind to A $\beta$  (Howlett *et al.*, 1999a; Howlett *et al.*, 1999b) a clear relationship between affinity for A $\beta$  and inhibition of toxicity has not been established for any series of compounds. This fact is primarily due to the lack of a robust or standard binding assay. Therefore, we proceeded to establish a satisfactory method to directly compare the affinity of a series of compounds for  $\beta$ -amyloid peptide.

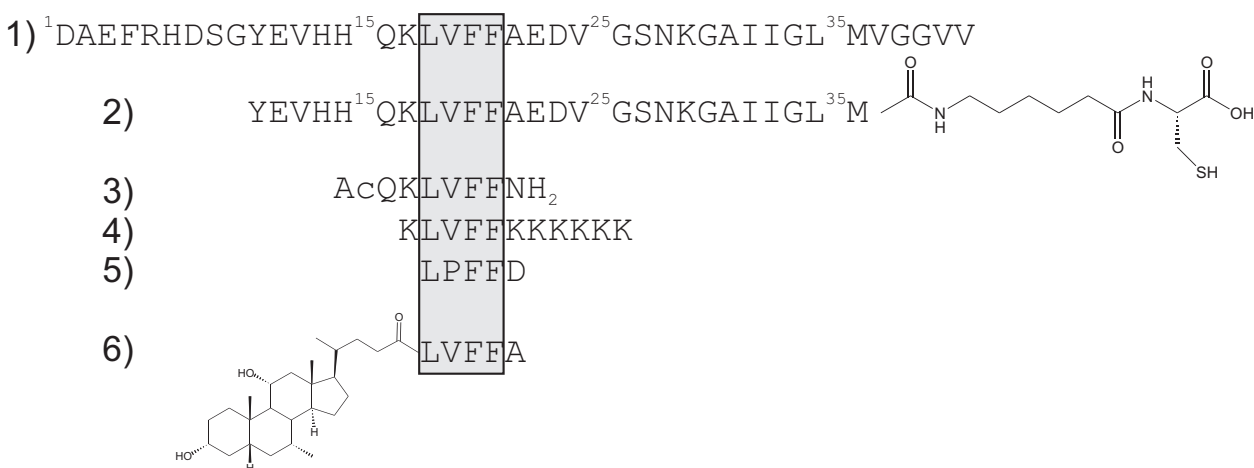
### 1.1.3. Design of direct binding assay using SPR

The direct binding assays reported to date for screening amyloid inhibitors require extrinsic dyes or the inclusion of either a fluorophore in the inhibitor (Kuner *et al.*, 2000) or a radionuclide in A $\beta$  (Esler *et al.*, 1997; Tjernberg *et al.*, 1997). Measurements that employ extrinsic dyes are particularly susceptible to optical artifacts, such as absorbance overlap by ligands and light scattering due to fibril formation. All reported assays consume amyloid peptide for each experiment, and significant effort must be taken to ensure consistent sample preparation (Zagorski *et al.*, 1999). Approaches that determine the affinity to a single preparation are advantageous and provide an opportunity to readily compare the activities of different compounds. These data could then be used to understand and optimize ligand activity.

We developed a new direct binding assay to identify small molecules that bind A $\beta$ . Through such an assay we wished to identify potential inhibitors of amyloid toxicity. Additionally, the mechanism of known inhibitors could be probed and new small molecules that bind A $\beta$  identified. We describe the development of a surface plasmon resonance (SPR) assay in which ligand binding to an immobilized form of A $\beta$  can be readily detected.

SPR has been used previously to investigate A $\beta$  interactions; however, these experiments were not designed to identify small molecule binding targets. Tjernberg and coworkers demonstrated a specific interaction of an immobilized peptide with full length A $\beta$  (Tjernberg *et al.*, 1997). Other studies have focused on observing the growth of immobilized amyloid fibrils (Myszka *et al.*, 1999). Neither of these general approaches is amenable to the screening of small molecules. Our strategy was to immobilize an easily

handled form of A $\beta$ , A $\beta$ (10-35) (Benzinger *et al.*, 2000), to a carboxymethyl dextran matrix, and measure the solution affinity of small molecules to this surface. A major advantage of this arrangement is that the surface density can be manipulated to minimize the density of the binding target, which may also limit its aggregation and therefore increase reproducibility. Moreover, with SPR detection, no labeling strategy for A $\beta$  is needed. Because a single surface is used for all experiments, there is no target variability between assays. Using this approach, we found that several compounds previously reported to prevent cellular toxicity are also high affinity ligands for A $\beta$ .



### Figure 1.1. Amyloid inhibitor design

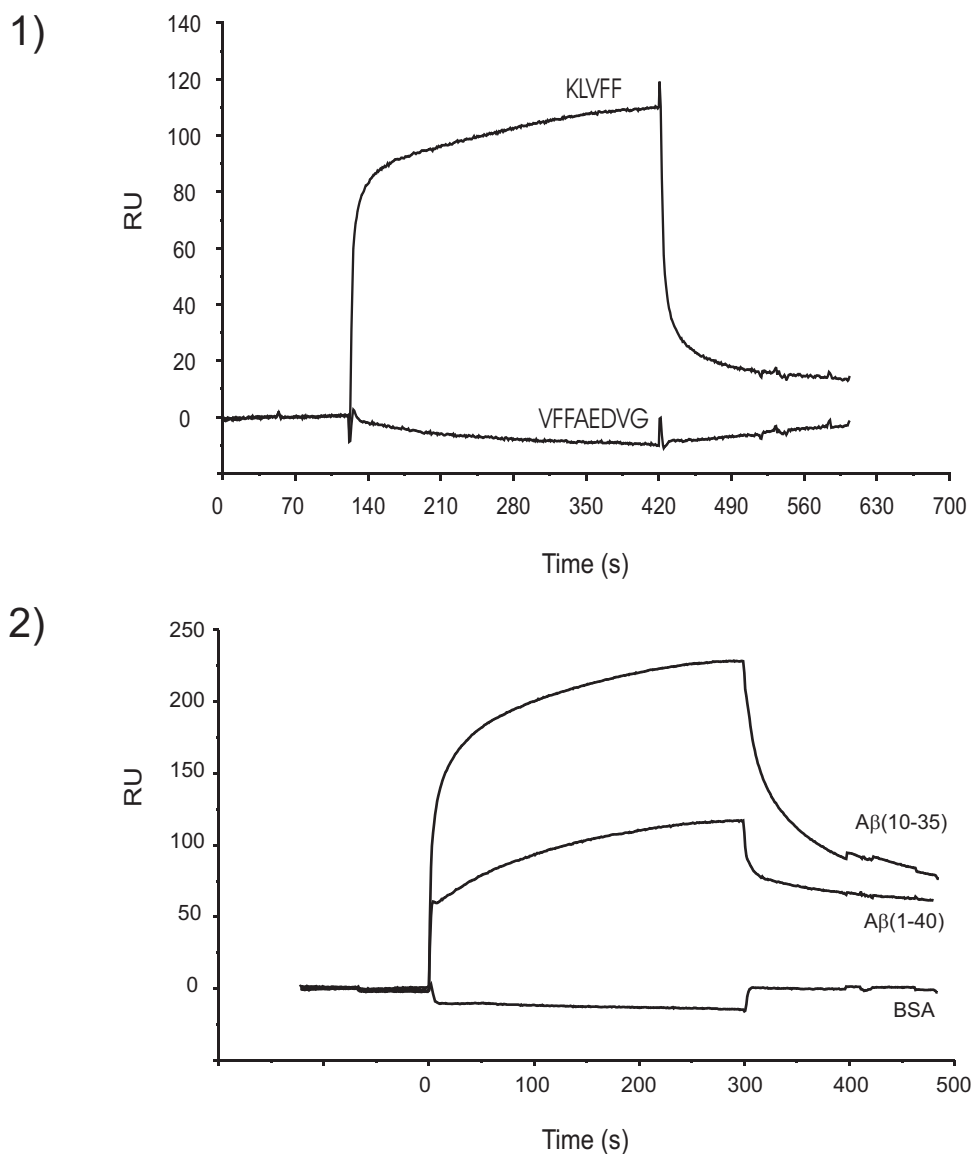
The binding target for these studies is the A $\beta$  peptide: 1) the full sequence of A $\beta$ (1-40) is shown, and 2) a portion of the native sequence, A $\beta$ (10-35), was used for SPR binding studies with C-terminal modifications to allow specific immobilization. Homologous binding elements from the A $\beta$ (1-40) sequence have been used by several researchers to design inhibitors of amyloid formation; the A $\beta$ (16-20) region has been used most frequently. Some examples are depicted in 3-6: 3) Tjernberg *et al.* (Tjernberg *et al.*, 1996); 4) Ghanta *et al.* (Ghanta *et al.*, 1996); 5) Soto *et al.* (Soto *et al.*, 1998); and 6) Findeis *et al.* (Findeis *et al.*, 1999).

### 1.2.1. Amyloid binding studies using CM5 Surfaces

To evaluate the affinity of ligands for A $\beta$ , we selected a surface that we expected to be compatible with our binding experiments. Our initial studies sought to determine whether a specific interaction between A $\beta$  immobilized at low density and small molecules in the desired molecular weight range could be observed. To evaluate whether the necessary sensitivity could be achieved, we immobilized A $\beta$ (10-35) on a carboxymethyl dextran surface (CM5 chip, Biacore AB). We chose A $\beta$ (10-35) as the immobilized target due to its competence to bind to A $\beta$ (1-40) plaques and its consistent aggregation properties (Benzinger *et al.*, 1998). Under appropriate conditions, A $\beta$ (10-35) has been shown to form aggregates of similar morphology to A $\beta$ (1-40) (Benzinger *et al.*, 2000), and NMR studies suggest that structured aggregates of A $\beta$ (10-35) and A $\beta$ (1-40) are similar (Antzutkin *et al.*, 2000; Benzinger *et al.*, 2000).

To generate the modified surface required for SPR, the target peptide was linked to the matrix using standard protocols for amide bond formation (O'Shannessy *et al.*, 1992). Although this method does not require any modification of A $\beta$ , several amines within the peptide could react; consequently, it is likely immobilized in multiple orientations. Ethanolamine was coupled to a separate activated surface to produce a control lane. The modified surfaces were exposed to solutions containing either of two potential peptide ligands, the pentapeptide KLVFF, A $\beta$ (16-20), and the peptide VFFAEDVG, A $\beta$ (18-25) (Figure 1.2.1). These peptides correspond to overlapping regions of the central hydrophobic domain of A $\beta$ , which contains key residues for A $\beta$ -A $\beta$  self-association (Tjernberg *et al.*, 1996). Previously we reported that A $\beta$ (16-20), but not A $\beta$ (18-25), inhibits the cellular toxicity

of A $\beta$ (Ghanta *et al.*, 1996; Pallitto *et al.*, 1999). Our SPR experiments revealed that A $\beta$ (16-20) interacted specifically with the immobilized target, but A $\beta$ (18-25) bound poorly. Full length A $\beta$ (1-40) and A $\beta$ (10-35) also bound specifically to immobilized A $\beta$ (10-35) (Figure 1.2.2). Control proteins such as bovine serum albumin (BSA) did not bind well to the surface. These initial results suggested that specific interactions of ligands with A $\beta$  could be detected using SPR.



**Figure 1.2. Specific interactions with immobilized A $\beta$ (10-35)**

1) Sensorgrams from a flow cell containing a CM5 surface derivatized using amine coupling. Specific interactions were seen with the peptide KLVFF (**1.1**), VFFAEDVG (**1.26**) did not show a significant response (responses for all peptides at 1 mM concentration in HBS). 2) Amyloid sequences A $\beta$ (10-35) and A $\beta$ (1-40) bind to a CM5 surface derivatized with A $\beta$ (10-35). Control experiments using BSA show negligible response. All proteins are at 50  $\mu$ M concentration in HBS buffer.

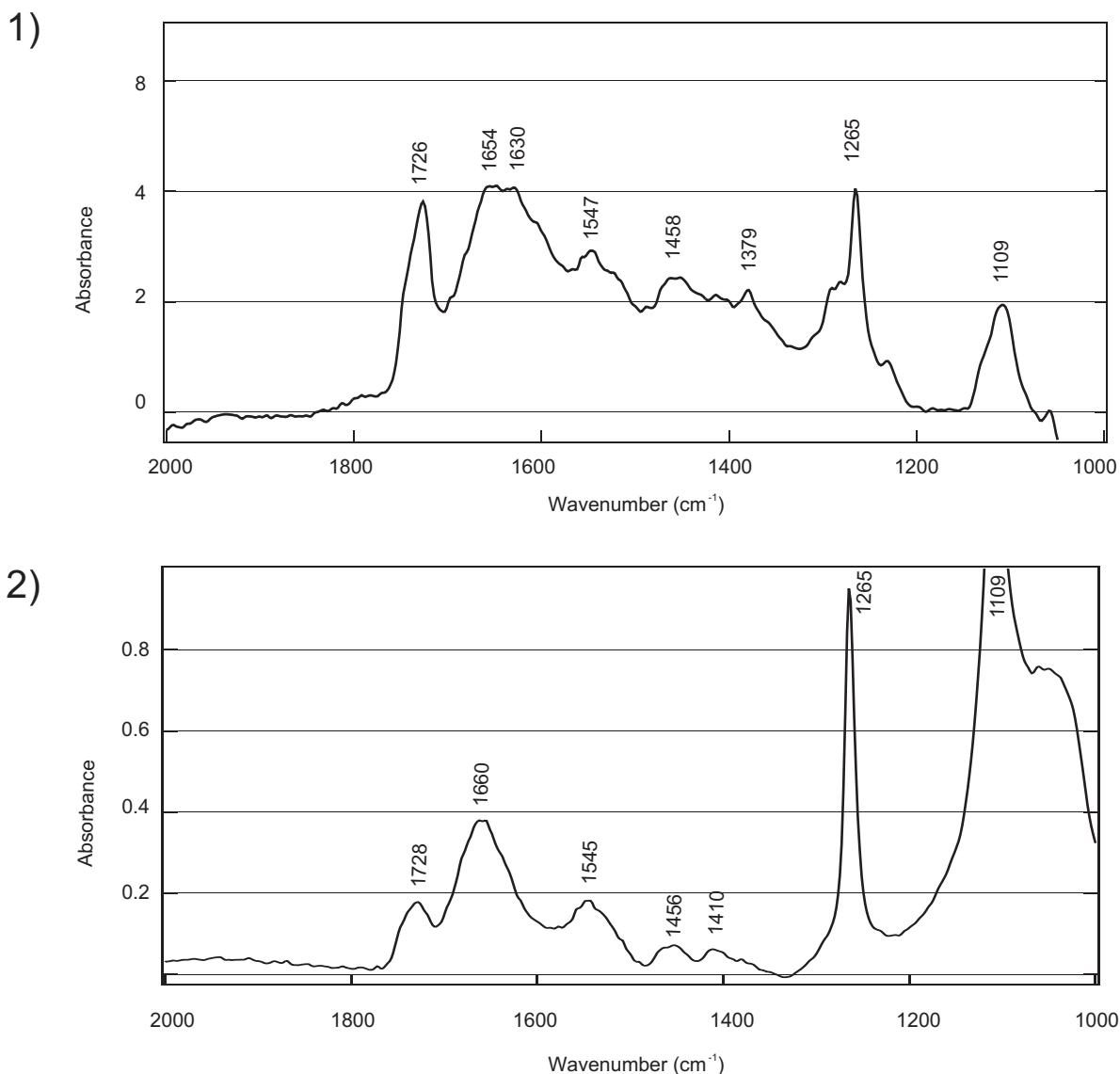
To confirm the presence of immobilized peptide on our surface, we attempted to characterize the resulting surface using surface IR techniques. Corn *et al.* have successfully applied polarization modulation Fourier transform infra-red reflection-absorption spectroscopy (PM-FTIRRAS) for studying the composition of self-assembled monolayers (SAM) on gold surfaces (Smith *et al.*, 2001). Spectra obtained for CM5 surfaces with immobilized peptide were obtained (Figure 1.3.1), as well as spectra for an underivatized surface as a control (Figure 1.3.2).

These spectra were unsuitable for high-resolution characterization of the surface due to the high background absorbances of the carboxylated matrix. This is unsurprising considering that a single flow cell is 1 mm<sup>2</sup> and should contain on the order of 2-5 pg/mm<sup>2</sup> of immobilized peptide; meanwhile the surface area coated with carboxymethyl dextran is 1 cm<sup>2</sup>. Additionally, it was observed that the intensity of PM-FTIRRAS measurements was highly variable due to *ad hoc* methods required for mounting a non-standard chip. The instrument mountings were designed for 3.0 cm<sup>2</sup> chips, and the chips used for our experiments were 1.0 cm<sup>2</sup>, this resulted in variable angles of reflection, and therefore variable absorbances between chips. The high variability in the magnitude of these absorbances prevented background correction for the dextran. Therefore, only qualitative assessment of these experiments is warranted. The underivatized surface (Figure 1.3.2) shows absorbances at 1728 and 1660 cm<sup>-1</sup> consistent with a hydrogen bonded C=O stretch of a carboxylic acid as expected. The derivatized surface (Figure 1.3.1) shows some additional features, although these are somewhat obscured by the absorbances of the carboxylated matrix. A new absorbance may be present at 1630 cm<sup>-1</sup>, consistent with an amide I stretch of a polypeptide. Amide II stretches should also be observed at 1560-1555 cm<sup>-1</sup>, however this region is



obscured. These data are therefore consistent with the immobilization of a polypeptide, but are not conclusive.

Despite the success of our initial binding experiments, we were concerned that Coulombic interactions between charged peptides and the anionic CM5 surface could complicate the evaluation of some ligands. Therefore, to expand the utility of the assay, we selected a surface with different charge density characteristics. Additionally, we employed a selective immobilization chemistry to maximize the uniformity of the binding sites on the surface.



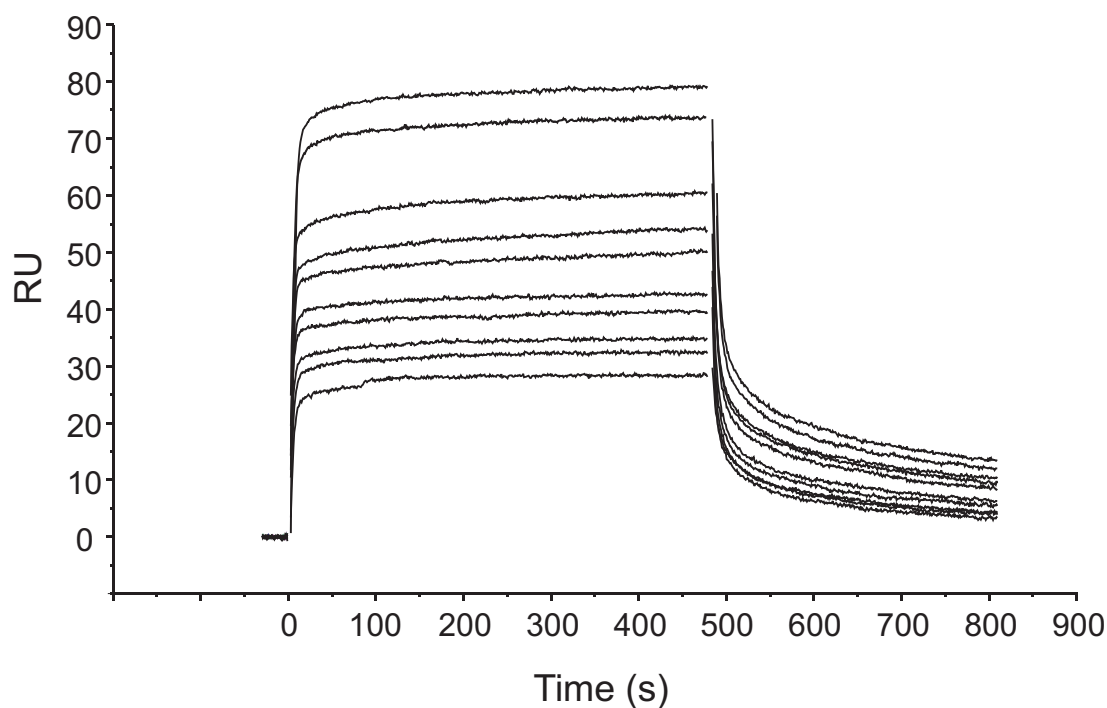
**Figure 1.3 PM-FTIRAS spectra of CM5 surface.**

1) PM-FTIRAS absorbance spectra for a CM5 surface with A $\beta$ (10-35) immobilized using amine crosslinking ( $\sim 2\text{-}5\text{ pg/mm}^2$  in each cell). The surface of the chip contained two derivatized flow cells ( $1\text{ mm}^2$  each) and the entire surface area of the chip was  $1\text{ cm}^2$ . The chip was mounted on a larger blank gold surface ( $3.0\text{ cm}^2$ ). 2) PM-FTIRAS absorbance spectra for a blank CM5 surface with no immobilized peptide. Note the difference in the magnitude of absorbances, as well as the appearance of all major peaks found for the surface containing immobilized peptide.

### 1.2.2. Amyloid binding studies using B1 surfaces

The B1 surface (Biacore AB) is composed of a carboxymethyl dextran matrix with approximately 10-fold fewer carboxylate sites than the CM5 surface. To ensure orientation-specific immobilization of the target, we introduced a C-terminal cysteine residue linked via an aminohexanoic acid (Aha) residue to the A $\beta$ (10-35) sequence (Figure 1.1.2).

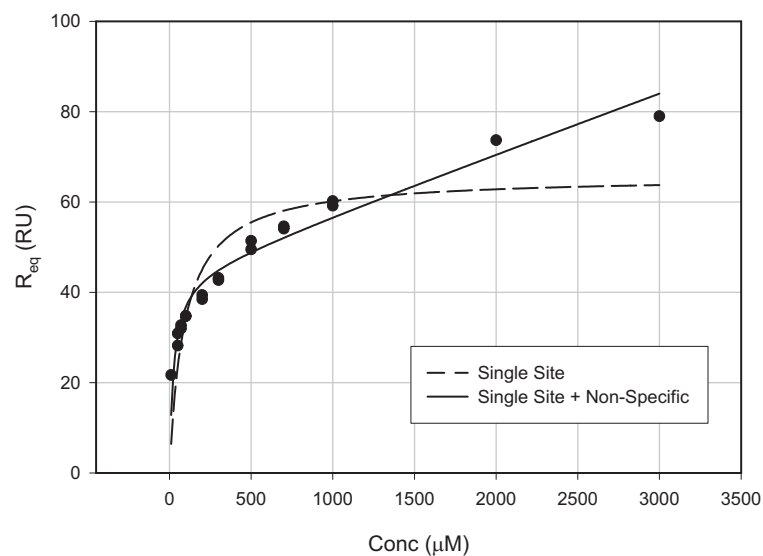
The cysteine side chain enables selective covalent bond formation to the matrix through conjugate addition of a cysteine thiolate to a maleimide (O'Shannessy *et al.*, 1992). To further reduce the likelihood of aggregation on the surface, we immobilized the target at low density. Thus, our conditions for surface modification are designed to minimize the immobilization of aggregates by using: 1) a truncated A $\beta$  sequence; 2) orientation-specific immobilization chemistry; and 3) target attachment at low density. The resulting surface was treated with a high salt denaturant, 4 M guanidine-HCl at pH 8.0, before and after injections of potential ligands to promote conformational homogeneity and dissociate any bound ligands. When A $\beta$ (16-20) was exposed to this surface, specific binding was observed. Multiple injections of identical samples afforded highly reproducible responses. To test the reproducibility of this procedure, the immobilization protocol was repeated on a fresh sensor chip. This preparation gave similar ligand binding responses and affinity. Given the reproducible results obtained with the modified B1 surfaces, we explored the binding interactions of candidate ligands for A $\beta$ .



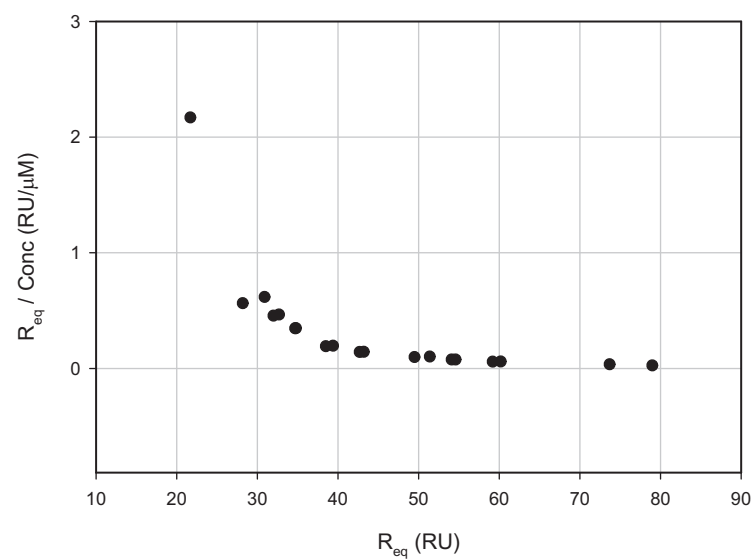
**Figure 1.4. Sensorgrams for compound 1.13.**

A representative set of binding data for KLVFFK<sub>6</sub> (**1.13**). All ten runs are overlaid for concentrations at 3000, 2000, 1000, 700, 400, 300, 200, 100, 70, and 50  $\mu$ M. The equilibrium response is determined as the average RU at 90% of contact time (430-440 sec) at each concentration. All sensorgrams have control lane data subtracted (subtraction artifacts at the start and end of each sensorgram have been removed for clarity).

1)



2)



**Figure 1.5. Binding isotherm of compound 1.13.**

Equilibrium analysis of binding data for KLVFFK<sub>6</sub> (**1.13**). 1) Regression analysis of binding affinity using the equilibrium values. Both single-site (eq. 1.1) and single-site with non-specific term (eq. 1.3) models are shown. 2) A linear transform of the equilibrium data for a Scatchard plot indicates heterogeneity in binding.

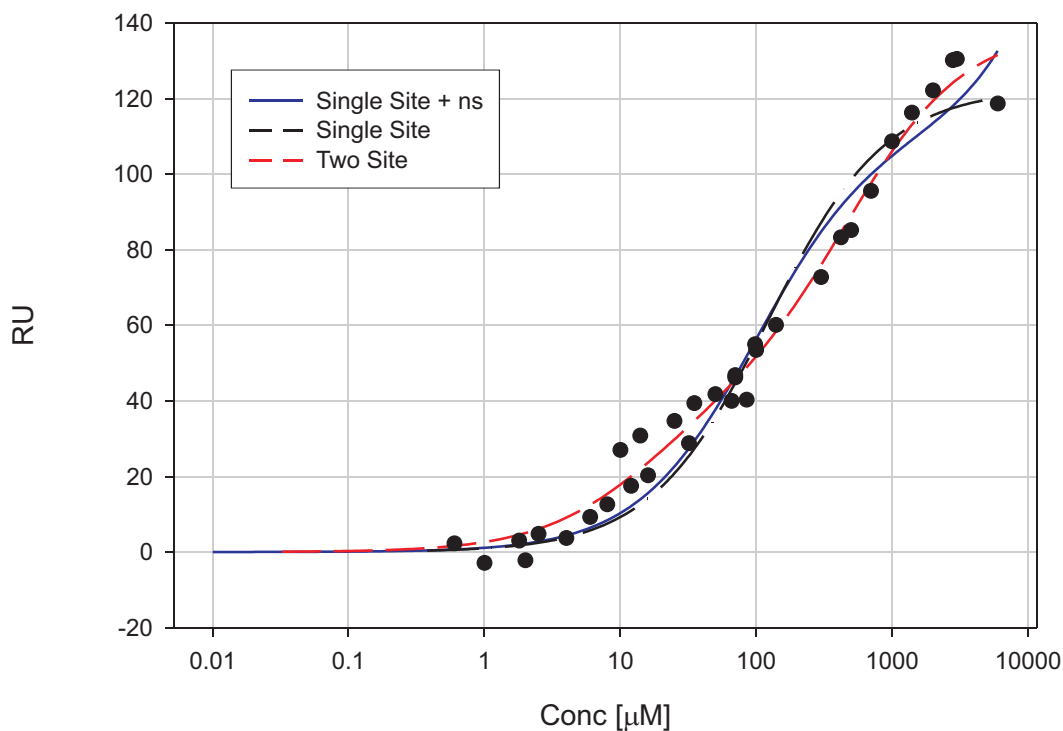
### 1.3. Peptide inhibitors binding to A $\beta$ (10-35)

To develop our method for determining the affinity of ligands for A $\beta$ , we examined the interactions of a well characterized inhibitor of toxicity, compound **1.13**. This compound is known as a potent inhibitor of amyloid toxicity and is able to alter the aggregation pathway and morphology of amyloid (Ghanta *et al.*, 1996; Pallitto *et al.*, 1999). Therefore we performed experiments using this compound to determine a binding isotherm and examine the mechanism of binding. For these experiments, the compound was injected over the amyloid surface and allowed to reach equilibrium (Figure 1.4). We corrected all binding measurements for changes in bulk refractive index by using reference-subtracted response levels at equilibrium to determine the binding isotherm (Karlsson and Stahlberg, 1995). Replicates over a range of concentrations provided the binding isotherm, and these data were plotted (Figure 1.5).

Initial examination of these data suggested that the binding of **1.13** did not follow the expected single site binding model (eq. 1.1). Additionally, examination of the same data using a Scatchard plot indicate that binding was heterogeneous, suggesting the presence of an additional binding site. Since a single site binding model was incapable of describing the data, we explored more complex models. The simplest model that introduces an additional binding site includes a single term for a second non-specific, or low-affinity, site (eq. 1.3). A slightly more complex model would include two new terms in order to describe an additional saturable binding site (eq. 1.4). The experiment shown in Figure 1.5 had been designed for increased throughput, and therefore we used a limited number (10 per compound) and range (10-3000  $\mu$ M) of concentrations. These conditions were designed to provide data able to

distinguish relative differences in affinity between compounds. To decide which model was more appropriate for analysis of the data, we first determined a more complete isotherm with a wider concentration range and more points. Additionally, we analyzed the binding of this and other compounds statistically to determine if use of the more complex binding model was appropriate. Experiments using an expanded concentration range (0.6-6000  $\mu\text{M}$ ) and increased replicates (35 concentrations over three experiments) were performed in order to test for evidence of multi-site binding in the assay (Figure 1.6).

1)



2)

**Fit Results:**

Eq.	Name	$K_d$		$R_{max}$		SS	F
1.1	single	120	+/- 10	123	+/- 4	2320	1.0
1.3	single+ns	100	+/- 10	110	+/- 6	1894	1.1
1.4	two site	16	+/- 6	41	+/- 8	785	3.0
—	—	500	+/- 130	99	+/- 7	—	—

**Figure 1.6. Detailed binding isotherm for compound 1.13.**

1) Semilogarithmic plot of a binding isotherm for compound **1.13**. The isotherm consists of 35 concentrations over three separate experiments using the same surface. The concentration range is 0.6-6000  $\mu\text{M}$ . 2) The data were fit to several models: single site (eq. 1.1), single site with non-specific binding (Single Site + ns, eq. 1.3), and independent two site binding (eq. 1.4). Parameters of the fits are shown including the sum of the squares of the residuals (SS) and the ratio of the SS to the single site model SS (F).

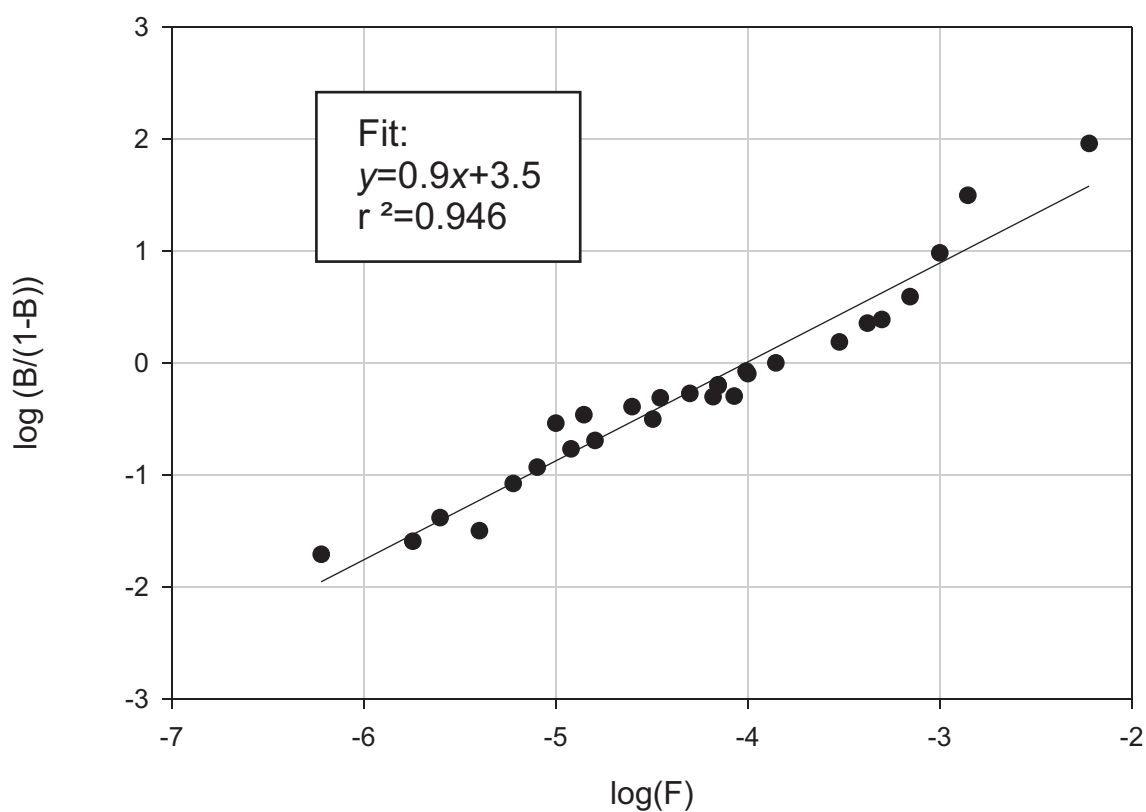


Examination of the fit in Figure 1.6 shows that using a two-site model (eq. 1.4) instead of a single-site model with a non-specific term (eq. 1.3) does provide a reduction in the sum of the squares of the residuals relative to the other models (Figure 1.6.2). Replotting the data in the form of a Hill plot gives a Hill coefficient of 0.9, consistent with non-cooperative binding sites (Figure 1.7). Although supportive of a non-cooperative second binding site, these results are not definitive and further investigation is required to confirm the validity of the independent two-site model. Interestingly, the saturation values ( $R_{\max}$ ) determined from these fits suggests that if a second site is present, it has a different point of saturation. The tighter affinity site has a saturation value of 40 RU [10%  $R_{\max}(\text{theoretical})$ ], while the lower affinity site has a saturation value of 100 RU [30%  $R_{\max}(\text{theoretical})$ ]. Because the mass of the peptide is invariant, the predicted saturation values in an ideal two-site interaction should be equivalent (eq. 1.2). Therefore, if this model is appropriate it suggests that there are two sites of different population on the surface.

Examination of the binding isotherms of other compounds screened for binding to amyloid also revealed that a two site model was not appropriate for the series of compounds in Table 1.3. Compounds **1.13-1.25** had been used to test for affinity on the same surface using a range of 50-3000  $\mu\text{M}$ . We fit these data with all three binding models to assess the ability of the model to describe multiple compounds. We found that using the single site model with the addition of the non-specific term (eq. 1.3) was able to reduce the residual sum of the squares ( $F = SS_i/SS_{ii}$ ) by 4-30 fold. Treatment of these data with the independent two-site model did improve the fit for **1.13**, however no other compounds showed an improvement in  $F$  (Table 1.1). Therefore, we used eq. 1.3 to analyze data from our assay. We discuss the potential origins of binding site heterogeneity in Section 1.5.

**Table 1.1. Analysis of binding model for compounds 1.13-1.25.**

<i>Compound</i>	$F_{ns}$ ( <i>eq. 1.1 vs. eq. 1.3</i> )	$F_2$ ( <i>eq. 1.3 vs. eq. 1.4</i> )
<b>1.13</b>	4.9	14
<b>1.14</b>	31	3.7
<b>1.15</b>	4.9	1.3
<b>1.16</b>	3.5	1.2
<b>1.17</b>	25	1.3
<b>1.18</b>	1.0	1.0
<b>1.19</b>	1.0	1.0
<b>1.20</b>	1.0	1.0
<b>1.21</b>	10	6.5
<b>1.22</b>	17	1.9
<b>1.23</b>	7.8	7.3
<b>1.24</b>	1.0	1.0
<b>1.25</b>	1.4	1.6



**Figure 1.7. Hill Plot for compound 1.13.**

Hill plot of data shown in Figure 1.6 to test for cooperativity between sites. The hill coefficient for the plot is  $n=0.9$ . A value of 1.0 suggests no cooperativity [free ligand concentration (F), bound ligand concentration (B)].

### 1.4.1. Affinities of peptide ligands for A $\beta$

We analyzed binding isotherms for compounds **1.13-1.25** using eq. 1.3 (Figure 1.5). The  $K_d$  values determined from our analysis are summarized in Table 1.3. Compound **1.13** (KLVFFK<sub>6</sub>) is an effective ligand for A $\beta$  ( $K_d = 40 \mu\text{M}$ ). This result indicates that a peptide domain lacking direct homology with A $\beta$  can play a significant role in binding. The increased affinities of sequences bearing lysine residues are not due to non-specific Coulombic interactions of KLVFFK<sub>6</sub> with the surface, as the affinities of compounds **1.17-1.20** and **1.22** indicate. Comparison of the affinities of compounds **1.13**, **1.14**, and **1.15** reveals that increasing the number of lysine residues from 4 to 6 does not afford more potent ligands. The position of the positively charged residues has a critical influence on A $\beta$  affinity. Placement of the positively charged residues close to position 20, as in **1.17**, gives rise to the most potent ligand of the four isomers. Placing the lysines three residues apart from the 16-20 region with intervening negatively charged residues (**1.18**) reduces the affinity by as much as 14-fold. Placement of positive charge at the *N*-terminus of the 16-20 sequence, as in **1.16**, results in lower activity than that of compounds **1.13-1.15**. These measurements support that affinities measured in this assay are interacting with the immobilized A $\beta$ (10-35) peptide. The observation that interactions of positively charged peptides have positional requirements strongly supports that observed binding is not an artifact of the negatively charged matrix.

With a method in place to analyze the affinity of candidate ligands, we examined several different classes of ligands including peptides and small molecules. First, we examined variants of A $\beta$ (16-20), which contained different aromatic side chains (Table 1.2). In these variants, one or both of the phenylalanine residues is substituted with tyrosine,

tryptophan, or histidine residues. Residues 19 and 20 have been shown previously to be important for plaque formation (Hilbich *et al.*, 1992), and we sought to determine if these interactions contribute to binding. Second, we tested peptides related to the KLVFFK<sub>6</sub> sequence, **1.13**, in which the *C*- and *N*-terminal sequence was varied (Tables 1.3 and 1.4). We demonstrated previously that **1.13** was a more potent inhibitor of A $\beta$  toxicity than was KLVFF (**1.1**) (Pallitto *et al.*, 1999). Thus, compounds designed to explore the importance of the lysine side chains in binding were assayed. Several small molecules previously reported to have effects on the aggregation or biological activities of A $\beta$  were also tested, including Congo red, rifampicin, melatonin, and the pentapeptide, LPFFD (Soto, 1999).

#### **1.4.2. Pentapeptide KLVxx compounds.**

In the case of pentapeptide ligands, we found that these compounds had universally low-affinity for immobilized A $\beta$ . Due to these low responses, we obtained only approximate determinations of affinity using a single-site model (eq. 1.1) by assuming the curves would reach a similar plateau. The relative affinity of these compounds could be compared using this method due to their similar mass and structure. This method is similar to that employed in other studies that determined the relative affinities of related compounds (Frostell-Karlsson *et al.*, 2000). It provides only a relative assessment of binding and should not be directly compared to dissociation constants. Additionally, the results from this analysis (Table 1.2) were similar to those obtained using graphical extrapolation methods for determining relative affinities (Klotz and Urquhart, 1948).

A series of variants of the KLVFF sequence were tested in the SPR assay. Truncation of the C-terminal phenylalanine (**1.2**) reduces affinity by approximately 10-fold. The D-amino acid sequence klvff (**1.3**) bound with similar affinity as **1.1**, as might be expected from previous reports (Findeis *et al.*, 1999; Tjernberg *et al.*, 1997). Substitutions of tyrosine at either the 19 or 20 position (**1.4**, **1.5**) did not alter the affinity; however, replacement of both phenylalanines with tyrosine (**1.6**) was detrimental. Substitution of histidine in position 19 (**1.8**), but not 20 (**1.7**), led to a substantial loss of binding; nevertheless, a double histidine substitution (**1.9**) partially restored binding. Substitution of tryptophan for phenylalanine residues gave mixed results. The sequence with a tryptophan residue at position 20 was less potent (**1.10**). When the analogous change was made at position 19 (**1.11**) or when substitutions were made at both positions (**1.12**), the resulting peptides afforded  $R_{eq}$  levels well above the theoretical  $R_{max}$  at high concentrations. This finding suggests that these peptides may aggregate in solution at high concentrations. Thus, the data from these compounds cannot be analyzed using a theoretical  $R_{max}$ . Still, the results demonstrate that compounds that interact by different mechanisms may be identified by this method.

Among the tetrapeptide and pentapeptide ligands screened, no sequences were found with greater potency than the original A $\beta$ (16-20) sequence, KLVFF. It has been observed previously that this ligand is capable of altering A $\beta$  aggregation and toxicity (Ghanta *et al.*, 1996; Pallitto *et al.*, 1999; Tjernberg *et al.*, 1996). We sought to determine if substitutions of the aromatic side chains might give rise to sequences with altered affinities. Compounds **1.1**-**1.12** all contained minor permutations of the A $\beta$ (16-20) sequence (Table 1.2). Because these variants bound weakly to immobilized A $\beta$ , only their relative binding abilities could be

evaluated. Many variations of the aromatic residues resulted in decreased binding relative to **1.1** (KLVFF). These data indicate that the phenylalanine residues contribute to the ability of the KLVFF sequence to bind A $\beta$ . Sequences with conservative changes at these positions, however, retain activity. Still, we were unable to find more potent sequences with standard amino acid substitutions. Our results suggest that peptidomimetic strategies are required to discover more potent analogs.

**Table 1.2. SPR results from steady state affinity determinations of pentapeptide ligands**

<i>Compound</i>	<i>Sequence</i>	<i>K<sub>rel</sub>(mM)<sup>a</sup></i>	<i>±SE</i>
<b>1.1</b>	KL <sup>+</sup> VFF	1.4	0.9
<b>1.2</b>	KL <sup>+</sup> VF	12	8
<b>1.3</b>	kl <sup>+</sup> vff	1.0	0.6
<b>1.4</b>	KL <sup>+</sup> VFY	1.6	0.6
<b>1.5</b>	KL <sup>+</sup> VYF	2.4	1.6
<b>1.6</b>	KL <sup>+</sup> VYY	6	2
<b>1.7</b>	KL <sup>+</sup> VFH	4	3
<b>1.8</b>	KL <sup>+</sup> VHF	ND <sup>b</sup>	
<b>1.9</b>	KL <sup>+</sup> VHH	4	2
<b>1.10</b>	KL <sup>+</sup> VFW	7	3
<b>1.11</b>	KL <sup>+</sup> VWF	ND <sup>c</sup>	
<b>1.12</b>	KL <sup>+</sup> VWW	ND <sup>c</sup>	

<sup>a</sup> Values reported were determined by fitting equilibrium values to a single site model and assuming the theoretical  $R_{max}$  as described in Materials and Methods (eq. 1.1, Section 1.8.2). Error is reported as the standard error of the fit.

<sup>b</sup>  $K_{rel}$  could not be determined due to insufficient response levels.

<sup>c</sup>  $K_{rel}$  could not be determined due to equilibrium values exceeding theoretical  $R_{max}$ .

**1.4.3. Composite peptides with charged domains.**

We reported previously that composite peptides containing short sequences composed of hydrophilic amino acids appended onto the Aβ(16-20) fragment are effective at inhibiting Aβ toxicity (Ghanta *et al.*, 1996; Lowe *et al.*, 2001; Pallitto *et al.*, 1999). The affinity of these composite sequences (comprising an Aβ recognition element appended to a more hydrophilic sequence) for Aβ is enhanced by positively charged residues at the C-terminus (Table 1.3). The differences in affinity between the composite sequences containing additional lysine residues, compounds **1.13-1.18**, reveal that the improvements in activity are due to the specific interactions of the C-terminal lysine residues with Aβ. The placement of the lysine



residues within a sequence greatly influences its binding affinity for the target. We postulate that these residues engage in complementary Coulombic interactions with negatively charged residues in the target sequence (e.g. E22 and D23). In accord with this model, the arginine-containing peptide **1.21** bound to immobilized A $\beta$  with an identical affinity to its lysine-substituted counterpart **1.13**.

The increased affinities of compounds **1.13**, **1.14**, and **1.21** for A $\beta$  relative to KLVFF may be due to the binding of these peptides in a parallel  $\beta$ -sheet mode. Parallel as well as anti-parallel binding modes have been invoked for assemblies of A $\beta$ -derived sequences (Antzutkin *et al.*, 2000; Balbach *et al.*, 2000; Benzinger *et al.*, 2000; Egnaczyk *et al.*, 2001; Rochet and Lansbury, 2000), suggesting that the specific sequence investigated might determine the binding mode. Additionally, cross  $\beta$ -sheet interactions involving charge-charge interactions can be exceptionally favorable (Smith and Regan, 1995). The lysine residues of compounds **1.13** and **1.14**, for example, could make favorable contacts with residues E22 and D23 within the target in the parallel mode. The arginine residues within peptide **1.21** would be expected to interact similarly. Interestingly, such contacts for compound **1.16** would only be accessible through an anti-parallel binding mode, and compound **1.14** binds more tightly to A $\beta$  than does **1.16**. Further characterization of the binding modes for different peptides will facilitate the optimization of A $\beta$  ligand structure.

The finding that the highest affinity compounds indicate a synergistic contribution of the hydrophobic recognition element (LVFF) and a positively charged sequence (oligo-lysine or -arginine) provides new directions for improving the affinity of A $\beta$  ligands. The results suggest new sites for interaction that can be used to generate compounds that make multi-

point contacts with A $\beta$ . In addition, composite sequences that contain recognition elements beyond the KLVFF sequence can bind with high affinity.

The data for Congo red (**1.25**) indicate that the SPR assay can report on the affinities of non-peptidyl small molecules for A $\beta$ . Additionally, the interactions of Congo red with immobilized A $\beta$  measured here provide indirect evidence for site isolation of the A $\beta$  target on the surface (Table 1.3). Congo red has been reported to interact with both monomeric A $\beta$  and fibrillar aggregates (Podlisny *et al.*, 1998). Our experiments with immobilized A $\beta$  result in a substantially weaker affinity for Congo red than that reported for binding to aggregated fibrils (Han *et al.*, 1996). Thus, the affinity of a ligand can be highly dependent upon the aggregation state of the target. This result highlights the advantages of our surface-based approach, and its potential to determine binding affinities for specific aggregation states.

Arginine-containing compound **1.21** was tested to determine the potency of compounds that incorporate positively charged residues other than lysine. These compounds possess activity similar to that of the lysine-containing compound **1.13**, suggesting that appending other positively charged sequences can afford compounds that exhibit enhancements in affinity relative to KLVFF. To examine the effects of altering the A $\beta$ (16-20) region in the context of a composite sequence, compounds **1.23** and **1.24** were tested. The activity of compound **1.23** is similar to that of **1.13**; however, **1.24** is less potent than might be expected from the relative activity of **1.10**.

Measurements of the affinities of several small molecules previously reported to alter fibrillogenesis and *in vitro* neurotoxicity were also conducted. We observed insignificant response levels (below 10 RU) for melatonin, rifampicin, and the peptide sequence LPFFD.

Congo red, however, did bind effectively to immobilized A $\beta$  in this assay. It was found to have reasonable affinity, although lower than that reported for aggregated A $\beta$  (Table 1.3).

**Table 1.3. SPR results from steady state affinity determinations**

<i>Compound</i>	<i>Sequence</i>	$K_d$ ( $\mu M$ ) <sup>a</sup>	$\pm SE$	%Viability <sup>f</sup>
<b>1.13</b>	KL VFFKKKKKK	40	9	88 <sup>c</sup>
<b>1.14</b>	KL VFFKKKK	37	5	78 <sup>c</sup>
<b>1.15</b>	KL VFFKK	80	40	72 <sup>c</sup>
<b>1.16</b>	KKK KL VFF	180	80	60
<b>1.17</b>	KL VFFKKKEEE	90	10	69
<b>1.18</b>	KL VFFEEEEKKK	1300	600	62
<b>1.19</b>	KL VFFEKEKEK	300	160	66
<b>1.20</b>	KL VFFEKEKEKE	ND <sup>b</sup>		62
<b>1.21</b>	KL VFFRRRRRR	40	10	92
<b>1.22</b>	KKKKKK	400	200	64
<b>1.23</b>	KL VWWKKKKKK	40	10	85
<b>1.24</b>	KL VFWKKKKKK	65	10	74
<b>1.25</b>	Congo Red	38	8	NA <sup>d</sup>
<b>1.26</b>	VFFAEDVG	ND		NA <sup>e</sup>

<sup>a</sup> Affinity was determined using eq. 1.3, as described in Materials and Methods (Section 1.8.3). Error is reported as the standard error of the fit.  $K_{ns}$  values were typically near 70  $\mu M$ .

<sup>b</sup>  $K_d$  could not be determined due to insufficient response levels.

<sup>c</sup> From Lowe, T. et al. (Lowe et al., 2001).

<sup>d</sup> From Klunk, W. et al., viability was recovered using 20:1 molar ratio of Congo red to A $\beta$ (25-35) (Klunk et al., 1998).

<sup>e</sup> From Ghanta, J. et al., viability was unchanged from control A $\beta$ (1-39) in PC12 cells (Ghanta et al., 1996).

<sup>f</sup> Untreated A $\beta$  samples gave 59% viability. The standard deviation in all cell viability measurements is  $\pm 2\%$ . Viability experiments were performed as described in Materials and Methods unless otherwise noted.

#### 1.4.4. Alanine replacements within KLVFF.

With a satisfactory method of measuring affinity for  $\beta$ -amyloid, we set out to explore structure-activity relationships. The data in Table 1.2 suggest that small peptides would provide inadequate response levels for affinity measurements. However, considering the positive results found in Table 1.3 we reasoned that peptides with appropriate characteristics could be used to ascertain new insights into the requirements for binding to the amyloid-derivatized surface. Several characteristics are apparent from the tight-binding peptides already studied: the sequences tend to have more than seven residues, they tend to have a net positive charge, and they require both a hydrophobic element and a charged element. With these requirements in mind, we set out to examine additional parameters such as stereochemical presentation of the sidechain, the inclusion of negatively charged elements, and modifications of the hydrophobic elements.

Our initial studies using pentapeptide ligands (compounds **1.1-1.12**) were directed at determining the requirements for binding of the aromatic region of the KLVFF sequence. Those studies suggested that alteration of the *C*-terminal phenylalanine position (residue 20 of  $\beta$ -amyloid) is severely detrimental to binding. Even conservative replacement with aromatic residues (Tyr, His) results in decreased binding. It remained to be established, however, what effect alterations of other hydrophobic residues in the sequence would have. We synthesized a set of peptides with alanine replacements of all residues within the 16-20 sequence (compounds **1.27-1.31**). Additionally we explored the polarity requirements of position 16 by using both serine (**1.32**) and glutamic acid (**1.33**) replacements.

**Table 1.4. SPR results from steady state affinity determinations**

<i>Compound</i>	<i>Sequence</i>	$K_d$ ( $\mu M$ ) <sup>a</sup>	$\pm SE$
<b>1.27</b>	KLVF <del>A</del> KKK	2000	4000
<b>1.28</b>	KLVA <del>F</del> KKK	210	120
<b>1.29</b>	KLAF <del>F</del> KKK	90	30
<b>1.30</b>	KAV <del>F</del> FKKK	130	40
<b>1.31</b>	ALV <del>F</del> FKKK	100	20
<b>1.32</b>	SLV <del>F</del> FKKK	140	90
<b>1.33</b>	ELV <del>F</del> FKKKK	4000	30000
<b>1.34</b>	LV <del>F</del> FKKK	200	80
<b>1.35</b>	klv <del>f</del> fk <del>k</del> kkk	110	50
<b>1.36</b>	ffv <del>l</del> kRRRRRR	7	5
<b>1.37</b>	kkkkklv <del>f</del> f	60	20
<b>1.38</b>	kkkkffv <del>l</del> k	19	3
<b>1.39</b>	ffv <del>l</del> kYGRKKRRQRR	50	10
<b>1.40</b>	KLVFFYGRKKRRQRR	40	10
<b>1.41</b>	EKELVFFFKKK	ND <sup>b</sup>	
<b>1.42</b>	KKKKKKKKLV <del>F</del> F	100	40
<b>1.43</b>	KLVFFEEEE	ND <sup>b</sup>	
<b>1.44</b>	EEEELV <del>F</del> FK	ND <sup>b</sup>	

*a* Affinity was determined using eq. 1.3, as described in Materials and Methods (Section 1.8.3). Error is reported as the standard error of the fit.  $K_{ns}$  values were typically near 70  $\mu M$ .

*b*  $K_d$  could not be determined due to insufficient response levels.

The alanine replacements of the 16-20 region confirmed our previous observations using pentapeptide ligands containing substitutions at the aromatic region. In those studies, we observed that truncation of the C-terminal phenylalanine reduced affinity by an order of magnitude. Using alanine substitutions in this series, we observe a similar effect: replacement of the C-terminal phenylalanine reduced affinity by as much as 50-fold (relative to KL~~V~~FFK~~K~~KKK, **1.14**). Substitution of alanine at the 19 position provided an approximately 5 fold loss of affinity (**1.28**). Replacement of leucine (**1.30**) and valine (**1.29**) also reduced the

measured affinity, however this change was no more than a two-fold reduction. The *N*-terminal position of the sequence appears to favor positively charged lysine over either alanine (**1.31**), serine (**1.32**), or glutamic acid (**1.33**) replacement. Truncation of the *N*-terminal position is also detrimental (**1.34**), and reduces affinity by as much as five-fold.

These data reinforce several features of peptide binding interactions for this system. Again, we observe that the phenylalanine residues (positions 19 and 20) are essential for binding, and the *C*-terminal position is the more critical of these two. Additionally, the hydrophobic residues leucine and valine are important for binding, even a conservative change of these residues to a smaller hydrophobic residue, alanine, showed measurable decreases in affinity. The *N*-terminal position appears to require a positive charge, as truncation or modification at this position reduces affinity.

#### **1.4.6. D-Amino acid sequences.**

To explore the effects of stereochemical modifications on affinity, we synthesized inverso and retro-inverso peptides containing the KLVFF motif and a positively charged element (Chorev and Goodman, 1993; Fletcher and Campbell, 1998). In our previous studies using L-amino acid sequences we found that positively charged residues placed at the *C*-terminus (**1.13**, **1.14**, **1.21**) of the KLVFF region were more favorable than placement at the *N*-terminus (**1.16**, **1.42**). Therefore, we constructed several variations of these sequences in order to determine the best placement of the positively charged element. Sequences with the same order of residues, but containing all-D-amino acids were used to construct inverso sequences **1.35** and **1.37**. Additional sequences were synthesized with a reversed order of all D-amino acids to construct retro-inverso peptides **1.36**, **1.38**, **1.39**. Affinity measurements of

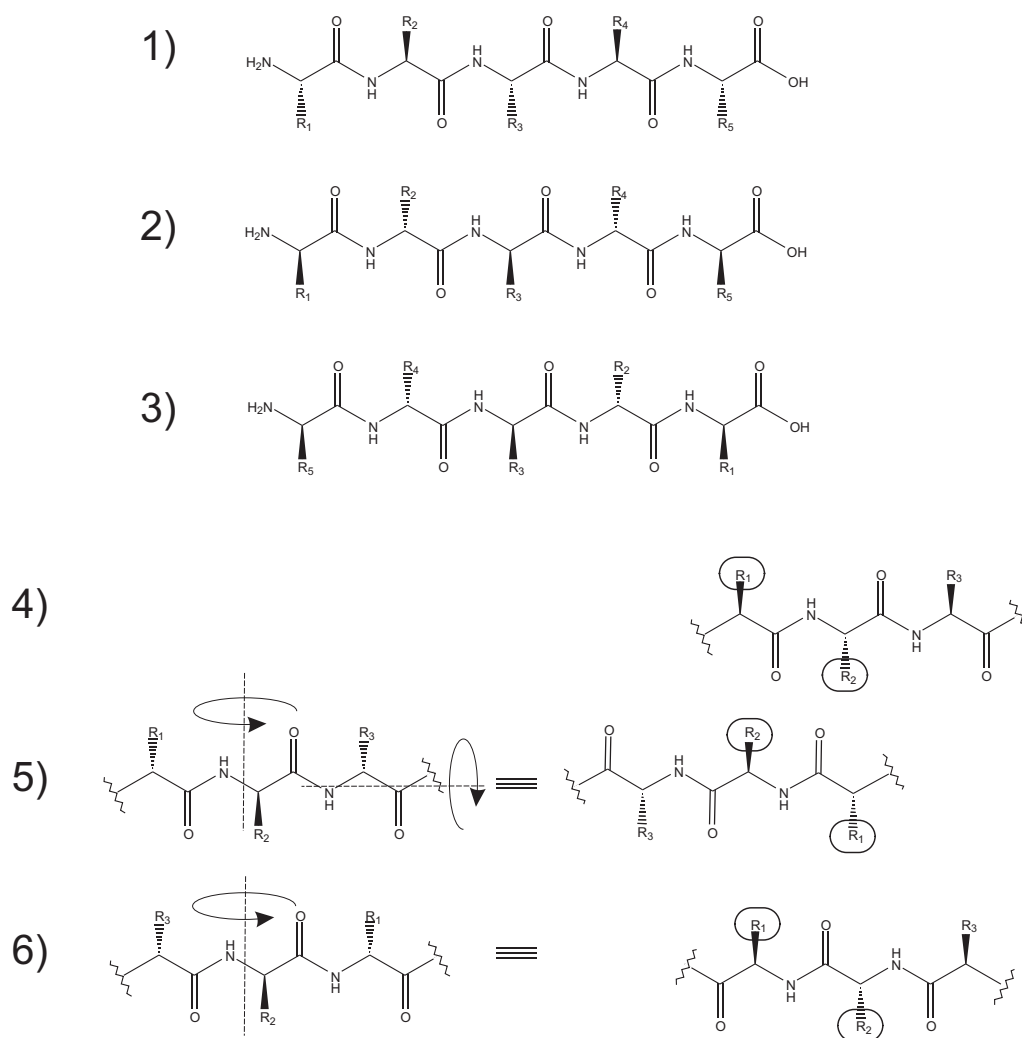
these peptides reveal that inverso peptides favor positively charged residues at the *N*-terminus, and retro-inverso peptides tolerate positive charges at both termini (Table 1.4).

These results may indicate that alternative binding modes are possible for these modified sequences. Previous experiments that appended residues to the KLVFF motif (Table 1.3) were consistent with a parallel  $\beta$ -sheet binding mode, which required 2-3 positively charged residues at the *C*-terminus and adjacent to the aromatic residues. Here, we find that this preference is reversed for the inverso sequences (**1.35**, **1.37**), and the retro-inverso sequences tolerate both *N*-terminal and *C*-terminal positive charge (**1.36**). It is clear that these results are not consistent with a parallel  $N \rightarrow C$  alignment of the sequences, in contrast to what is hypothesized for the previous sequences. Rather, these results may be rationalized by considering the orientations of the pair of phenylalanine residues in each sequence. If the sidechain orientations are maintained in these interactions, then the similar affinity of these ligands suggests that interactions between the amide backbones are not critical for binding (Figure 1.8). This model would predict that positive charges would be favorable at the *N*-terminus of both inverso and retro-inverso sequences. This is consistent with the measured affinity of the inverso sequences. The retro-inverso sequences tolerate both arrangements well; therefore, these sequences are also consistent with the model.

The critical nature of aromatic-aromatic interactions suggested by this model of binding is consistent with our previous results as well as those from other groups. Modifications of phenylalanine residues within the amyloid sequence are known to alter aggregation and conformational properties of the peptide (Esler *et al.*, 1996; Janek *et al.*, 2001). Studies of amyloid binding to immobilized small molecules also suggests that phenylalanine interactions are essential for binding (Tjernberg *et al.*, 1996; Tjernberg *et al.*,

1997). We find that alanine substitutions of these residues within eight residue inhibitors are most detrimental, leading to as much as a 50-fold reduction in affinity. In our studies of pentapeptides, truncations of aromatic residues were the most destructive to binding interactions. Aromatic interactions are well known as important elements of protein structure, and have been proposed to be essential for amyloid aggregation (Gazit, 2002; McGaughey *et al.*, 1998; Scrutton and Raine, 1996). Our observations here reinforce the importance of the central hydrophobic domain of A $\beta$ (1-40), and in particular the aromatic residues of this region appear to be extremely important for self-recognition of the peptide.





**Figure 1.8. Binding model for retro-inverso peptides.**

Structures of 1) an L-amino acid peptide, 2) a D-amino acid retro peptide, and 3) a D-amino acid retroinverso peptide. To orient both D-amino sequences to mimic the presentation of  $R_1$  and  $R_2$  in the L-amino acid sequence (4). 5) Rotation of the peptide backbone presents  $R_1$  and  $R_2$  sidechains, but results in a reversal of the peptide backbone, and exchange of  $R_1$  and  $R_2$ . 6) Reversal of the peptide backbone results in alignment of  $R_1$  and  $R_2$  similar to the L-amino acid configuration, but again reverses the backbone.

#### 1.4.7. Alternative charged domains.

To further explore the requirements of charged residues in amyloid binding peptides, we synthesized sequences with both positive and negative charged elements. Our previous work had suggested that positive charged residues (lysine or arginine) were favored when positioned C-terminal to the KLVFF motif. Therefore, we synthesized sequences containing alternative positively charged elements. For compounds **1.39** and **1.40**, we employed the cationic protein transduction domain from HIV TAT protein (Mi *et al.*, 2000; Schwarze *et al.*, 1999). These peptides could have potential *in vivo* applications due to their ability to penetrate cell membranes. These peptides showed similar affinity to compounds able to inhibit amyloid toxicity. Unfortunately, cell viability experiments with both of these compounds suggested that the peptide itself was toxic to cells. Experiments with PC12 cells showed that compound **1.40** at concentrations used for our assays (25  $\mu$ M) reduced cell viability to  $75 \pm 9\%$  and compound **1.41** reduced cell viability to  $87 \pm 6\%$ . Therefore these compounds could not be used for biological experiments.

To determine the length requirements of the charged domain, we studied different length polylysine domains. Extended polylysine sequences at the N-terminus (**1.42**) failed to improve affinity over shorter sequences at the same position (**1.16**). Peptides with a net negative charge did not provide measurable responses in our binding assay. We tested sequences containing multiple glutamic acid residues at both the N- and C-termini of the KLVFF motif (**1.42**, **1.43**), and found that both peptides failed to show any response. This result may be due to the characteristics of the surface used for binding studies. The surface consists of a negatively charged dextran matrix, and therefore the partitioning of net negative

peptides into this material will be unfavorable. Therefore, these data suggest a notable limitation to our assay design.

#### **1.4.8. Structure activity relationships for binding to A $\beta$ -derivatized surfaces.**

The structure activity relationships determined here provide the most detailed model of the binding interactions of  $\beta$ -amyloid presented to date. With the advent of a medium-throughput direct binding assay, we have been able to determine the structural requirements for high affinity binding. Further studies will be required to uncover the detailed mechanisms of activity, and a more defined structural model for these interactions. Still, our data still provide a useful empirical description of the requirements for small molecule binding to immobilized  $\beta$ -amyloid peptide.

We find several important characteristics for tight binding ligands in our assay. First, the presence of two neighboring aromatic groups (either phenylalanine or tryptophan) is essential for binding. Replacements using tyrosine or histidine are generally detrimental. The combination of effective aromatic and charge interactions in putative ligands also appears to be essential. Charged domains appear to be the most effective when located at the C-terminus of the KLVFF motif, and can consist of either arginine or lysine. These domains should be of at least 2 residues in length, however longer sequences sometimes improve affinity. Alteration of either of these key elements in a peptide ligand appears to prevent effective binding in virtually all cases studied here.

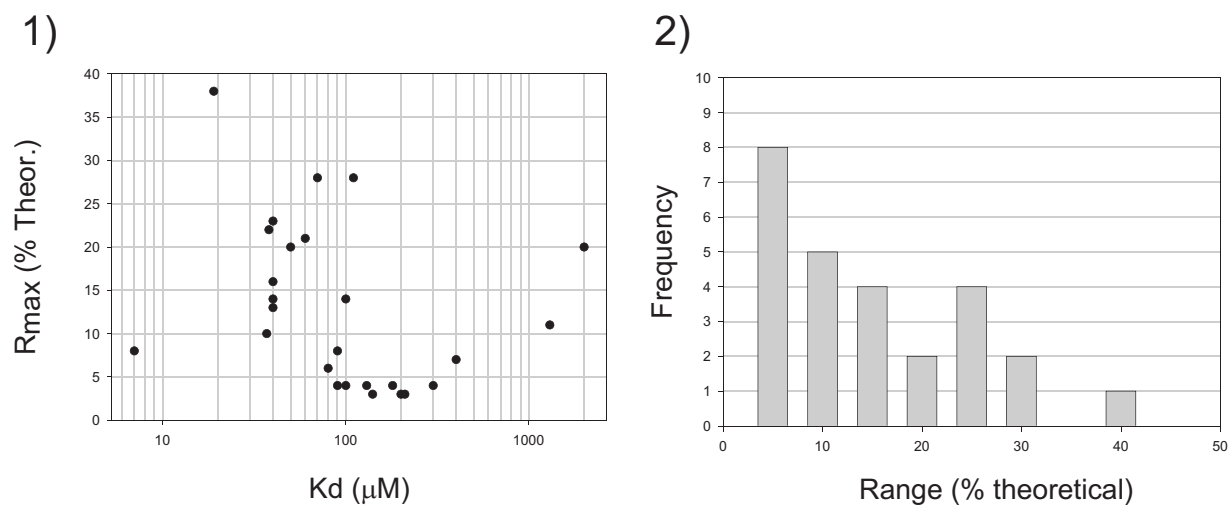
### 1.5. Designing peptide inhibitors for distinct oligomerization states

Our analysis of the data suggests that there is an additional class of binding sites found on the prepared surface. What are the potential causes of this additional interaction? Given our selective immobilization strategy, it is unlikely that multiple orientations of the A $\beta$  target are responsible for the observed heterogeneity. We propose that the observed heterogeneity arises from an additional independent binding site contained within the immobilized sequence or due to the presence of aggregates. Multiple binding sites within the peptide itself have been detected previously in studies that examined the binding of radiolabeled A $\beta$ (1-40) to short homologous peptides (Tjernberg *et al.*, 1996). In addition to identifying the primary A $\beta$  self recognition sequence as A $\beta$ (16-20), a secondary site was also found within the A $\beta$ (24-34) sequence. We suspect that this region could provide an additional weak-binding site within the immobilized peptide that accounts for the observed heterogeneity.

An alternative proposal also presents itself in light of the unusual saturation values observed for the two-site model (Figure 1.5). Two separate classes of sites could be present on the surface, and differences in populations between these sites could provide disparate  $R_{\max}$  values. This heterogeneity of the surface could be accounted for by several possibilities, including the presence of alternate conformations or immobilization of different oligomerization states. Considering the aggregation-prone nature of the immobilized peptide, we favor the presence of a quantity of  $\beta$ -amyloid oligomers on the surface. Although we designed our conditions for immobilization to avoid the inclusion of oligomers, these data would be consistent with their presence.

If this analysis is correct, it implies that the binding assay is capable of determining the affinity for separate states of oligomerization. In the current configuration, this appears to be possible on the same surface; however, it is unclear what aggregation state can be assigned to particular sites from the binding isotherm. Comparison of our affinity measurements using Congo red to those performed with aggregated fibrils suggests that this compound binds tighter to higher aggregation states (Han *et al.*, 1996). Therefore, we hypothesize that the low affinity site found here is due to monomeric  $\beta$ -amyloid, and the high affinity site is due to  $\beta$ -amyloid dimers or small oligomers (Harper *et al.*, 1997; Koo *et al.*, 1999; Walsh *et al.*, 1997). This possibility is particularly interesting considering that we have found our surface preparations to be consistent over separate experiments and stable over long periods of time. Therefore, the configuration of our assay may provide a simple means to immobilize and study the binding interactions of separate oligomeric species.

Reconsideration of our initial binding studies also lends support to the presence of multiple classes of sites on the surface. Tabulation of the saturation values fit from the binding isotherms of compounds in Tables 1.3 and 1.4 show a non-uniform distribution of these values. The majority of compounds (65%) have saturation values between 5-15% of the theoretical saturation (normalized for the mass of each peptide), the remaining compounds have values between 20-40% of saturation (Figure 1.9). The measured  $R_{\max}$  values do not appear to correlate with affinity (Figure 1.9). The range of observed  $R_{\max}$  values may indicate that certain compounds have an intrinsic selectivity for a particular aggregation state found on the surface.



**Figure 1.9. Distribution of  $R_{\max}$  values.**

1) Semilogarithmic plot of  $R_{\max}$  values vs. measured affinity. 2) Histogram of  $R_{\max}$  values from binding data in both Tables 1.3 and 1.4. Values have been normalized to the molecular weights of each compound, and are calculated as percent of theoretical (using eq. 1.2).

Results from several laboratories suggest that specific states of aggregation are responsible for amyloid toxicity (Harper *et al.*, 1997; Koo *et al.*, 1999; Walsh *et al.*, 1997). Specifically, small amyloid oligomers (dimers to tetramers) appear to be early species in the process of aggregation. These oligomeric species (also known as  $\beta$ -amyloid derived diffusible ligands, or ADDLs) have been proposed to be the relevant toxic species in AD (Klein *et al.*, 2001; Koo *et al.*, 1999). These oligomers have been observed by a variety of techniques including atomic force microscopy (Harper *et al.*, 1997), transmission electron microscopy (Ward *et al.*, 2000), and size exclusion chromatography (Pallitto and Murphy, 2001; Shen *et al.*, 1993; Tseng *et al.*, 1999; Walsh *et al.*, 1997).

Until recently the association between soluble oligomers and amyloid toxicity was relatively obscure. *In vitro* and *in vivo* data is consistent with ADDLs being neurotoxic (Koo *et al.*, 1999; Walsh *et al.*, 2002). However, evidence that ADDLs are present in the AD brain is still lacking. Murphy and coworkers have developed the most detailed *in vitro* model of the amyloid aggregation pathway to date. The model is based on size exclusion chromatography, dynamic light scattering, and static light scattering (Pallitto and Murphy, 2001). This development was facilitated by conditions that provide a homogeneous preparation of monomeric peptide as a starting point for aggregation experiments. The model suggests that formation of intermediate aggregates, referred to as filaments, associate to form amyloid fibrils. Murphy *et al.* have shown that this model is able to predict several elements of the *in vitro* aggregation event, more importantly, these authors have been able to exploit the model to develop conditions in which particular intermediate species predominate. This development will be particularly useful for testing the *in vitro* toxicity of such species.

This model of toxicity inhibition is counterintuitive, and contrary to the accepted strategy of aggregation inhibition. Considering the aggregation models refined by Murphy *et al.* and studies of peptide inhibitors of toxicity by Murphy and Kiessling *et al.*, it becomes clear that acceleration of aggregation is a viable strategy for designing new inhibitors of toxicity (Ghanta *et al.*, 1996; Pallitto *et al.*, 1999). As discussed above, we propose that the surfaces we have used for these studies are capable of harboring stable  $\beta$ -amyloid oligomers. Conceivably, immobilization conditions could be developed for particular oligomerization states of interest. In this way experiments could be performed that measure the affinity of compounds for separate oligomerization states. The identification of compounds that could selectively target intermediate species would be invaluable for both *in vitro* and *in vivo* studies of AD.

#### **1.6.1. Biological activity of peptide inhibitors.**

Several biological models are used to test the ability of potential ligands to alter the toxicity of  $\beta$ -amyloid. Two critical components of any assay are the choice of the biological model and the conditions used to produce toxic aggregates. The most common tissue culture models used in the literature are rat neuronal cells (PC12) and human neuroblastoma cells (SH-SY5Y) (Li *et al.*, 1996; Shearman *et al.*, 1994). Several labs developing small molecule inhibitors of amyloid toxicity have employed these models (Ghanta *et al.*, 1996; Lowe *et al.*, 2001; Pallitto *et al.*, 1999). Toxicity is assessed by determining the activity of the cell mitochondria after challenge (Shearman *et al.*, 1994). A decrease in MTT reduction, which indicates loss of mitochondrial function, is an early indicator of  $A\beta$ -mediated toxicity

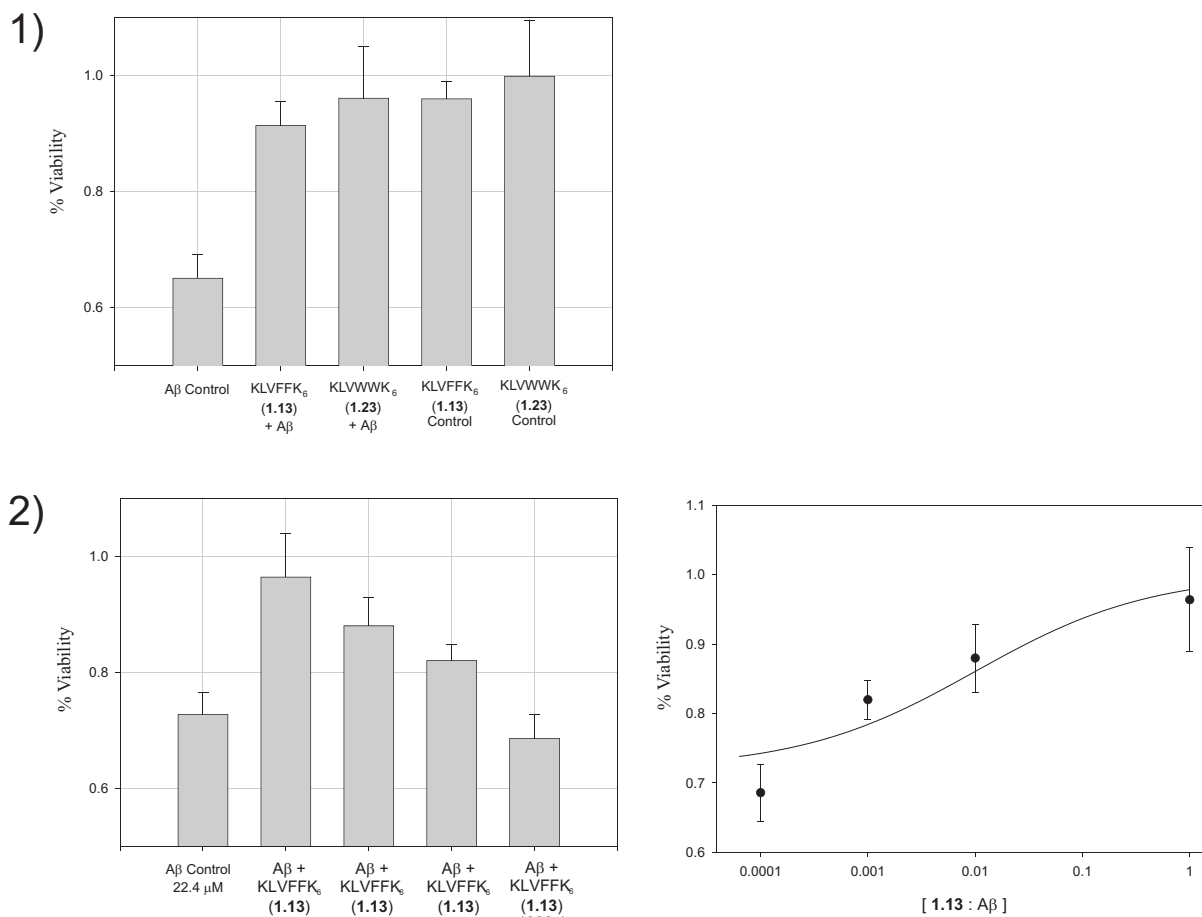


(Shearman *et al.*, 1994). We have previously used this assay to show that compounds related to **1.13** are effective inhibitors of A $\beta$  toxicity (Ghanta *et al.*, 1996; Lowe *et al.*, 2001; Pallitto *et al.*, 1999). Several conditions are available for the preparation of toxic amyloid, for our studies we have used dissolution of the peptide with small concentrations of a strong acid, trifluoroacetic acid (TFA) (Shen and Murphy, 1995).

The ability of **1.13** to prevent amyloid toxicity has been previously characterized using this assay in both PC12 and SH-SY5Y cells (Ghanta *et al.*, 1996; Lowe *et al.*, 2001; Pallitto *et al.*, 1999). We used the PC12 cell model to further characterize the activity of compounds **1.13** and **1.23**. We first tested the ability of both compounds to prevent the toxicity of A $\beta$  at 1:1 molar ratios of A $\beta$  to inhibitor (Figure 1.10.1). We found that both compounds were able to inhibit toxicity, and our results were consistent with previously published studies (Ghanta *et al.*, 1996; Lowe *et al.*, 2001; Pallitto *et al.*, 1999). Additionally, we confirmed that this effect was dose-dependent by repeating the experiment with reduced concentrations of the inhibitor peptide (Figure 1.10.2). The inhibition of toxicity was dose-dependent and treatment of these data as an IC<sub>50</sub> gives an approximate value of 0.001 equivalents inhibitor to amyloid.

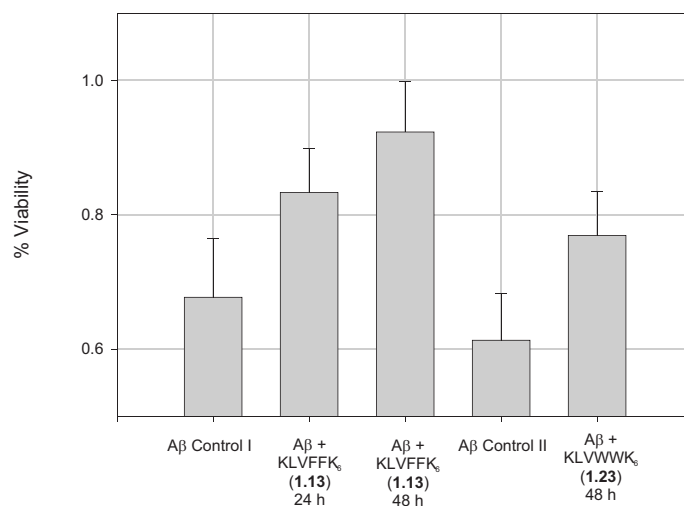
Although we were able to observe that peptide inhibitors such as **1.13** are able to prevent the formation of toxic amyloid aggregates, we also wanted to test if these same compounds could reverse the toxicity of already formed aggregates. Therefore, using identical conditions as above, we prepared toxic amyloid aggregates and used inhibitors to reverse toxicity (Figure 1.11). For these experiments we first aggregated an amyloid sample for 48 h at 37 °C. The sample was then allowed to incubate for another 48 h at 37 °C. Importantly, for the second portion of the incubation, peptide inhibitors were added either 24 or 48 h prior to

the end of the incubation. Therefore, recovery of toxicity relative to control should be an indication of the ability of the peptide inhibitor to reverse the toxicity of amyloid aggregates. We observed that compound **1.13** was able to reverse toxicity with 24 or 48 h of exposure to the aggregates. Compound **1.23** was also able to reverse toxicity with 48 h of incubation.



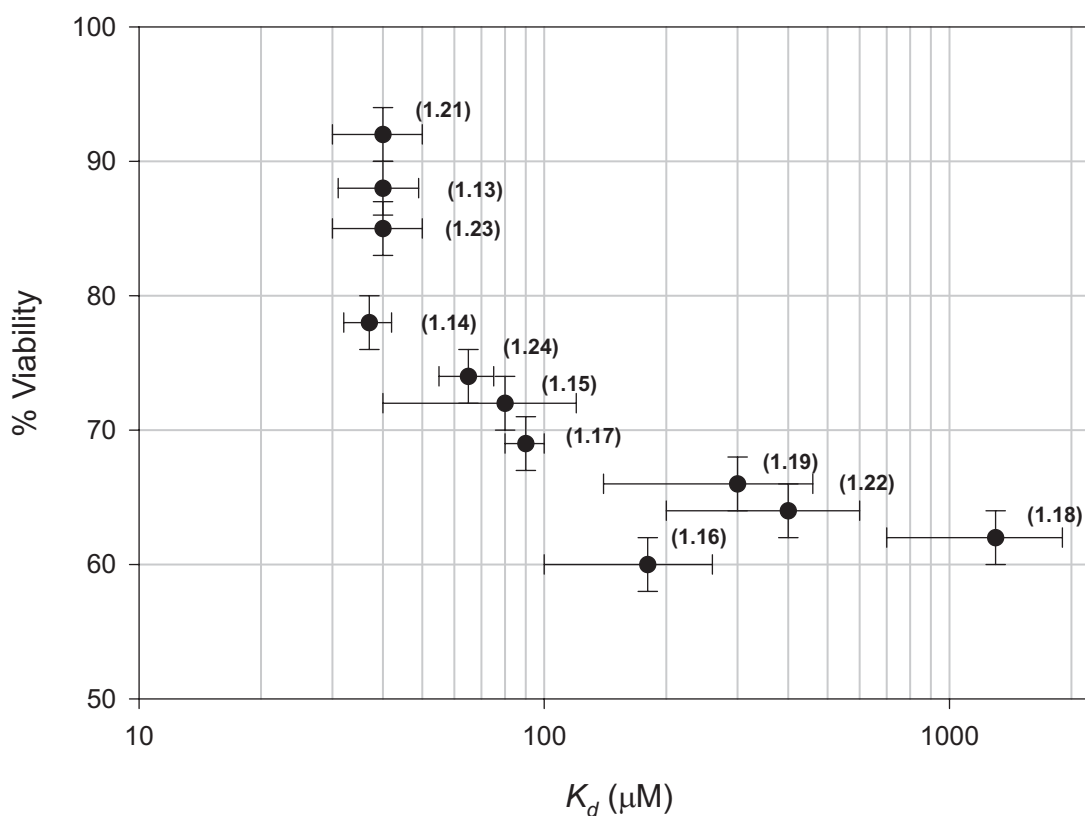
**Figure 1.10. Prevention and concentration dependence of toxicity.**

1) To test the biological activity of some tight binding ligands for Aβ, PC12 (rat neuronal) cells were challenged with aggregated Aβ in the presence and absence of peptide inhibitors. Co-incubation of both compounds **1.13** and **1.23** during aggregation inhibits amyloid toxicity. Amyloid was dissolved initially in 0.5 % TFA before aggregation. Samples were aggregated for 48 h at 37 °C with (25 μM final concentration) Aβ and (25 μM final concentration) peptide inhibitor. Points shown represent 5-7 replicates and error is shown as the standard error of the mean. 2) To test the concentration dependence of this effect, decreasing molar ratios of inhibitor to Aβ were used. Compound **1.13** was able to partially inhibit toxicity with a molar ratio as low as 1000:1 Aβ to peptide present. Points shown represent 5 replicates each, and error is given as the standard error of the mean.



### Figure 1.11. Reversal of toxicity.

To test the ability of peptide inhibitors to reverse already toxic A $\beta$  aggregates, we aggregated A $\beta$  at 37 °C for 48 h (after initial dissolution in 0.5% TFA). After this incubation, the aggregated solution was incubated at 37 °C for another 48 h. Peptide inhibitors (1:1 ratio of A $\beta$ :inhibitor) or buffer (control) were added at either 24 h or 48 h before the end of the second incubation. Therefore, increased viability is a measure of the *reversal* of amyloid toxicity. Data shown are the mean of 5 replicates, and error is given as the standard error of the mean.



**Figure 1.12. Correlation of Affinity with in vitro inhibition of toxicity.**

Correlation of affinity measured by SPR with prevention of cellular toxicity of A $\beta$ (1-40). Compounds shown are all from Table 1.3. For toxicity experiments, the final A $\beta$  concentration was 25  $\mu\text{M}$ , and the A $\beta$ :peptide molar ratio was 1:1. Cellular viability was assessed with the MTT assay.(Shearman, 1999) Each value represents the mean of results from 2 separate runs with seven replicates per run.

### 1.6.2. Ligand affinity is a predictor of toxicity inhibition

To examine the ability of the remaining A $\beta$  ligands to influence cellular toxicity, we examined their potency using the MTT assay and SH-SY5Y cells (Shearman, 1999). Previously, we and others have identified compounds that alter A $\beta$ -A $\beta$  association processes (Findeis *et al.*, 1999; Ghanta *et al.*, 1996; Gordon *et al.*, 2001; Lowe *et al.*, 2001; Pallitto *et al.*, 1999; Soto *et al.*, 1996; Soto *et al.*, 1998; Tjernberg *et al.*, 1996; Tjernberg *et al.*, 1997). Although some of these compounds have been found to block the cellular toxicity of A $\beta$ , the relationship between A $\beta$  binding affinity and inhibition of toxicity has been obscure (Howlett *et al.*, 1999b).

We reasoned that compounds that bind A $\beta$  would be likely to alter its aggregation pathways and thereby prevent its toxicity. Compounds with these characteristics serve as useful probes of the molecular mechanisms underlying amyloid formation and pathology and as leads for the design of therapeutic agents. Using an immobilized form of a target protein fragment A $\beta$ (10-35), the relative affinities for small molecules can be assessed with SPR. A key to this success is an immobilization protocol that provides a consistent preparation of the target, A $\beta$ (10-35). In any solution-based assay, A $\beta$  monomers readily aggregate to generate a diverse mixture of different targets. By immobilizing a form of A $\beta$  at low density, a surface that affords consistent binding results is obtained. Another benefit of our approach is that the surface modified with A $\beta$ (10-35) is stable for several weeks and can be used for multiple assays. With this assay method, the relative affinities of several groups of small molecules were measured and compared to their ability to prevent A $\beta$  cellular toxicity. The results of these viability experiments are given in Table 1.3 and Figure 1.12.

To test our hypothesis that the most effective ligands for A $\beta$  would be effective inhibitors of its toxicity, we developed an assay to determine relative affinities of a series of compounds for A $\beta$ . The results of toxicity experiments with new compounds analyzed here given in Table 1.2, and they show excellent agreement with the measured affinities from SPR (Figure 1.12). Compounds with measured dissociation constants lower than approximately 50  $\mu$ M (**1.13**, **1.14**, **1.21**, **1.23**) afforded protection against toxicity with cell viability levels above 80%. The compounds (**1.16**, **1.18**, **1.19**, **1.20**, **1.22**) that were less effective ligands in our binding assay (i.e. with  $K_d$  values greater than 100  $\mu$ M) were less effective at preventing the cellular toxicity of A $\beta$ .

A key finding from our results is that a direct binding assay can identify compounds that alter A $\beta$  toxicity. Several of the compounds examined here were previously identified as inhibitors of toxicity (i.e., compounds **1.1**, **1.13**, **1.14**, **1.15**, and **1.25** (Lowe *et al.*, 2001; Pallitto *et al.*, 1999; Soto, 1999)). Our results suggest that their mechanism of action depends on high affinity binding to A $\beta$ . Not all compounds reported to interfere with A $\beta$  toxicity were found to bind to the immobilized A $\beta$  species in this assay. For example, several other compounds with reported biological activity were ineffective in our assay (i.e. melatonin, rifampicin, and LPFFD). Their lack of activity in this assay suggests that these compounds may act by a different mechanism. Alternatively, these compounds may not bind effectively to the A $\beta$ (10-35) sequence used here or they may only interact with higher order assemblies of A $\beta$ , which we have attempted to minimize on our surface. In addition to providing leads for inhibitors of toxicity, our ability to directly monitor binding to A $\beta$  allows us to dissect the role of A $\beta$  affinity in inhibitor function.

## 1.7. Conclusions

In summary, we have presented a new method for determining the affinity of small molecules for  $\beta$ -amyloid peptide. Using this method, we have developed detailed structure activity relationships for the binding of ligands to amyloid. We find that modified sequences containing the central hydrophobic domain ( $A\beta(16-20)$ ) can provide ligands of high affinity for amyloid. Additionally, we have shown that the aromatic residues of the sequence are an essential feature of this recognition event. Composite sequence containing positively charged elements were also used to demonstrate that additional Coulombic interactions can provide significant and synergistic enhancements in the affinity of ligands. Using *in vitro* cell viability assays we demonstrate that ligands of high affinity are often potent inhibitors of amyloid toxicity. Together these methods provide a straightforward means of designing new inhibitors of amyloid toxicity.

Our direct binding assay for determining the affinity of small molecules to  $A\beta$  serves as a highly effective method to identify compounds that bind  $A\beta$ . Significantly, the SPR assay is convenient, reproducible, and has the necessary sensitivity to detect the interaction of low molecular weight ligands with the  $A\beta$  target. Our finding that ligands for immobilized  $A\beta$  are effective at preventing  $A\beta$  toxicity in cell culture provides support for the hypothesis that ligands for  $A\beta$  can function as effective inhibitors of its toxicity. The assay we describe provides the means to identify such inhibitors.

Many amyloid diseases are known, and few strategies for therapy are currently available. Emerging evidence suggests that there are many common features between these



diseases, in particular soluble oligomers (ADDLs) seem to be the primary toxic species in several systems. Our results reported here provide general methods to identify specific ligands for  $\beta$ -amyloid peptide; these will facilitate studies of the mechanisms of aggregation, and ultimately amyloid diseases.

### 1.8.1. Experimental procedures

*Reagents.* All reagents were purchased from Sigma (St Louis, MO) or Fisher Scientific (Pittsburgh, PA) unless otherwise noted.

*Peptide synthesis.* Protected peptide residues and resins were purchased from Advanced Chemtech (Louisville, KY). Peptides used in this study were assembled by solid-phase peptide synthesis procedures appropriate for monomers equipped with fluorenylmethoxycarbonyl protecting groups (Fmoc). Peptides were purified by reverse-phase high-performance liquid chromatography (RP-HPLC) using a Vydac C18 column and water/acetonitrile mobile phase. All peptides were analyzed by matrix-assisted laser desorption/ionization time-of-flight (MALDI-TOF) spectroscopy on a BRUKER REFLEX II mass spectrometer.

*A $\beta$ (10-35).* A $\beta$ (10-35)-amide used in the initial studies was purchased from QCB Biosource International (Camarillo, CA). The amino acid sequence is YEVDHQLVFFAEDVGSNKGAIIGLM-NH<sub>2</sub>. The reported mass is 2902 and the purity is >97% (purity based on HPLC peak area). The A $\beta$  (10-35)-Aha-Cys (Figure 1.1.2) was synthesized using a Synergy 432A Peptide Synthesizer (Applied Biosystems, Foster City, CA). The cysteine used for surface immobilization was introduced to the peptide at the C-terminus through an intervening aminohexanoic acid (Aha) spacer. The amino acid sequence is YEVDHQLVFFAEDVGSNKGAIIGLM-Aha-C. The peptide was purified by RP-HPLC (purity was 88% based on peak area). The mass of the peptide is 3120, and its sequence was confirmed by amino acid analysis. All protected peptide reagents were purchased from

Novabiochem (La Jolla, CA), and the coupling reagents were purchased from Applied Biosystems.

*SPR Assay.* Sensor chips were purchased from BIAcore (Uppsala, Sweden). All SPR experiments were run on a BIAcore 2000 instrument. Reagents for immobilization (EDC, NHS, ethanolamine) were purchased from Aldrich Chemical Company (Milwaukee, WI). The buffer used to immobilize the peptide through amide bond formation was 10 mM sodium acetate (pH 5.0), the regeneration buffer was 4 M guanidine-HCl in 10 mM Tris-HCl (pH 8.0); running buffer was HEPES-buffered saline (HBS) containing 10 mM HEPES and 150 mM sodium chloride (pH 7.4). All buffers were filtered (0.22  $\mu$ m, nylon) prior to use. For immobilization via cysteine thiolate addition to maleimide, HBS buffer (pH 7.4) was used for all steps unless otherwise noted. The bifunctional coupling reagent *m*-maleimidobenzoyl-*N*-hydroxysulfosuccinimide ester (Sulfo-MBS) was purchased from Pierce Chemical Company (Rockford, IL), ethylenediamine (EDA) and cysteine were purchased from Aldrich and used as provided.

*A $\beta$  Immobilization.* Attachment of A $\beta$ (10-35)-amide to the CM5 chip followed standard amide bond-forming conditions as reported elsewhere (O'Shannessy *et al.*, 1992). The flow rate employed for all steps was 5  $\mu$ L/min to maximize contact time. The carboxymethyl dextran matrix was activated by injection of a 1:1 mixture of *N*-ethyl-*N'*-(dimethylaminopropyl)-carbodiimide (EDC) and *N*-hydroxysuccinimide (NHS) (70  $\mu$ L, 200 mM EDC, 50 mM NHS). The  $\beta$ -amyloid peptide (10-35) fragment was then injected into the activated flow cell (0.5 mg/ml peptide in sodium acetate buffer). Unreacted NHS esters were capped with ethanolamine (70  $\mu$ L, 1 M, pH 8.5) to afford a surface that gave a final change in

response units (RU) of 2700 in the A $\beta$  sample flow cell. The control flow cell was reacted under the same protocol using an injection of ethanolamine buffer (70  $\mu$ L) instead of the peptide to produce a control cell with reduced charge. The B1 surface was prepared using standard maleimide chemistry (O'Shannessy *et al.*, 1992); the surface was activated as above using NHS/EDC, then reacted with EDA (70  $\mu$ L, 1 M, pH 8.5) to generate free amine groups on the surface. Sulfo-MBS (70  $\mu$ L, 50 mM in HBS) was then injected to generate a surface modified with maleimide groups. For the conjugate addition of the A $\beta$  sequence, the cysteine-containing peptide was dissolved in immobilization buffer containing 10% DMSO at a concentration of 5 mg/ml. The resulting mixture was injected immediately after dilution to afford a final concentration of 50  $\mu$ g/ml in immobilization buffer with 0.1% DMSO. Cysteine (70  $\mu$ L, 100 mM in 10 mM NaOAc, pH 5.0) was injected to eliminate free, unreacted maleimide groups. The change in RU corresponding to A $\beta$  immobilization was 1350. The surface was washed with regeneration buffer in short pulses to remove non-covalently associated peptide (5  $\mu$ l  $\times$  20), this gave a final response of 800 RU. The control lane was prepared as above and then blocked with an injection of cysteine after injection of sulfo-MBS.

*SPR of peptide analytes.* Peptide samples were prepared by dilution into running buffer after lyophilization. Each peptide was diluted at ten concentrations (3000, 2000, 1000, 700, 400, 300, 200, 100, 70, and 50  $\mu$ M) and injected in multichannel mode (40  $\mu$ L KINJECT, 5  $\mu$ L/min). The surface was then exposed to running buffer for 300 sec to observe dissociation. The chip surface was regenerated by injection of the regeneration buffer (10  $\mu$ L). The control lane data was subtracted from raw data obtained from the flow cell with

immobilized A $\beta$ . The response at equilibrium ( $R_{eq}$ ) was then plotted versus concentration (M) using the graphing program Sigma Plot.

### 1.8.2. Binding models.

For the compounds listed in Table 1.2, the isotherms did not reach a final plateau; thus, the data were fit to a standard binding curve with a fixed  $R_{max}$  value (eq. 1.1) (Attie and Raines, 1995; Frostell-Karlsson *et al.*, 2000; Karlsson and Stahlberg, 1995). Here,  $R$  is the response in RU,  $F$  is the concentration of free ligand, and  $K_d$  is the fitted dissociation constant.

$$R = \frac{R_{max} F}{K_d + F} \quad (1.1)$$

The  $R_{max}$  was calculated as the theoretical plateau determined from eq. 1.2, using the molar mass of each analyte ( $MW_A$ ), the molar mass of the immobilized ligand ( $MW_L$ ), and the RU of immobilized ligand ( $RU_L$ ).

$$R_{max} = \frac{MW_A}{MW_L} \times RU_L \quad (1.2)$$

This analysis is intended only to provide a relative assessment of binding; it does not yield absolute affinities. This fitting procedure afforded  $K_{rel}$  values, a nomenclature used to distinguish them from true affinities. To determine affinities for compounds listed in Tables 1.3-1.4, a non-specific binding term was added to equation 1.1 (Attie and Raines, 1995), and data were fit by linear regression to equation 1.3:

$$R = \frac{R_{max} F}{K_d + F} + K_{ns} F \quad (1.3)$$

For these analyses,  $R_{max}$ ,  $K_d$  and  $K_{ns}$  were left as independent variables. Alternatively, a model including an additional saturable binding site could be used to fit the data, as in equation 1.4:

$$R = \frac{R_{\max 1} F}{K_{d1} + F} + \frac{R_{\max 2} F}{K_{d2} + F} \quad (1.4)$$

*Prevention of A $\beta$  cellular toxicity in SH-SY5Y cells.* All cell culture medium, antibiotics and serum were purchased from Life Technologies (Gaithersburg, MD). All other chemicals were purchased from Sigma-Aldrich (St. Louis, MO) unless stated otherwise. A $\beta$ (1-40) was purchased from AnaSpec, Inc. (San Jose, California) and used without further purification. The identity and purity of the peptide were assessed by mass spectrometry and amino acid analysis. The amino acid sequence of the peptide is DAEFRHDSGYEVHHQKLVFFAEDVGSNKGAIIGLMVGGV. The reported molecular weight was 4331.3 and the reported purity was greater than 95.8%. Lyophilized A $\beta$  was stored at  $-70^{\circ}\text{C}$  until use. For toxicity experiments, lyophilized A $\beta$  was dissolved in pre-filtered 0.1% TFA at 10 mg/mL, then incubated 1 hour at  $37^{\circ}\text{C}$ . A $\beta$  stock solution was then diluted to 0.5 mg/mL (115  $\mu\text{M}$ ) with sterile-filtered phosphate-buffered saline (PBS) containing penicillin and streptomycin (PBS: 0.01 M  $\text{K}_2\text{HPO}_4$ /  $\text{KH}_2\text{PO}_4$ , 0.14 M NaCl, pH 7.4). The samples were allowed to aggregate at  $37^{\circ}\text{C}$  for 48 hours, and then diluted to 25  $\mu\text{M}$  with fresh media for plating. Human neuroblastoma (SH-SY5Y) cells obtained from ATCC (Rockville, MD) were used as model neurons. Cells were stored in liquid nitrogen and thawed in a  $37^{\circ}\text{C}$  water bath. Cells were cultured to confluence on poly-lysine coated T-flasks in medium containing 44% minimal essential medium (MEM) modified to contain 1.5 g/L

sodium bicarbonate, 44% Ham's modification of F-12 medium, 10% fetal bovine serum (FBS), 1% 3.6 mM L-glutamine, and 1% penicillin/streptomycin antibiotics (10,000 units/ml). Flasks were incubated in a humidified 37 °C incubator with 5% CO<sub>2</sub>. Cells were harvested using 0.4 mM EDTA and 0.05% trypsin, centrifuged at 750 G for 10 minutes, then resuspended in fresh medium, with mild aspiration used to break up clumps. Cells were counted using a haemocytometer (Hausser Scientific), and plated in 96-well poly-lysine coated plates with approximately 10,000 cells per 100 µL medium per well. Plates were incubated in a humidified 37 °C incubator, 5% CO<sub>2</sub> for 24 hours to allow cell attachment, then 80 µL of medium was removed and 80 µL of Aβ or control medium was added to cells. Plates were then incubated for an additional 24 hours at 37 °C. Cell viability was assessed using an MTT (3-(4,5 dimethylthiazol-2-yl)-2,5 diphenyltetrazolium bromide) toxicity assay with 20 µL of 2.5 mg/mL MTT in medium per well (Shearman, 1999). After MTT addition, plates were incubated at 37 °C for 4 hours then formazan crystals, produced by healthy mitochondria, were dissolved in 100 µL of 50% DMF, 20% SDS (pH 4.7) at 37 °C 8 to 12 hours. Absorbance at 570 nm was detected with a microplate reader (Bio-Tek Instruments, Winooski, VT) using background subtraction. Cell viability percentages, %*V*, were calculated as follows:

$$\%V = \frac{S - B}{C - B} \quad (1.5)$$

where *S* is the sample absorbance, *C* is the buffer control absorbance, and *B* is the background absorbance. Sample, background and control absorbances were averaged over 7

replicates. Background samples contained cell culture medium, unreduced MTT, and the SDS/DMF solution.

*Prevention of Ab cellular Toxicity in PC12 cells.* All cell culture reagents were obtained from GIBCO BRL. Amyloid samples were aggregated following the above procedure. Phosphate Buffered Saline (PBS) was prepared as 7.5 mM  $\text{Na}_2\text{HPO}_4 \cdot 7\text{H}_2\text{O}$ , 2.5 mM  $\text{NaH}_2\text{PO}_4$ , 140 mM NaCl, 100 units/mL Streptomycin/Penicillin, pH 7.4 and the solution was sterile filtered. Amyloid peptide ( $\text{A}\beta(1 \rightarrow 40)$ ) was obtained from Biosource International/QCB (Camarillo, CA) as a lyophilized powder. The peptide was dissolved in ddH<sub>2</sub>O with 0.1% TFA at 10 mg/mL. The peptide solution was immediately diluted into PBS buffer (with or without inhibitors present) to a final concentration of 125  $\mu\text{M}$  in epindorf tubes. Inhibitor concentrations were typically equimolar with  $\text{A}\beta$ , or at lower concentrations as indicated. The samples are then sealed with parafilm and incubated for 48 h at 37 °C.

Aggregated samples were cooled to room temperature and then diluted 5:1 using RPMI 1640 culture media and vortexed immediately before use. Culture media for PC12 cells was prepared as 84% RPMI 1640 containing L-glutamine and phenol red, 10% heat inactivated horse serum (HIHS), heat inactivated fetal bovine serum (FBS), 1% penicillin/streptomycin (10,000 units/mL).

PC12 cells (below pass 10) were harvested from confluent culture by treatment with Trypsin/EDTA (0.025 % trypsin) solution for 2-5 min. Trypsin was quenched by addition of fresh media. Cells were then centrifuged at 2100 rpm for 10 minutes. The solution was aspirated and cells were resuspended in fresh media and vortexed to achieve a monodisperse sample. An aliquot of the solution was then diluted 2:1 with trypan blue (4 %) and counted by

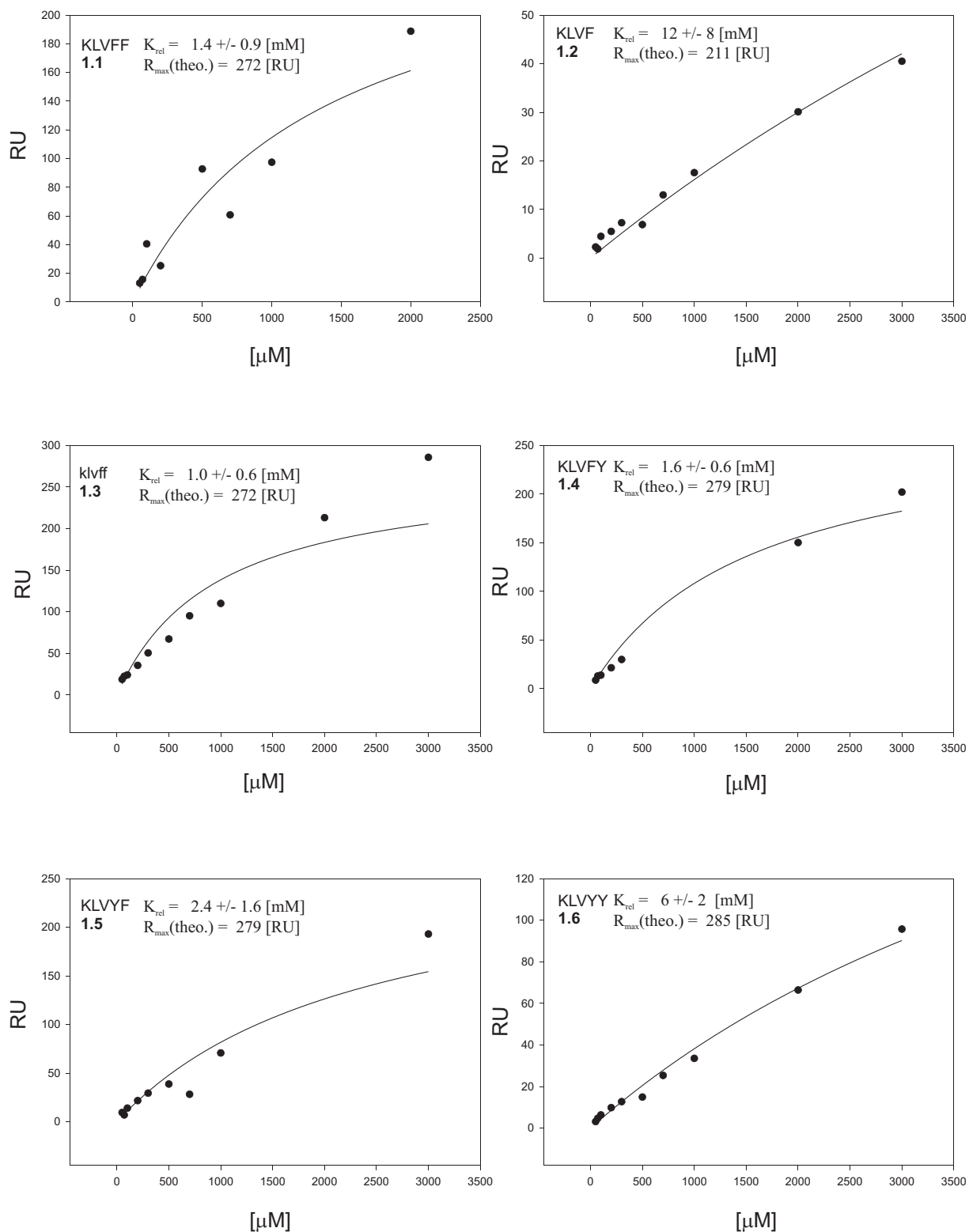


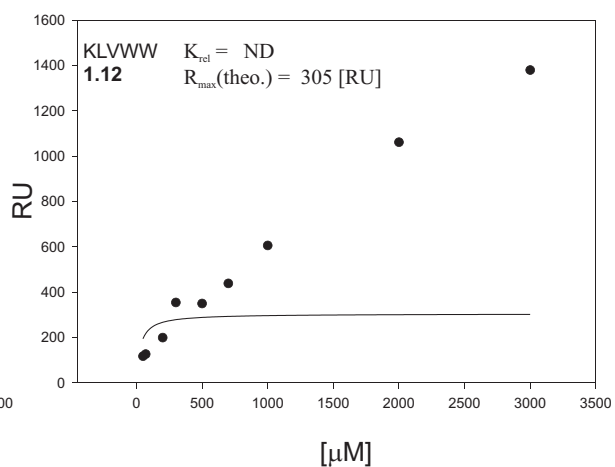
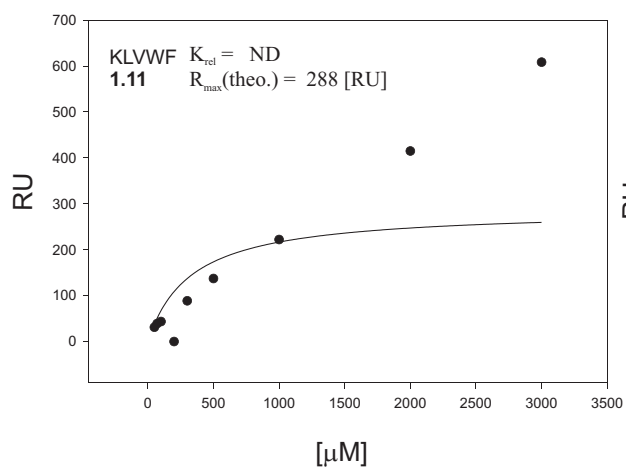
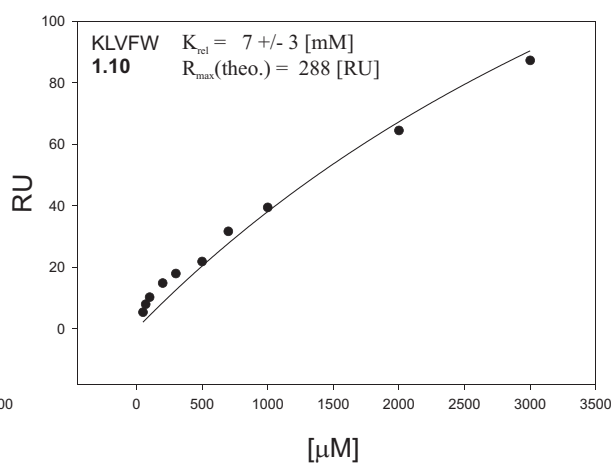
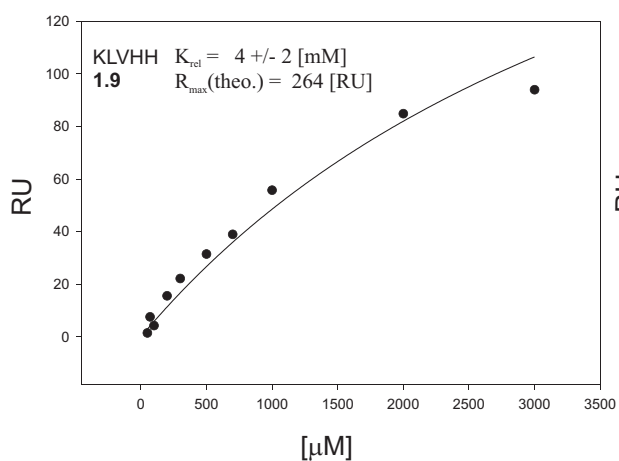
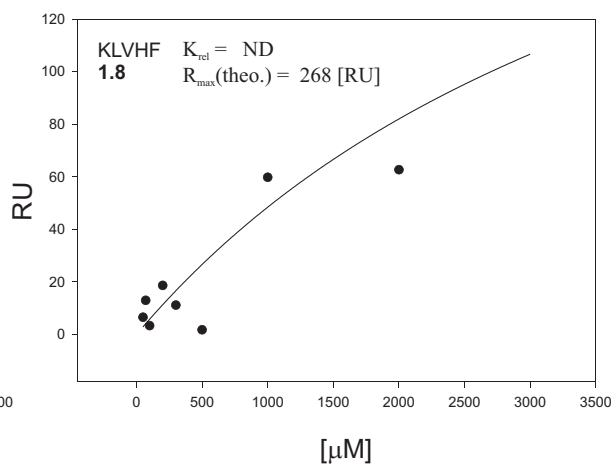
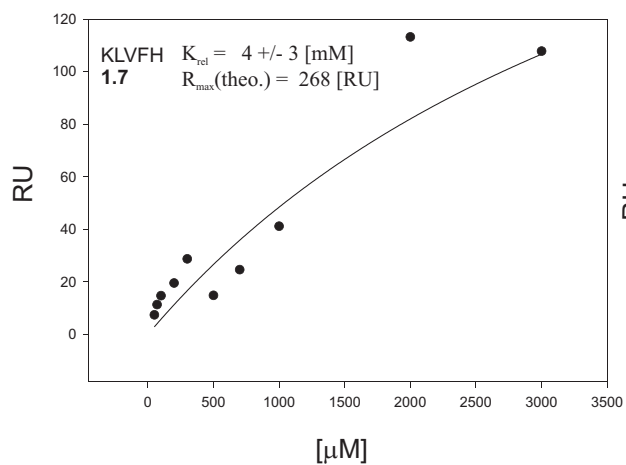
haemocytometer. Cells were then plated to a sterile 96 well plate at 15,000 cells/well in 100  $\mu$ L of fresh media. The plate was incubated for 24 h at 37 °C to allow cells to attach. The media was removed and amyloid samples were added to the plate. Samples were run with 5-7 replicates each. Control samples contained vehicle diluted into media. A background control was provided by co-addition of lysis buffer and MTT to untreated wells. Samples were incubated for another 24 h at 37 °C, at the end of the incubation 10  $\mu$ L of a fresh solution of MTT (5mg/ml) was added to each well. The plate was incubated for another 6 h, at the end of which 100  $\mu$ L of lysis buffer was added to all wells (except background control). Lysis buffer was prepared as 10 g sodium dodecyl sulfate (SDS), 15 mL H<sub>2</sub>O, and 25 mL dimethyl formamide (DMF) adjusted to pH 4.7. The plate was then incubated at 37 °C for 12 h, and then read at 570 nm. Cell viability was calculated as described above.

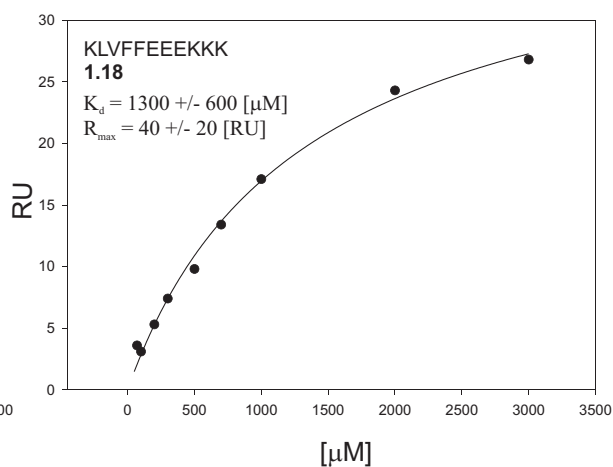
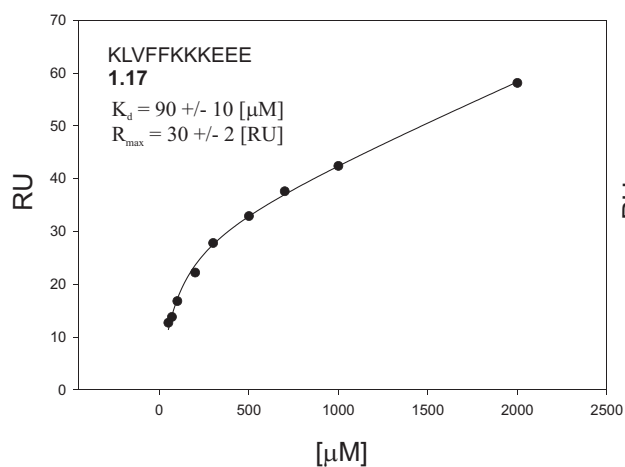
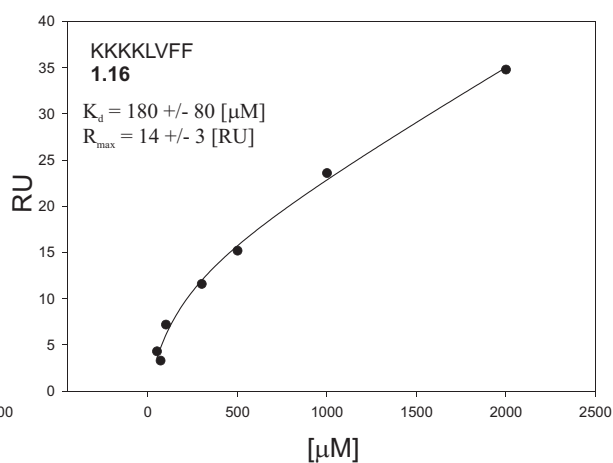
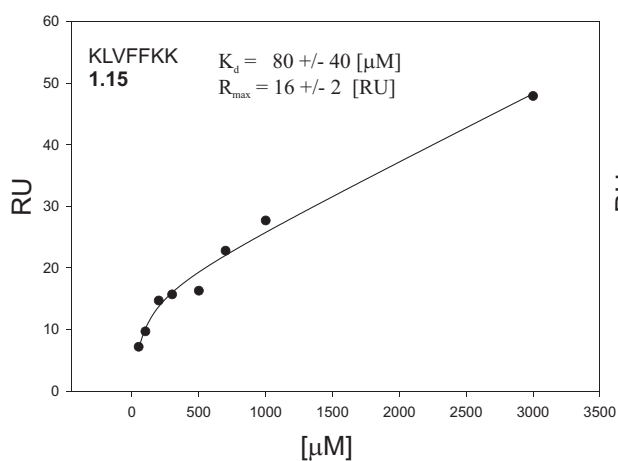
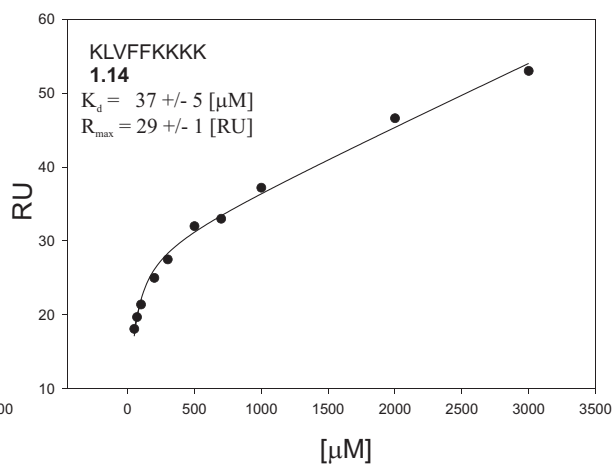
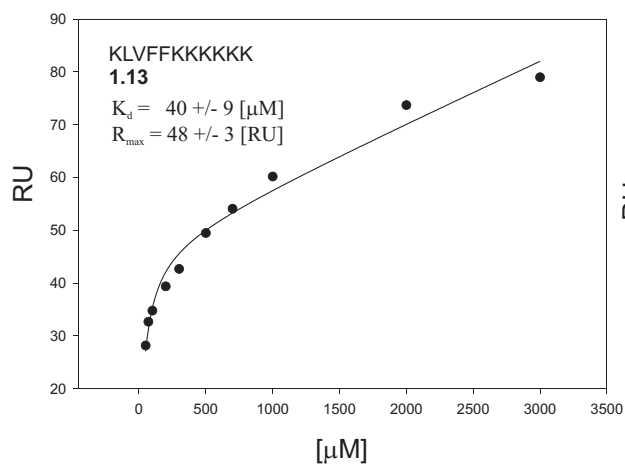
*Reversal of A $\beta$  cellular toxicity in PC12 cells.* Amyloid samples were aggregated as above for 48 h at 37 °C in PBS buffer. Samples were then incubated for an additional 48 h period at 37 °C in sealed epindorf tubes. As indicated, equimolar concentrations of peptide inhibitors were added to the incubating samples at 24 or 48 h prior to the end of the 4 d incubation. Therefore, samples marked 24 h were co-incubated with inhibitor for only 24 h prior to the end of this period, and samples marked 48 h were co-incubated for 48 h prior to the end of this period.

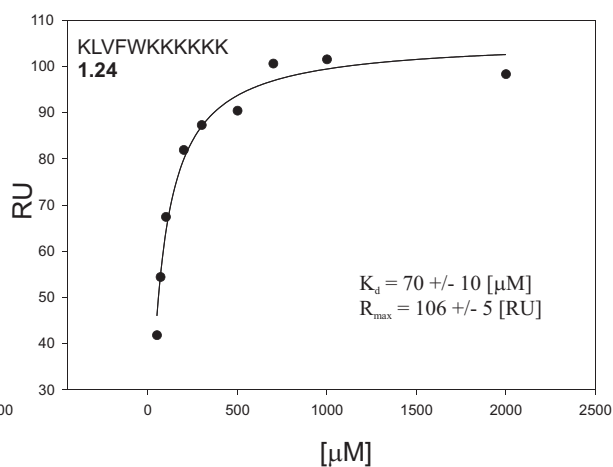
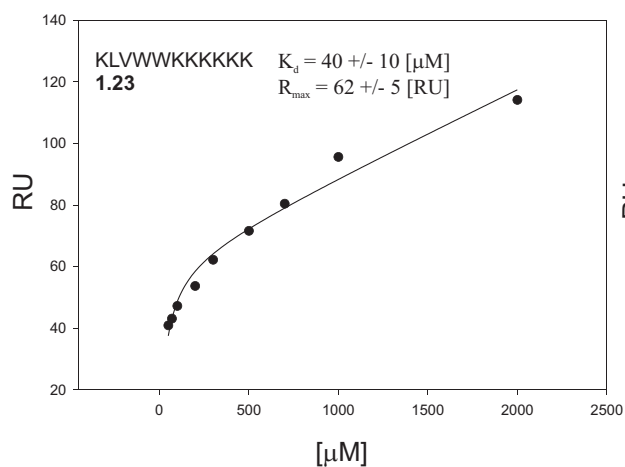
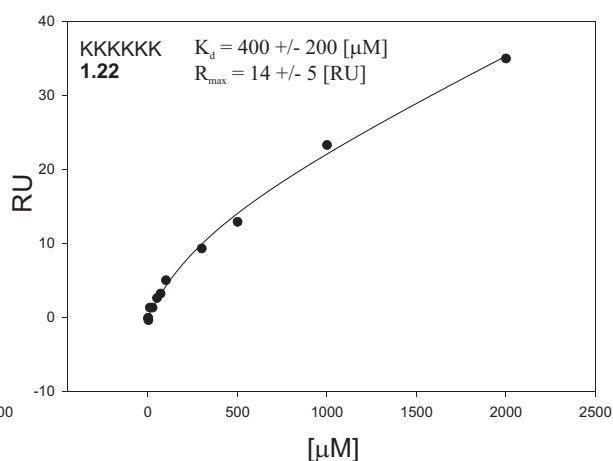
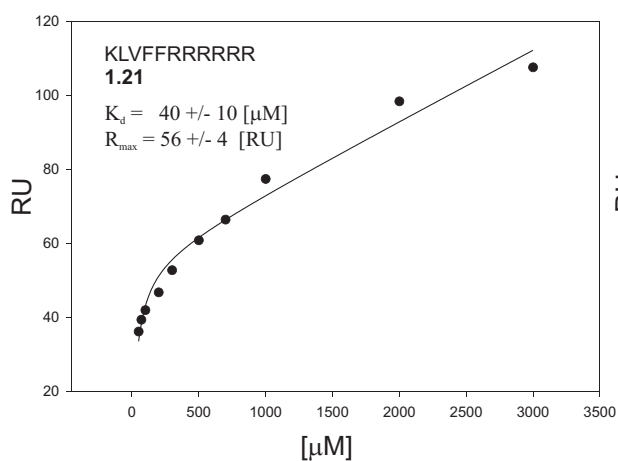
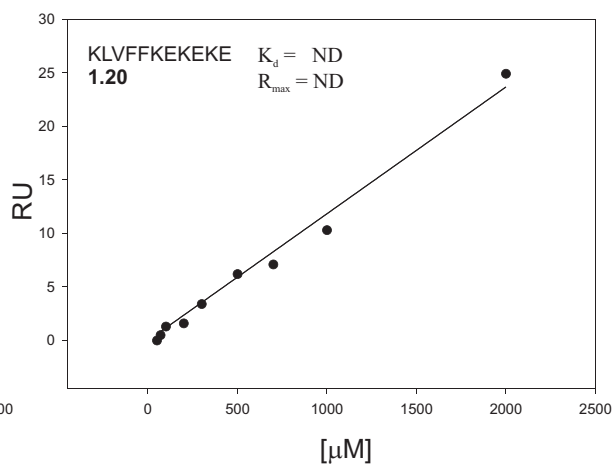
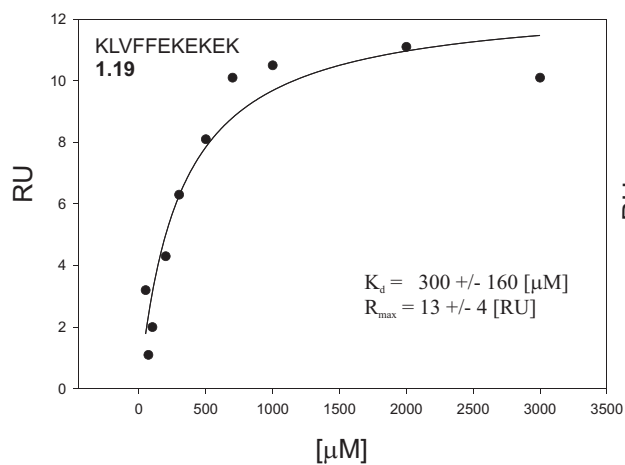
At the end of the 96 h incubation, samples and A $\beta$  controls were diluted 5:1 into fresh RPMI media, and added to wells containing 10,000 PC12 cells/well as described above. Samples were incubated with the cells for 24 h, and cell viability was determined by addition of MTT identical to the above procedure.

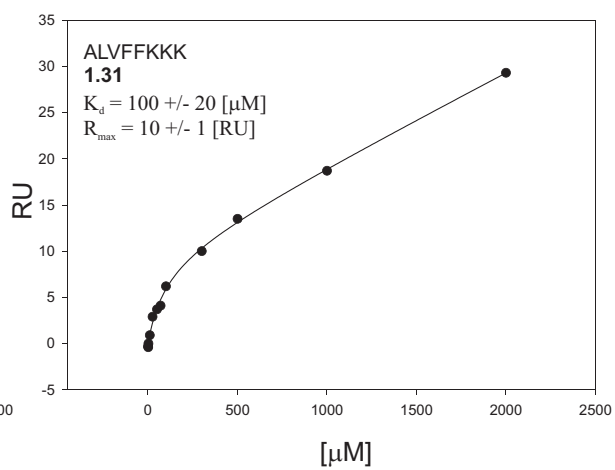
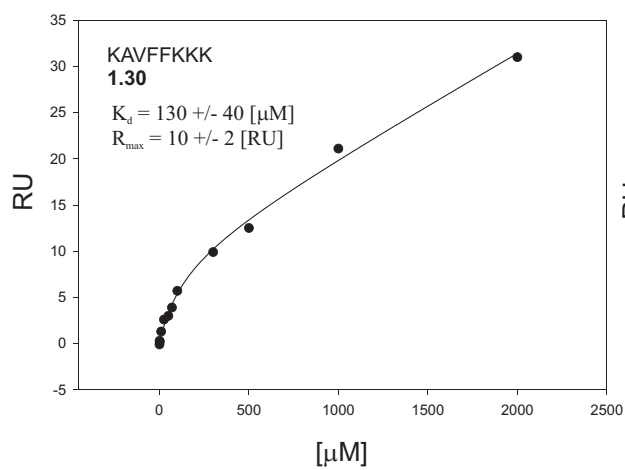
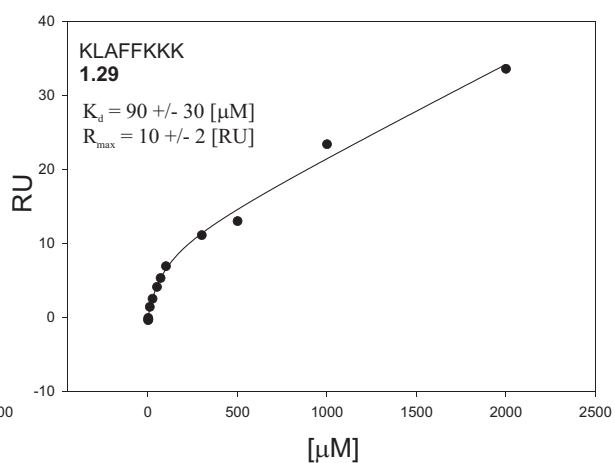
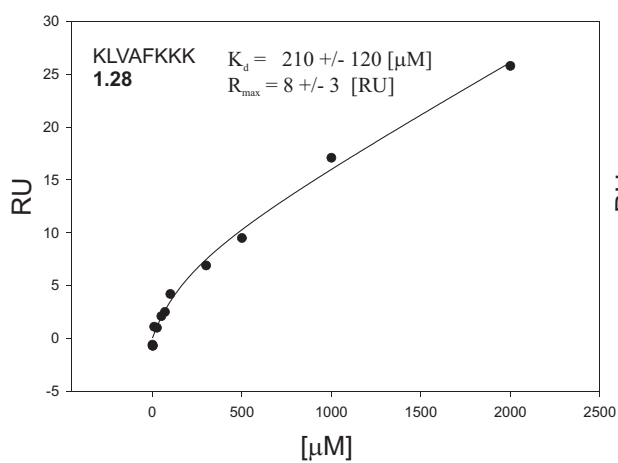
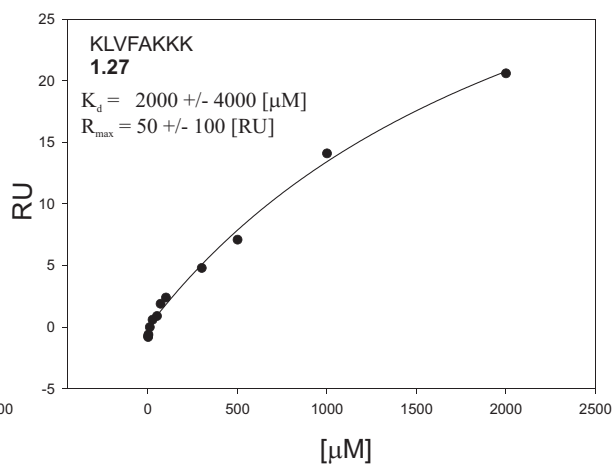
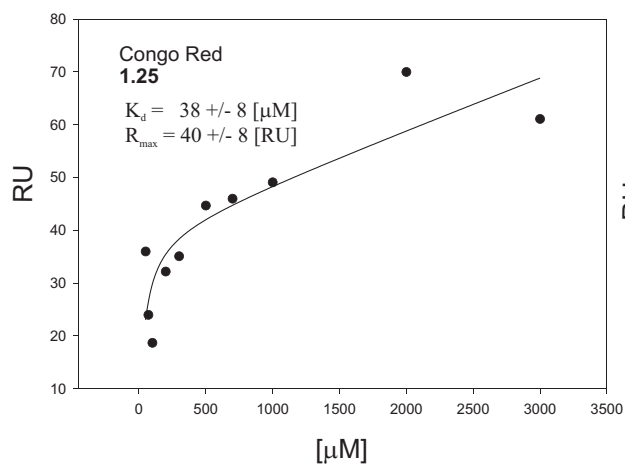
### 1.8.3. Raw binding data for SPR binding experiments.

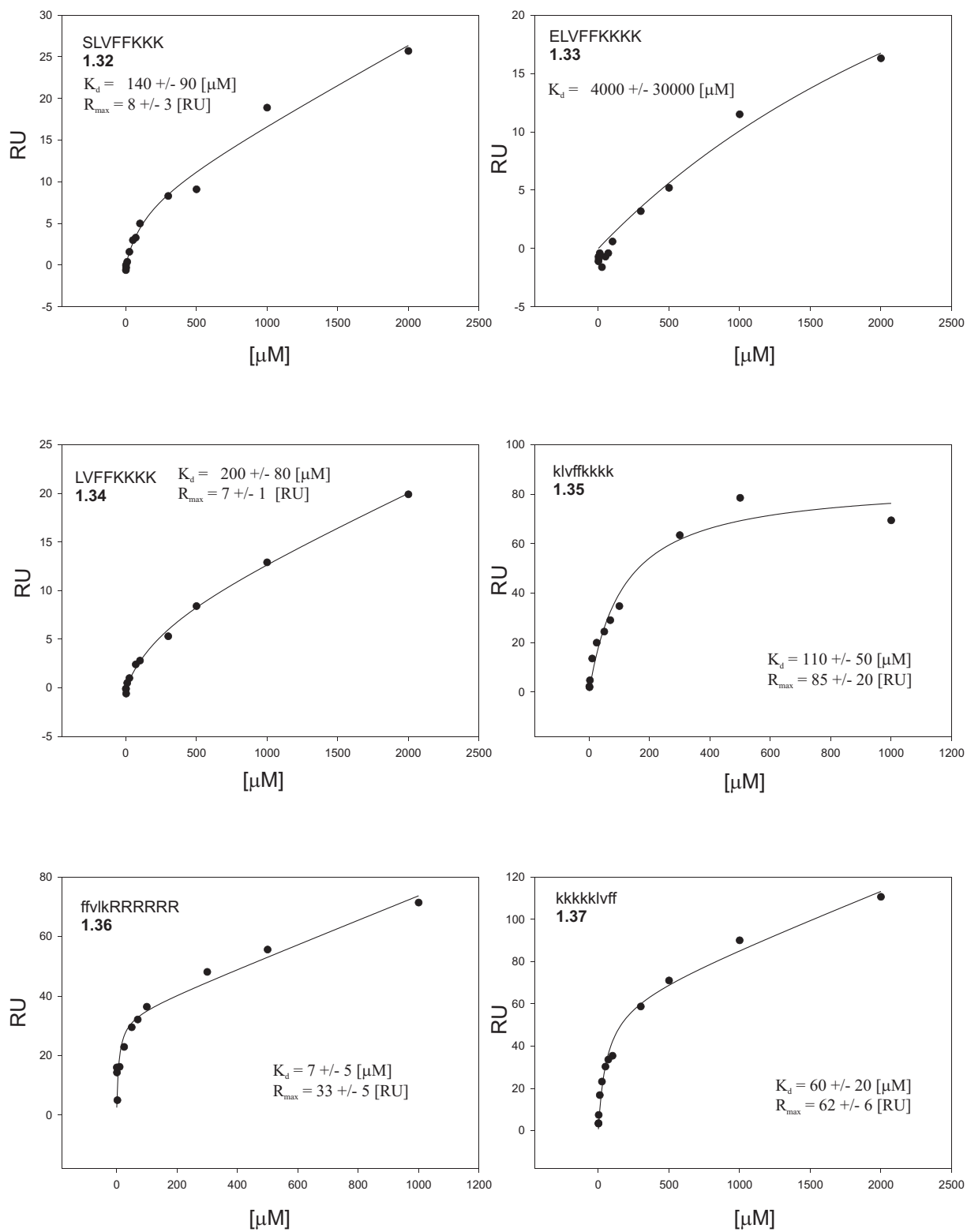


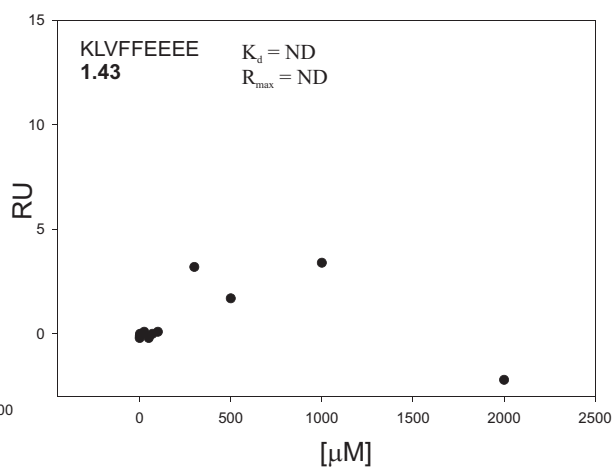
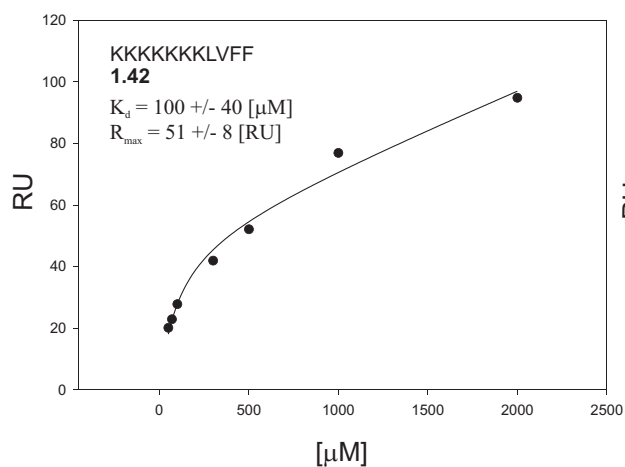
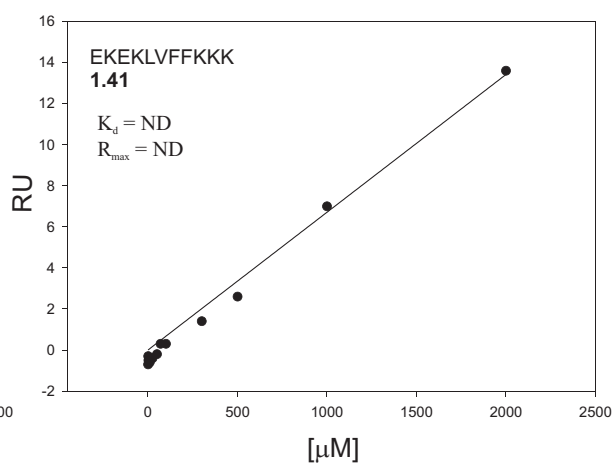
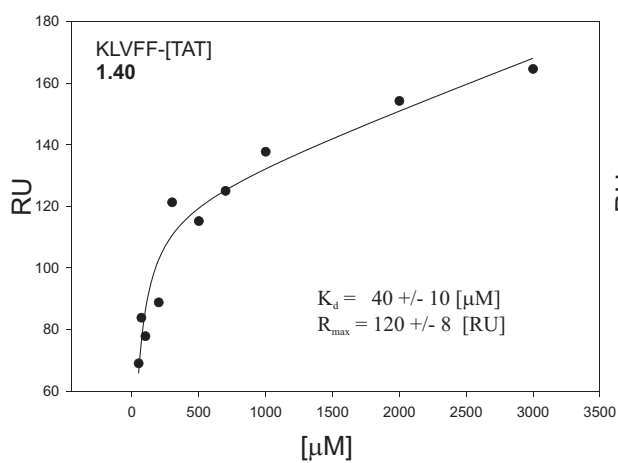
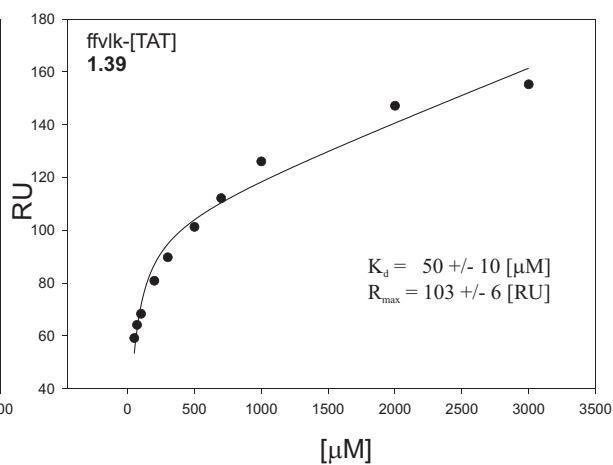
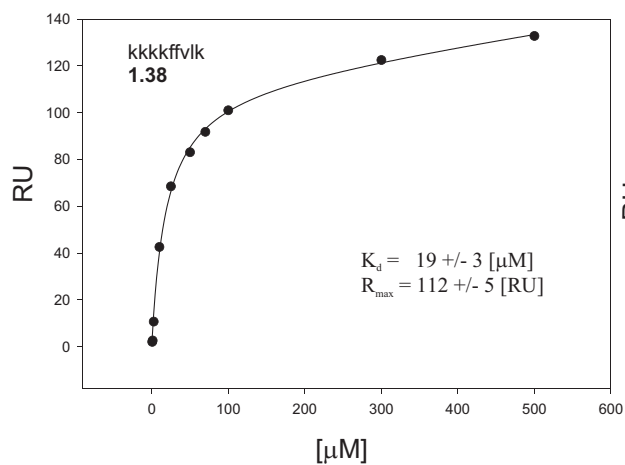




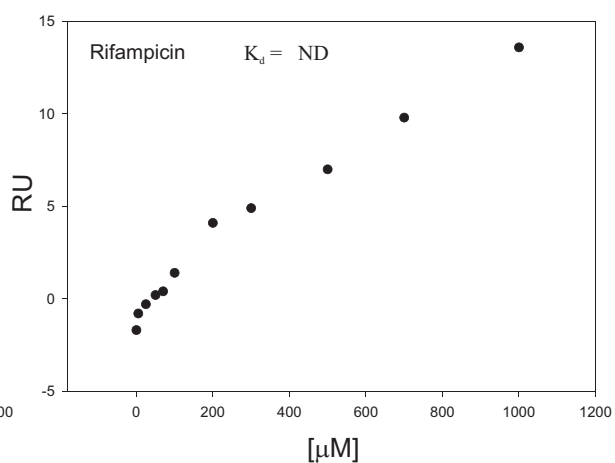
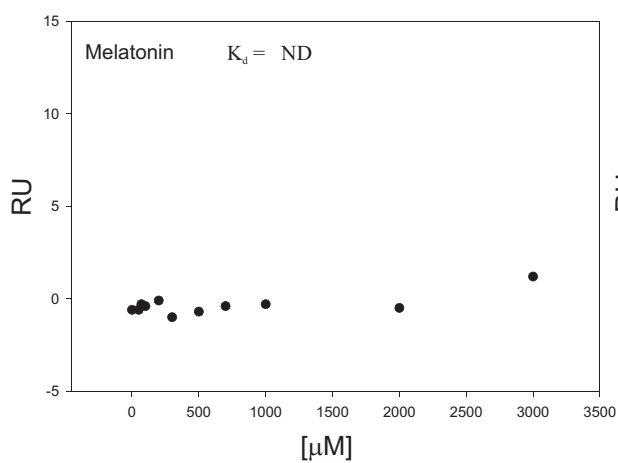
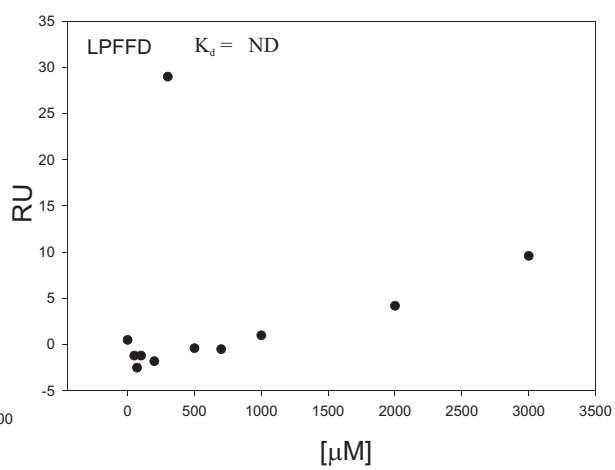
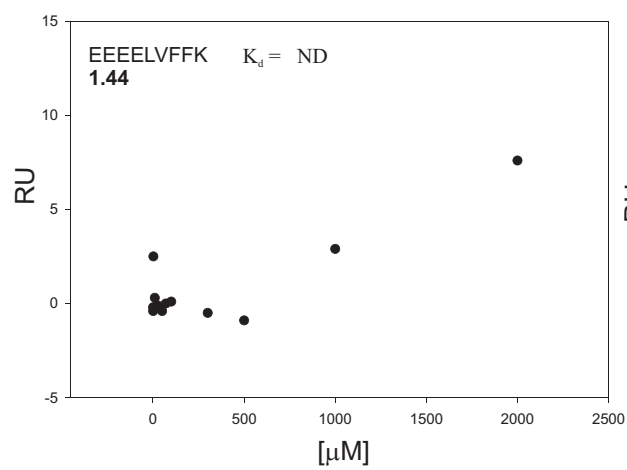












## Chapter 2. Structure Based Design of Multivalent Ligands

## **2.1. Abstract.**

In this chapter, general structural considerations for the design of multivalent ligands are discussed. Multivalent ligands present unique design problems for the macromolecular chemist. In contrast to monovalent ligand design in which the molecular complementarity of a small molecule must be optimized for its protein binding site, multivalent ligands must accommodate the topography of multiple binding sites. Binding sites may be located on the same oligomeric protein, or on entirely separate proteins. Therefore, multivalent ligand designs must take into account the spatial arrangement of the target binding sites. Although examples of successful multivalent ligand design are found in the literature, principles for multivalent ligands design are not as well appreciated. We summarize here diverse examples of multivalent carbohydrate ligands that have been used to target two commonly studied multivalent proteins: the tetrameric plant lectin, concanavalin A (Con A), and the family of pentameric AB<sub>5</sub> bacterial toxins. Our summary contrasts the activity of general ligand structures for these two disparate multivalent protein structures. General guidelines in the design of multivalent ligands can be drawn. Finally, we suggest general methods for more effectively determining guidelines in multivalent ligand design targeted at specific protein structures.

### 2.2.1. Mechanisms of multivalent binding.

The design of synthetic molecules for use in biological systems generally focuses on binding to, or inhibiting the binding of a native ligand. This is a powerful approach and the generation of small molecule ligands has become a well-developed process that has resulted in unprecedented advances in clinical therapies. Multivalent ligands have been recognized as some of the most potent synthetic inhibitors known (Fan *et al.*, 2000a; Kiessling and Pohl, 1996; Mammen *et al.*, 1998a). The design of multivalent ligands as effective inhibitors is an emerging field that requires empirical optimization of ligand design (Kiessling *et al.*, 2000b). We propose that the topographic features of multivalent ligands can be optimized for a desired activity. Here, we discuss examples of multivalent ligands that have been developed for two different receptors, the plant lectin concanavalin A (Con A) and the class of AB<sub>5</sub> bacterial toxins. These two examples demonstrate not only the importance of optimal ligand design but also the essential consideration of the mechanism of ligand activity.

Although multivalent ligands are potent inhibitors of binding, these ligands also can participate in more complex biological processes. A common mechanism for signal transduction is the non-covalent association of cell surface receptors into clusters (Heldin, 1995; Klemm *et al.*, 1998). Multivalent ligands are unique in their ability to control the association of multiple receptors, providing tools that are able to form complexes ranging from dimers to infinite lattices (Olsen *et al.*, 1997). Promoting receptor clustering using multivalent ligands is rapidly emerging as a method to deconvolute signal transduction pathways (Gestwicki and Kiessling, 2002; Sacchettini *et al.*, 2001). Due to this unique activity of multivalent ligands, it has been proposed that multivalent ligands able to engage in receptor clustering events can act not only as *inhibitors* but also as *effectors* (Kiessling *et al.*,

2000a). Two primary challenges remain for effective implementation of this strategy – the synthesis of new ligands with optimum activity and the development of assays capable of differentiating between the available binding modes for these ligands. Only with a mechanistic basis for measured activity will it be possible to associate ligand structure with observed potency.

Multivalent binding interactions are inherently complex due to the multiple binding modes available. Several distinct binding modes have been proposed for these events (Figure 2.1) (Kiessling, L. L. *et al.*, 2001; Kiessling and Pohl, 1996; Mammen *et al.*, 1998a). Each of these additional binding modes has the potential to enhance the functional affinity of multivalent ligands. To generate a ligand with particular biological properties, however, a single binding mode could be required. For example, a response due changes in the proximity of receptors at the cell surface would be triggered only by ligands able to cluster receptors well. Alternatively, inhibition of a natural ligand binding to an oligomeric receptor would be best mediated by ligands with high functional affinity (avidity). For this discussion, we define activity as the functional affinity, that is, the measured affinity, of a ligand. However, it is important to consider that mechanisms, such as receptor clustering, may have activity in a biological context that does not fit this definition. Examples of proposed binding modes for multivalent ligands are summarized below:

- 1) **Subsite binding.** Subsite binding is defined as ancilliary interactions at the same or a separate low affinity site. Branched oligosaccharides often interact with carbohydrate-binding proteins by this mechanism. The terminal residues of the oligosaccharide might interact at a separate site near the high affinity site providing enhancements in functional affinity (Quesenberry *et al.*, 1997).

- 2) **Local Concentration Effects.** Increased effective concentrations in intramolecular reactions are well known (Kiessling, L. L. *et al.*, 2001; Page and Jencks, 1971). By extension, it has been hypothesized that upon binding of a single epitope of a multivalent ligand, the receptor experiences an enhanced local concentration due to the enforced proximity of multiple un-bound epitopes.
- 3) **Chelate effect.** The chelate effect has been invoked to account for the increased inhibitory potency of multivalent ligands of sufficient size to span multiple binding sites on a single receptor. This mode of binding is believed to be favorable because only one translational entropic cost is paid (Jencks, 1981; Page and Jencks, 1971). This mechanism has been invoked for linear polymers and branched oligosaccharides (Lee and Lee, 2000; Mann *et al.*, 1998). This is clearly seen in the co-crystal structure reported by Bundle, Read and coworkers (Kitov *et al.*, 2000).
- 4) **Receptor Clustering.** The clustering of a receptor by a multivalent ligand is often invoked as a mechanism of enhanced potency. This mechanism has been invoked for small molecules, polymers, and dendrimers (Burke *et al.*, 2000; Cairo *et al.*, 2002; Corbell *et al.*, 2000). Clustering is often observed in co-crystal structures of lectins with branched oligosaccharides (Hester and Wright, 1996; Mandal and Brewer, 1992; Olsen *et al.*, 1997).
- 5) **Steric Stabilization.** Steric stabilization of a receptor is defined as the steric inhibition of access to unligated binding sites using a multivalent ligand (Mammen *et al.*, 1998a). For example, large polymer structures that bind only a few sites on a cell surface could effectively inhibit the binding of other ligands to unbound sites due to their steric bulk.

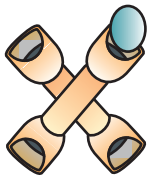
This mechanism has primarily been invoked in the inhibition of viral adhesion to cells using polyacrylamide polymers (Mammen *et al.*, 1995).

The array of binding modes available to multivalent interactions presents a unique problem for the study of these events (Lundquist and Toone, 2002). In a typical monovalent bimolecular binding event a single assay that relates to bound ligand can provide the fundamental descriptor of binding, the association constant ( $K_a$ ). The association constant then describes the free *versus* bound state of the ligand and receptor at any given concentration. In the case of multivalent ligands the situation is much more complex. For example, in a system where both clustering and chelate binding modes are active, a given measurement of bound ligand does not distinguish between ligand bound to a single receptor or to two separate receptors. Therefore, it is generally the case that no single parameter can describe the binding of a multivalent ligand in the presence of multiple binding modes. Any successful approach to the mechanistic study of multivalent interactions will depend on multiple assays that report on separate modes of binding, and/or the design of compounds that exclude particular binding modes. Comparisons of ligand activities in a single assay should be valid in systems where a single binding mode dominates.

Considering the diverse interactions that multivalent ligands engage in, it is no surprise that optimization of their activities is challenging. The synthesis of multivalent ligands for the inhibition of viral adhesion, lectin agglutination, inhibition of bacterial toxin binding, and the clustering of cell surface receptors has been described (Gestwicki and Kiessling, 2002; Kitov *et al.*, 2000; Lundquist and Toone, 2002; Mammen *et al.*, 1998a). From these studies, a diverse group of structures and multivalent ligand receptor interactions

have been investigated. Unfortunately, comparison of results from these studies is difficult. They are often conducted in disparate systems with unrelated assay methods. As a result, the accumulation of general structure-activity relationships is difficult. There is a definitive need for large-scale systematic studies of multivalent ligands to determine whether specific scaffolds have general properties. Using data from the literature, we analyze two systems that feature relatively uniform methods of activity determination and use similar receptor targets. From these examples, important structural considerations particular to each receptor can be ascertained.

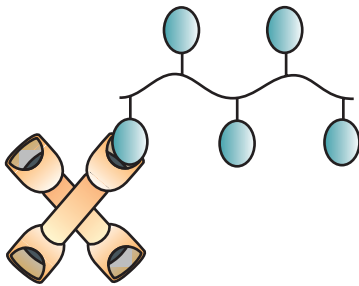
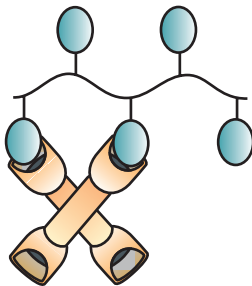




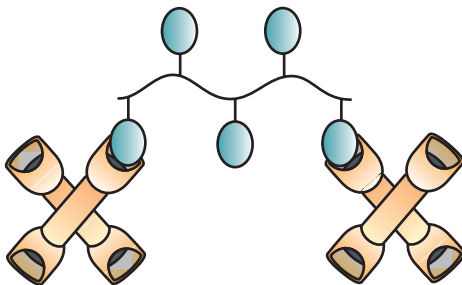
1) Monovalent Binding



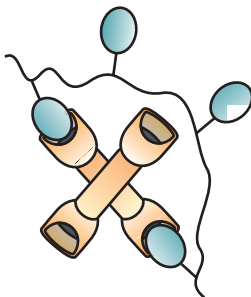
2) Subsite Binding

3) Local Concentration  
(Statistical Effect)

4) Chelate Binding



5) Crosslinking



6) Steric Stabilization

**Figure 2.1. Mechanisms of multivalent binding.**

The binding of multivalent ligands to multivalent receptors is inherently complex due to the diverse modes of binding available to these systems.

- 1) A monovalent ligand binds to only one site.
- 2) A multivalent ligand may make additional contacts within a single binding site, or at an ancilliary site. This binding mode is termed subsite binding.
- 3) A multivalent ligand engaged at a single site results in an increased local concentration due to the additional copies of the binding epitope.
- 4) A multivalent ligand of appropriate length can engage multiple sites on the same receptor complex; this mode of binding is termed the chelate effect.
- 5) A multivalent ligand can also engage multiple receptors, resulting in receptor clustering.
- 6) Multivalent ligands can also sterically block unbound sites on multivalent receptors, this binding mode is termed steric stabilization.

### 2.2.2. Variables to consider in multivalent ligand design.

Multivalent ligand design requires the consideration of a number of separate macromolecular parameters (Figure 2.3) (Kiessling *et al.*, 2000b). These parameters are distinct from the typical parameters required for monovalent ligand design (Figure 2.2). Although appropriate choice of a specific ligand is required for multivalent binding, the challenge of multivalent ligand design lies in the optimal presentation of multiple epitopes for the desired activity. The primary issues to be considered are the covalent attachment of the ligand to the polyvalent presentation (attachment point and linker composition), the number of active sites presented (valency and density of sites), and the nature of the polyvalent scaffold. We will refer to the collective description of these parameters as the ligand *architecture*. Few systematic studies of the influence of ligand architecture on ligand activity are known (Chapter 3). We expand on these individual parameters and provide some examples below:

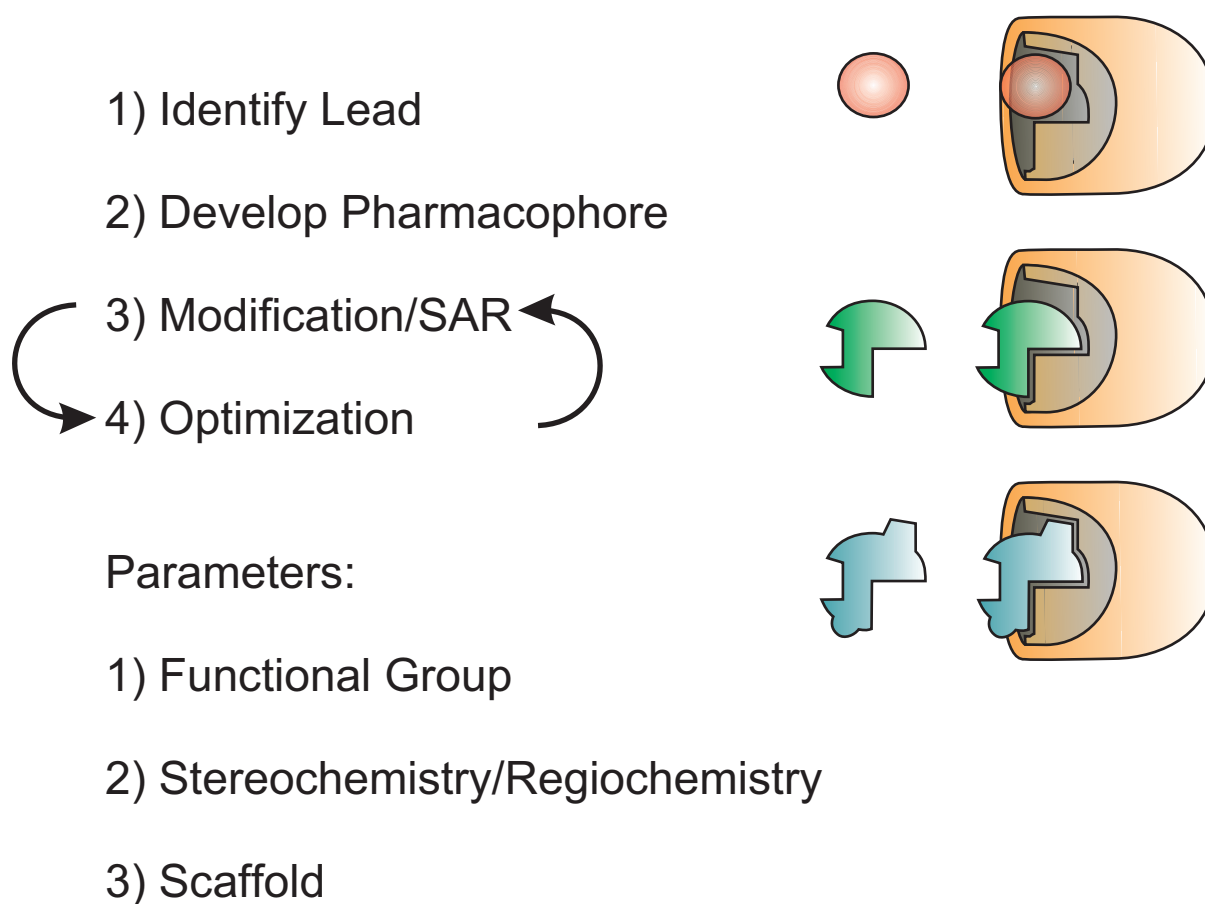
**Linker length.** Early work with dimeric compounds designed to inhibit influenza adhesion to cells provided some of the first experimental evidence for the influence of linker length on multivalent binding (Glick *et al.*, 1991). These studies found that dimers of appropriate length achieved enhanced inhibitory potencies by bridging multiple receptors, and optimal linker lengths were essential to this activity. Recent studies using large dendrimeric structures as inhibitors of AB<sub>5</sub> toxins optimized the appropriate linker lengths for binding multiple sites on the same protein surface and this variable was found to be critical to activity (Fan *et al.*, 2000b). Additionally, increased linker length may be required to provide access to deep binding clefts (Gestwicki *et al.*, 2001).

**Valency.** Many separate studies have found increases in ligand valency affect potency; systematic studies within ligand structural classes are available for dendrimers, linear polymers, and protein conjugates (Kanai *et al.*, 1997; Mammen *et al.*, 1998a; Page *et al.*, 1996b; Weigel *et al.*, 1979; Woller and Cloninger, 2001). This parameter is necessary and sufficient for the classification of a molecule as a multivalent ligand; however, its optimization is often overlooked. Each of the aforementioned studies has identified notable differences between ligands of different valencies, and these trends can be hard to predict.

**Density.** The density of sites on a multivalent ligand is defined here as the number of potentially active binding epitopes relative to inactive epitopes. Therefore, the density of binding epitopes on a multivalent ligand is essentially a measure of the spacing between sites. In systems with an invariant scaffold (*e.g.*, a globular protein) an increase in density is equivalent to an increase in valency. In scaffold structures that can change with valency (*e.g.*, a living polymer), an increase in density is distinct from an increase in valency. The effects of altered epitope density were first observed using glycosylated proteins (Ashwell and Morell, 1974; Weigel *et al.*, 1979). Recent efforts have examined these effects in linear polymers, and have found that epitope density is an important determinant of ligand potency (Cairo *et al.*, 2002; Mammen *et al.*, 1996).

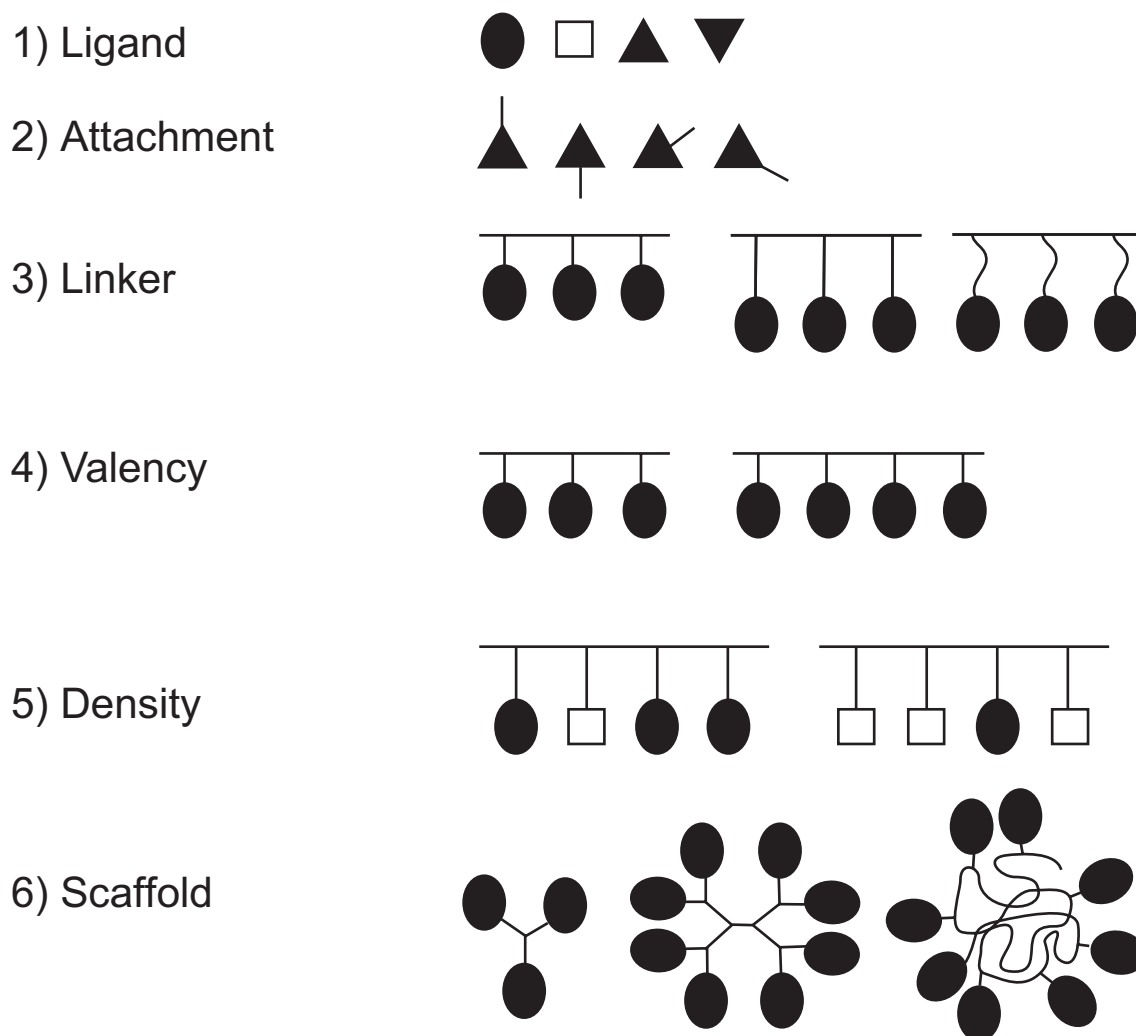
**Ligand Scaffold.** The three dimensional presentation of epitopes in a multivalent ligand can be critical for its activity. This effect can be seen in the range of activities observed for different multivalent structures, even when targeting similar receptors (Reuter *et al.*, 1999; Roy *et al.*, 1998; Yi *et al.*, 1998). Although there are very few systematic examples that measure these effects, it is clear that these parameters may be one of the most important considerations for activity. For example, the difference in activity between a linear polymer

and a dendrimer structure often is not compared within the same assay. Thus, information on whether different types of scaffolds are especially suited to a specific application is generally lacking. Still, some inroads into this problem are being made, and these are discussed in this chapter.



**Figure 2.2. Monovalent ligand design.**

General strategy and parameters used to optimize the activity of monovalent ligands. 1) A specific binding lead compound is first identified. 2) The identified lead is structurally modified in order to determine the essential components of the pharmacophore. 3) Modifications of the lead that improve binding are combined and (4) optimized to provide a tight binding inhibitor of the target. The general features of the ligand used for optimization of activity are the functional groups used, the stereochemistry and regiochemistry of their presentation and the scaffold on which the groups are presented.



**Figure 2.3. Multivalent ligand design.**

Multivalent ligand design requires the consideration of several parameters distinct from monovalent ligand design. 1) The selection of an appropriate specific ligand is a prerequisite for successful design. 2) The attachment of the ligand to the polyvalent scaffold requires chemical modification of the ligand at a site that does not disrupt binding. 3) The linker used to attach the ligand to the scaffold must accommodate binding and its composition, length, and flexibility should be considered. 4) The number of binding sites, or valency, of the ligand is a key determinant of ligand activity. 5) The density of binding sites on the ligand backbone can also influence ligand activity. 6) The presentation of binding sites on a particular scaffold can also be an important determinant of the activity of the ligand.

### **2.3.1. Multivalent ligand architecture influences activity**

Based on the number of variables able to influence multivalent ligand activity, multivalent ligand design is expected to be difficult. Moreover, the relationship between ligand structure and its activity is likely to be complex because different binding modes could occur simultaneously. Although there are currently no comprehensive studies of the broad effects of ligand structure on multivalent activity, there are examples of particular systems that have been intensively studied across multiple laboratories. Data from these systems can provide useful general observations. Empirical conclusions regarding the influence of ligand structure on multivalent binding can still be drawn.

In the following sections the activity of diverse multivalent ligand structures to interact with the tetrameric plant lectin Con A and the family of pentameric AB<sub>5</sub> bacterial toxins. For each set of examples, data comparing the activity between general classes of ligand structure will be discussed. Because the data are often collected using slightly different experimental configurations, caveats to data interpretation will be discussed. The activities of general ligand structures between different receptor classes have been analyzed. We find that optimal ligand activity can be associated with the general structural class of the ligand, and this may be due to the particular receptor and its natural mechanisms of activity.

### **2.3.2. Designed multivalent ligands for inhibition of Con A binding.**

The plant lectin, Con A, is often used as a model for multivalent lectins. Con A binds monovalent  $\alpha$ -mannosides with relatively weak affinity ( $\sim 0.1$  mM) and interacts with branched oligosaccharides with somewhat tighter affinity (2  $\mu$ M, trimannoside) (Williams *et*



*al.*, 1992). The lectin has four binding sites presented in a tetrahedral arrangement (Becker, J. W. *et al.*, 1976). The physiological activity of Con A is unknown; however, it is a potent agent for the clustering of cell surface glycoproteins and the agglutination of cells (Chapter 4). Because it is readily available and has been extensively characterized, Con A is often used as a model of multivalent receptor interactions.

The tetrahedral arrangement of Con A binding sites may be important for its ability to become clustered in the presence of multivalent ligands. This arrangement provides the lectin with the ability to form three-dimensional lattices when bound to multivalent ligands (Mandal and Brewer, 1992). The ability to form lattices may be a general property of lectins with this fold, as other lectins have been observed to form these types of lattices in the presence of divalent ligands (Hester and Wright, 1996). Interestingly, the packing of Con A lattices in the crystal depends on the ligand used, and thus it may provide a means for generating selectivity in binding (Hamelryck *et al.*, 2000; Mandal and Brewer, 1992; Olsen *et al.*, 1997). Although these interactions are likely different in solution, they suggest a mechanism for increasing specificity in the formation of homo-aggregates with multivalent lectins.

Several researchers have designed and tested multivalent ligands for binding to and inhibiting the activity of Con A (Kiessling and Pohl, 1996; Lundquist and Toone, 2002; Page *et al.*, 1996a; Woller and Cloninger, 2002). These examples may constitute the most comprehensive exploration of the structure-activity relationships for multivalent ligands with any single receptor class. A notable feature of these studies is that many use hemagglutination inhibition assays (HIA) to compare relative enhancements in activity. Although interpretation of data from this assay does have some inherent difficulties, the studies provide a uniform comparison of activity between ligands and across laboratories. The assay configuration used

measures the ability of a given multivalent ligand to inhibit the agglutination of cells by Con A. Potent inhibitors are effective at blocking Con A – glycan interactions, however, this activity could derive from multiple binding modes (*e.g.* receptor clustering, chelate effect, subsite binding, etc.)



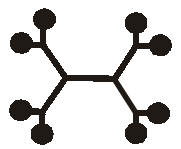
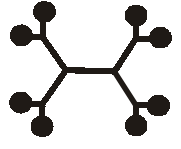
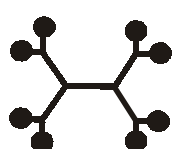


We have summarized the spectrum of multivalent ligand structures that have been used as ligands for Con A below (Table 2.1). Three general classes of scaffolds are represented: small molecules, dendrimers, and linear polymers. The majority of these examples have used HIA to compare activity, and these data are provided where appropriate. All activities presented are relative to that of monovalent mannose saccharides.

How do each of these structural classes fare as inhibitors of Con A activity? Small molecules, such as dimers, trimers and macrocycles, tend to have the smallest enhancements in activity (0.8 – 21 fold *per saccharide*). Dendrimers provide the largest range of activity within a single class – small dendrimers ( $n < 30$ ) show between 30-300 fold enhancements, while larger dendrimers can have as much as 660 fold enhancements. The most potent ligands for Con A in HIA are linear polymers, these ligands are able to provide as much as a 2000 fold enhancement of activity on a *per saccharide* basis. Competitive binding assays using SPR or enzyme linked lectin assays (ELLA) provide further qualitative confirmation of these conclusions.

Optimal design of multivalent ligands for inhibition of Con A in HIA likely rests on the ability of these ligands to effectively cluster the lectin and not the ligands functional affinity (Corbell *et al.*, 2000). The activity of Con A to stimulate T cells and to induce apoptosis derives from its ability to form homo-clusters of cell surface receptors, and therefore optimal ligands would provide ideal arrangement of the lectin for lattice-like

assembly (Anderson, J. *et al.*, 1976; Cribbs *et al.*, 1996). We propose that linear polymers derive their enhanced activity in HIA from efficient Con A lattice formation. Indeed, experiments that quantitate the stoichiometry of Con A – ligand complexes after precipitation have shown surprisingly high ratios compared to many other ligands (Cairo *et al.*, 2002; Gestwicki *et al.*, 2002b). Optimal ligands for lattice formation would be expected to perform well in HIA as they would more efficiently remove binding sites from solution; therefore, our analysis here may be skewed for this activity. However, our conclusions suggest that consideration of the native biological function of the target can be a valuable tool for guiding multivalent ligand design.

**Table 2.1. Multivalent ligands for Con A inhibition.**

<i>Reference</i>	<i>Structure</i>	<i>Valency (n)</i>	<i>Rel. Potency (per n)</i> <i>(Assay Used)<sup>a</sup></i>
(Burke <i>et al.</i> , 2000)	macrocycle 	3	30 (10) <b>(FRET)</b>
(Roy <i>et al.</i> , 1998)	dendrimer 	3 4	616 (205) 1200 (300) <b>(HIA)</b>
(Dimick <i>et al.</i> , 1999)	dendrimer 	3 4 8	2 (0.8) 124 (31) 104 (13) <b>(HIA)</b>
(Page and Roy, 1997)	PAMAM dendrimer 	2 3 4 8 16 32	24.3 (12.2) 62.9 (21.0) 75 (18.8) 224 (28.0) 301 (18.8) 402 (12.6) <b>(ELLA/yeast mannan)</b>
(Woller and Cloninger, 2002)	PAMAM dendrimer 	8 16 29 55 95 172	8 (1) 24 (1.5) 1 x 10 <sup>3</sup> (45) 2 x 10 <sup>4</sup> (275) 5 x 10 <sup>4</sup> (510) 1 x 10 <sup>5</sup> (660) <b>(HIA)</b>
(Mann <i>et al.</i> , 1998)	ROMP 	10 33 143	200 (20) 920 (28) 5 x 10 <sup>3</sup> (37) <b>(SPR)</b>
(Kanai <i>et al.</i> , 1997)	ROMP 	10 25 52 143	1 x 10 <sup>3</sup> (100) 1 x 10 <sup>4</sup> (400) 8 x 10 <sup>4</sup> (1500) 2 x 10 <sup>5</sup> (2000) <b>(HIA)</b>

a. The activity of multivalent ligands is given relative to mannose. The activity is also given on a per saccharide basis in parenthesis. The most similar assay results have been chosen for comparison, however experimental configurations may be different.

### 2.3.3. Designed multivalent ligands for inhibition of AB<sub>5</sub> toxins.

The family of carbohydrate binding AB<sub>5</sub> toxins have been the subject of intense research in the field of medicinal chemistry (Fan *et al.*, 2000a; Merritt and Hol, 1995). These structurally related bacterial toxins are produced by several notorious pathogens, best known among these are cholera and the shigella toxins. The AB<sub>5</sub> complex itself is the agent responsible for the deadly symptoms of these infections (Acheson, D. W. K. *et al.*, 2000; Alouf, J. E., 2000). The B subunits are required for specific binding of the toxin to target cells within the host. Upon binding at the surface of host cells the catalytically active A subunit is delivered into the cytoplasm where it then disrupts the cell by a variety of mechanisms (Falnes and Sandvig, 2000; Fan *et al.*, 2000a). The specificity of the toxin complex is imparted by the carbohydrate binding sites of the B subunits, which bind cell surface glycolipids, such as GM1. As a result of the millions of deaths caused by these pathogens every year, there is great interest in the development of inhibitors that target this class of carbohydrate-binding proteins (Crowcroft, 1994; Ivanoff and Robertson, 1997; Kotloff *et al.*, 1999).

Although a great deal of work has focused on the optimization of monovalent inhibitors for B subunit binding, these studies have met with extremely limited success (Fan *et al.*, 2000a). Even the best of these is of equal potency to the native oligosaccharide, and many are thousands of times weaker (Bernardi *et al.*, 1999; Minke *et al.*, 1999b; Minke *et al.*, 1999a). In recent years however, several groups have hypothesized that multivalent ligands could provide exceptionally active inhibitors of these interactions. To this end, researchers have synthesized multiple classes of ligand structures, designed to block different specific toxins. The carbohydrate-binding specificities of each toxin is different, and some of these

complexes are proposed to bind to more than five carbohydrate epitopes simultaneously (Ling *et al.*, 1998). These factors all complicate the direct comparison of activity between receptor and ligand structural features. For our analysis we have tabulated the measured inhibitory potencies of these ligands. The method used to determine their activity as well as the toxin used are also tabulated (Table 2.2). All data are shown relative to the corresponding monovalent epitope to allow for comparisons between structures.








Our survey reveals different structural trends for multivalent ligands that bind to AB<sub>5</sub> toxins than those that bind Con A. Small molecules (dimers and small dendrimers,  $n = 2-8$ ) provide limited enhancements of inhibition. In fact some small dendrimers are unable to provide any enhancement when compared on a per saccharide basis to their monovalent counterpart. Linear polymers can provide impressive enhancements of inhibitory potency as shown by Gargano *et al.* in their studies of SLT-1. By far, the greatest enhancements observed were found using large dendrimeric structures designed specifically to complement the binding sites of the B subunits within the toxin complex. The enhancements observed for these ligands were as high as  $5 \times 10^5$  on a per saccharide basis.

The two most active inhibitors for AB<sub>5</sub> toxins found to date are dendrimers that are both extremely similar in design and structure. Additionally, both of these ligands demonstrate similar enhancements in activity, even though specific features of their design are different. Both groups used previously known crystal structure data to determine the optimal presentation of carbohydrates (Ling *et al.*, 1998). In addition, Fan *et al.* optimized the linker lengths used for presentation of the sugar epitopes and found that this feature was vital to ligand activity. It is very likely that the ability of these ligands to mimic the surface

presentation of glycolipids is responsible for their impressive gains activity, and these two studies provide an outstanding example of successful rational design.

The mechanism of binding for large dendrimer structures to AB<sub>5</sub> toxins cannot be inferred from inhibition experiments; however, structural insights have been provided by Kitov *et al.* The crystal structure data obtained provides an indication of the potential mechanisms (Figure 2.4) (Kitov *et al.*, 2000). The determined structure of the pentavalent ligand bound to SLT-1 shows the presence of two binding modes simultaneously. Although originally designed to bind a single AB<sub>5</sub> complex at 10 sites by chelation, the crystal structure shows the ligand binding to 5 sites on two separate AB<sub>5</sub> complexes using both chelated and crosslinked binding modes (Figure 2.4). Although these data are not necessarily indicative of the solution binding mode of the ligand, they provide a clear demonstration of the complexity of multivalent binding events.

**Table 2.2. Multivalent ligands for AB<sub>5</sub> toxins.**

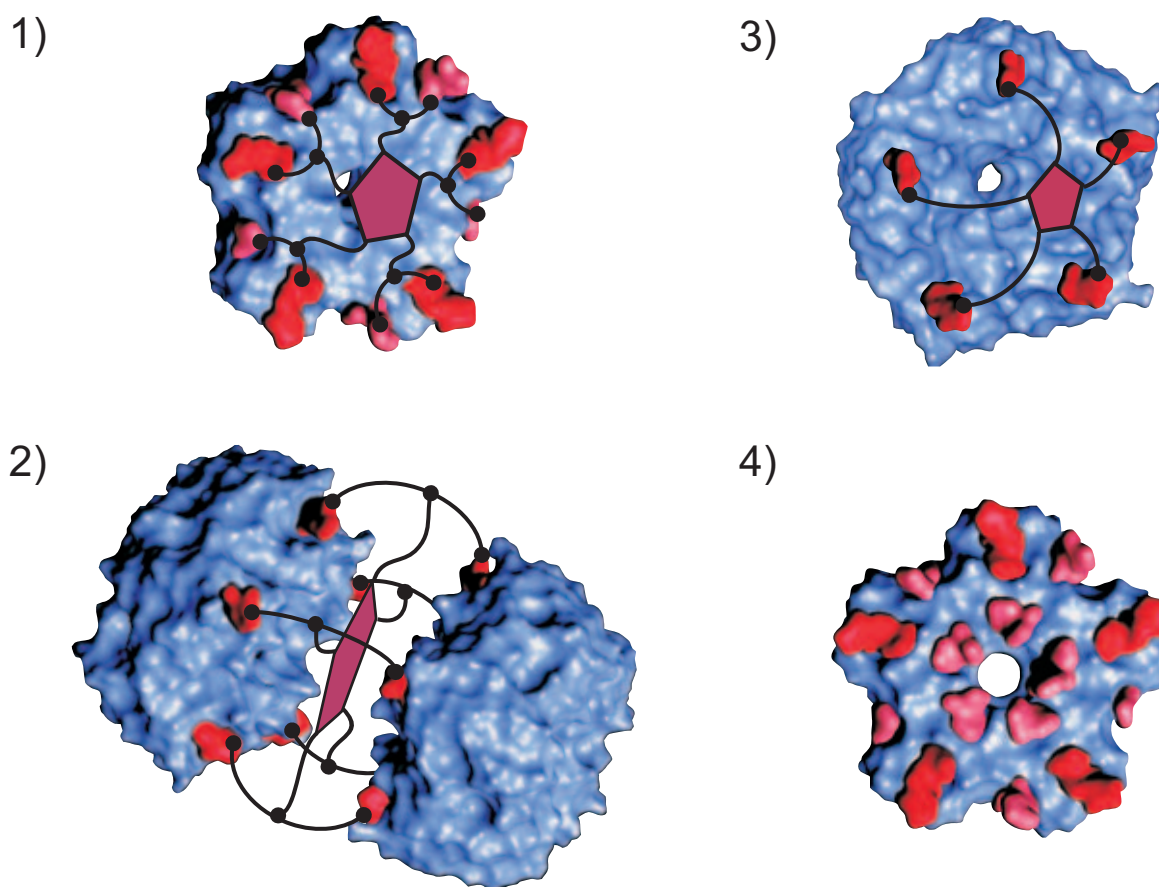
<i>Reference</i>	<i>Structure</i>	<i>Valency (n)<sup>a</sup></i>	<i>Rel. Potency (per n) (Target/Assay Used)<sup>b, c</sup></i>
(Lundquist <i>et al.</i> , 2000)	dimer peptide 	2	75 (38) (SLT-1/ELISA)
(Thompson and Schengrund, 1997)	dendrimer 	4	10 (2.5) (HLT/ <sup>125</sup> I binding)
(Vrasidas <i>et al.</i> , 2001)	dendrimer 	2 4 8	77 (38) 182 (46) 545 (68) (CLT/Fluorescence titration)
(Fan <i>et al.</i> , 2000b)	dendrimer 	5	1 x 10 <sup>5</sup> (2 x 10 <sup>4</sup> ) (HLT/ELISA)
(Kitov <i>et al.</i> , 2000)	dendrimer 	2 10	40 (20) 5 x 10 <sup>6</sup> (5 x 10 <sup>5</sup> ) (SLT-1/ELISA)
(Dohi <i>et al.</i> , 2002)	polyacrylamide 	~800 ( $\chi=0.2$ )	25 (0.03) (SLT-1/HIA)
(Gargano <i>et al.</i> , 2001)	polyacrylamide 	NR	5 x 10 <sup>3</sup> (NR) (SLT-1/cell toxicity)

a. Valency is given where applicable (NR = not reported). Compounds with site density other than 100% are noted by  $\chi$  values.

b. The activity of multivalent ligands is given relative to the corresponding monovalent saccharide. The activity is also given on a per saccharide basis in parenthesis. The most similar assay results have been chosen for comparison, however experimental configurations may be different.

c. Abbreviations used for AB<sub>5</sub> ligands: CLT (cholera toxin), HLT (heat-labile enterotoxin), SLT (shiga-like toxin).





**Figure 2.4. Binding modes of STARFISH ligands for SLT-1.**

Schematic of multivalent binding modes possible for binding to verotoxin homopentamers. 1) Initially proposed binding mode for STARFISH ligands. 2) Observed binding mode of STARFISH ligand found by X-ray crystallography. (Kitov *et al.*, 2000) 3) Proposed binding mode for HLT ligands. 4) Face-on view of SLT-1 showing monovalent ligands bound at Site 1 (light red), Site 2 (dark red), Site 3 (light red, center).

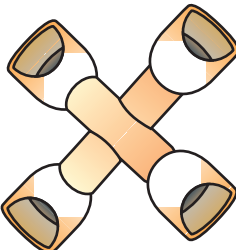
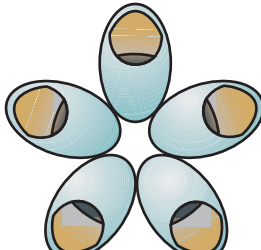

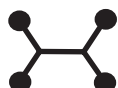



Our survey of Con A and AB<sub>5</sub> ligand structure-activity indicates that distinct ligand architectures are optimum for each receptor class (Figure 2.5). In the case of Con A, we propose that ligands able to form efficient clusters of the lectin are the most active. Optimal ligands for the tetrameric Con A tend to be dendrimers and linear polymers. Inhibitors of AB<sub>5</sub> toxin binding are optimal when they effectively mimic the cell-surface presentation of glycolipids. Inhibition of binding is most efficient in the case of structures that are able to span the face of the toxin binding sites. Both long polymers and dendrimers with long linkers are able to accommodate these features and are the most potent inhibitors. Although these structural requirements could be predicted upon consideration of the function of each receptor, such a general principle has not been established in the literature. The juxtaposition of multivalent ligand activity with receptor structure provides a general conclusion regarding multivalent ligand activity: Macromolecular complementarity is essential for optimum activity – a multivalent ligand must accommodate the spatial presentation of receptor binding sites. In light of multiple ligand structure-activity studies we can determine which structural parameters are required in particular cases. Additionally, the deconvolution of the mechanisms of binding responsible for activity would assist our analysis and might also identify common structural features that result in particular binding modes.

#### **2.4.1. Conclusions.**

We have surveyed the relative potencies of multivalent ligands directed at the inhibition of the plant lectin Con A and the family of AB<sub>5</sub> toxins. We find in this survey that individual receptor architectures require specific multivalent ligand structures for optimal activity. Importantly, we observe that in these two cases the optimal structural class of

multivalent ligands is different. Therefore, the determination of optimal ligand design is certain to benefit from systematic approaches to multivalent ligand design that explore multiple ligand architectures for any given receptor.

The rational design of synthetic multivalent ligands is currently in an early stage of development. In contrast to the well-established methodology available to the medicinal chemist, the macromolecular chemist often designs ligands without general rules for activity and cannot predict the mechanism of binding that the ligand will engage in. Both of these facets of multivalent ligand design require new approaches to both the design and study of these systems. Studies able to systematically explore the influence of particular ligand parameters will be absolutely essential to the rational design of new ligands with optimal properties. Additionally, the development of assay methods that yield practical information with regard to the mechanisms of binding are lacking. These improvements will be especially useful when ligands from multiple structural classes can be compared within identical assay configurations.

Ligand Architecture vs. Receptor Architecture		Concanavalin A	AB <sub>5</sub> Toxins
Structural Class	Valency (n)		
	2-3	1-20 +	20-40 +
	4-30	30-300 ++	1-3 -
	31-172	300-700 +++	NA
	5-10	NA	20,000-500,000 +++++
	10-1200	100-2,000 +++++	8,000 +++++

**Figure 2.5. Interplay of ligand and receptor architecture in multivalent binding.**

Both ligand and receptor architecture are key determinants of multivalent binding. The inhibitory potency of general structural classes of ligands is summarized for the two receptor architectures discussed here. Activities of each class are disparate between receptor classes. Optimal ligands for Con A are large dendrimers and linear polymers. Optimal ligands for AB<sub>5</sub> toxins are large dendrimers that mimic the surface presentation of glycolipids. Ranges of activity in *related* assays are summarized on a *per saccharide* basis (using HIA for Con A and ELISA for AB<sub>5</sub>).

## Chapter 3. Influence of Ligand Structure on Multivalent Interactions

Portions of this work are published in:

“Control of Multivalent Interactions by Binding site Density”, C.W. Cairo, J.E. Gestwicki, M. Kanai, and L.L. Kiessling, *J. Am. Chem. Soc.*, **2002**, 124, 1615-1619.

“Cell Aggregation By Scaffolded Receptor Clusters”, J.E. Gestwicki, L.E. Strong, C.W. Cairo, F.J. Boehm, L.L. Kiessling, *Chem. Biol.*, **2002**, 9, 163-169.

“Designed Potent Multivalent Chemoattractants for *Escherichia coli*”, J.E. Gestwicki, L.E. Strong, S.L. Borchardt, C.W. Cairo, A.M. Schnoes, L.L. Kiessling, *Bioorg. Med. Chem.*, **2001**, 9, 2387-2393.

“Structurally Diverse Multivalent Ligands Reveal the Influence of Architecture on Receptor-Binding Mechanisms”, J.E. Gestwicki, C.W. Cairo, L.E. Strong, K.A. Oetjen, L.L. Kiessling, *submitted for publication*.

Contributions:

Compounds **3.21-3.35** were contributed by M. Kanai.

Compounds **3.5-3.10, 3.11, 3.12, 3.14-3.16** were contributed by L.E. Strong

Compounds **3.13, 3.17-3.20, 3.36-3.38**, chemotaxis and QP assays were contributed by J.E. Gestwicki.

FRET and solid-phase binding assays were contributed by J.E. Gestwicki and K.A. Oetjen.

GGBP binding studies (Figure 3.6) were performed by J.E. Gestwicki and N. Reiter.

### 3.1. Abstract

The clustering of cell-surface receptors is a common mechanism used to activate signaling pathways. Multivalent ligands can be used to control receptor clustering, and therefore the resulting signal transduction. In principle, multivalent ligand features can control clustering and the downstream signals that result, but the influence of ligand structure on these processes is incompletely understood. In this chapter, efforts towards understanding the underlying principles that guide multivalent ligand activity are described. Specifically, an example of structure-based design of multivalent ligands for the glucose/galactose binding protein (GGBP) is described. Using molecular modeling and crystal structures of the target receptor monomer units for multivalent ligand synthesis were designed, and the resulting ligands are potent new bacterial chemoattractants. Secondly, the development of assays that report on distinct aspects of multivalent binding events are detailed. To validate the assays used, the influence of a single parameter of multivalent ligand structure (binding epitope density) on receptor clustering events was analyzed. Finally, the activities of a structurally diverse group of compounds in these assays to determine the effects of ligand structure on multivalent binding were compared. Using this battery of assays the effect of changing epitope density, valency, and overall architecture of multivalent ligands was studied.

#### 3.2.1. Structure based design of multivalent ligands for GGBP

The signaling pathway that controls chemotactic response in *Escherichia coli* (*E. coli*) is a particularly well-characterized signaling system. The bacteria use this system to detect changes in their chemical environment, and respond by altering their locomotion (Hazelbauer *et al.*, 1993). This versatile system is able to recognize an array of both attractants and

repellents using only a few cell surface receptors (Adler *et al.*, 1973; Grebe and Stock, 1998). Moreover, the bacteria are able to detect minute changes in the concentrations of these molecules over as many as five orders of magnitude.

*E. coli* is known to undergo taxis in response to many different saccharides (Adler *et al.*, 1973). Chemotaxis towards saccharides in *E. coli* is initiated by the binding of a chemoattractant to the periplasmic binding protein glucose-galactose binding protein (GGBP) (Grebe and Stock, 1998; Hazelbauer *et al.*, 1993). GGBP then binds to the transmembrane receptor, Trg. Trg is one of the five methyl-accepting chemotaxis proteins (MCPs) known in *E. coli*. Upon activation by ligated GGBP, Trg becomes methylated by the methyl-transferase CheB. Methylation of the MCP leads to activation of the flagellar motor proteins by a two-component system that consists of the kinase, CheA, and the response regulator, CheY. Reports have suggested that several components of this system may act in concert, either as homo-dimers or tetramers (Grebe and Stock, 1998).

Although the molecular details of each step of the pathway are known, the mechanisms used by the system to respond to such a large dynamic range of concentrations remain obscure. Models have been proposed in the literature that suggest receptor clustering as a potential mechanism (Bray *et al.*, 1998; Shimizu *et al.*, 2000). Gestwicki *et al.* have shown that clustering of Trg receptors using multivalent ligands is a potent means of modulating chemotactic signaling (Gestwicki *et al.*, 2000a). Additionally, Gestwicki and Kiessling have shown that clustering of Trg results in potentiation of signaling through other MCPs, such as the serine receptor, Tsr (Gestwicki and Kiessling, 2002). This work has been further supported by recent genetic studies (Ames *et al.*, 2002). Although it has been known that these receptors are localized to the poles of the bacteria, receptor-receptor interactions are

not well characterized. These studies have lent convincing support to models of homo- and hetero-dimer communication within bacterial chemotaxis, and suggest that the development of ligands for this system could provide useful insights to the biological mechanisms responsible for signaling.

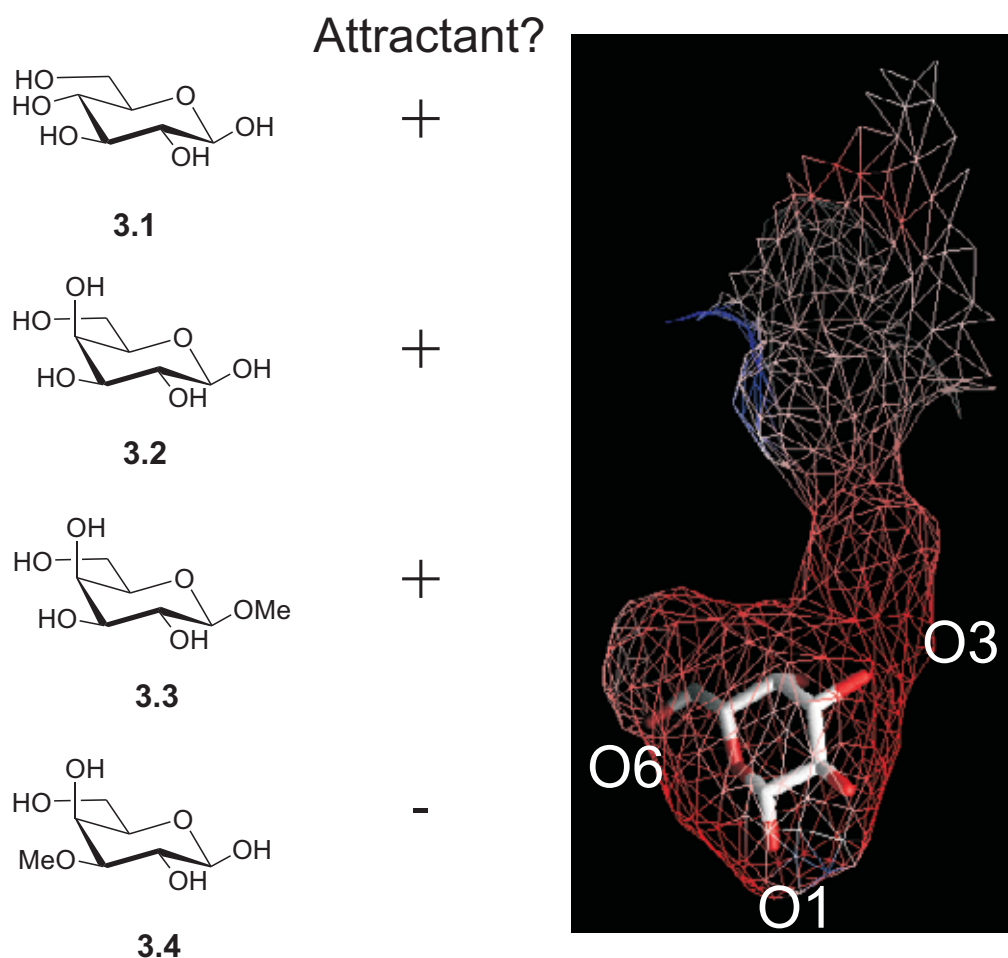
In the course of developing ligands for studies of bacterial chemotaxis, we became interested in the structural requirements of these ligands. In particular, we sought to optimize the activity of multivalent ligands that were known to be chemoattractants for *E. coli*. Therefore, using both biological and structural information available in this system, we designed and synthesized a series of mono- and multivalent ligands for the periplasmic binding protein, GGBP, and tested their ability to cause chemotaxis in bacteria.

### **3.2.2. Attachment point.**

To design ligands for GGBP, we used the extensive crystallographic data on this saccharide-binding protein (Vyas *et al.*, 1987; Vyas *et al.*, 1988). The structure of GGBP consists of two major lobes with a deep binding cleft near a hinge region of the protein (Figure 3.2.1). Upon binding, the protein undergoes a conformational change through the hinge region that closes the binding cleft around the ligand (Shilton *et al.*, 1996; Vyas *et al.*, 1988). GGBP is able to bind to both anomers of glucose and galactose. The saccharide is engages in multiple hydrogen bonds from aspartate residues within the cleft, as well as van der Waals interactions with tyrosine and tryptophan residues. The available crystallographic data reveal that all four sugars bind in the same orientation, with the anomeric hydroxyl group directed into the binding cleft (Vyas *et al.*, 1994).



To design multivalent ligands for this receptor, we needed to identify appropriate attachment points to introduce new functionality without significantly disrupting the binding interactions of the saccharide. The crystallographic data described above suggest that the anomeric position is an untenable site for a linker; however, the O3 position appeared to be a solvent accessible group that could accommodate a linker to a multivalent scaffold. Analysis of the available chemotactic data for methylated sugars, however, offered a conflicting view (Adler *et al.*, 1973). Adler *et al.* tested the chemotactic activity of several methylated derivatives of both galactose and glucose. They observed that monosaccharides with a substituent at the O3 position were not chemoattractants, but those with anomeric substituents were. To provide insight into this apparent discrepancy, we performed molecular modeling studies of monosaccharides and alkylated monosaccharides in the binding site of GGBP.



**Figure 3.1. Selected monosaccharides chemoattractants for *E. coli*.**

Monosaccharides that have been tested for bacterial chemotaxis (**3.1-3.4**). (Adler *et al.*, 1973) Alkyl substitution is tolerated at the anomeric position of galactose, but not at the O3 position. A surface representation of the GGBP binding site is shown with the native ligand, galactose. The O1, O3, and O6 positions have been noted. Based on the co-crystal the O3 position is expected to be tolerant of methylation.

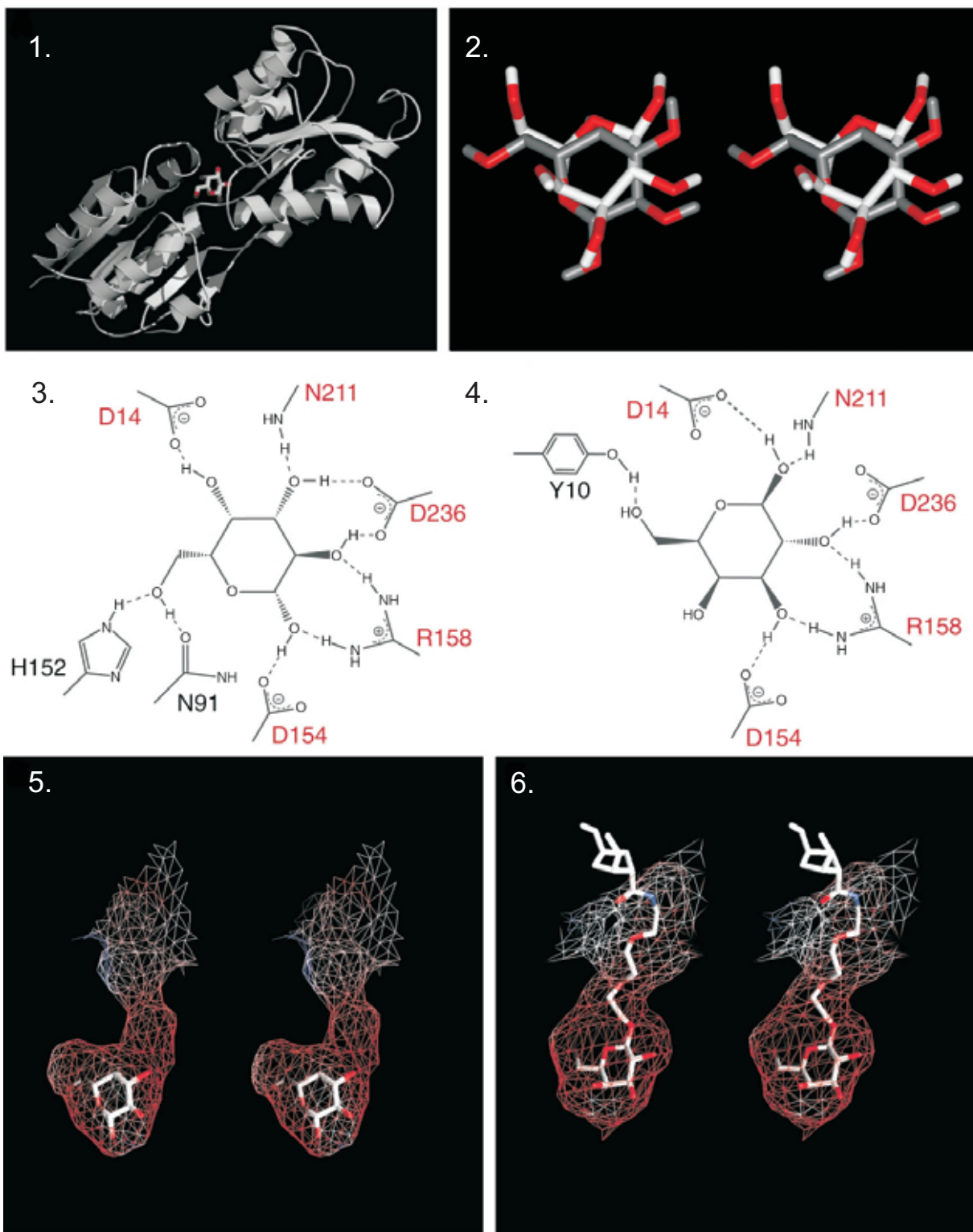
We hypothesized that there might be an alternate binding mode that could reconcile these data. We reasoned that any alternate orientation would likely retain several key features of the binding interactions observed in the co-crystal. 1) The plane of the saccharide (C1-C2-C4-C5) would not be altered so that van der Waals contacts and hydrogen bond interactions with equatorial hydroxyl groups could be maintained; and 2) the largest ring substituent, C6-O6, would remain in the same area of the binding pocket. The only transformation capable of meeting these two criteria is a rotation of the saccharide through a C2-C6 axis (Figure 3.2.4). This orientation would satisfy our criteria for binding to the protein, as well as reorient the anomeric hydroxyl group to a solvent-exposed position.

To test our hypothesis, we performed docking calculations able to predict alternate orientations of the ligand within the binding site. We expected that these calculations could confirm the potential of this alternate orientation, and might suggest how prevalent this conformer might be. Automated docking calculations have been found to be a useful tool for similar studies, and software to perform these calculations is available (Morris *et al.*, 1996). Olson and coworkers have obtained excellent results from docking studies of several small molecules to receptors, including  $\beta$ -trypsin, cytochrome P-450, streptavidin, HIV-1 protease, and influenza hemagglutinin using the program AutoDock. This method employs simulated annealing conformational searches using AMBER-based force fields for energy calculations (Goodsell and Olson, 1990; Weiner *et al.*, 1984). The method can dock both rigid and flexible molecules to fixed binding sites. Typical calculations generate populations of potential orientations, which are then sorted into clusters by relative energies.

Docking calculations of galactose, glucose and mannose anomers were conducted using AutoDock 2.4 (Figure 3.3). Monosaccharides were docked to the ligated structure of

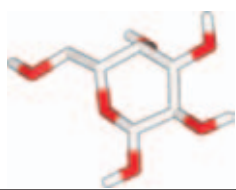
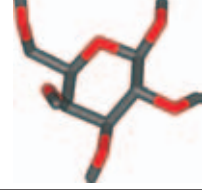
GGBP (PDB: 1GLG, with the saccharide removed). Orientations produced by the calculation were sorted into clusters of related orientations. The results were consistent with an alternate saccharide orientation (Figure 3.2.2), and the majority of all orientations found were consistent with either the crystal structure or the alternate orientation (> 85%). In the case of galactose, docking calculations predicted that the  $\beta$ -anomer would favor the alternate orientation. For glucose, both anomers were predicted to favor the alternate orientation. Both anomers of mannose were predicted to favor the orientation found using x-ray crystallography.

The alternate orientation identified by these calculations maintains several important non-covalent interactions found in the co-crystal structure (Figure 3.2.3, 3.2.4). Several sets of hydrogen bonding interactions between the hydroxyl groups of the saccharide and aspartate residues D14, D154, and D236 are maintained. Comparison of the coordinates of the heavy atoms of the structures suggests that these two orientations are very similar, giving an root-mean squared deviation (rmsd) value of  $1.54 \text{ \AA}^2$  for pseudo-symmetric heavy atoms (rmsd is calculated using coordinates of *transformed* atoms; e.g., C1 $\rightarrow$ C3, C6 $\rightarrow$ C6, etc.) The positions of pseudo-symmetric oxygen atoms are exceptionally well maintained.



**Figure 3.2. Alternate orientations of galactose within GGBP.**

- 1) Ribbon diagram of the galactose-GGBP co-crystal (1GLG).
- 2) An alternate orientation of galactose predicted by docking studies of the GGBP binding site. The crystal structure orientation is shown in dark grey, and the alternate orientation is shown in light grey. The overlay is shown crossed stereoview, in similar orientation to the structure shown in (1).
- 3) Two-dimensional representation of important hydrogen bonding interactions found for the crystal structure orientation of galactose.
- 4) Two-dimensional representation of important hydrogen bonding interactions found for the alternate orientation of galactose.
- 5) Crossed-stereo view of the internal surface of the binding pocket of GGBP with the crystal structure orientation.
- 6) Crossed-stereo view of the internal surface of the binding pocket of GGBP after minimization with an alkylated galactose monomer.

						
Autodock Orientations found using 1GLG	Crystal Structure Orientation (Frequency)	%	Alternate Orientation (Frequency)	%	Other Orientations (Frequency)	%
D-galactose						
$\alpha$ -anomer	7	35	12	60	1	5
$\beta$ -anomer	10	74	2	14	2	14
D-glucose						
$\alpha$ -anomer	3	23	8	61	2	15
$\beta$ -anomer	6	38	9	56	1	6
D-mannose						
$\alpha$ -anomer	11	73	2	13	2	13
$\beta$ -anomer	6	60	3	30	1	10

**Figure 3.3. Autodock results for docking of galactose to GGBP.**

Results of docking studies for monosaccharides to 1GLG using Autodock 2.4 (Goodsell *et al.*, 1996). Coordinates of docked saccharides were first filtered to examine only those within the binding site. Then cluster analysis was used to group similar orientations. The resulting groups were then compared to the crystal structure orientation and tabulated. The populations are given as the raw number of structures found as well as each orientations percentage of the total orientations found in the binding site.

These calculations, therefore, support our hypothesis that an alternate saccharide orientation could be accommodated in the saccharide binding site of GGBP. The predicted orientation is consistent with available data for chemotactic ligands. Importantly, our theoretical binding model predicted that the anomeric position of monosaccharides would be tolerant of substituents. We therefore proceeded to determine the ability of the GGBP binding channel to accommodate alkyl linkers for attachment to a polymer backbone.

### **3.2.3. Linker length.**

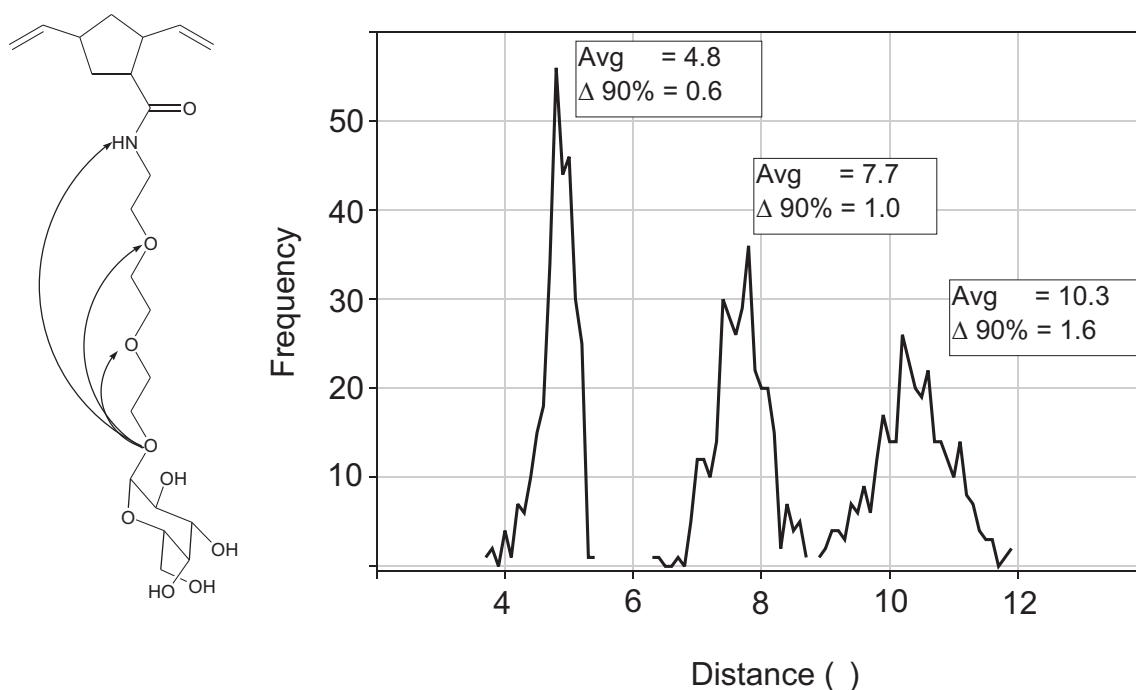
With a clear idea of an appropriate attachment point, we set out to determine what type of linker could be best accommodated by the GGBP binding channel. We first noted that the channel is relatively narrow and consists predominantly of polar residues (Asn, Asp, Thr). Therefore, ethylene glycol units were chosen to link the saccharide to the bulky polymer backbone. To determine the optimum length requirement for the linker, molecular modeling was used.

We designed a monomer unit containing multiple ethylene glycol units appended in a  $\beta$ -linkage to the anomeric position of D-galactose. The ring-opened norbornene structure was then docked into the binding site using the alternate orientation predicted by our calculations. The structure was minimized and then subjected to molecular dynamics (sidechains within 5 Å were allowed to move). During these calculations, we monitored the intra-chain distances between the saccharide and each ethylene glycol unit (Figure 3.4).

Our calculations indicate that compounds containing one and two ethylene glycol units were extremely confined within the GGBP binding channel. Specifically, a narrow distribution of intra-chain distances was observed for these linker regions during the course of



the calculations. The average distance found for one and two ethylene glycol units was 4.8 and 7.7 Å, respectively. The range occupied for 90% of the observed values was 0.6 and 1.0 Å. In contrast, after addition of the third ethylene glycol unit, the distribution of these values is much wider with 1.6 Å at an average distance of 10.3 Å, suggesting motion is less restricted for compounds with this chain length.



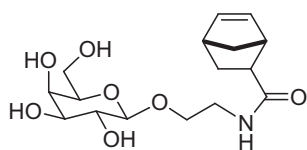
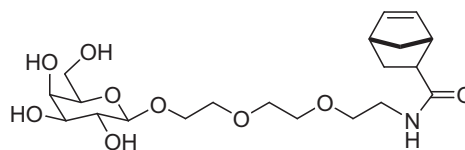
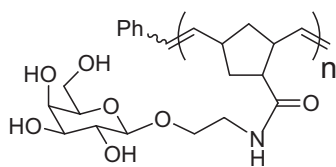
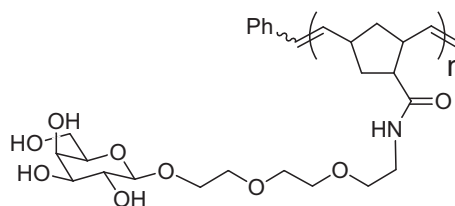
**Figure 3.4. Determination of optimal linker lengths using molecular dynamics.**

To determine the optimal linker lengths of monomer units for binding GGBP, a monomer with three PEG units was minimized into the binding site in the alternate orientation identified by docking studies. The resulting structure was then subjected to molecular dynamics simulations, and the intra-chain distances were monitored. Histograms of these distances reveal that a minimum of three PEG units are required to provide relatively free motion of the terminal region of the monomer. The average distance for each PEG unit is given, along with the distance range occupied by 90% of the values.

### 3.2.4. Chemotactic activity of designed ligands.

Based on our analysis of the binding site requirements of GGBP, we designed and synthesized a series of mono- and multivalent saccharide ligands as potential chemoattractants (Figure 3.5). ROMP was used to produce multivalent ligands displaying galactose residues using norbornene-derived monomers (Gestwicki *et al.*, 2000a; Strong and Kiessling, 1999). To test our predictions for required linker lengths to bind GGBP, we synthesized ligands with both short (**3.5-3.7**, Figure 3.5) and long (**3.8-3.10**) linker lengths. Additionally, each series contained both short ( $n = 10$ ) and long ( $n = 25$ ) polymers to test the effect of increased valency on chemotaxis.

We tested whether these ligands were active chemoattractants using capillary accumulation assays and found that they were active (Table 3.1) (Gestwicki *et al.*, 2001). Additionally, we confirmed that monomer units **3.5** and **3.8** were able to bind to GGBP by monitoring the internal fluorescence of tryptophan (Figure 3.6) (Boos *et al.*, 1972; Gestwicki *et al.*, 2001). To assess relative chemotactic activity, we employed a motion analysis assay using video microscopy. This method allows the quantification of bacterial motion as angular velocity over time. Due to its analysis of single bacterial paths, this technique is often more sensitive to small changes in activity between ligands. The results of these experiments with the designed chemoattractants (**3.5-3.10**) are summarized in Table 3.1 (Gestwicki *et al.*, 2001).

**3.5****3.8****3.6**  $n = 10$ **3.7**  $n = 25$ **3.9**  $n = 10$ **3.10**  $n = 25$ 

**Figure 3.5. Structures of designed chemoattractants.**  
Structures used in studies of bacterial chemotaxis.

**Table 3.1. Chemoattractant activity of synthetic galactose ligands.**

Compound	<i>n</i> (linker)	Chemoattractant	Rel. Potency <sup>a</sup>	Reference
<b>3.1</b> β-glucose	NA	+		(Adler <i>et al.</i> , 1973)
<b>3.2</b> β-galactose	NA	+	1	(Adler <i>et al.</i> , 1973; Gestwicki <i>et al.</i> , 2001)
<b>3.3</b> β-methyl-galactose	NA	+		(Adler <i>et al.</i> , 1973)
<b>3.4</b> β-3-methyl-galactose	NA	-		(Adler <i>et al.</i> , 1973)
<b>3.5</b>	1 (short)	+	1	(Gestwicki <i>et al.</i> , 2000a; Gestwicki <i>et al.</i> , 2001)
<b>3.6</b>	10 (short)	+	1	(Gestwicki <i>et al.</i> , 2000a; Gestwicki <i>et al.</i> , 2001)
<b>3.7</b>	25 (short)	+	10	(Gestwicki <i>et al.</i> , 2000a; Gestwicki <i>et al.</i> , 2001)
<b>3.8</b>	1 (long)	+	1	(Gestwicki <i>et al.</i> , 2001)
<b>3.9</b>	10 (long)	+	10	(Gestwicki <i>et al.</i> , 2001)
<b>3.10</b>	25 (long)	+	100	(Gestwicki <i>et al.</i> , 2001)

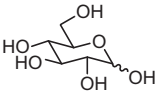
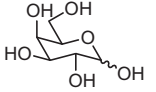
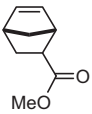
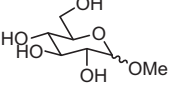
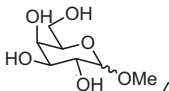
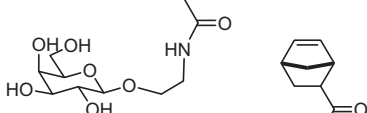
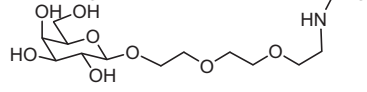

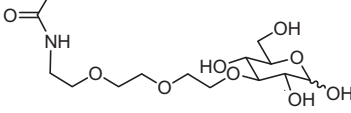
*a. Relative potencies were determined by motion analysis, and represent changes in the minimum concentration required for initiating chemotaxis. All concentrations compared on a per saccharide basis.*

These experiments confirmed that GGBP binds sugars with anomeric alkyl substituents, and that such compounds are attractants. Even very large substituents appear to be well tolerated. Additionally, we confirmed that these ligands could bind to GGBP using tryptophan fluorescence experiments (Boos *et al.*, 1972) (Figure 3.6). Examination of the relative potencies of these ligands as chemoattractants suggests that alkyl substituents are tolerated only at the anomeric position, and that longer linkers enhance activity. Comparison of the relative activities of the two monomers (**3.5** and **3.8**, Figure 3.5) initially suggests that increased linker length does not impart additional activity to these ligands. However, multivalent ligands with galactose residues tethered through the longer linkers had different activities than those possessing shorter linkers. Specifically, only the highest valency polymers containing a short linker (**3.6-3.7**) exhibited increased potency ( $n = 25$ , **3.7**) relative to the monomer. Both multivalent ligands that possess a longer linker (**3.9-3.10**) showed increased activity relative to the monomer. The short polymer ( $n = 10$ , **3.9**) showed a 10-fold increase in activity. The most potent ligand studied, ( $n = 25$ , **3.10**) was 100-fold more active than galactose alone. Thus, both linker length and valency of the ligand are critical to improved activity of these multivalent ligands. Our observation that multivalent presentation is required for the bacteria to distinguish between these ligands is consistent with models of chemotaxis signaling that use receptor clustering to potentiate activity (Ames *et al.*, 2002; Bray *et al.*, 1998; Gestwicki *et al.*, 2000a; Gestwicki *et al.*, 2001; Gestwicki and Kiessling, 2002; Shimizu *et al.*, 2000).

These results provide an example of how structure based-design can guide the production of potent multivalent ligands. Using both experimental results and the tools of molecular modeling we predicted a new putative binding mode for our ligands, and using this,

optimized their ability to bind to the target receptor. This example is unique in its exploration of the effects of altering both the attachment point, valency, and linker lengths of a series of multivalent ligands.

From these studies we found that some features of multivalent ligand design are amenable to rational design approaches (attachment point, linker length). However, we also found that other parameters require empirical study to determine optimum activity (valency). There are few examples of systematic studies of structural parameters of multivalent ligands. Although many multivalent ligands have been used in different systems, no comprehensive studies have analyzed multiple parameters in multiple assays. To more thoroughly explore the effects of multivalent ligand structure on activity we chose to study a model multivalent protein, the plant lectin concanavalin A. Using this system, we identified a battery of assays to provide orthogonal measurements of multivalent ligand activity. With these methods in hand we then screen a small library with diverse ligand architecture in order to determine the general contributions of ligand structure to activity.

Compound		Attractant?	Binds GGBP?	$K_d$ (nM)
glucose <b>3.1</b>		+	+	220
galactose <b>3.2</b>		+	+	500
methyl ester norbornene		-	-	n.a.
1-methyl glucoside		+	+	60
1-methyl galactoside <b>3.3</b>		+	+	410
galactose monomer (short) <b>3.5</b>		+	+	110
galactose monomer (long) <b>3.8</b>		+	+	1.1
3-methyl glucoside <b>3.4</b>		-	+	n.a.
glucose 3-monomer		-	+	4.0

**Figure 3.6. Binding of ligands to GGBP.**

The binding of synthetic ligands to GGBP was monitored by tryptophan fluorescence to determine their affinity.(Boos *et al.*, 1972; Gestwicki *et al.*, 2001) Compounds were also tested for their ability to attract *E. coli*. using capillary accumulation assays.(Gestwicki *et al.*, 2000a)



### **3.3.1. Assays for studying multivalent binding.**

Studies of multivalent carbohydrate ligands have generally focused on determinations of increases in functional affinity (avidity) (Kiessling and Pohl, 1996; Mammen *et al.*, 1998a). To this end, several types of assay design are generally employed to measure avidity effects (Kiessling, L. L. *et al.*, 2001). This analysis almost universally finds that multivalent ligands have avidities many fold greater than their monovalent forerunners. As a result, many researchers have attempted to discover the mechanisms of this enhancement. Efforts to dissect these effects have suggested that explaining the thermodynamic basis of these enhancements can be unexpectedly complex (Lundquist and Toone, 2002; Mammen *et al.*, 1998b; Rao *et al.*, 1998). However, empirical studies of avidity effects in multivalent ligands have provided a variety of structures to consider in the design of new ligands. We summarize here the primary techniques currently used in the literature for these studies.

#### **3.3.1.1. Hemagglutination.**

A range of multivalent carbohydrate ligands have been used as inhibitors of lectin binding. One of the primary assays for comparing lectin activity is analysis of the ability of these proteins to cause agglutination of cells. These multivalent proteins are effective agents for causing clustering of cell surfaces, leading to large cell-cell aggregates that drop out of solution. Therefore, to determine inhibition of this activity, lectins are incubated with agglutinating cells with increasing concentrations of lectin inhibitors. In this way, relative activities of these inhibitors can be assessed (Mortell *et al.*, 1996; Page *et al.*, 1996b; Schnebli, H. P., 1976; Sigal *et al.*, 1996). Agglutination assays provide a straightforward method of comparing inhibitory activities; however, they have several key drawbacks. For

example, there is an inherent 2-fold error in any activity determination. Additionally the multivalent nature of both the ligands and the lectins used can complicate the data. For example, some multivalent ligands may crosslink lectins in solution, and therefore give uninterpretable assay results (Corbell *et al.*, 2000). Therefore, more direct means of determining lectin inhibition have been sought.

### **3.3.1.2. Isothermal titration calorimetry.**

Isothermal titration calorimetry (ITC) has been used in several studies of multivalent interactions (Dam *et al.*, 2000; Dam and Brewer, 2002; Lundquist and Toone, 2002; Rao *et al.*, 1998; Weatherman *et al.*, 1996). This method has the potential to dissect the thermodynamic components of entropy and enthalpy in a binding event (Cooper, A. *et al.*, 1994a; Fisher and Singh, 1995). This is accomplished by directly measuring the heat released from the binding event (Ladbury and Chowdhry, 1996; Wiseman *et al.*, 1989). Recent applications of this technique to multivalent binding have demonstrated that the results of ITC experiments using multivalent lectins often do not agree with hemagglutination experiments (Corbell *et al.*, 2000). This is expected, considering that HIA experiments measure only inhibition, and ITC should measure affinity.

It should be noted that calorimetry measurements can suffer from precipitation artifacts in multivalent systems. For example, multivalent binding can occur such that the ligand clusters multiple receptors in solution. Under appropriate conditions, this event can lead to precipitation, a change in the concentration of soluble protein and ligand and therefore the measured heat of the system. The effects of precipitation are well known to be problematic for calorimetric experiments (Cooper, A. *et al.*, 1994b). Quantitative precipitation

experiments using identical conditions to the calorimetric experiment can provide an assessment of the extent of precipitation. Indeed “turbid” solutions are often found at the end of calorimetric titrations although the ramifications with regard to data interpretation are often unclear (Dimick *et al.*, 1999).

Several calorimetry studies in the literature have reported unexplained  $\Delta S^\circ$  measurements for multivalent interactions. For example, investigations of complex formation of synthetic trimeric vancomycin structures and trimeric analogs of D-Ala-D-Ala binding partner have provided measurements of the energetics of multivalent binding (Rao *et al.*, 1998). The authors use ITC to measure the affinity of this binding event, and they observe that the functional affinity of the multivalent ligands is due to an increase in the enthalpic term. Enthalpic contributions of binding scaled linearly with the number of binding sites, however the entropic contributions were approximately 1.5-fold less favorable than expected. This additional entropy is not due to error and is not accounted for in the proposed binding model. Similar entropic effects have been observed in multivalent carbohydrate systems (Dam *et al.*, 2000). In a study of small di-, tri-, and tetra-valent carbohydrate ligands which bind to the lectins Con A and Dioclea grandiflora (DGL) entropic contributions for higher valency compounds are again 1.5-fold less favorable than expected. These enthalpic contributions also scale with valency for the high affinity ligands. The authors suggest that the entropic effects could be indicative of clustering multiple lectin molecules in solution, a mechanism that is consistent with the ITC model fits. Similar mechanisms have been proposed to account for glycodendrimer ligand binding to Con A (Corbell *et al.*, 2000). Calorimetric methods also have been used to study the cooperativity of multivalent binding events using Con A. It is

interesting to note that these authors observe precipitation under the conditions used for calorimetry (Dam *et al.*, 2000; Dam *et al.*, 2002a; Dam *et al.*, 2002b).

#### **3.3.1.3. Quantitative precipitation.**

Quantitative precipitation assays can provide an assessment of the ability of a multivalent ligand to cause precipitation of its receptor (Khan *et al.*, 1991). Experiments are performed at low temperature and using high salt concentrations to increase precipitation. Importantly, these assays can provide stoichiometric information about the complexes formed between the multivalent ligand and its receptor. By determining the concentration of ligand at which the precipitation curve reaches saturation, the molar ratio of ligand to receptor is found. The assay therefore reports on the stoichiometry of multivalent complexation; however, this value should be treated as the stoichiometry of the final precipitate not that of discrete complexes. This information can have important ramifications for biological applications of these interactions. Receptor clustering is a common mechanism for initiating signal transduction, therefore being able to predict the ability of multivalent ligands to control clustering is useful (Heldin, 1995; Klemm *et al.*, 1998). For example, signaling events that are modulated by the number of bound receptors might be enhanced by multivalent binding (Cochran *et al.*, 2000). Therefore, these assays may provide a method to identify ligands with improved biological activity (Stone *et al.*, 2001).

#### **3.3.1.4. Turbidity.**

Turbidity assays are often used for determinations of the rate of aggregation of multivalent proteins (Easterbrook-Smith, 1993; Murphy *et al.*, 1988; Sittampalam and Wilson, 1984). These experiments were first conducted using antibodies, and similar

experiments are often used to study multivalent carbohydrate interactions. For example, multivalent mannose-substituted dendrimers have been studied using turbidimetric assays to determine relative rates of Con A clustering (Roy *et al.*, 1998). Rates of receptor clustering are known to be important in several biological systems. Moreover, receptor clustering events at the cell surface have been observed to occur over many orders of magnitude from seconds to days (Petrie *et al.*, 2000; Sugiyama *et al.*, 1997). Therefore, turbidity assays may provide an important indicator of the activity of multivalent ligands in these systems. Determining the structural features of a ligand that influence rates of clustering will be useful for the design of ligands to be used in systems that require specific rates of clustering to achieve a specific functional output.

#### **3.3.1.5. Fluorescence resonance energy transfer.**

Fluorescence resonance energy transfer (FRET) can provide important structural information about multivalent interactions (Ballerstadt and Schultz, 1997; Matko and Edidin, 1997). The assay exploits distance dependent transfer of energy between two differentially labeled receptors, one labeled with a donor and one with an acceptor. Decreases in the observed fluorescence of a label indicate decreased distance between the labels, and therefore is an indicator of inter-receptor distances. FRET efficiency varies as the sixth power of the distance between labels, and therefore is extremely sensitive to changes in proximity.

This method has been used extensively in biological systems to look at inter-receptor distances of proteins *in vitro* and *in vivo* (Matko and Edidin, 1997). FRET has been successfully used for studies of multivalent interactions by Kiessling and coworkers for small trimeric molecules and multivalent polymers (Burke *et al.*, 2000; Cairo *et al.*, 2002;

Gestwicki *et al.*, 2002c). These studies have shown that multivalent ligands can form soluble receptor clusters, and that the structure of these clusters is dependent on the structure of the ligands. A change in FRET signal can be interpreted as a defined change in distance or as an average change within a population.

FRET assays have several advantages over other assays described here. First, FRET uses minimal quantities of both ligand and receptor and is adaptable to microtiter plate format. Second, the assay is able to provide structural information about *soluble* receptor-ligand complexes. Therefore, FRET experiments are extremely useful for the study of multivalent interactions.

#### **3.3.1.6. Transmission electron microscopy.**

Transmission electron microscopy has recently emerged as a powerful analytical tool for imaging of multivalent ligand – receptor complexes. Using proteins labeled with gold nano-particles, the proximity of individual labels can be assessed. Gestwicki *et al.* have used this method to characterize discrete populations of dimeric, trimeric, and tetrameric complexes of the lectin Con A bound to multivalent mannose-substituted polymers (Gestwicki *et al.*, 2000b). These results were consistent with those from precipitation assays (Cairo *et al.*, 2002). This method is unique in its ability to give a visual representation of single complexes. Electron microscopy has also been used to observe the orientation of engineered multivalent constructs (Lawrence *et al.*, 1998).

### **3.3.1.7. Surface plasmon resonance.**

Optical biosensors using surface plasmon resonance (SPR) have been employed for both kinetic and thermodynamic studies of bio-molecular interactions (Morton and Myszka, 1998; Myszka, 2000; Rich and Myszka, 2000; Schuck, 1997). Several studies of multivalent interactions using this technique have been reported using lectins and carbohydrates. For example, the technique has been used as a method to identify lectin specificity, the kinetics of multivalent lectin binding, and the stoichiometry of galectin binding (Haseley *et al.*, 1999; Shinohara *et al.*, 1994; Shinohara *et al.*, 1997; Symons *et al.*, 2000). Mann *et al.* have used SPR to characterize the competitive binding of multivalent mannose-substituted polymers to Con A (Mann *et al.*, 1998). Rao *et al.* used SPR studies to characterize the binding of synthetic divalent ligands for vancomycin (Rao *et al.*, 1999).

These examples demonstrate the versatility of surface binding studies for evaluation of both kinetic events and binding affinity. SPR measurements are often in excellent agreement with other solution techniques (Rich and Myszka, 2000). It should be noted however that surface presentation can often affect the observed rates (Horan *et al.*, 1999). Therefore, SPR measurements of any interaction should be carefully evaluated for such artifacts by varying the density of immobilized receptor.

### **3.3.2. Multiple assays are required for study of complex interactions.**

It is apparent from this brief survey of methods for assessing multivalent ligand activity that no single assay can provide a comprehensive description of these complex events. As discussed in Chapter 2, multivalent ligand interactions can engage in multiple binding mechanisms, and therefore a single parameter, such as affinity, is not easily related to

more complex properties, such as receptor clustering, without experiment. Complex events, including receptor clustering, chelate binding, or precipitation could be obscured in analyses of a single parameter of binding. Receptor clustering events are an excellent example of non-affinity effects related to multivalent binding. In a given clustering event, functional affinity (or avidity) will predict the equilibrium concentration of bound ligand, however properties such as the distance between receptors, or the rate of their complexation must be measured independently.

Receptor clustering governs many biological processes, including immune responses and growth factor signaling (Heldin, 1995; Kiessling and Pohl, 1996; Klemm *et al.*, 1998; Mammen *et al.*, 1998a). Parameters known to be important for receptor clustering include the stoichiometry of binding (Cochran *et al.*, 2000), the rate of cluster formation (Petrie *et al.*, 2000; Sugiyama *et al.*, 1997), and the proximity of receptors (Livnah *et al.*, 1999). Understanding the molecular features of a multivalent ligand that influence these parameters would provide insight into how natural multivalent interactions are regulated. Additionally, the properties of synthetic ligands can be optimized so that they serve as regulators for systems of interest.

We hypothesized that to develop a useful interpretation of the impact of ligand structure on the processes of receptor clustering multiple assays would be required. Therefore, we identified a panel of assays that would provide a broad range of information about receptor clustering events. Importantly, the results of these non-affinity assays were also compared to functional affinity measurements. In this way, we intend to demonstrate that guidelines for multivalent ligand design can be extracted.



### 3.3.3. Multivalent binding assays to study receptor clustering.

The assays we used for our studies were selected to provide insight into receptor clustering events in solution (Figure 3.7). The majority of these assays were not expected to be directly related to inhibitory activity, and therefore could provide insights beyond typical binding assays. QP assays were used to determine both the ligand concentrations required to cause precipitation and the stoichiometry of the resulting complexes. Turbidity assays were used to compare the initial rates of clustering in solution. FRET assays were used to observe changes in proximity between receptors in the complex. Finally, measurements of functional affinity were provided by a competitive binding assay.

To test the merit of our approach, we selected a series of multivalent mannose-substituted polymers that varied only in binding epitope density. We expected that assessment of the activities of these ligands in the selected assays would allow us to observe the effect of binding epitope density. These studies would provide a useful description of binding epitope density effects in multivalent binding, and more generally, would provide insight into multivalent ligand function.

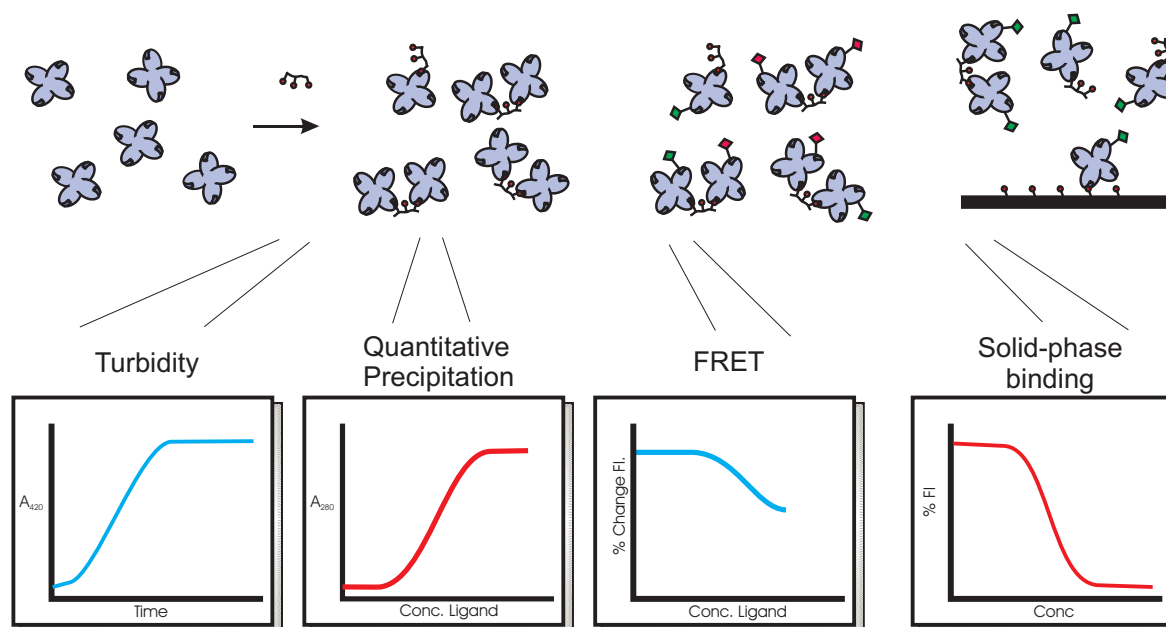
### 3.3.4. Concanavalin A as a model receptor.

Many proteins that participate in multivalent interactions are oligomeric. One of the most studied members of this class is the tetrameric lectin, concanavalin A (Con A) (Liener, I. E., 1976). At neutral pH, the lectin exists as a homotetramer that presents four distinct binding sites for mannopyranosides ( $K_d \sim 0.1$  mM) (Becker, J. W. *et al.*, 1976; Liener, I. E., 1976; Williams *et al.*, 1992). Con A is a well-known activator of cellular signaling (Anderson, J. *et al.*, 1976). The oligomeric state of Con A can influence its signaling activity, and the formation of macromolecular Con A-ligand assemblies on the cell surface appears to be

important for signal transduction (Cribbs *et al.*, 1996). Although Con A-induced signaling has been well-studied, its physiological relevance is unknown. Con A is structurally similar to many animal and bacterial lectins implicated in signaling events (Kogelberg and Feizi, 2001; Lis and Sharon, 1998; Vijayan and Chandra, 1999). One class of these, the galectins, are galactose-binding lectins that can regulate cell adhesion, cell proliferation, and cell survival (Barondes *et al.*, 1994; Bouckaert *et al.*, 1999; Perillo *et al.*, 1998). As with Con A, the abilities of the galectins to cross-link cell surface receptors have been implicated in initiation of signal transduction (Perillo *et al.*, 1998). Thus, both Con A and galectin-mediated signaling appears to depend on the formation of macromolecular assemblies on the cell surface.

Multivalent ligands that bind and cluster lectins can serve as scaffolds for the assembly of macromolecular displays. For example, multivalent arrays of mannose have been shown to promote the formation of higher order assemblies containing multiple copies of Con A (Figure 3.12) (Gestwicki *et al.*, 2002c). In the case of Con A, these macromolecular complexes can possess many unoccupied sugar binding sites poised for interaction. For example, we have found that scaffolded displays of Con A bind more avidly to surfaces presenting mannose residues (Burke *et al.*, 2000). Such macromolecular complexes are more effective than Con A itself at promoting cell – cell associations (Gestwicki *et al.*, 2002c). Thus, multivalent ligands that cluster lectins without saturating their carbohydrate-binding sites can be used to cross-link cell surface glycoproteins and thereby initiate signaling (Gestwicki *et al.*, 2000a; Gestwicki *et al.*, 2002c; Kiessling *et al.*, 2000a). Multivalent interactions of saccharide ligands with Con A have been studied using a wide range of methods, including electron microscopy (Gestwicki *et al.*, 2000b), calorimetry (Dimick *et al.*, 1999), and x-ray crystallography (Olsen *et al.*, 1997). Because of the signaling properties of

Con A and the abundance of information on its complexes, it is an excellent model for examining ligand features that impact receptor clustering.



**Figure 3.7. Assays employed for studies of multivalent binding.**

Multivalent binding events were studied using multiple assays. Turbidity and precipitation assays are used to determine rates and stoichiometries of multivalent interactions. FRET assays are used to test for changes in receptor proximity within complexes. Additionally, competitive binding experiments were used to determine the inhibitory activity of each ligand.

### 3.4.1. Density effects in multivalent binding.

We studied the influence of multivalent ligand binding epitope density on the clustering of the model receptor, Con A. We analyzed four aspects of receptor clustering: the functional affinity of binding, the stoichiometry of the complex, the rate of cluster formation, and receptor proximity. Our experiments reveal that the density of binding sites on a multivalent ligand strongly influences each of these parameters. In general, high binding epitope density results in higher functional affinity, greater numbers of receptors bound per polymer, faster rates of clustering, and reduced inter-receptor distances. Ligands with low binding epitope density, however, are the most efficient on a binding epitope basis. Our results provide insight into the design of ligands for controlling receptor – receptor interactions and can be used to illuminate mechanisms by which natural multivalent displays function.

The binding epitope density of a multivalent ligand has been shown to influence its activity (Horan *et al.*, 1999; Krantz *et al.*, 1976; Mammen *et al.*, 1995). Often these increased activities have been attributed to increases in functional affinity (Kiessling *et al.*, 2000a; Kiessling and Pohl, 1996; Mammen *et al.*, 1998a). We hypothesized that binding epitope density could also affect kinetic and structural parameters important in cluster formation. To test this hypothesis, we investigated a series of multivalent ligands varying in binding epitope density. Polymeric carbohydrate displays that vary in the density of binding sites presented are known (Horan *et al.*, 1999; Krantz *et al.*, 1976; Mammen *et al.*, 1995). The compounds employed in prior studies were synthesized by increasing the ratio of unfunctionalized to functionalized monomer to decrease binding epitope density. The unfunctionalized monomer units were typically smaller and of different hydrophobicity than the functionalized units;

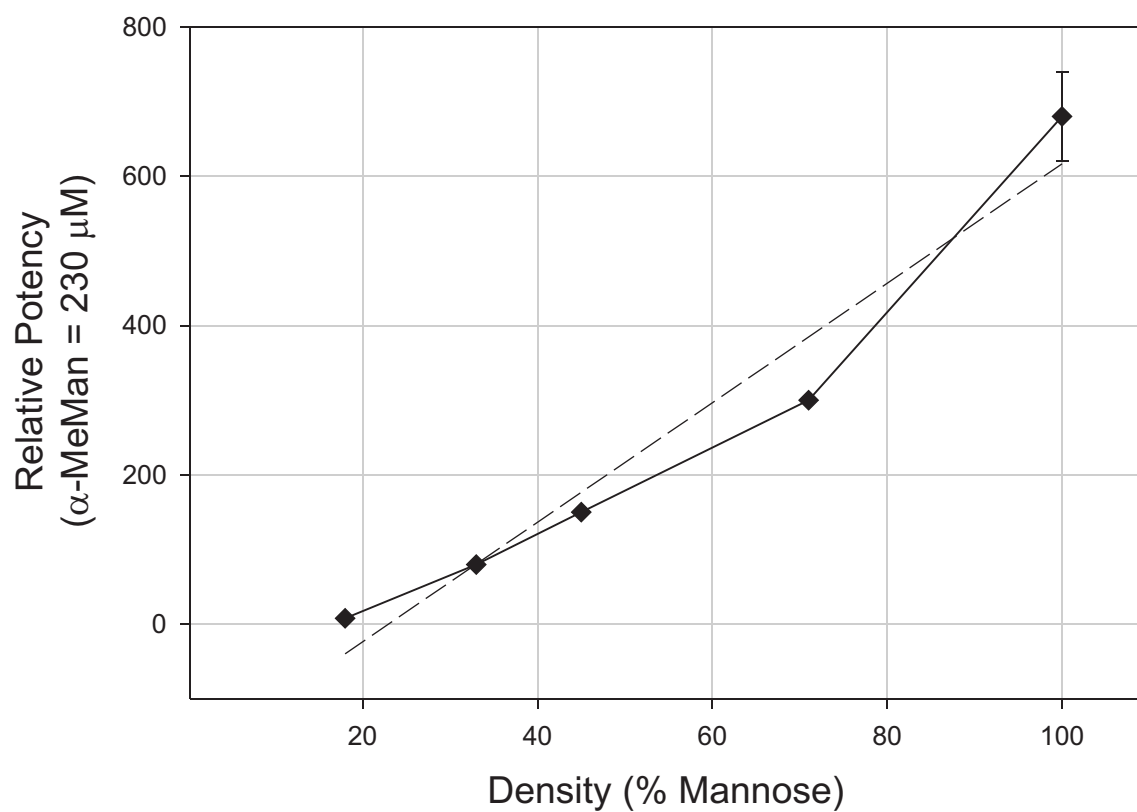
consequently, the resulting polymers did not present a uniform steric and electronic environment. To allow selective analysis of the impact of changes in binding epitope density on receptor clustering, we devised a method to synthesize multivalent ligands with monomer units that varied only in their binding activity. Moreover, we employed a battery of assays to characterize different parameters relevant to receptor clustering.

We used the ring-opening metathesis polymerization (ROMP) to synthesize polymers that vary only in the density of mannose residues (Table 3.2) (Kanai *et al.*, 1997; Kanai and Kiessling, 2002). Con A binds mannose but does not recognize the sterically similar moiety galactose (Goldstein, I. J., 1976); consequently, we altered the ratio of mannose- and galactose-substituted monomers in copolymerization reactions. Using this approach and the functional group-tolerant ruthenium initiator  $[\text{Ru}=\text{CHPh}(\text{Cl})_2(\text{PCy}_3)_2]$  (Trnka and Grubbs, 2001), we could readily produce materials with different mannose densities (compounds **3.29-3.35**, Figure 3.13). Differences in the mannose to galactose monomer ratios employed in the polymerization reactions were preserved in the final materials. Thus, ligands could be produced with similar length, polarity, and steric properties that differ only in their proportion of binding sites. With these compounds, we examined the influence of epitope density on the formation of Con A clusters. Our investigations reveal that the density of binding sites presented by a multivalent ligand influences critical features of receptor clustering.

### 3.4.2. Functional affinity of multivalent ligands.

The functional affinity (avidity) of multivalent ligands is well known to increase with valency (Kiessling and Pohl, 1996; Mammen *et al.*, 1998a; Mann *et al.*, 1998). The effect of binding epitope density has not been as well studied. Functional affinity enhancements for multivalent ligands are generally measured using either competition assays (which yields an inhibitory constant) or direct binding assays (Mann *et al.*, 1998; Rao *et al.*, 1998). Hemagglutination assays are also used as a general measure of ligand activity; however, these measurements may suffer from precipitation artifacts as discussed above. To compare the functional affinity of our ligands, we implemented a competitive plate-binding assay. The assay uses an immobilized 2-aminoethyl  $\beta$ -D-mannopyranoside, and the ability of ligands to inhibit fluorescently labeled Con A binding to the surface is determined.

Using this method, the functional affinity of compounds **3.31-3.35** (Figure 3.13) was determined and compared to that of  $\alpha$ -methyl-mannose. The results of these experiments are shown in Figure 3.8. Interestingly, we observed that increasing the binding epitope density of the ligands leads to a direct increase of the functional affinity. This is a surprisingly large effect, resulting in an 80-fold increase in affinity as the density of the ligand is increased from 20% to 100% mannose. Therefore, in regards to functional affinity, optimum compounds should contain 100% epitope density.



**Figure 3.8. Measured inhibitory potency of polymers with variable binding epitope density.**

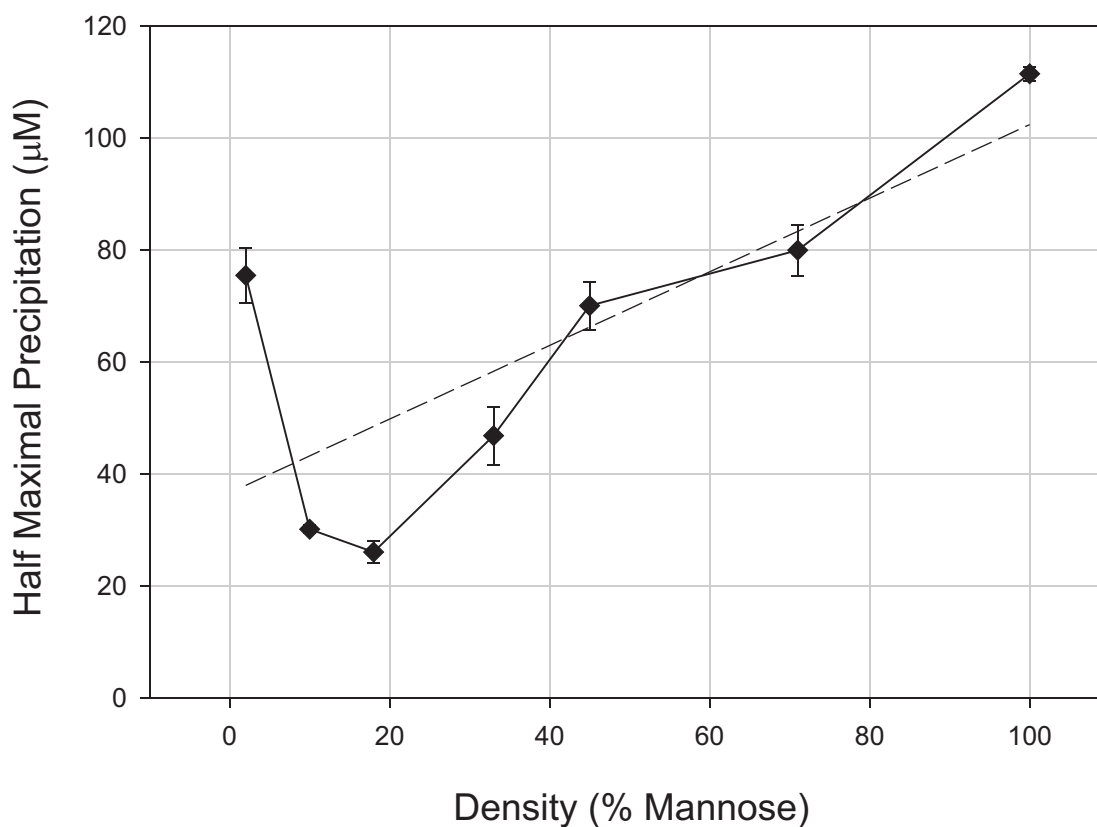
The ability of each ligand (**3.29-3.35**) to inhibit the binding of fluorescently-labeled Con A tetramers to a surface derivatized with mannose was tested. The activity of each ligand is shown relative to  $\alpha$ -MeMan (230  $\mu$ M). Concentrations were calculated on a per saccharide basis. (Linear regression of the data give  $r^2 = 0.95$ , dashed line). Compound structures are shown in Figure 3.13.



### 3.4.3. Relative stoichiometry of Con A to ligand within the cluster.

The number of Con A tetramers bound that bind to ROMP-derived ligands depends on the degree of polymerization (length) of the multivalent ligand (Gestwicki *et al.*, 2000b). Steric effects preclude the binding of Con A tetramers to every mannose residue on a fully elaborated polymer generated by ROMP (Schuster *et al.*, 1997). To determine the effect of binding epitope density on the stoichiometry of the Con A – ligand complex, compounds **3.29-3.35** (Figure 3.13) were used in quantitative precipitation (QP) assays. These experiments determine the concentration of ligand required to maximally precipitate the lectin from solution. Therefore, the results provide a determination of the stoichiometric composition of the precipitate (Khan *et al.*, 1991).

The initial aggregates formed in QP experiments likely consist of isolated complexes; however, crosslinked lattices may form in later stages (Olsen *et al.*, 1997). The data from these experiments reveal that the number of tetramers bound per polymer increases with increasing epitope density (Table 3.2, Figure 3.9). The observed stoichiometry agrees well with our previous experiments using transmission electron microscopy, in which we examined the stoichiometry of isolated multivalent ligand-promoted clusters of Con A (Gestwicki *et al.*, 2000b). The fully elaborated polymer binds the greatest number of tetramers, but reducing the mannose epitope density to 70% does not significantly alter the stoichiometry of the precipitate. Polymers in which 2-20% of the residues are mannose bind the greatest number of receptors per residue. Thus, on a mannose residue basis, the most efficient compounds are those with the lowest density of binding sites. In contrast, the polymers that display the greatest number of binding sites generate the largest clusters.



**Figure 3.9. Precipitation of Con A by polymers with variable binding epitope density.**

Quantitative precipitation assays were used to determine the relative ability of each ligand (3.29-3.35) to precipitate the lectin (Khan *et al.*, 1991). These data are represented as the half maximal per saccharide concentration required for precipitation. The data can also be used to determine the stoichiometry of the complex (Table 3.2) (Linear regression of the data gives an  $r^2$  value of 0.58, dashed line). Compound structures are shown in Figure 3.13.

**Table 3.2. Binding epitope density of multivalent polymers influences the stoichiometry of Con A complexation.**

<i>Compound</i>	<i>valency (DP)<sup>a</sup></i>	<i>%Man<sup>b</sup></i>	<i>Stoichiometry<sup>c</sup></i>	<i>Mannose/Con A<sup>d</sup></i>
<b>3.29</b>	143	100	16	9
<b>3.30</b>	145	71	15	7
<b>3.31</b>	115	45	9	6
<b>3.32</b>	86	31	7	4
<b>3.33</b>	102	18	6	3
<b>3.34</b>	116	10	3	3
<b>3.35</b>	129	2	1	2

*a. The degree of polymerization (DP) was determined by NMR integration of polymer end groups versus internal olefin resonances, to give the valency (see: Experimental Methods).*

*b. Ratio between incorporated mannose and galactose used in the polymerization is given as % mannose.*

*c. Stoichiometry of the complex is calculated using QP experiments. The ratio is reported as the ratio of Con A tetramers per polymer backbone.*

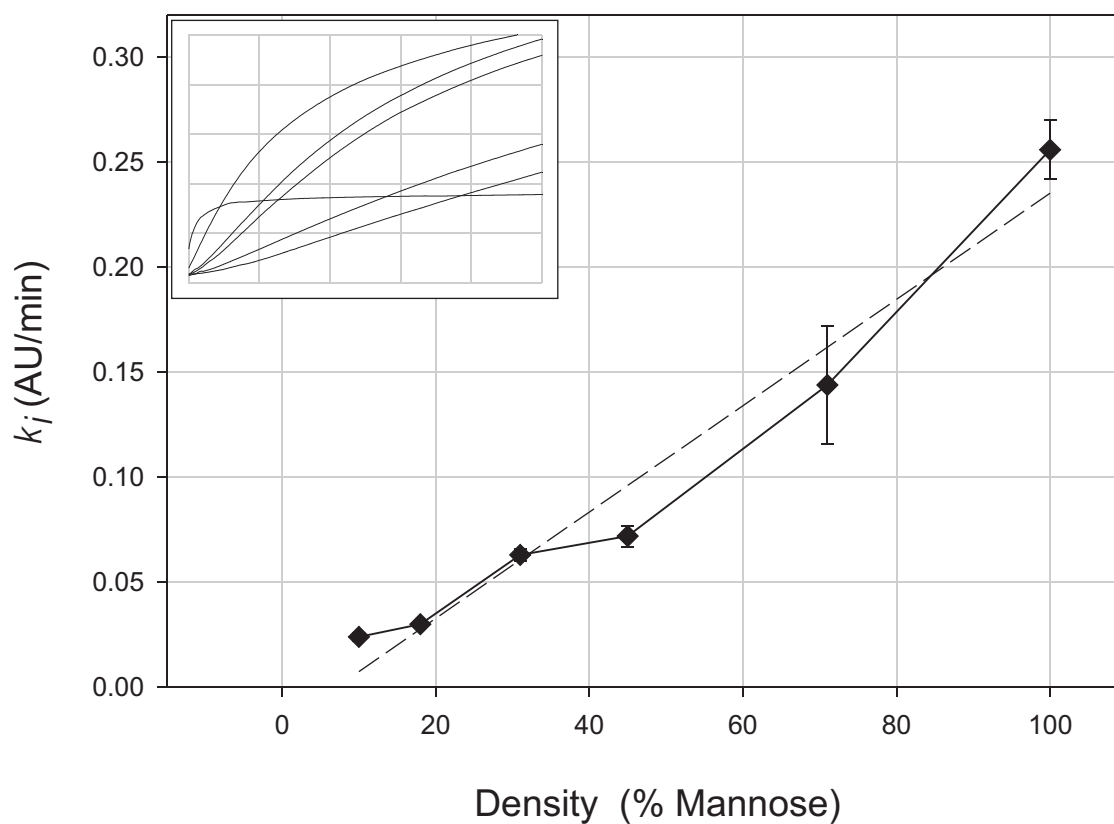
*d. The ratio of mannose residues to Con A tetramers is calculated as DP/stoichiometry.*

#### **3.4.4. Rate of cluster formation.**

QP provides information about an endpoint of receptor clustering, yet a critical parameter for biological systems is the rate of complex assembly. Cell-surface receptor clustering processes occur on time scales that range from seconds to days (Petrie *et al.*, 2000; Sugiyama *et al.*, 1997). To measure the effects of epitope density on the kinetics of receptor clustering, we employed a turbidimetric assay to monitor the rate of formation of lectin clusters in solution (Kitano *et al.*, 2001; Roy *et al.*, 1998; Ueno *et al.*, 1997).

In the turbidity assay, Con A is mixed with a 10-fold excess of multivalent ligand, a process that induces rapid precipitation (see: Figure 3.10, inset). The initial rate of change in turbidity is related directly to the rate of receptor - receptor association mediated by the polymer backbone (Lichtenbelt *et al.*, 1974; Puertas *et al.*, 1998; Puertas and delasNieves, 1997). By determining the initial slope of the curve a measurement of the rate of Con A clustering is obtained. These initial values should relate to the formation of isolated complexes; however, at later time points, secondary interactions between complexes obscure analysis. For example, in the presence of the highest density ligand **3.29** (Figure 3.13), Con A rapidly aggregates and then reaches a plateau value (see: Figure 3.10, inset). Alternatively, the absorbance for assemblies formed in the presence of ligands **3.30-3.34** (Figure 3.13) continues to increase over time. This result is consistent with the formation of higher order, cross-linked complexes in presence of ligands **3.30-3.34**, the cross-linked complexes are expected to be more prevalent when precipitation is slower. We, therefore, have restricted our analysis to the initial rates of complexation.

The rate of Con A complexation depends on the epitope density of the multivalent ligand. The highest density polymer induces clustering at a rate approximately 10-fold faster than that of the lowest density polymers. Subtle decreases in binding epitope density (e.g. from 100% to 70%), can decrease the rate of clustering by as much as 2-fold. In contrast, this change in epitope density produced little or no change in the stoichiometry of the clusters. Thus, the binding epitope density of a multivalent ligand has a considerable effect on the rate at which it mediates receptor clustering.



**Figure 3.10. Rate of Con A precipitation using variable binding epitope density polymers.**

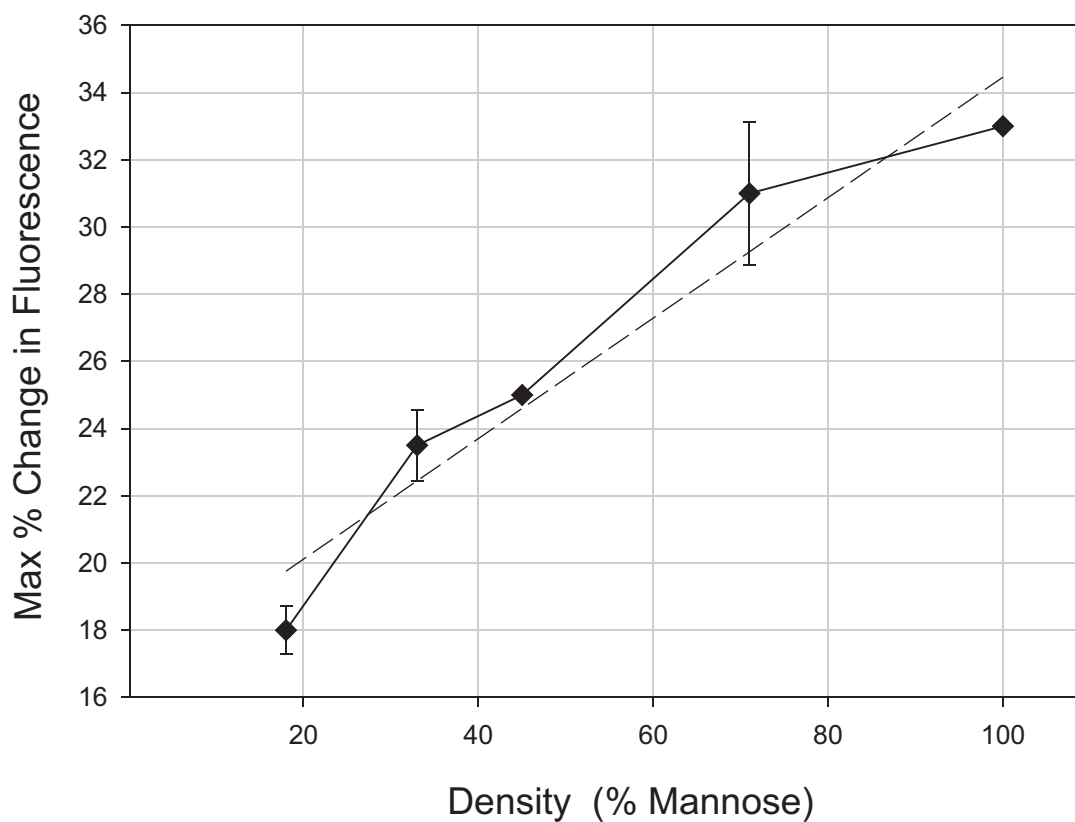
Initial rates of precipitation were determined from three independent experiments, error shown is the standard deviation. Some error bars are smaller than the symbols. Inset:  $A_{420}$  vs. time shows raw turbidity curves. Concentrations were calculated on a per saccharide basis. (Linear regression of the data give  $r^2 = 0.96$ , dashed line). Compound structures are shown in Figure 3.13.

### 3.4.5. Receptor proximity.

Multivalent ligands can alter the proximity of receptors on the cell surface (Gestwicki *et al.*, 2000a; Heldin, 1995; Klemm *et al.*, 1998; Mann *et al.*, 1998; Rao *et al.*, 1998). Changes in receptor proximity can dramatically influence biological processes. To explore the influence of binding epitope density on multivalent ligand-induced receptor clustering, we exploited fluorescence resonance energy transfer (FRET) as a method to assess changes in receptor proximity (Ballerstadt and Schultz, 1997; Matko and Edidin, 1997). These measurements rely on the distance-dependent transfer of energy between two differentially labeled receptors. Here, fluorescein- and tetramethylrhodamine (TMR)-labeled Con A were used as donor and acceptor, respectively (Burke *et al.*, 2000).

Decreases in the fluorescence emission of the fluorescein donor are an indication of the proximity of Con A tetramers in the assembly. Compounds **3.29-3.33** (Figure 3.13) were added to a solution containing differentially labeled Con A, and the fluorescein emission was monitored (Figure 3.11). As the binding epitope density of the ligand increased, the maximum percent change in fluorescence emission elicited also increased. FRET efficiency varies as the sixth power of the separation distance (Matko and Edidin, 1997). Thus, this change is anticipated if the average distance between Con A tetramers in the polymer-lectin complex decreases. Alternatively, the change may also reflect an increase in the population of Con A tetramers in close proximity. Although these data do not distinguish between either scenario, both represent relevant changes in receptor clustering. Applying the average distance analysis, the changes in FRET for compounds **3.29-3.33** (Figure 3.13) indicate that altering the binding epitope density from 20% to 100% results in a decrease of the average inter-Con A distances of approximately 15%. This change is less pronounced for small reductions in

binding epitope density; comparison of the highest mannose density ligands **3.29** and **3.30** (100% and 70% mannose residue incorporation), shows that little to no change in FRET is observed. This result is consistent with studies of the stoichiometry determined from quantitative precipitation experiments, in which the stoichiometry of complexes formed from compounds **3.29** and **3.30** was similar.



**Figure 3.11. FRET induced by variable density ROMP-derived ligands.**

FRET is assessed by determining the percent decrease in emission of the fluorescent donor (520 nm) on Con A in the presence of multivalent ligands. The donor and acceptor used are fluorescein and rhodamine. FRET of labeled Con A induced by compounds **3.29-3.35**. Each point represents the average of three separate experiments, each over a concentration range of 0.001- 100  $\mu$ M mannose. Concentrations were calculated on a per saccharide basis. Error shown is the standard deviation. (Linear regression of the data give  $r^2 = 0.93$ , dashed line). Compound structures are shown in Figure 3.13.



### 3.4.6. Changes in binding epitope density affect multivalent binding

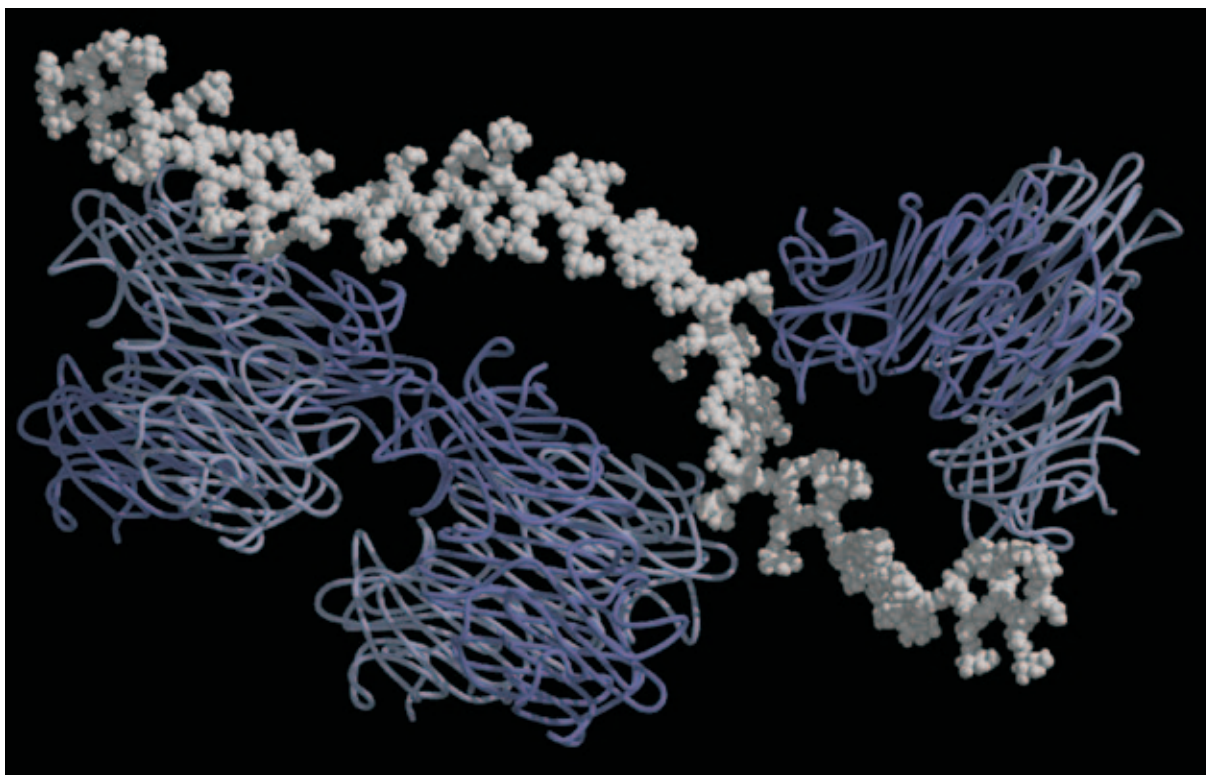
Multivalent ligands are useful biological probes due to their increased functional affinity and their ability to engage in multiple binding mechanisms. Multivalent ligands that influence receptor clustering can be used to illuminate and manipulate diverse physiological processes (Gestwicki *et al.*, 2000a; Kiessling *et al.*, 2000a). We hypothesized that the binding epitope density of a multivalent display influences parameters beyond its functional affinity. These include: the stoichiometry of complexation, rate of cluster formation, and receptor proximity. Little is known about the influence of multivalent ligand structure on these parameters. Using a series of multivalent ligands that differ only in their binding epitope density, we explored mechanistic parameters relevant for receptor clustering events.

Applying assays that report on the assembly of Con A complexes, we investigated the effects of changing the binding epitope density of multivalent ligands. The stoichiometric composition of the multivalent ligand – receptor complexes was determined by QP assays. These results indicate that lower density ligands bind fewer receptors. Surprisingly, they also reveal that these ligands provide the most efficient interactions per recognition element. As anticipated, the ligands that display the most binding sites clustered the most receptors per polymer. Interestingly, increasing the binding epitope density beyond 70% mannose residues did not increase the number of receptors bound per multivalent ligand. FRET experiments showed that changes in binding epitope density afforded similar trends with regard to the proximity of receptors within the cluster. Increases of binding epitope density from 20-70% resulted in decreases in average inter-receptor distances. Again, increasing binding epitope density from 70% to 100% produced no measurable changes in FRET.

Turbidimetric experiments allow quantitation of the relative rates of clustering induced by the polymers. We observed that the rate of clustering is directly related to binding epitope density; the highest density ligands showed the fastest rates of assembly. In contrast to both QP and FRET experiments, the rate of clustering for ligands with binding epitope densities of 70% and 100% were different. The highest density ligand **3.29** exhibited a 2-fold increase in rate of clustering of Con A over ligand **3.30** (Figure 3.13). This result suggests that the rate of clustering is more sensitive to small changes in the multivalent scaffold than the other parameters measured.

The results presented here demonstrate that binding epitope density is an important parameter that influences receptor clustering. In addition, there is interplay between epitope density and cluster formation. Traditionally, research on multivalent interactions has focused on optimizing activity on a binding epitope basis. Our results reveal other parameters may be critically influenced by changes in ligand structure. We found that epitope density can be decreased to complex a greater number of receptors per binding element. In contrast, increasing the mannose density of a multivalent ligand increased the number of receptors bound per polymer, increased initial rates of complexation, and decreased the inter-Con A distances in the complex. Thus, when receptor proximity is essential, density should be increased to reduce inter-receptor distances. For interactions requiring fast kinetics, the highest possible binding epitope density may be optimal. Our studies indicate that ligand microstructure plays a key role in controlling the outcome of multivalent binding events. Thus, it is a critical design parameter in creating multivalent ligands with tailored biological activities (Bertozzi and Kiessling, 2001; Kiessling *et al.*, 2000b).

Multivalent interactions govern many important biological responses, yet there is little known about the influence of multivalent ligand structure on these processes. It has been suggested that natural polyvalent ligands (e.g. mucins, heparan sulfate) may use variations in binding epitope density to modulate biological interactions and the responses that result (Gerken *et al.*, 1998; Lindahl *et al.*, 1998; Perrimon and Bernfield, 2000). Our results suggest mechanisms by which binding epitope density could influence the regulation of natural multivalent interactions to yield the range of kinetic parameters and structural features that these processes require.



**Figure 3.12. Scaffolded receptor clusters.**

A theoretical model of a ROMP ligand ( $n = 50$ ) complexed with three Con A tetramers. The model is intended to convey a sense of scale for the complexes discussed in this chapter.

### 3.5.1. Multivalent ligand architecture.

Our studies of polymers with variable binding epitope density (Section 3.4) support the hypothesis that multivalent ligand architecture can influence protein binding modes. Specifically, our results suggest that a single parameter, such as density, can have diverse effects on binding. Using a panel of four different assays, we found that the rate of clustering, the stoichiometry of the complex, the proximity of receptors, and the inhibitory potency were all influenced by changes in binding epitope density. These results are of direct application in the design of new multivalent ligands; however, there are additional structural features that might provide equally profound effects on multivalent binding modes.

We hypothesized that other ligand features, such as valency and three-dimensional architecture, could also influence multivalent interactions. The assays that we have already implemented for examining changes in receptor clustering are ideal for addressing the propensity of a ligand to engage in different binding modes. We required a diverse array of compounds to investigate the influence of structural features, such as valency and architecture. Therefore, we prepared a collection of multivalent ligands that can be grouped into five different structural classes of ligands. Within each class, we varied both the valency and density of binding epitopes. Each of these compounds (with the exception of control compounds) were derivatized with  $\alpha$ -mannosides for binding to Con A. For comparison, we included the compounds already examined in Section 3.4 for analysis. For all assays, the binding epitope concentrations were normalized by using a hexose assay. All data is presented in saccharide concentrations (except for the stoichiometric ratios given in Figure 3.15). Therefore, differences between ligands are due only to changes in *presentation* – not concentration – of saccharide.

The structures we chose are members of five general classes of molecules (Figure 3.13):

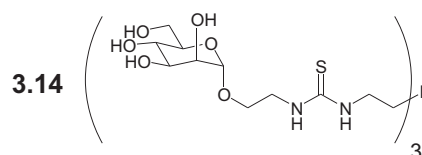
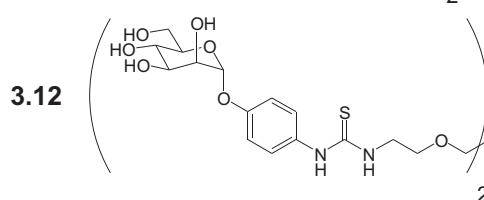
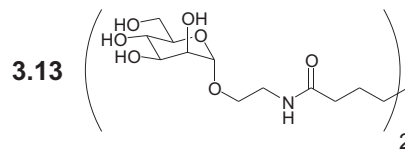
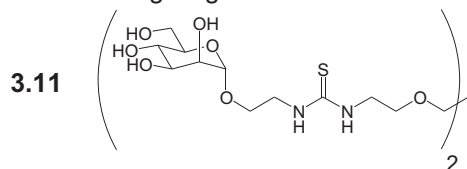
- 1) Low molecular weight compounds (**3.11-3.14**). This class contains both dimeric and trimeric structures with few binding epitopes (< 5 sites). Low molecular weight structures (ca. < 1000 Da) were generated and functionalized with an  $\alpha$ -mannoside according to previously described methods (Lindhorst and Kieburg, 1996; Woller and Cloninger, 2001).
- 2) Dendrimers (**3.15-3.16**). We chose poly(amidoamine) (PAMAM) dendrimers as representatives of this class of medium size multivalent molecules (ca. < 7500 Da) (Esfand and Tomalia, 2001). The interactions of similar compounds with Con A have been studied by other research groups (Page and Roy, 1997; Woller and Cloninger, 2002).
- 3) Globular Proteins (**3.17-3.20**). A common method for constructing multivalent carbohydrate ligands is to derivatize globular proteins, such as bovine serum albumin (BSA), with saccharides (Krantz *et al.*, 1976; Roseman and Baenziger, 2001). These ligands are generally large (~250,000 Da) and of medium valency (5-100 sites). Therefore, we prepared BSA conjugates with variable amounts (density) of mannose residues.
- 4) Linear Polymers (**3.22-3.35**). Multivalent saccharide-substituted polymers generated by ROMP have provided exceptionally active ligands for a number of different systems (Gestwicki and Kiessling, 2002; Manning *et al.*, 1997; Maynard *et al.*, 2001). An advantage of using ROMP for the production of these polymers is that the resulting materials can be of low polydispersity and possess a wide range of functional

groups (Fraser and Grubbs, 1995; Schrock *et al.*, 1995; Trnka and Grubbs, 2001). In addition to the variable-density ligands used for Section 3.4 (**3.29-3.35**), a series of variable valency polymers (**3.21-3.29**) was included to more completely represent this class of ligands (Kanai *et al.*, 1997; Kanai and Kiessling, 2002).

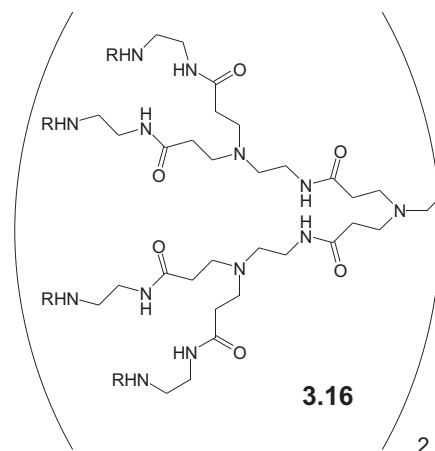
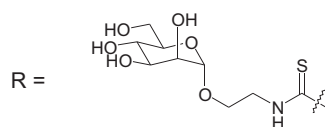
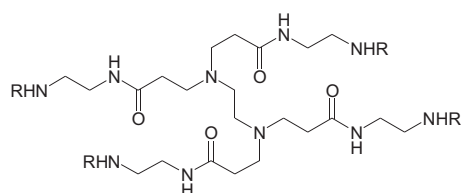
- 5) Polydisperse Polymers (**3.36-3.38**). We selected another polymer backbone with different characteristics from ROMP-derived ligands. Polyethylene-maleic anhydride (PEMA) polymers are commercially available and easily functionalized to provide multivalent saccharide presentations (Lu and Chung, 2000). These ligands are generally of high molecular weight (~100,000 Da) and of high valency (~700 sites). The polymers are generally of high polydispersities.

Our library consists of five general classes of ligands that vary in structure, and within each class we explore the influence of valency and epitope density. This library is intended, therefore, to provide a general survey of multivalent ligand architecture. Each of these ligands were tested with the battery of assays described. Analysis of these results provides some insight into the general features of each class.

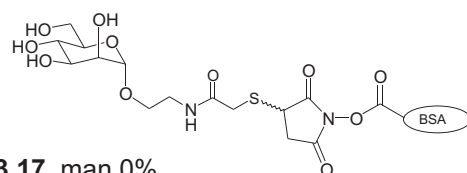
## Low molecular weight ligands



## Dendrimers



## Globular Proteins



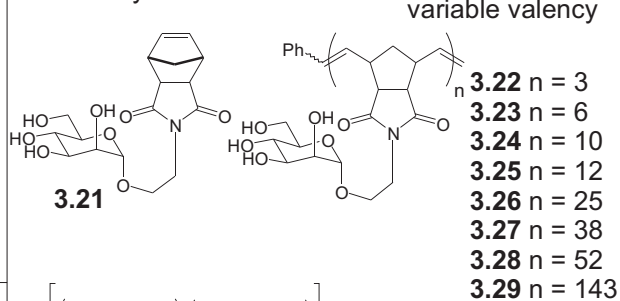
**3.17** man 0%

**3.18** man 56%

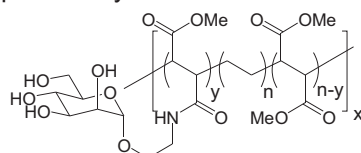
**3.19** man 23%

**3.20** man 13%

## Linear Polymers



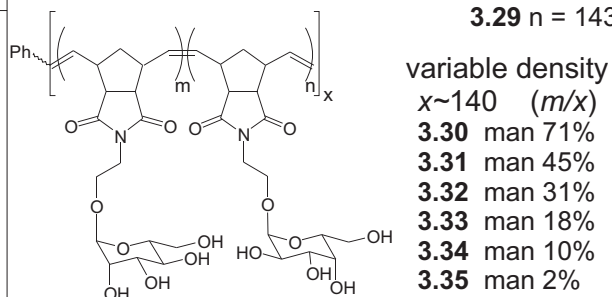
## Polydisperse Polymers



**3.36** y ~ 0 man 0%

**3.37** y ~ 200 man 50%

**3.38** y ~ 100 man 25%





**Figure 3.13. Structures of multivalent ligands used.**

In order to study the effects of ligand architecture, we assembled a small library of diverse multivalent ligands. The library consisted of small molecules (**3.11-3.14**), dendrimers (**3.15, 3.16**), protein conjugates (**3.17-3.20**), linear polymers (**3.22-3.35**), and polydisperse polymers (**3.33-3.38**). Several of these groups contained members with altered *density* and *valency* of binding sites.

### 3.5.2.1. Low molecular weight compounds.

Low molecular weight multivalent ligands used in our assays were effective inhibitors of Con A binding; however, they were poor clustering agents. Considering the low valency of these ligands ( $n = 2-3$ ), they achieve exceptionally good increases in functional affinity (avidity), as much as 60-fold using our inhibition assay (**3.12**). In addition, these compounds were able to crosslink receptors; however, they had very weak activity in QP assays, complexing  $\sim 1$  tetramer per molecule. Similarly, the rate of clustering was too slow to observe on the timescale of the turbidity experiments (10 min). Compound **3.12** was active in FRET assays, causing as much as a 40% change in FRET.

### 3.5.2.2. Dendrimers.

The dendrimer ligands used here showed modest gains in functional affinity, and were reasonably good clustering agents. The dendrimers we generated contain between 4-8 mannose residues; the best inhibitors showed as much as 300-fold increases in potency (**3.16**). Additionally, the dendrimers were able to cluster multiple Con A tetramers, 2-8 tetramers per ligand by QP. The dendrimers showed good rates of clustering based on turbidity measurements ( $< 0.25$  AU/min). Surprisingly, these ligands were incapable of eliciting any change in FRET signal in our experiments. The lack of FRET is likely due to the orientation or spacing of Con A tetramers in the complex.

### **3.5.2.3. Globular proteins.**

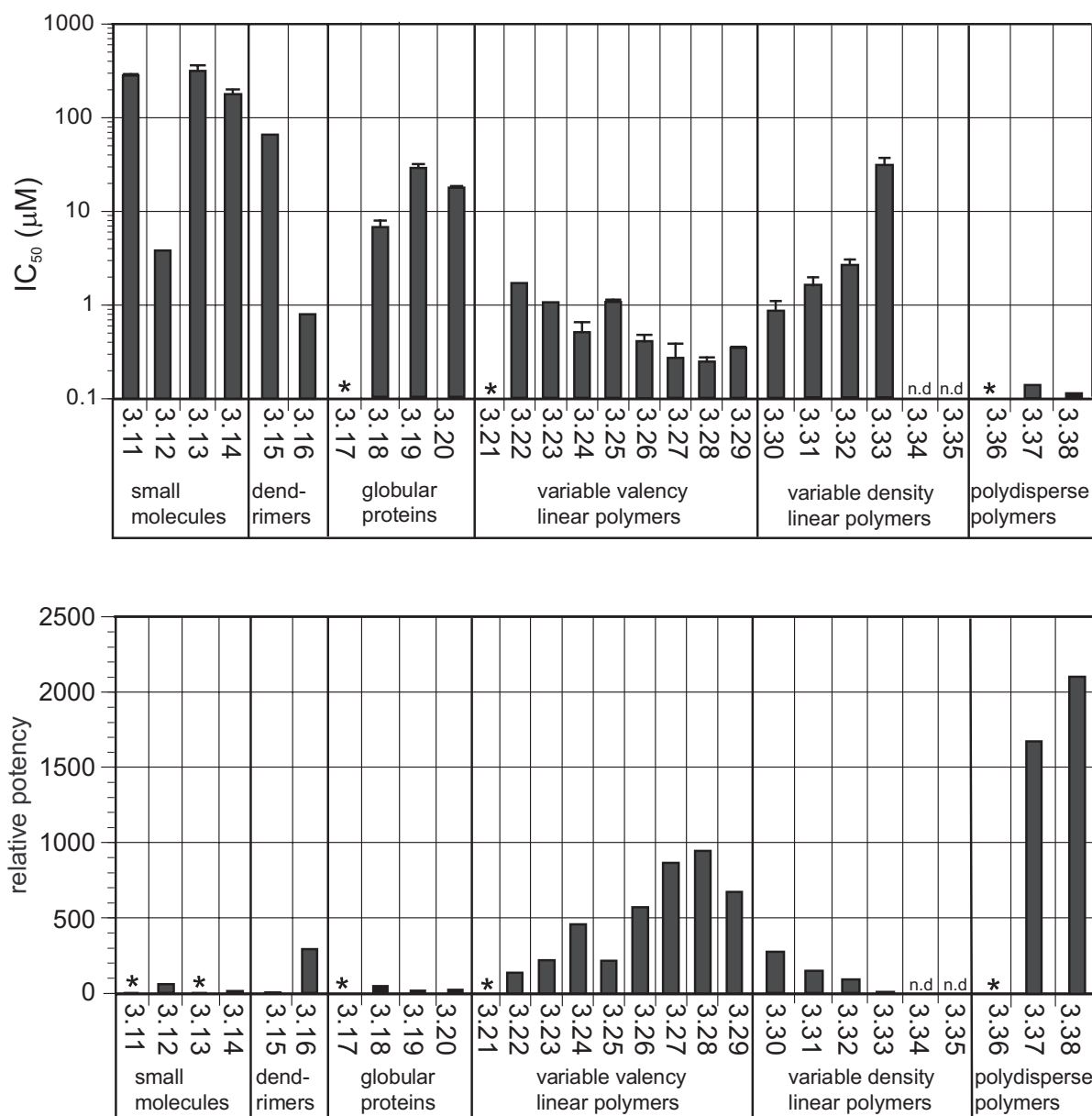
Protein conjugates were effective as both inhibitors and as mediators of clustering. The conjugates showed only modest improvements in functional affinity, generally they were 10-40-fold more effective inhibitors than  $\alpha$ -methyl-mannose. Mannose-substituted protein conjugates were able to complex 4-10 Con A tetramers per conjugate. Additionally, the rate of clustering was generally slow ( $< 0.1$  AU/min) and some conjugates with low binding epitope densities did not show any clustering over the course of the turbidity experiment. Globular proteins were able to induce modest changes in FRET, providing a maximum of 10% FRET in the highest density studied.

### **3.5.2.4. Linear polymers.**

Linear polymers were represented here by ligands produced using ROMP. These polymers consisted of two series, one series contains variable valency polymers and the other contains variable density polymers. Overall, these polymers showed excellent activity in every assay. The high density and high valency polymers were 900-fold more effective inhibitors than  $\alpha$ -methyl-mannose. QP assays showed that these ligands were capable of forming clusters of as many as 20 Con A tetramers per polymer. Ligands with the highest binding epitope densities gave the fastest rates of clustering ( $\sim 0.5$  AU/min) and these events quickly reached saturation. This class of ligands were superior for inducing changes in FRET, causing as much as 55% change in FRET signal.

#### **3.5.2.5. Polydisperse polymers.**

PEMA polymers represented a class of high-molecular weight polydisperse polymers. These polymers were superior in several assays, including inhibition of Con A binding and QP. Enhancements in inhibitory potency of these ligands were the largest observed in our study (> 2000-fold). PEMA-derived polymers also provided the highest stoichiometric ratios of Con A to ligand; they were capable of complexing more than 400 tetramers per polymer. In addition, these ligands were able to cause receptor clustering at good rates (0.1-0.3 AU/min). However, only small changes in FRET (20%) were observed in the presence of these ligands, indicating that the Con A tetramers in the complex were not in close proximity.

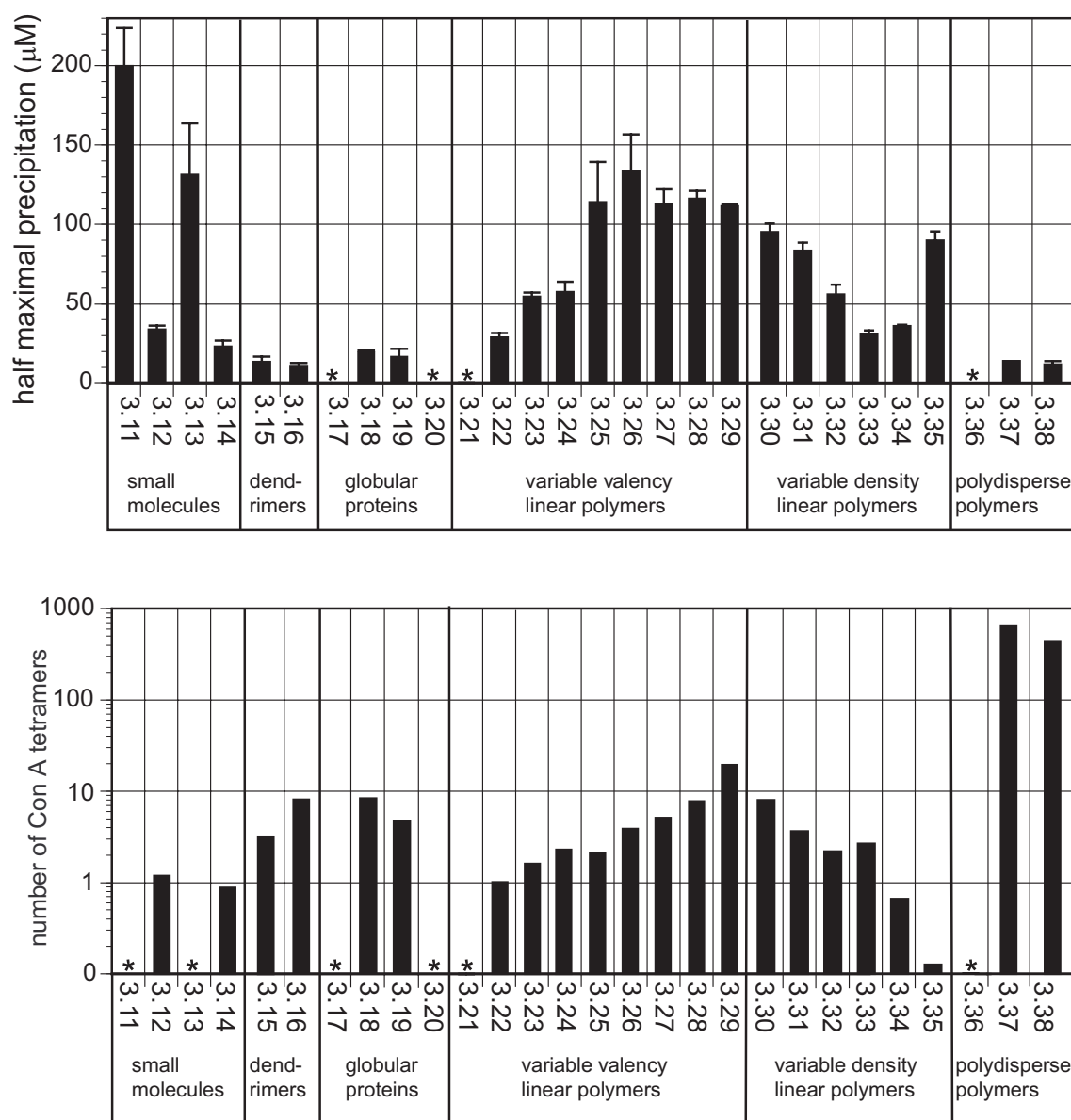


**Figure 3.14. Functional affinity of Con A binding to multivalent ligands.**

(Top) Solid-phase binding assays were used to determine the inhibitory potency of each ligand.  $IC_{50}$  values were determined by non-linear regression of inhibition curves derived from seven ligand concentrations. Concentrations were calculated on a per saccharide basis. Error bars represent the standard deviation. Asterisks denote compounds that were unable to inhibit Con A binding ( $IC_{50} > 1$  mM).

(Bottom) Inhibition data are represented potencies relative to  $\alpha$ -MeMan given as unity (230  $\mu M$ ). Asterisks denote compounds with  $IC_{50} > \alpha$ -MeMan.

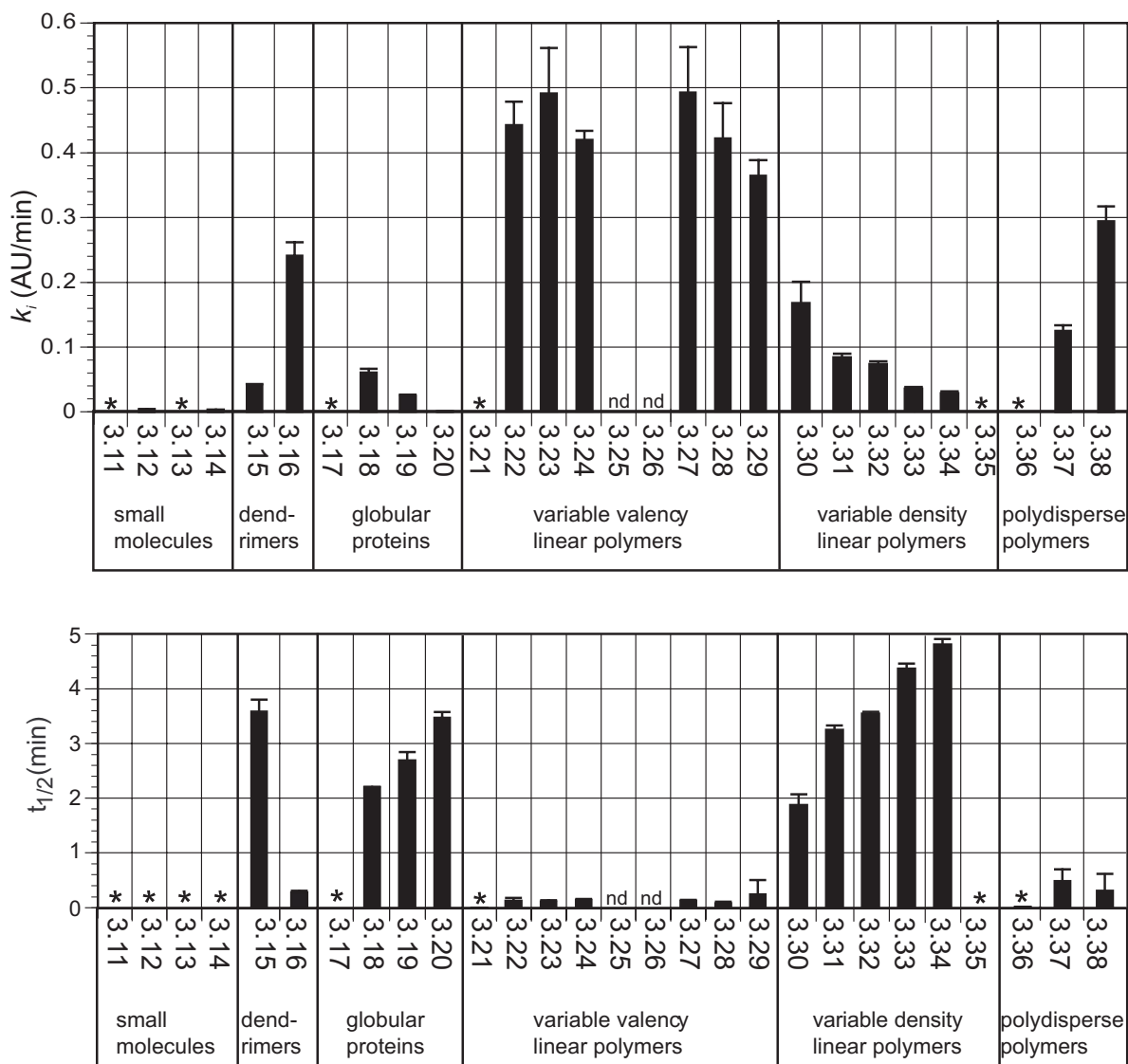
Compound structures are shown in Figure 3.13.



**Figure 3.15. Precipitation of Con A by multivalent ligands.**

(Top) Quantitative precipitation assays were used to determine the half maximal concentration required for Con A precipitation. Ligand concentrations were between 0.01- 300 μM or 0.001- 75 μM for compounds **3.17-3.20**. Each point represents the average of at least two replicates performed in duplicate. Concentrations were calculated on a per saccharide basis. The resulting curves were fit by non-linear regression to determine the half maximal concentration required for precipitation. Error bars represent standard deviation. Asterisks denote that precipitation was not observed.

(Bottom) Analysis of QP assays to determine the relative stoichiometries of Con A-ligand complexes. The values are extracted from the inflection point of the precipitation curve as described elsewhere. (Khan *et al.*, 1991) Asterisks indicate that no precipitation was observed or that analysis of the curve for stoichiometry could not be performed. Compound structures are shown in Figure 3.13.

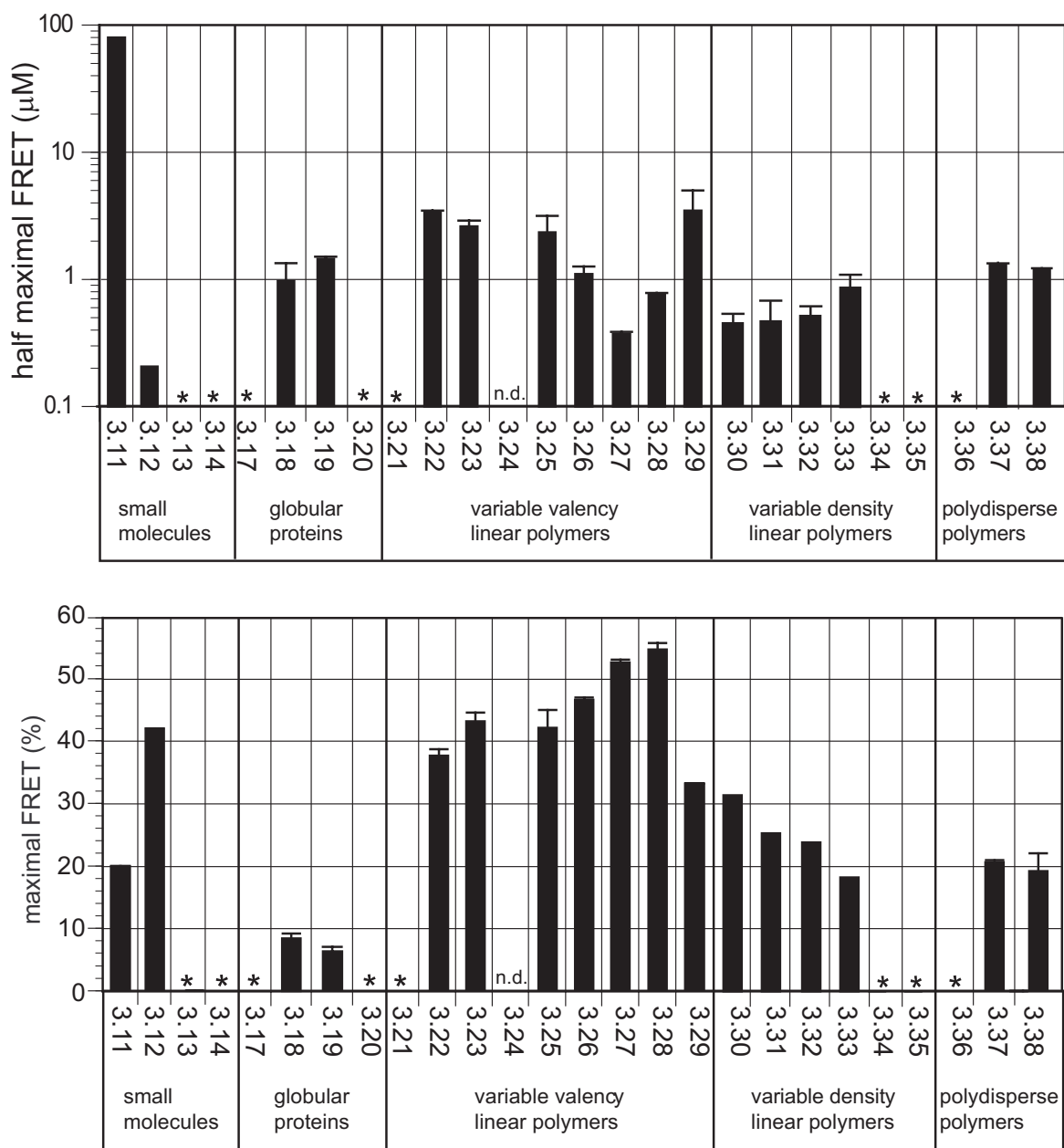


**Figure 3.16. Rate of precipitation of Con A by multivalent ligands.**

(Top) Turbidity experiments were performed in order to determine the rate at which complexation of Con A occurs in the presence of multivalent ligands. Analysis of the initial linear portion of the curve (peak rate) provides a determination of the relative rates of aggregation ( $k_i$ ). Each point represents three replicates, error bars represent the standard deviation of these determinations. All experiments were performed at the same per saccharide concentration. Asterisks denote that no precipitation was observed.

(Bottom) In the case of turbidity profiles that reached saturation, the time required for reaching half-maximal turbidity was determined ( $t_{1/2}$ ). Asterisks denote that no precipitation was observed or that the precipitation did not reach saturation within 10 minutes. nd = not determined.

Compound structures are shown in Figure 3.13.

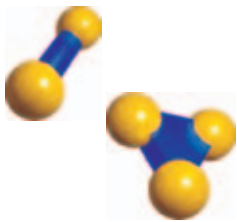

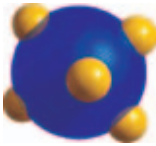




**Figure 3.17. FRET analysis of Con A complexes formed by multivalent ligands.**

(Top) FRET experiments were performed with fluorescein- and TMR-labeled Con A in solution at a total final concentration of 80 nM. Fluorescein emission was monitored relative to untreated control, and the results were fit by non-linear regression to determine the half maximal concentration for FRET. Each point represents the average of three experiments with a range of 10-12 concentrations between 0.001-50  $\mu\text{M}$ . Concentrations were calculated on a per saccharide basis. Error bars represent the standard deviation. Asterisks indicate that there was no change in FRET observed up to 50  $\mu\text{M}$  of ligand.

(Bottom) The maximal percent change in FRET signal for the Con A donor-acceptor pairs observed in the presence of each multivalent ligand. Asterisks indicate that there was no change in FRET observed up to 50  $\mu\text{M}$ . Compound structures are shown in Figure 3.13.



	Small Molecules	Dendrimers	Globular Proteins (BSA)	Linear polymers (ROMP)	Polydisperse polymers (PEMA)
					
Size (Da)	small 600-700	small 1,500-7,500	large ~250,000	medium 3,000-34,000	large ~100,000
Maximum Valency	low 2-3	variable 4-16	medium 5-100	variable 5-100	high 700
Inhibition	+	+	+	++	+++
Cluster size	+	++	++	++	++++
Rate	+	++	+	+++	++
FRET	++	-	+	+++	++

**Figure 3.18. Summary of the influence of different ligand architectures on Con A binding.**

General structural features of the ligands studied are summarized, including molecular weight and valency. The activities of each of these ligands are summarized for the assays used here.

*Inhibitory Potency (solid-phase binding assay):*

Average relative potency for each class 1-200 (+), 200-1000 (++), >1000 (+++).

*Stoichiometry (QP assay):*

Average ratio of receptor-ligand < 2 (+), 2-10 (++), 10-100 (+++), >100 (++++).

*Rate of aggregation (turbidity assay):*

Average  $k_i$  < 0.1 (+), 0.1-0.3 (++), > 0.3 (+++)(AU/min).

*Proximity of Receptors (FRET assay):*

Average maximum change in FRET < 10% (+), 10-30% (++), >30% (+++).

### 3.5.3. The architecture of a multivalent ligand affects its binding mode(s).

Using a library of compounds that vary in architecture, valency, and epitope density, we have shown that ligand structure has an important influence on receptor clustering and functional affinity. The assays employed provide determinations of the inhibitory potency, stoichiometry of clustering, rate of clustering, and proximity of receptors. Testing a diverse compound library in mechanistic assays provides insights into multivalent ligand function. These studies suggest the structural features that provide optimum activity for ligands that recognize their targets through a specific binding mode.

Each of the clustering assays we used provide an indication of a separate facet of the receptor clustering event. The Con A binding inhibition assay reports on which ligands are the most potent inhibitors. Activity in QP assays is an indication of the number of receptors a single ligand can interact with upon cluster formation. Therefore ligands with optimum activity in this assay could cluster the greatest number of receptors. Ligands that demonstrate fast rates in the turbidity assay should promote events that require rapid clustering. Finally, ligands that produce large changes in the fluorescence emission of donor- and acceptor-labeled receptors upon binding due to FRET should be able to bring individual receptors into close proximity.

What general structural trends do we observe for activity in each of these assays? (Figure 3.19) We find that linear polymers (derived from ROMP or functionalization of PEMA, **3.22-3.35**, Figure 3.13) are the most avid binders, showing as much as 2000-fold increases in inhibitory potency. Dendrimers (**3.15-3.16**), globular proteins (**3.18-3.20**) and small molecules (**3.11-3.14**) all show less enhancement over monovalent ligands. Linear polymers are the best ligands for interacting with large numbers of receptors in precipitation

assays. Dendrimers and globular proteins have less pronounced effects on precipitation. The fastest clustering reactions occur in the presence of high density ROMP-derived ligands, however both functionalized PEMA polymers and dendrimers induce moderate rates of clustering. Finally, ROMP-derived ligands are also superior for causing changes in proximity as observed by FRET, but both PEMA-functionalized compounds and small molecules are only moderately active.

Based on these results, we conclude that the presentation of binding sites in a linear polymer is generally optimum for Con A clustering activity. Defined polymers of medium length and high density tend to be optimal for high rates of clustering and FRET. Long polydisperse ligands of medium density tend to be optimum for increased inhibitory potency and binding of multiple receptors.

Using a structurally diverse library of multivalent ligands in combination with multiple assays we have been able to identify highly effective ligands for promoting Con A clustering. Our exploration of multivalent ligand architecture provides conclusions that may be general for the design of ligands that cause clustering. To establish generality, further investigations of the interaction of a multivalent ligand library with different receptors is required. Our studies here have been restricted to a single receptor structure, Con A. However, receptors with different numbers or orientation of binding sites could have different preferences for interaction. In part, the data presented here provide incentive for the pursuit of such questions. They demonstrate the value of structural optimization of multivalent ligand activity.

#### 3.5.4. Deciphering the rules of multivalent ligand design.

An intended goal of the studies described in this chapter is to determine whether general structural rules for multivalent ligand design can be developed. Full realization of this goal would require an extensive library consisting of series within each structural class that vary in parameters such as valency and density. Our current data set only contains systematic variations within a single structural class. The library sampled polymer displays derived from ROMP with variable valency (3.21-3.28) and variable density (3.29-3.35) and the results of this characterization may contain useful trends (Figure 3.13).

We have considered both series in our analysis above; however, comparison of both sets of data reveals some differences. The variable density series shows linear trends in all assays, with the exception of QP assays (Figure 3.8-3.11). Specifically, as the density of mannose residues increases the inhibitory potency, the rate of clustering, and the change in fluorescence due to FRET increases. The half maximal concentrations required for precipitation in QP also increased with increased density. The extremely low density polymers tested in QP assays were outside these trends, and showed greatly reduced activity in QP experiments. Presentation of the variable valency series in the same manner suggests similar linearity in both inhibition and FRET assays (Figure 3.18). It should be noted that very long polymers (3.29) disrupt this trend.

We suggest that these regions of linearity for these two series can provide useful guidelines for ligand design. It is important to emphasize that this empirical analysis does not provide a mechanistic interpretation for the trends, it only quantifies our observations. As seen here, deviation from these trends at the extremes of each parameter strongly support the

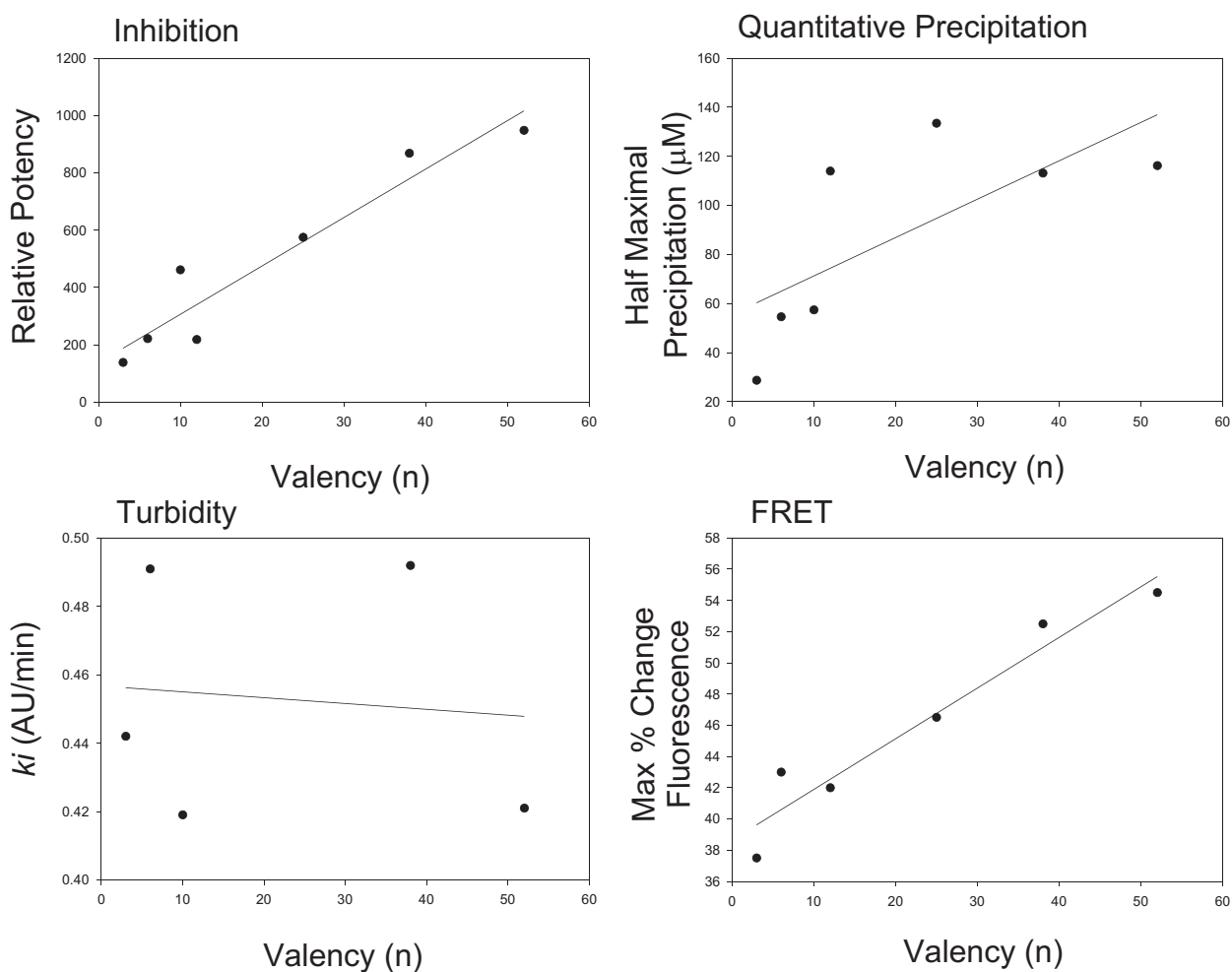
expectation that these trends may be oversimplified. With these caveats in place, a linear analysis of these results is a useful exercise.

Linear regression of assay results for compounds generated by ROMP are summarized in Table 3.3. For each assay, the quality of the fit ( $r^2$ ) and the slope of the fit ( $m$ ) are given. In the valency series, only the inhibitory potency and FRET results appear to follow a linear trend for polymer lengths of  $n = 3 - 52$  ( $r^2 > 0.9$ ). In the density series, all four assays follow linear trends between 10-100% ( $r^2 > 0.93$ ). For brevity, we relate each dependence to inhibitory potency measurements using a proportionality constant (Table 3.3). Therefore, comparison of the magnitude of the proportionality constants should provide a relative assessment of the resulting dependence of each activity on the parameter of density or valency.

Using this method of comparison, general relations within the data can be identified. We find that inhibitory potency is attenuated more dramatically by valency ( $m = 17$ ), rather than density ( $m = 8$ ). We also find that changes in FRET signal are attenuated equally well by both parameters ( $m = 0.2$  and  $0.3$ ). Therefore, we could conclude that to more efficiently design high avidity compounds that induce maximal FRET signal (*i.e.* close proximity of receptors), a polymer of high density and high valency should be employed.

Once trends have been described within a series, the proportionality constant ( $K_{av}$ ) becomes a predictive tool. In the density series we have found linear trends for all assays. Therefore, using the proportionality constants in each assay, we can predict the activity of new compounds in three assays from a single measurement of any other. For example, a measurement of a new compound's inhibitory potency could provide direct predictions of QP, turbidity, and FRET results.

We have restricted our analysis to linear trends, as these are the simplest to deconvolute. In the absence of data from more compounds, the determination of more complex relationships is untenable. Our current data set does provide useful trends within limited ranges. As mentioned above, the extreme regions of these parameters warrant more detailed investigation, and may require more complex descriptors of activity.



**Figure 3.19. Correlations between ligand valency and measured parameters.**

Plots of ROMP ligands (3.22-3.28) in each of the assays used versus the length of each polymer is shown. Each plot is fit by linear regression, a summary of these relations is given in Table 3.3. For comparison see Figures 3.7-3.10 with variable density ROMP ligands. Compound structures are shown in Figure 3.13.

**Table 3.3. Correlations for density and valency of polymers produced by ROMP.**

Valency      Compounds				
3.22-3.28      (n=3-52)				
	Functiona l Affinity	Turbidity	QP	FRET
r <sup>2</sup>	0.91	0.01	0.51	0.93
m <sup>a</sup>	17	-2	2	0.3
K <sub>av</sub> <sub>b</sub>	-	NA	0.09	0.02

Density      Compounds				
3.29-3.34      (100%-10%)				
	Functiona l affinity	Turbidity	QP	FRET
r <sup>2</sup>	0.95	0.96	0.96	0.93
m <sup>a</sup>	8.0	3.0	0.9	0.2
K <sub>av</sub> <sub>b</sub>	-	0.4	0.1	0.03

a. The units for slope of the fit are:

Functional affinity [Rel. Potency/n] or [Rel. Potency/%n].

Turbidity [(AU/min)/n] or [(AU/min)/%n].

QP [ $\mu$ M/n] or [ $\mu$ M/%n].

FRET [% Max. Change in Fl./n] or [% Max. Change in Fl./%n].

b. The proportionality constant  $K_{av}$  is derived by calculating the ratio of the fit slope of each parameter ( $m_i$ ) to the slope of the functional affinity ( $m_{av}$ ).  $K_{av}=(m_i)/(m_{av})$



### 3.6. Conclusions

The interaction of multivalent ligands with their receptors is generally complex, because it can involve multiple modes of binding. As a result, these interactions are difficult to characterize, and the design of new ligands for specific activity is often challenging. Here we have described the design of multivalent ligands for two different receptors: GGBP and Con A. In each case we examine the effect of structural parameters on multivalent binding. These studies provide useful examples of the controlling influence of multivalent ligand structure on binding interactions.

In contrast to monovalent ligand design, the design of multivalent ligands requires consideration of parameters such as attachment point, linker length, ligand valency, and ligand density. Additionally, the overall architecture of a multivalent ligand can influence its activity. We have used two series of multivalent ligands that differ in some or all of these parameters in order to assess the influence of these variables on multivalent ligand activity.

In our studies of multivalent ligands for GGBP, we designed potent new bacterial chemoattractants. Using molecular modeling, we determined the optimal attachment point and linker length for saccharides presented on a multivalent ROMP-derived ligand. The activities of ligands that varied in linker length to the polymer backbone support our molecular modeling predictions: the most potent attractants were those predicted to best accommodate the binding site of GGBP. Interestingly, optimized linker lengths only showed increased activity when presented on polymers of high valency. These studies support previous findings that multivalent presentation can provide improved selectivity. Additionally, the design of these ligands required consideration of attachment point, linker length, and valency of the multivalent ligands.

To more thoroughly explore the effects of ligand structure on multivalent binding, we studied the interactions of multivalent mannose ligands with the lectin Con A. Our approach to this problem required the implementation of multiple binding assays to report on different aspects of binding. A structurally diverse library of multivalent ligands was evaluated in these assays. This combination of diverse assays and compounds provides one of the most comprehensive studies of this kind. Our results suggest that, in the case of Con A, ROMP-derived ligands provide the most efficient presentation of binding sites. These ligands are some of the most potent inhibitors, and are of superior activity in turbidity and FRET assays to other ligands studied. Therefore, ROMP-derived ligands are highly effective at complexing multiple receptors and will remain a useful instrument in biological studies of receptor clustering.

Finally, we observe that systematic variation of multivalent ligand structure can provide useful indications of ligand activity. Variation of ROMP-derived ligands in both valency and density of binding epitopes provided several notable trends within individual assays. Determination of these trends could provide the means for *de novo* design of ligands with desired activity. Future investigations will require detailed exploration of these parameters within different structural classes of ligands. Studies that also compare the function of these ligands among different receptor structures will be of critical importance. Ultimately, the relation of observed trends for ligand activity between receptor classes will provide general guidelines for ligand design based solely on receptor structure.

### 3.7. Experimental materials and methods

#### *General Methods*

Con A and tetramethylrhodamine-labeled Con A (6.3 mol/mol average loading density) were obtained from Vector Laboratories, Inc. Burlingame, CA. Fluorescein-labeled Con A (7.5 mol/mol average loading density) was purchased from Sigma, St. Louis, MO. All other reagents were obtained from Sigma unless otherwise noted. All experiments were conducted using HEPES-buffered saline (HBS) unless otherwise noted (HEPES 10 mM, NaCl 150 mM, and CaCl<sub>2</sub> 1 mM adjusted to pH=7.4 and filtered using 0.2  $\mu$ m nylon filters). Concentrations of polymer stock solutions were estimated by gravimetric analysis and confirmed by the hexose assay (Dubois *et al.*, 1956; Fox and Robyt, 1991).

#### *Molecular Modeling*

Extended isotactic ROMP-derived polymers (**3.7**) were built *in silico* using Macromodel 6.5 (Schrodinger Inc., Portland, Oregon). These structures were minimized initially using distance constraints to induce an extended conformation, then minimized again without constraints. All calculations used the AMBER\* force field *in vacuo*.

Con A tetramer coordinates were retrieved from the protein data base as 1CVN. Multiple tetramers were generated by symmetry operations to produce Con A dimers with lattice symmetry. A random conformation of isotactic ROMP-derived polymer (**3.7**), n=50, was then arranged to interact with the binding sites of the tetramers. These components were arranged and then minimized in SYBYL 6.3 (Tripos Inc., St. Louis, MO). Images of the resulting coordinates were generated using Molscript 2.1 and Raster 3D.

Surfaces of the binding site of glucose-galactose binding protein (GGBP) were generated in GRASP 1.2 using coordinates retrieved from the protein data bank (PDB ID:

1GLG and 1GCG). Monosaccharides were docked to GGBP (PDB ID: 1GLG) using Autodock 2.4 (Goodsell *et al.*, 1996; Goodsell and Olson, 1990). For these runs the hydroxyl groups of the saccharides were allowed to rotate freely. Grid files for the docking simulations were 60 Å on each side. Resulting conformations were analyzed by cluster methods.

Optimal lengths for ethylene glycol linkers were determined by introducing monomer units with varying ethylene glycol linkages into the binding site of GGBP (1GLG with original ligand removed) using Macromodel 6.5. Each monomer was subjected to substructure molecular dynamics for 200 ps using the AMBER\* force field and GBSA water solvation. Each run was then analyzed by observing the interchain distances over the course of the simulation.

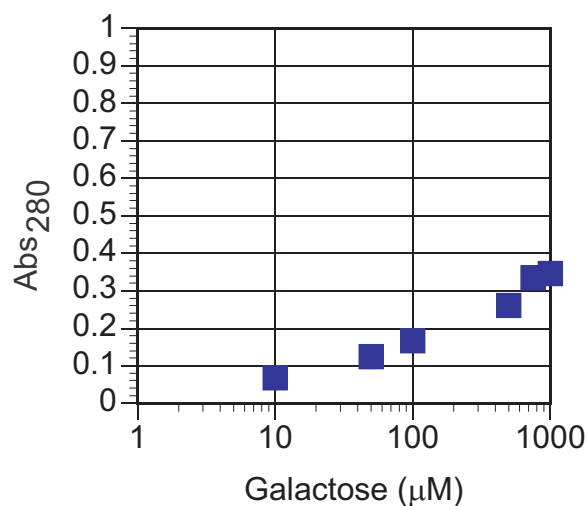
*Solid-phase binding assay.*

Micro-titer well plates activated with maleic anhydride (Reacti-bind polystyrene 96-well plates, Pierce, Inc.) were derivatized with mannose by the addition of a solution of 2-aminoethyl  $\beta$ -D-mannopyranoside (50  $\mu$ L, 1 mg/mL) in HBS. Plates were incubated for 60 minutes at 22 °C. Wells were washed twice with phosphate-buffered saline containing 0.1% Tween-20 and 1 mM  $\text{CaCl}_2$  (PBST- $\text{Ca}^{2+}$ ). Solutions of 50  $\mu$ g/mL fluoresceinated Con A (Vector Laboratories, Burlingame, CA) and mannose-bearing ligands **1-28** in PBST- $\text{Ca}^{2+}$  were incubated in the wells for 30 minutes at 22 °C. Wells were washed twice with PBST- $\text{Ca}^{2+}$  and once with HBS. Remaining fluoresceinated Con A was detached for analysis by the addition of 100  $\mu$ L of 100 mM methyl  $\alpha$ -D-mannopyranoside. After a 15 minute incubation, these solutions were transferred to cluster plates (Costar black with clear bottom cluster plate, Corning Inc., Corning NY) suitable for fluorescence analysis. Fluorescein emission intensity

was determined on a BioLumin plate reader using 5 nm slit widths, a PMT voltage of 850 V, an excitation wavelength of 480 nm, and emission wavelength of 520 nm.

#### *Quantitative Precipitation*

Quantitative precipitations and analysis were carried out by a method modified from that previously described by Khan, *et al.* (Khan *et al.*, 1991). Briefly, Con A and ligand were prepared in precipitation buffer (0.1 M Tris-HCl pH 7.5, 90 mM NaCl, 1 mM CaCl<sub>2</sub>, 1 mM MnCl<sub>2</sub>), vortexed briefly to mix, and then incubated for 5 h at 22 °C. The final concentration of Con A was 30 µM (assuming Con A tetramers with a molecular weight of 104,000 Da). White precipitates were pelleted by centrifugation at 5000 x g for 2 min. Supernatants were removed by pipette and pellets were gently washed twice with cold buffer. Pellets were then resuspended in 600 mL of 100 mM methyl α-D-mannopyranoside, and were completely dissolved after a 10 min incubation at room temperature. Protein content was determined by measuring the absorbance at 280 nm by UV-Vis spectroscopy on a Varian Cary 50 Bio using a 100 mL volume quartz cuvette with a 1 cm pathlength. Measurements are the average of three independent experiments with 2 scans performed in each experiment. Experiments also were performed using control polymers bearing only galactose residues (Figure 3.20) to demonstrate that polymeric galactose is unable to cause significant precipitation of Con A.



**Figure 3.20. Precipitation of Con A by galactose polymers.**

To test the ability of the “non-binding” galactose residue used in the variable density mannose polymers (compounds **3.29-3.35**), we performed QP experiments with galactose homo-polymers (n=50). The resulting precipitation profile is shown. These data support that galactose is a weak ligand for Con A, and that precipitation caused by galactose residues for compounds **3.29-3.35** should not be significant. Compound structures are shown in Figure 3.13.

*Turbidimetric Assay*

Con A was diluted fresh for all experiments. The lectin was dissolved at ~1 mg/mL in HBS buffer, and the resulting solution was mixed and sterile filtered (2  $\mu$ m). The concentration of the Con A stock solution was determined using UV absorbance at 280 nm ( $A_{280} = 1.37 \times [\text{mg/mL Con A}]$ ). The solution was then diluted to 1  $\mu$ M (based on Con A tetramer at 104,000 Da). Turbidity measurements were performed by adding 100  $\mu$ L of the diluted Con A solution to a dry quartz micro-cuvette (100  $\mu$ L volume, 1 cm pathlength). A solution of the ligand of interest in HBS buffer was then added (10  $\mu$ L at 500  $\mu$ M, final concentration was 50  $\mu$ M per mannose residue). Upon addition, the solution was mixed vigorously for 5 s using a micropipette and then placed in the spectrometer. Absorbance data were recorded at 420 nm for 10 min at 1 Hz. Each sample was run three times, the steepest portion of the initial aggregation was then fit to determine the rate of aggregation. Error was determined as the standard deviation of the three rates. Curves shown are the average of all three runs. To establish that the aggregation process was a result of specific binding of saccharide epitopes to the lectin, competition experiments were also performed. Complexes between Con A and multivalent ligands were produced as above (5  $\mu$ M Con A, 50  $\mu$ M saccharide). The resulting solutions were allowed to stand for 1 hr at room temperature. The turbid solution was then placed in a dry quartz micro-cuvette (100  $\mu$ L volume, 1 cm pathlength) and the absorbance at 420 nm was recorded (T=0 min). A solution of methyl- $\alpha$ -D-mannopyranoside was then added (10  $\mu$ L at 54  $\mu$ M, final concentration 5  $\mu$ M) and mixed for 5 seconds. The change in absorbance (at 420 nm) was monitored as a function of time. The final absorbance (T=10 min) was determined as an average of the last 10 seconds of this run.

The percent change in absorbance was determined as  $(T_0 - T_{10})/T_0$ , the results are represented in Table 3.4. The resulting data indicate that the ability of monovalent methyl- $\alpha$ -D-mannopyranoside to disrupt the aggregates depends on the binding epitope density of the multivalent ligand template employed.

**Table 3.4. Reversal of aggregation by a competitive ligand.**

<i>Compound (Density)</i>	$T_0$	$T_{10}$	$\%Change(T_0 - T_{10})/T_0$
<b>3.29</b> (100%)	0.34	0.24	29.6
<b>3.30</b> (71%)	0.56	0.27	51.8
<b>3.31</b> (45%)	0.61	0.22	64.4
<b>3.32</b> (31%)	0.75	0.16	78.9
<b>3.33</b> (18%)	0.64	0.11	83.5
<b>3.34</b> (10%)	0.67	0.11	84.0

#### *Fluorescence Resonance Energy Transfer*

Stock solutions of tetramethyl rhodamine-Con A and fluorescein-Con A were resuspended in HBS to 400 mg/mL. Ligand was suspended in distilled H<sub>2</sub>O to 10x of the final concentration by serial dilution from a 20  $\mu$ M stock. Ligand and Con A solutions were mixed in 96-well plates (Costar black with clear bottom cluster plate, Corning Inc., Corning NY). The final concentrations of rhodamine-Con A and fluorescein-Con A were each 4 mg/mL. The final concentration of ligand is varied over the concentration range of 0.001-100  $\mu$ M mannose residues. The final volume was brought to 100  $\mu$ L with HBS. Solutions were mixed by gentle tapping and then incubated at 22 °C for 30 min in the dark. Fluorescein emission was measured on a BioLumin plate reader using 5 nm slit widths, a PMT voltage of 850 V,



excitation wavelength of 485 nm, and emission wavelength of 520 nm. Results are the average of two experiments performed in duplicate. Error represents the standard error of the mean. The maximum percent change in fluorescence to calculate the change in average distance between receptors is shown in Table 3.5. It should be noted that a similar change in fluorescence could result from changes in the population of proximal receptors rather than changes in the average distance between receptors.

**Table 3.5. Average distance calculations for FRET (Compounds 3.29-3.35).**

<i>%</i>	<i>r</i>	+/ -
<i>Mannose</i>		
100	60	2
71	62	1
45	63	1
33	67	1
18	70	1
10	ND	
2	ND	

Calculation of Average Inter-Receptor Distances. Average inter-Con A distances were calculated using the maximum % change in FRET as described previously (Matko and Edidin, 1997). The Förster distance used for calculations was 54 Å (Wu and Brand, 1994).

*High throughput FRET assay.*

The FRET experiments were performed with some minor modifications to the procedure described previously (Burke *et al.*, 2000; Gestwicki *et al.*, 2002c). The

modifications were made to allow more rapid analysis of samples in 96-well plates. Con A derivatives with fluorescent labels (4  $\mu\text{g/mL}$  of fluoresceinated and rhodamine-labeled Con A, Vector Laboratories, Burlingame, CA) and ligand were added to the wells of black cluster plates in a final volume of 100  $\mu\text{L}$ . The buffer was calcium-enriched HBS (HBS with 1 mM  $\text{CaCl}_2$ ). Solutions were mixed by gentle tapping and then incubated at 22  $^\circ\text{C}$  for 30 minutes in the dark. Fluorescein emission was measured on a BioLumin plate reader using 5 nm slit widths, a PMT voltage of 850 V, excitation wavelength of 485 nm, and emission wavelength of 520 nm. Ligands had negligible fluorescence at 520 nm. Half-maximal fluorescence values were determined by fitting data to non-linear curves.

*Ligand synthesis.*

Precursors to ligands **3.11-3.20** and **3.36-3.38** were obtained from commercial sources, as indicated. Mannose residues were appended to these scaffolds using the reagents 2-aminoethyl  $\beta$ -D-mannopyranoside, [*p*-isothiocyanato]-phenyl  $\alpha$ -D-mannopyranoside or [2-isothiocyanato]-ethyl  $\alpha$ -D-mannopyranoside. These were generated from mannose using known procedures (Lindhorst and Kieburg, 1996; Page and Roy, 1997). The concentrations of all ligands were calculated by hexose determination, as described (Dubois *et al.*, 1956; Fox and Robyt, 1991), using mannose as a standard. The concentrations of **3.17** and **3.36** could not be calculated in this fashion, as these ligands did not bear saccharide modifications. The concentration of these control compounds was determined by gravimetric or spectrophotometric analysis, and the concentrations employed corresponded to the maximum functionalized scaffold concentrations used (e.g. the concentration of **3.16** employed was the same as the concentration of **3.38**).

*Low molecular weight compounds (3.11-3.14):*

Compound **3.11**. 2,2'-(Ethylenedioxy)bis(ethylamine) (3.2  $\mu$ L, 0.022 mmol, 1 equivalent, Pierce, Inc. Rockford, IL) was reacted with [2-isothiocyanato]-ethyl  $\alpha$ -D-mannopyranoside (17.6 mg, 0.066 mmol, 2.5 equivalents) in water. The product was dialyzed (100 molecular weight cutoff (mwco), 24 hours, 4x250 mL), and compound **3.11** was isolated as a solid (14.6 mg) in 98% yield. The product was purified by column chromatography using a 5:4:1  $\text{CH}_2\text{Cl}_2$ :MeOH:H<sub>2</sub>O solvent system. <sup>1</sup>H NMR (300 MHz, 80% DMSO- $d_6$ , 20% D<sub>2</sub>O)  $\delta$  4.6 (s, 2H);  $\delta$  3.6-3.3 (m, 30 H);  $\delta$  1.2 (t, 4H). MALDI-TOF:  $m/z$  = 701.4 [ $\text{M}^+\text{Na}^+$ ] ( $\text{M}^+\text{Na}^+$  cal. 701).

Compound **3.12**. 2,2'-(Ethylenedioxy)bis(ethylamine) (2.5  $\mu$ L, 0.0168 mmol, 1 equivalent, Pierce, Inc. Rockford, IL) was treated with [p-isothiocyanato]-phenyl  $\alpha$ -D-mannopyranoside (12.3 mg, 0.042 mmol, 2.5 equivalents) and triethylamine (7 mL 0.0506 mmol, 3 equivalents) in a methanol/water mixture (1:1 200  $\mu$ L total volume). The product was dialyzed (100 mwco, 24 hours, 4x250 mL) and compound **3.12** was isolated (4.7 mg) in 36% yield. <sup>1</sup>H NMR (300 MHz, 80% DMSO- $d_6$ , 20% D<sub>2</sub>O)  $\delta$  6.9 (s, 8H);  $\delta$  5.4 (d, 2H);  $\delta$  4.0 (m, 2H);  $\delta$  3.8 (dd, 2H);  $\delta$  3.6-3.4 (m, 20H). MALDI-TOF:  $m/z$  = 797.3 [ $\text{M}^+\text{Na}^+$ ] ( $\text{M}^+\text{Na}^+$  cal. 797).

Compound **3.13**. Bis(sulfosuccinimidyl) suberate (5 mg, 0.00874 mmol, 1 equivalent, Pierce, Inc. Rockford, IL) was treated with 2-aminoethyl  $\beta$ -D-mannopyranoside (7.79 mg, 0.0349 mmol, 4 equivalents) in 200  $\mu$ L dimethylsulfoxide (DMSO). The reaction was allowed to proceed for 3 hours at 22 °C. Water was added to allow dialysis (500 mwco, 24 hours, 2x1000 mL). The resulting solution was lyophilized to afford compound **3.13** as a solid (4.2

mg) in 83% yield.  $^1\text{H}$  NMR (300 MHz, 80% DMSO- $\text{d}_6$ , 20%  $\text{D}_2\text{O}$ )  $\delta$  4.7 (s, 2H);  $\delta$  3.8-3.2 (m, 20H);  $\delta$  2.0 (m, 4H);  $\delta$  1.4 (m, 4H);  $\delta$  1.2 (s, 4H). MALDI-TOF:  $m/z$  = 607.3 [ $\text{M}^+\text{Na}^+$ ] ( $\text{M}^+\text{Na}^+$  cal. 607.2).

Compound **3.14**. Tris(2-aminoethyl)amine (2.4  $\mu\text{L}$ , 0.0159 mmol, 1 equivalent, Pierce, Inc. Rockford, IL) was reacted with [2-isothiocyanato]-ethyl  $\alpha$ -D-mannopyranoside (19 mg, 0.0717 mmol, 4.5 equivalents) in water. The product was dialyzed (100 mwco, 24 hours, 4x250 mL) and compound **3.14** was purified by column chromatography using a 5:4:1  $\text{CH}_2\text{Cl}_2$ :MeOH: $\text{H}_2\text{O}$  solvent system. Compound **3.14** was obtained as a solid (7.5 mg) in 50% yield.  $^1\text{H}$  NMR (300 MHz, 80% DMSO- $\text{d}_6$ , 20%  $\text{D}_2\text{O}$ )  $\delta$  4.6 (s, 2H);  $\delta$  3.6-3.4 (m, 18H);  $\delta$  3.3 (m, 18H);  $\delta$  2.6 (m, 12H). MALDI-TOF:  $m/z$  = 964.4 [ $\text{M}^+\text{Na}^+$ ] ( $\text{M}^+\text{Na}^+$  cal. 964).

*Dendrimers (3.15-3.16)*: Starburst PAMAM dendrimers were obtained from Aldrich as 20 wt% solutions in methanol. Dendrimers **3.15** and **3.16** were prepared as described by Woller and Cloninger (Woller and Cloninger, 2001). Compound **3.15**  $^1\text{H}$  NMR (300 MHz, 80% DMSO- $\text{d}_6$ , 20%  $\text{D}_2\text{O}$ )  $\delta$  4.3 (s, 4H);  $\delta$  3.8-3.1 (m, 56H);  $\delta$  2.7 (m, 8H);  $\delta$  2.5 (s, 4H);  $\delta$  2.3 (m, 8H). MALDI-TOF:  $m/z$  = 1577.7 [ $\text{M}^+$ ] (cal. 1577). Compound **3.16**  $^1\text{H}$  NMR (300MHz, 80% DMSO- $\text{d}_6$ , 20%  $\text{D}_2\text{O}$ )  $\delta$  4.6 (s, 8H);  $\delta$  3.8-3.2 (m, 48H);  $\delta$  3.1 (m, 48H);  $\delta$  2.7-2.5 (m, 36H);  $\delta$  2.4-2.0 (m, 48H). MALDI-TOF:  $m/z$  = 3312.8 [ $\text{M}^+\text{Na}^+$ ] ( $\text{M}^+\text{Na}^+$  one unreacted site cal. 3311).

*Globular protein conjugates (3.17-3.20)*: A thiol was appended to 2-aminoethyl  $\beta$ -D-mannopyranoside (3 mg/mL in DMSO) by reaction with the *N*-hydroxysuccinimidyl ester of *S*-acetylthioacetic acid (SATA, 2 equivalents, Pierce, Inc. Rockford, IL). The reaction was conducted for 2 hours at 22  $^\circ\text{C}$ . Remaining SATA was removed by scavenger resin (100-fold

molar excess of amines). After removal of the resin, the thioester was treated with 0.5 M hydroxylamine (100  $\mu$ L, 10 mM phosphate buffer, 25 mM EDTA, pH 7.2, 15 minutes) to reveal the thiol group. The thiol-containing mannose derivative was added to 10 mg/mL IMJECT BSA (maleimide-activated bovine serum albumin, Pierce, Inc. Rockford, IL) in phosphate buffered saline (PBS) pH 7.1. IMJECT BSA contains approximately 20 maleimides per BSA, according to manufacturer specifications. Mannosylation reactions were performed for 2 hours at 22  $^{\circ}$ C on a rotary shaker. Cysteine (100  $\mu$ L, 30  $\mu$ M) was added to quench the unreacted maleimides. Shaking was continued for 1 hour at 22  $^{\circ}$ C. The resulting solution was dialyzed (7000 mwco, 2x1000 mL) overnight against 10 mM HBS (10 mM HEPES, 150 mM NaCl, pH 7.5). Compounds **3.18-3.20** were isolated. Control compound **3.17** was not treated with 2-aminoethyl  $\beta$ -D-mannopyranoside, but otherwise received identical treatment.

*Linear defined polymers (3.21-3.35):*

The syntheses and characterization of **3.21-3.35** are reported elsewhere (Kanai *et al.*, 1997; Kanai and Kiessling, 2002). Polymer length (degree of polymerization) was confirmed by integration of  $^1\text{H}$  NMR peaks. Briefly, to the solution of the mannose bearing monomer (36 mg, 0.098 mmol) and dodecyltrimethylammonium bromide (DTAB) (48 mg, 0.16 mmol, 1.6 eq) in water (310  $\mu$ L), was added catalyst  $[\text{Ru}=\text{CHPh}(\text{Cl})_2(\text{PCy}_3)_2]$  (0.8 mg, 0.00098 mmol, 0.01 eq) in  $\text{CH}_2\text{Cl}_2$  (150  $\mu$ L). The mixture was stirred vigorously for 20 hr at room temperature. After workup and purification, polymer **3.29** was obtained as a colorless film (24 mg, 67%). The degree of polymerization determined from  $^1\text{H}$  NMR is 143 (**3.29**).

*Characterization of Multivalent Ligands (3.29-3.35):*

$^1\text{H}$  and  $^{13}\text{C}$  NMR spectra were recorded on a Bruker WP-300 or a Bruker AM-500 Fourier Transform NMR spectrometer. Polymers were synthesized using emulsion conditions with a monomer to catalyst ratio of 100:1 ( $\text{M/C} = 100$ ) as previously described (Kanai *et al.*, 1997), using various ratios of mannose and galactose monomers (Kanai and Kiessling, unpublished results). The ratio of the two saccharides within the polymer was analyzed from the intensity of the anomeric protons by  $^1\text{H}$  NMR: (mannose-1-H at 4.86 ppm and galactose-1-H at 4.93 ppm). As shown in Table 3.6, the polymers obtained reflect the mannose/galactose ratios employed in their synthesis. These data indicate that there is no detectable reactivity difference between mannose- and galactose-bearing monomers.

**Table 3.6. NMR Characterization of DP for compounds 3.29-3.35.**

Entry	% Man <i>a</i>	% Man (NMR) <i>b</i>	<i>n</i> <sup>c</sup>	yield/% <sup>d</sup>
<b>3.29</b>	100	100	143	67 (95)
<b>3.30</b>	71	71	145	78 (89)
<b>3.31</b>	45	45	115	81 (85)
<b>3.32</b>	31	33	86	77 (83)
<b>3.33</b>	18	18	102	47 (69)
<b>3.34</b>	10	10	116	70 (85)
<b>3.35</b>	2	ND	129	87 (95)

- a.* Percent mannose incorporation based on ratio of mannose to galactose monomers used in the polymerization.
- b.* Percent mannose incorporation based on integration of mannose- and galactose-1-H by <sup>1</sup>H NMR.
- c.* The value *n* is defined as the degree of polymerization (DP) for the reaction determined from <sup>1</sup>H NMR.
- d.* Isolated yield. Yields estimated from NMR are in parentheses.

*Polydisperse polymers (3.36-3.38):* 2-Aminoethyl β-D-mannopyranoside (4.42 mg, 0.5 equivalents, 0.1 mg/mL) and polyethylene maleic-anhydride (PEMA) polymers (10 mg, 35 mg/mL, Polysciences Inc., Warrington, PA) were dissolved in DMSO. The PEMA was considered to be an average molecular weight of 100,000 (according to manufacturer specifications), which constitutes an average of 400 maleic anhydride and 400 ethylene units per polymer chain. The conjugation reaction was agitated for 3 hours at 22 °C on a rotary shaker. The remaining maleic anhydride groups were quenched with addition of 100 μL distilled water and the product was treated with a 2-fold molar excess of TMS-diazomethane

to methylate any carboxylic acid groups. Solutions were brought to <25% DMSO by the addition of distilled water, dialyzed overnight (7000 mwco, 2x1000 mL), and compound **3.38** was isolated. Similar conditions were used to generate compound **3.37**. Control polymer **3.36** was generated by addition of ethanolamine in place of the mannose-derivative.



## Chapter 4. Controlling Receptor Clustering *in vitro* using Synthetic Multivalent Ligands

Portions of this work are in preparation:

“Modulation of Con A toxicity using Synthetic Multivalent Ligands,” Cairo, C.W., Gestwicki, J.E., Kiessling, L.L., *in preparation*.

Contributions:

Compounds **4.1** and **4.2** were contributed by F.J. Boehm and R.M. Owen.

Compound **4.4** was contributed by B.R. Griffith.

IC<sub>50</sub> determination of  $\alpha$ -Fas IgM was contributed by E. Underbakke (Figure 4.10.3).

#### 4.1. Abstract.

With the methods to quantitate the activity and binding mechanisms of multivalent ligands outlined in Chapter 3, we sought to apply information from those assays to interactions at the cell surface. Specifically, we wanted to test if our model studies using lectin clustering could be directly applied to activate signaling through receptors in the cell membrane. In the first part of Chapter 4, we describe our results from testing the ability of scaffolded lectins to cluster cell surface receptors in sensitive cell lines. In the second part, we explore the generality of our findings using a specific cell surface target, the Fas receptor. In both systems synthetic multivalent ligands function as powerful reagents for the control of signal transduction. Our findings are consistent with findings in Chapter 3 that suggest linear polymers are able to assemble lectin complexes.

Oligomeric lectins are well known as potent mitogens and cell activators (Anderson, J. *et al.*, 1976). This activity is due to their ability cluster cell surface receptors. As a result, lectins have been used to activate signal transduction. For example, the lectin concanavalin A (Con A) is known to induce apoptosis in sensitive cell types by clustering glycosylated cell-surface receptors (Cribbs *et al.*, 1996). This apoptotic activity is dependent on whether the dimeric or tetrameric form of the lectin is employed; the tetrameric form is active but the dimeric form is not. Therefore, ligands that modulate the oligomerization state of Con A could be used to control its toxic effects. We anticipated that multivalent mannose-substituted polymers could be used as scaffolds to assemble multiple copies of Con A (Gestwicki *et al.*, 2002c). These complexes could bind to and cluster cell-surface glycoproteins. Thus, we reasoned that multivalent mannose-displaying ligands could modulate the toxic effects of Con A. Because tumor cells often have patterns of glycosylation that are distinct from normal cells

(Kim and Varki, 1997), such ligands could be useful for promoting apoptosis of unwanted cells.

Using three cell lines that undergo apoptosis in response to Con A treatment (PC12, SW837, and HCT15), we characterized the ability of multivalent ligands to modulate Con A-induced apoptosis. In the presence of mannose-bearing polymers, the toxic effects of Con A can be enhanced by at least 40-fold. Fluorescence microscopy experiments reveal that Con A – polymer complexes cluster cell-surface receptors more effectively than Con A alone. Together these data indicate that oligomeric assemblies of soluble lectins can function as powerful mediators of signaling events that depend on receptor clustering.

In the second part of Chapter 4, studies directed at examining the generality of our approach are illustrated. We identified a signal transduction event with potential for biotechnological applications: crosslinking of the Fas receptor. Fas is a member of the TNF family of cell surface receptors and is found on many cells in the immune system and some cancerous cells (Weller *et al.*, 1998). Clustering of Fas results in apoptosis in sensitive cells (Belshaw *et al.*, 1996). Several tumor lines are known to produce Fas, and these cells are found in predominantly Fas(-) tissue (Weller *et al.*, 1998). Therefore, reagents for clustering of this receptor could have potential as chemotherapeutics. We designed a semi-synthetic conjugate that incorporates antibody Fab' fragments that bind Fas. Treatment of appropriate cells with conjugates that present Fas-binding units on a multivalent backbone should cause Fas clustering on relevant cell surfaces, thereby leading to apoptosis. Using cultured Fas(+) cells, we demonstrate that this strategy is feasible and that the multivalent conjugates are more potent than more conventional clustering agents, such as antibodies.

#### **4.2.1. Receptor clustering using multivalent lectins.**

Multivalent lectins have long been used as reagents for the study of cell surface receptors (Anderson, J. *et al.*, 1976). They often are used as reagents for the detection of cell surface glycoproteins (Anderson, J. *et al.*, 1976; Lis and Sharon, 1998). Additionally, many are well known as T-cell activators and mitogens (Kilpatrick, 1999). Under appropriate conditions, lectins are also known to have cytotoxic effects (Gorelik, E., 1998; Schwarz *et al.*, 1999). For example, the sensitivity of transformed cells to Con A is often different from normal tissue; which is consistent with studies showing tumor cells can have glycosylation patterns distinct from normal cells (Kim and Varki, 1997). As a result, lectin toxicity has been explored as a potential tumor-targeting strategy (Nicolson, G. L., 1976). A major disadvantage of using lectins as cytotoxic agents for tumor cells is that these proteins can cause systemic mitogenicity and toxicity. As a result, methods to control the toxicity of lectins would improve the prospects for this strategy.

#### **4.2.2. Con A-induced apoptosis.**

One of the best-characterized lectins is the tetrameric plant lectin, Con A. Con A binds mannose-containing oligosaccharides with good affinity ( $K_d \sim 2 \mu\text{M}$ ), and it also can bind monosaccharides, such as mannose, albeit more weakly ( $K_d \sim 0.1 \text{ mM}$ ) (Toone, 1994). Con A is toxic to a number of cell types including murine neuronal cells (Cribbs *et al.*, 1996), and human colorectal (Kiss *et al.*, 1997) and melanoma cells (Lorea *et al.*, 1997) (Table 4.1). The mechanism of lectin-induced apoptosis is not completely understood; however, key features have been established.

Lectin toxicity requires the presence of lectin-binding sites at the cell surface. Presumably, the lectin binds to glycosylated cell-surface proteins. This condition is necessary, but not sufficient, for activity. Cell death caused by Con A is the result of apoptosis (Cribbs *et al.*, 1996; Kim *et al.*, 1993; Kulkarni *et al.*, 1998; Kulkarni and McCulloch, 1995; Nagase *et al.*, 1998; Schwarz *et al.*, 1999). As a result, the toxicity of lectins can be readily measured using cell viability assays (Cribbs *et al.*, 1996; Gieni *et al.*, 1995).

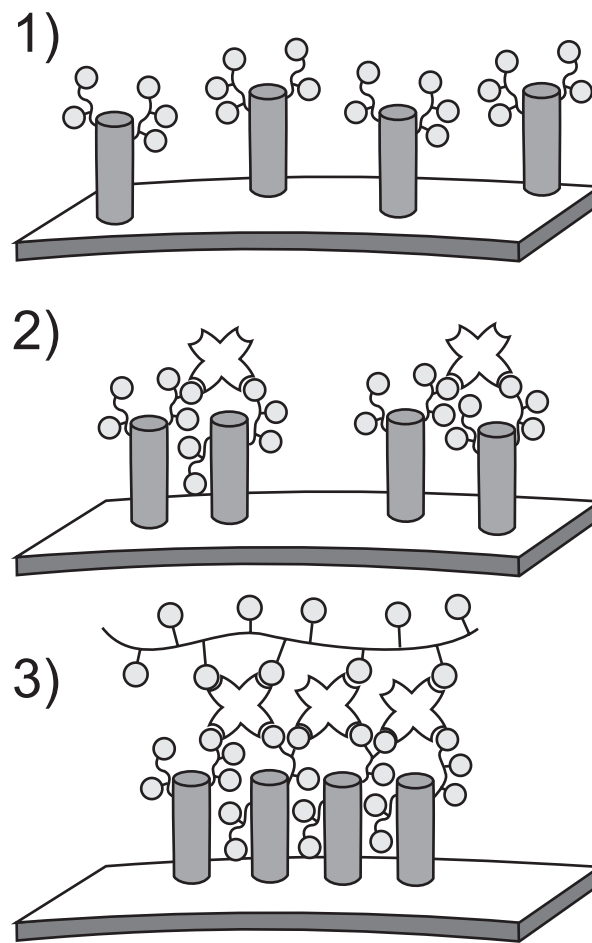
Examination of lectin binding to the cell surface has shown that cell-surface glycoproteins are clustered by treatment with multivalent lectins (Cribbs *et al.*, 1996). Glycoprotein clustering induced by Con A is dependent on whether the lectin is a dimer or a tetramer (Cribbs *et al.*, 1996; Wang, J. L. *et al.*, 1976). Con A exists as a homotetramer that presents four binding sites in a tetrahedral orientation; however, succinylation of Con A results in a dimeric form with two intact binding sites (sCon A) (Wang, J. L. *et al.*, 1976). In cells normally sensitive to Con A toxicity, sCon A is not toxic and is unable to cause receptor clustering at the cell surface (Cribbs *et al.*, 1996; Mannino *et al.*, 1978). Together, these data suggest that the mechanism of toxicity induced by Con A treatment requires the formation of glycoprotein clusters at the cell surface (Figure 4.1).

The specific binding partner(s) of Con A in mammalian cells is not definitively known; however, recent work has identified the protein zero receptor (PZR) as a potential binding partner in both murine and human cell lines (Zhao *et al.*, 2002). Importantly, cells expressing an inactive PZR mutant are resistant to Con A-mediated toxicity and agglutination. These results suggest that PZR is the primary binding partner for Con A in these cell types, and that crosslinking of this receptor is required for toxicity.

**Table 4.1. Characterized lectin toxicity.**

<b>Lectin</b>	<b>Cell Lines or Source</b>	<b>Species/Type</b>	<b>Reference</b>
<b>Con A</b>	HT29, Caco2	human/colorectal, adenocarcinoma	(Ryder <i>et al.</i> , 1994)
<b>Con A*</b>	HGF	human/fibroblast	(Kulkarni <i>et al.</i> , 1998)
<b>Con A</b>	3T3, SV3T3, H. normal, H. SV40, H. DMNA, H. Polyoma	murine/fibroblast, hamster/fibroblast	(Shohan <i>et al.</i> , 1970)
<b>Con A*</b>	3T3, HGF	murine/fibroblast, human/fibroblast	(Kulkarni and Mcculloch, 1995)
<b>Con A</b>	3T3, HT-1080, HEK293, HeLa	murine/fibroblast, human/fibrosarcoma, human/kidney, human/adenocarcinoma	(Zhao <i>et al.</i> , 2002)
<b>Con A*</b>	cortical neurons	murine/neuron	(Cribbs <i>et al.</i> , 1996)
<b>Con A*</b>	TC, SPC	murine/T cell, murine/spleen cell	(Nagase <i>et al.</i> , 1998)
<b>Con A, PNA, WGA, GSA-IA4, PHA-L</b>	SK-MEL-28, HT-144, C32	human/melanoma	(Lorea <i>et al.</i> , 1997)
Con A, sCon A	3T3, SV3T3	murine/fibroblast	(Mannino <i>et al.</i> , 1978)
<b>Con A, WGA, GSA, PHA-L, PNA</b>	LoVo, HCT15, SW837	human/colorectal carcinoma	(Kiss <i>et al.</i> , 1997)
<b>Con A*, WGA, sWGA, PHA-L</b>	BxPC, MIA, Panc-1, CFPAC, ASPC, HS-766T, HTB-147, CaPan-1, CaPan-2	human/pancreatic	(Schwarz <i>et al.</i> , 1999)
PNA	human rectal	human/colorectal	(Ryder <i>et al.</i> , 1998)
WGA*, GSAB4	BL6-8, BL6-12, CL8-1, WEHI-164, YAC-1, MCA102, L929	human/melanoma	(Kim <i>et al.</i> , 1993)
WGA, MAL, STL, TML1, TML2, GML, PPL, AIL, LCL, NPA, AAL	H3B, Jar, B16, ROS	human/hepatoma, human/choriocarcinoma, human/melanoma, human/osteosarcoma	(Wang <i>et al.</i> , 2000)

\* - cells were characterized as undergoing apoptosis on treatment with the indicated lectin



**Figure 4.1. Secondary clustering of cell surface receptors.**

(1) Cell-surface receptors bearing mannose residues become clustered when treated with a multivalent lectin. (2) This clustering can trigger signal transduction. Treatment of the cells with lectin and a multivalent presentation of mannose (3) enhances the ability of the lectin to promote receptor clusters.

#### 4.2.3. Examining the toxicity of Con A in the presence of multivalent ligands.

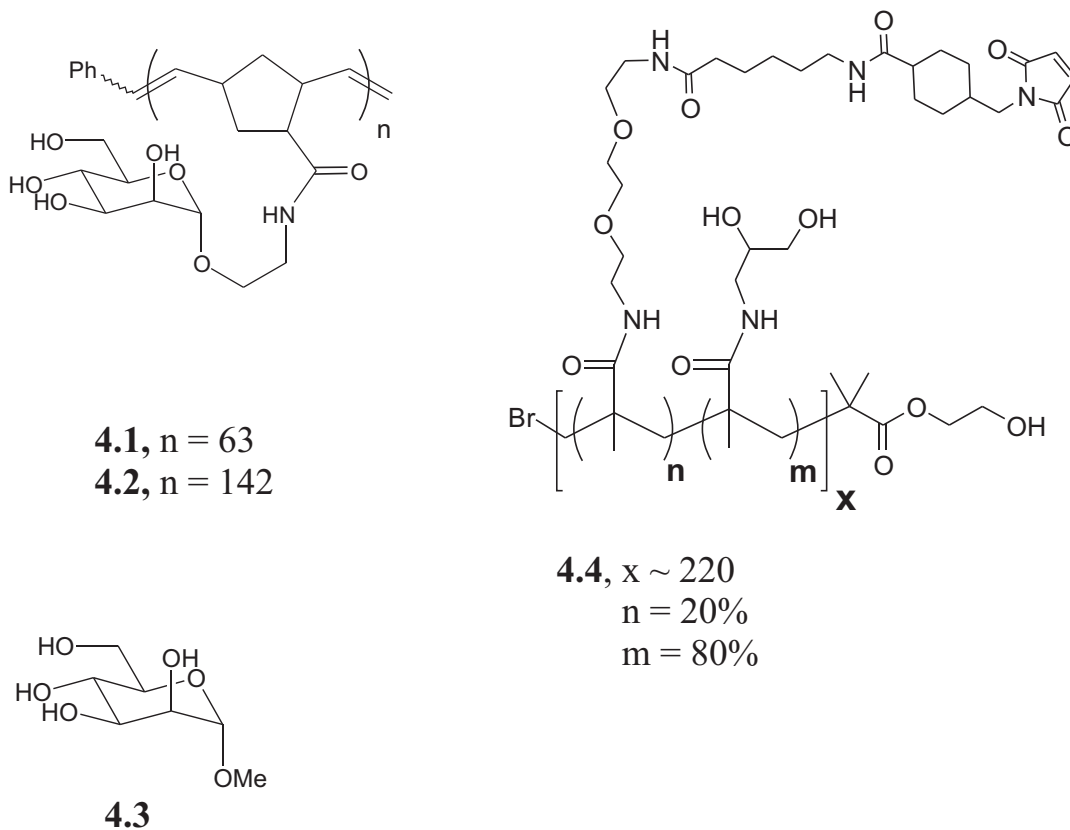
We have explored the use of multivalent polymers as scaffolds for the assembly of multiple copies of Con A (Cairo *et al.*, 2002; Gestwicki *et al.*, 2000b; Gestwicki *et al.*, 2002c). Ring-opening metathesis polymerization (ROMP) provides polymer backbones of defined length (valency) that can be easily derivatized with saccharide residues. These multivalent displays of saccharides can function as scaffolds for the assembly of multiple Con A tetramers. The resulting Con A complexes present their saccharide binding sites with altered spatial proximity and increased functional affinity relative to Con A alone (Gestwicki *et al.*, 2002c). As a result, the polymers should be able to modulate the ability of Con A to bind and cluster glycosylated proteins. Thus, we hypothesized that Con A toxicity could be potentiated by controlling the oligomerization state of the lectin by assembling multiple copies of it on multivalent saccharide polymers (Figure 4.1).

In our study, three cell lines sensitive to Con A toxicity were employed to evaluate the activity of Con A in the presence of multivalent saccharide polymers (Figure 4.2). We found multivalent polymers modulated the activity of Con A in a dose-dependent manner. Apoptotic responses were found at significantly reduced Con A concentrations (*e.g.* 40-fold lower). Thus, we demonstrate that the assembly of Con A onto a multivalent scaffold can modulate the clustering of cell-surface proteins and therefore the activity of the lectin. Modulation of Con A toxicity by synthetic ligands demonstrates that scaffolded lectin clusters on the cell surface can be used to manipulate cellular responses (Sacchettini *et al.*, 2001).

The development of general strategies to study and manipulate lectin-induced receptor clustering will be relevant for many biological systems. The lectin-fold and saccharide



specificity of Con A is homologous to lectins important for signaling, including the galectins and the Flt3 receptor-interacting lectin (FRIL) (Hamelryck *et al.*, 2000; Kogelberg and Feizi, 2001; Vijayan and Chandra, 1999). Galectins are known to regulate cell adhesion, cell proliferation, and cell survival (Perillo *et al.*, 1998). The activity of these lectins is proposed to require multivalent interactions with cell surface receptors (Barondes *et al.*, 1994; Bouckaert *et al.*, 1999). Lectins that regulate cell proliferation, such as FRIL, have potential application in the cultivation of stem cells (Colucci *et al.*, 1999). These lectins are known to form oligomerized structures in the presence of appropriate ligands and clustering of the lectin may affect both its specificity and its interaction with cell surface glycoproteins (Hamelryck *et al.*, 2000). Therefore, synthetic multivalent ligands may provide useful tools to manipulate the specificity and activity of lectins at the cell surface (Kiessling *et al.*, 2000a; Sacchettini *et al.*, 2001).



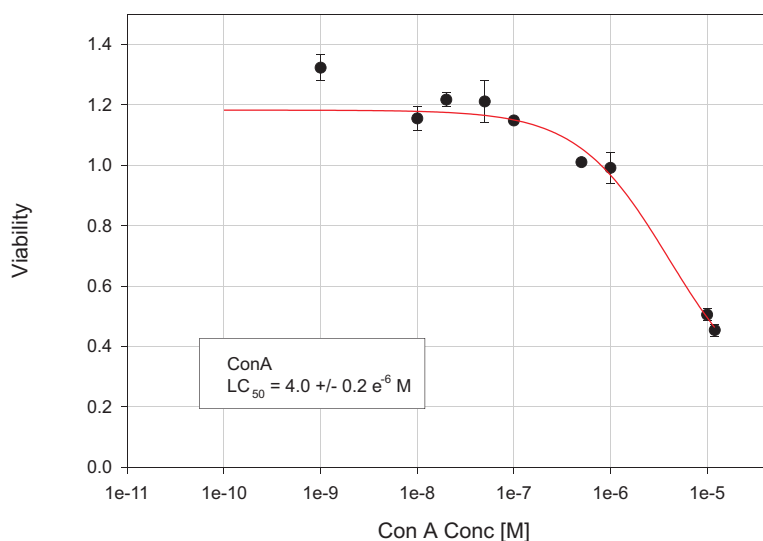
**Figure 4.2. Structures of polymers.**

Structures of synthetic ligands used in this chapter. Studies of lectin toxicity used mannose-substituted polymers derived from ROMP (**4.1**, **4.2**) that were prepared by post-polymerization modification described elsewhere (Strong and Kiessling, 1999). Valency ( $n$ ) was determined by using  $^1\text{H}$  NMR integration.  $\alpha$ -Methyl mannose (**4.3**) was used as a control compound for lectin toxicity experiments. Polymers prepared by atom transfer radical polymerization (ATRP) were generated following previously described methods (**4.4**) (Matyjaszewski and Xia, 2001).

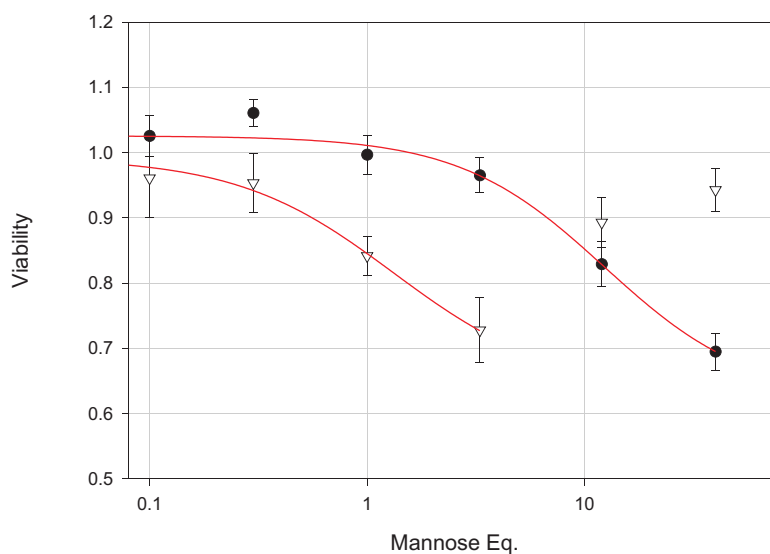
#### 4.3.1. Con A toxicity in PC12, SW937, and HCT15 cells.

The lectin toxicity for the cell lines of interest was characterized. Cell viability assays were used to determine the lethal concentration ( $LC_{50}$ ) for Con A in three separate cell lines. Murine neuronal cells are known to be sensitive to Con A toxicity (Cribbs *et al.*, 1996); therefore we anticipated that PC12 cells, a pheochromocytoma cell line often used as an *in vitro* neuronal model, would show a similar response. SW837 cells are a human rectal cancer cell line that has been previously characterized for sensitivity to a number of lectins including Con A (Kiss *et al.*, 1997). HCT15 cells are a human colon cancer cell line that is also sensitive to Con A, and it is similar to the SW837 cell line (Kiss *et al.*, 1997). All cell lines were obtained from ATCC and characterized for dose-dependent Con A toxicity (Figure 4.3-4.5). Viability assays were performed by quantifying the amount of 3-(4,5-dimethylthiazol-2-yl)-2,5-diphenyltetrazolium bromide (MTT) reduced to formazon by the cells after exposure to samples. Cells with decreased mitochondrial function give reduced conversion of MTT relative to controls (observed by  $A_{570}$ , see: Materials and Methods, Section 4.7). This assay has been shown to correlate well with other measures of cell viability in response to lectin toxicity, such as trypan blue dye-exclusion and thymidine incorporation assays (Cribbs *et al.*, 1996; Gieni *et al.*, 1995). All cell lines had similar responses to tetrameric Con A: PC12 cells responded at an  $LC_{50}$  value of  $4 \times 10^{-6}$  M, HCT15 cells responded with an  $LC_{50}$  value of  $0.2 \times 10^{-6}$  M, and SW837 cells responded with an  $LC_{50}$  of  $0.2 \times 10^{-6}$  M lectin (Figure 4.3-4.5).

1)



2)



**Figure 4.3.1. Toxicity of Con A in PC12 Cells**

PC12 cells were exposed to lectin at the indicated concentrations (in HBS) for 48 h, then cell viability was measured using an MTT assay. Viability is shown relative to control wells treated only with buffer. Linear regression using eq. 4.2 gives an  $LC_{50} = 4 \pm 0.2 \times 10^{-6}$  M.

**Figure 4.3.2. Modulation of Con A toxicity in PC12 cells in the presence of multivalent ligands.**

PC12 cells treated with Con A at a constant concentration ( $1 \times 10^{-7}$  M) in the presence of increasing equivalents of mannose presented on ROMP ligands **4.1** (●) and **4.2** (▽). Cells were incubated with samples in low serum media for 48 h, and then viability was measured using MTT reduction. Each point represents the average of 6 replicates. Curves were fit using a standard  $IC_{50}$  formula (see: Experimental Methods), and error bars represent the standard error of the mean. Compound structures are shown in Figure 4.2.

#### **4.3.2. Modulation of Con A toxicity using multivalent mannose-substituted polymers 4.1 and 4.2.**

We tested our hypothesis that the presentation of multiple copies of Con A oligomerized by multivalent ligands could modulate lectin toxicity. Cell viability assays were performed in the presence of a non-toxic dose of Con A. Under these conditions, we expected changes in viability to result from changes in Con A oligomerization state. We used two different mannose-substituted polymers of different length. Based on previous studies of similar compounds, we predicted that increases in the length of the polymer would increase the number of Con A tetramers complexed with each polymer and also bring these complexes into closer proximity (Gestwicki *et al.*, 2000b; Gestwicki *et al.*, 2002c; Gestwicki *et al.*, 2002b). Therefore, we would expect to observe differences in the activity of these two polymers if the number of cell-surface receptors complexed or the proximity of those receptors affects signaling in the cell types of interest.

MTT assays were conducted on both cell lines using a fixed sub-lethal concentration of Con A ( $1 \times 10^{-7}$  M), and conditions were considered 100% viability. When PC12 cells were treated with Con A or mannose-substituted polymers alone no effect on cellular viability was observed (Table 4.2). In contrast, when cells were exposed to Con A in the presence of mannose-substituted polymers the toxicity of Con A was potentiated (Figure 4.3-4.5). This toxicity depends on the valency and the concentration of the multivalent mannose derivative employed. Polymer activity was plotted in terms of the total concentration of mannose residues in each sample relative to the concentration of Con A binding sites (mannose equivalents). This unit incorporates the concentration of Con A binding sites and the concentration of mannose; therefore, it allows comparison of activity between polymers and

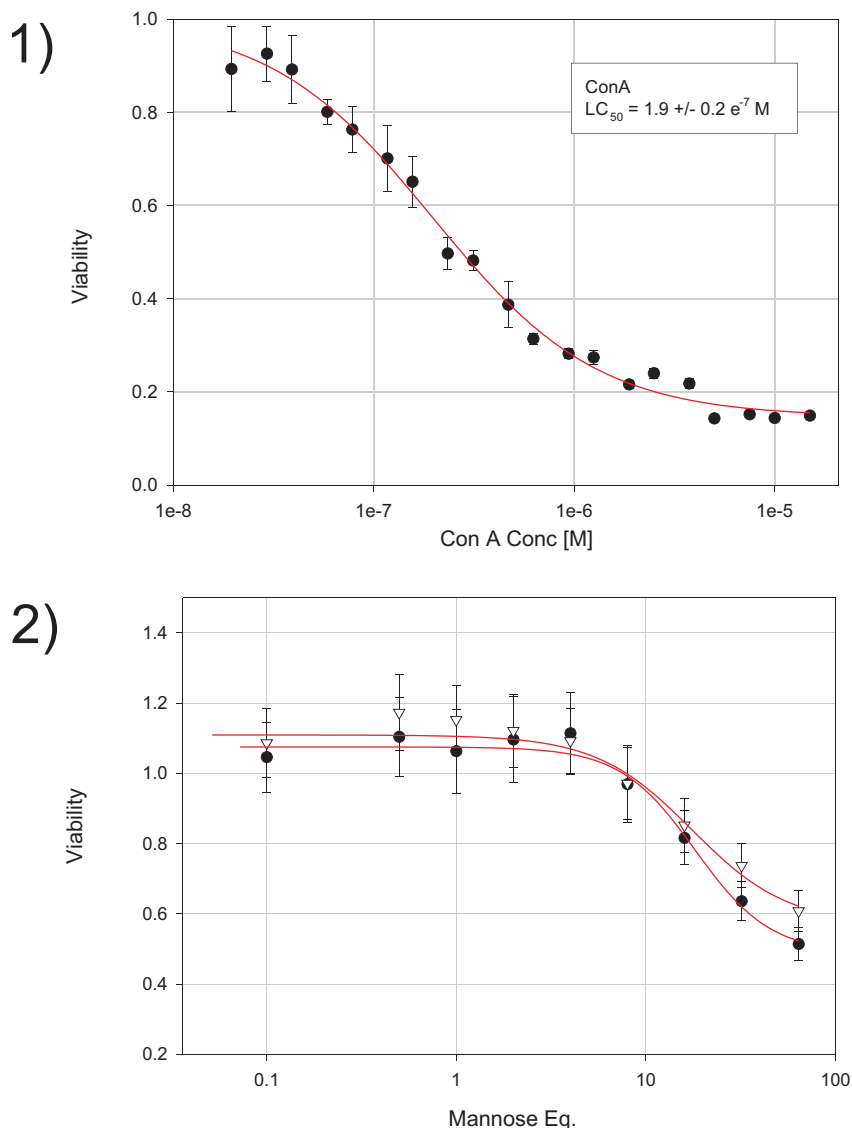
mannose ligands without any bias due to the valency of the ligand or the Con A concentration used. Additionally, the activity of each ligand is given as an absolute concentration.

We first tested the ability of two mannose-substituted polymers of different lengths to potentiate Con A toxicity in PC12 cells. The polymers had different effects on Con A toxicity. Compound **4.1** (DP = 63) gave an EC<sub>50</sub> of  $12 \pm 7$  mannose equivalents ( $1.2 \pm 0.7$   $\mu$ M saccharide,  $19 \pm 11$  nM polymer), and compound **4.2** (DP = 142) gave an EC<sub>50</sub> of  $1.3 \pm 1.2$  mannose equivalents ( $130 \pm 120$  nM saccharide,  $0.92 \pm 0.85$  nM polymer) (Figure 4.3). These results demonstrate that treatment of PC12 cells under these conditions with either **4.1** or **4.2** induces Con A toxicity at  $1 \times 10^{-7}$  M, 40-fold below the LC<sub>50</sub> of Con A alone. Interestingly, at high concentrations of **4.2**, viability of the cells returned to control levels. This result is consistent with previous observations that suggest Con A binding site saturation occurs at high concentration of multivalent ligand (Gestwicki *et al.*, 2002c). Con A binding site saturation occurring at high concentrations. Under these conditions, excess polymer can occupy all vacant Con A binding sites thereby preventing the binding of Con A to cell surface glycoproteins (*vide infra*) (Gestwicki *et al.*, 2002c).

These data suggest that SW837 and PC12 cells have different responses to clustering of Con A. Experiments with SW837 cells reveal that treatment with Con A or mannose-substituted polymers alone did not affect cell viability (Table 4.2). As with PC12 cells, treatment of the SW837 cells with Con A in the presence of mannose-substituted polymers potentiated the toxicity of the lectin (Figure 4.4). Con A in the presence of the shorter polymer (**4.1**) gave an EC<sub>50</sub> value of  $18 \pm 3$  mannose equivalents ( $1.8 \pm 0.3$   $\mu$ M saccharide,  $29 \pm 5$  nM polymer), and when the longer scaffold was present (**4.2**), it had a similar EC<sub>50</sub> value

of  $18 \pm 8$  mannose equivalents ( $1.8 \pm 0.8$   $\mu$ M saccharide,  $13 \pm 6$  nM polymer) (Figure 4.4). Thus, in contrast to the results with PC12 cells, polymers of either length gave identical  $EC_{50}$  results when compared on a saccharide residue basis.

Experiments with HCT15 cells in the presence of Con A or mannose-substituted polymers alone did not affect cell viability (Table 4.2). Treatment of cells with Con A in the presence of mannose-substituted polymers resulted in potentiated lectin toxicity as described for the other two cell lines above (Figure 4.5). In the presence of Con A, the 63mer (**4.1**) gave an  $EC_{50}$  value of  $12 \pm 4$  mannose equivalents ( $1.2 \pm 0.4$   $\mu$ M saccharide,  $19 \pm 6$  nM polymer), and the 142mer (**4.2**) gave an  $EC_{50}$  of  $8 \pm 4$  mannose equivalents ( $0.8 \pm 0.4$   $\mu$ M saccharide,  $6 \pm 3$  nM polymer). These results are similar to those with SW837 cells, as could be expected from their related origin (Kiss *et al.*, 1997).



**Figure 4.4.1. Toxicity of Con A to SW837 Cells**

SW837 cells were exposed to lectin at the indicated concentrations (in HBS) for 48 h, then cell viability was measured using an MTT assay. Viability is shown relative to control wells treated only with buffer. A representative experiment is shown with an LC<sub>50</sub> = 1.1 +/- 0.2 x 10<sup>-6</sup> M.

**Figure 4.4.2. Modulation of Con A toxicity in SW837 cells in the presence of multivalent ligands.**

SW837 cells were treated with Con A at a constant lectin concentration (1 x 10<sup>-7</sup> M) in the presence of increasing amounts of mannose presented on either a 63- or 142-mer ROMP-derived polymer **4.1** (●) and **4.2** (▽). Cells were incubated with samples in low serum media for 48 h, and then viability was measured using MTT reduction. Each point represents the average of 3 experiments, with 8 replicates in each experiment. Curves were fit using a standard IC<sub>50</sub> formula (see: Experimental Methods), error bars represent the standard error of the mean. Compound structures are shown in Figure 4.2.



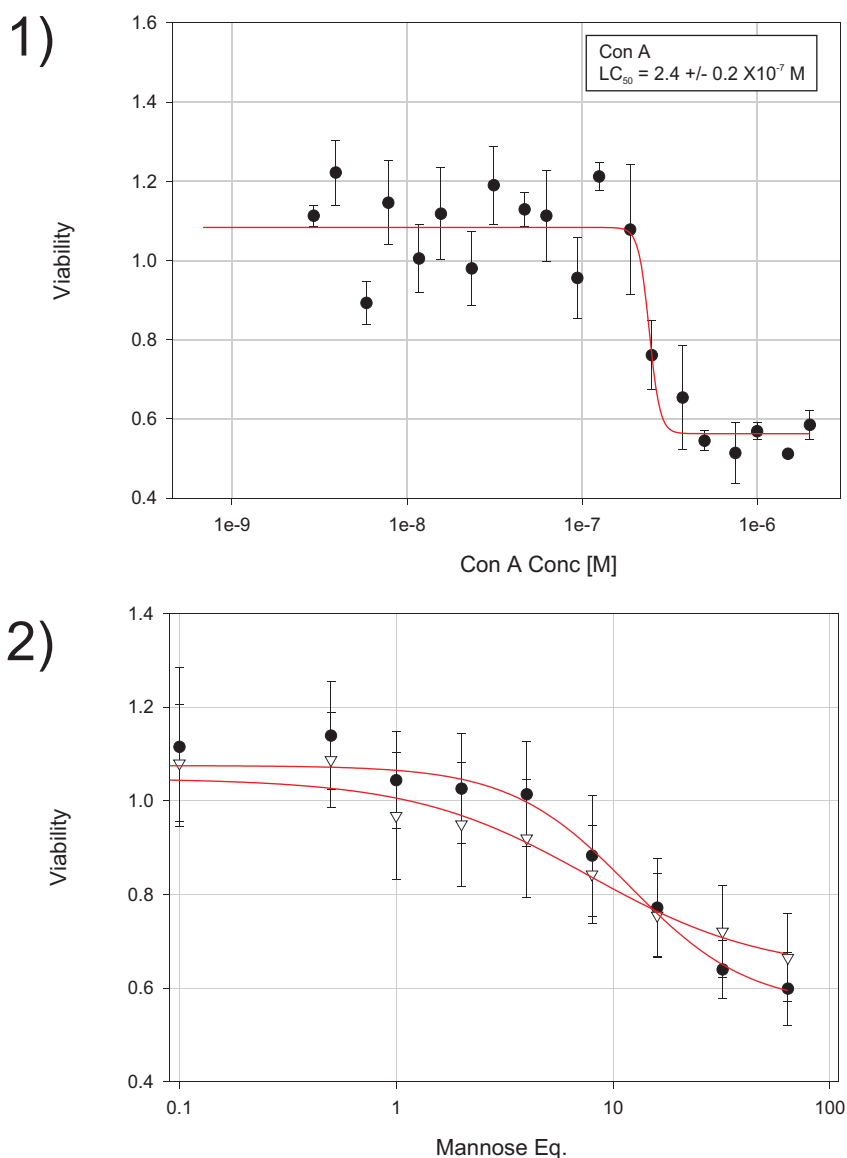
#### **4.3.3. Polymer – Con A complexes elicit an apoptotic cell morphology.**

In a number of cell lines, treatment with Con A affords cell morphologies and biochemical changes consistent with programmed cell death (Cribbs *et al.*, 1996; Kulkarni and McCulloch, 1995). We anticipated that light microscopy experiments could therefore reveal whether similar morphological features are observed under conditions determined to be lethal in our cell viability experiments. Accordingly, cells were exposed to Con A and mannose-substituted scaffold under conditions determined to be lethal (*vide supra*), and the cellular morphology of PC12 and SW837 cells was monitored [Figure 4.6.1 (PC12) and Figure 4.6.2 (SW837)]. Because SW837 and HCT15 cells are similar, HCT15 cells were not studied by microscopy. In the presence of the multivalent ligands and Con A, both cell lines used showed characteristic membrane blebbing and the appearance of apoptotic bodies as indicated by visible microscopy (Hacker, 2000). At the concentrations used, Con A alone did not elicit these morphological changes. These results indicate that the Con A-mediated toxicity observed in cell viability assays results from apoptosis.

#### **4.3.4. Clustering of cell-surface glycoproteins by Con A and multivalent ligands.**

To study the mechanism of Con A toxicity in the presence of multivalent ligands, we performed microscopy experiments to visualize clustering of Con A on the cell surface. Treatment of the cell lines with fluorescein-labeled Con A resulted in clustering of Con A on the cells, consistent with other reports (Cribbs *et al.*, 1996; Mallucci, L., 1976). To compare the degree of clustering of Con A at the cell surface induced in the presence of the multivalent mannose substituted scaffolds, we used a Con A derivative that does not cause clustering on

its own. Succinylated Con A is known to have a reduced ability to cluster glycoproteins, presumably because it has only two binding sites. We have previously shown that multivalent polymers are able to assemble sCon A oligomers in solution (Gestwicki *et al.*, 2002c). Thus, we anticipated the sCon A could cluster glycoproteins in the presence of the multivalent ligands. As expected, fluorescein-labeled sCon A (Fl-sCon A) alone was unable to cluster surface glycoproteins in either cell line (Figure 4.6); however, upon treatment with either **4.1** (Figure 4.6) or **4.2** (Figure 4.6) characteristic Con A fluorescence that is indicative of protein capping was observed. Notably, clustering appeared to be more distinct in both cell lines when treated with the higher valency ligand (**4.2**) vs. the lower valency ligand (**4.1**). Improved clustering in the presence of polymer **4.2** could be an indication of the formation of larger sCon A complexes, and therefore larger clusters of cell-surface binding partners, by the higher valency polymer.

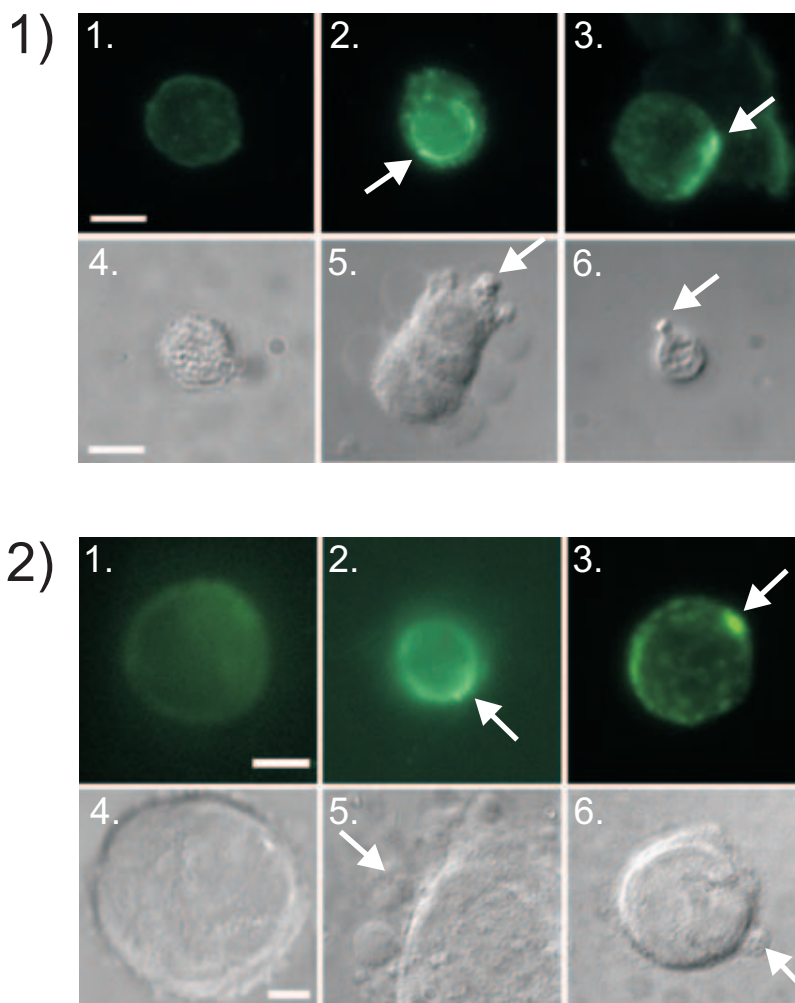


**Figure 4.5.1. Toxicity of Con A in HCT15 Cells**

HCT15 cells were exposed to lectin at the indicated concentrations (in HBS) for 48 h, then cell viability was measured using an MTT assay. Viability is shown relative to control wells treated only with buffer. A representative experiment is shown with an  $LC_{50} = 2.4 \pm 0.2 \times 10^{-6} \text{ M}$ .

**Figure 4.5.2. Modulation of Con A toxicity in HCT15 cells in the presence of multivalent ligands.**

HCT15 cells were treated with Con A at a constant concentration ( $1 \times 10^{-7} \text{ M}$ ) in the presence of increasing equivalents of mannose presented on either a 63- or 142-mer ROMP-derived polymer **4.1** (●) and **4.2** (▽). Cells were incubated with samples in low serum media for 48 h, and then viability was measured using MTT reduction. Each point represents the average of 3 experiments, with 8 replicates in each experiment. Curves were fit using a standard  $IC_{50}$  formula (see: Experimental Methods), error bars represent the standard error of the mean. Compound structures are shown in Figure 4.2.



**Figure 4.6. Clustering of Con A on the surface of PC12 and SW837 cells results in apoptotic morphology.**

1) PC12 cells were grown on glass cover slips in 6-well plates and fixed. Cells were treated with Fl-sCon A ( $1 \times 10^{-6}$  M) for 2 h in the presence of 1) buffer; 2) **4.1** ( $3 \times 10^{-7}$  M); 3) **4.2** ( $2 \times 10^{-7}$  M). For visualization of apoptotic morphology, cells were treated with Con A ( $1 \times 10^{-7}$  M) for 48 h in the presence of 4) buffer; 5) **4.1** ( $2 \times 10^{-8}$  M); 6) **4.2** ( $8 \times 10^{-9}$  M). Scale bar is 10  $\mu$ m.

2) SW837 cells were grown on glass cover slips in 6-well plates and fixed. Cells were treated with Fl-sCon A ( $1 \times 10^{-6}$  M) for 2 h in the presence of 1) buffer; 2) **4.1** ( $3 \times 10^{-7}$  M); 3) **4.2** ( $1 \times 10^{-7}$  M). For visualization of apoptotic morphology, cells were treated with Con A ( $1 \times 10^{-7}$  M) for 48 h in the presence of 4) Buffer; 5) **4.1** ( $3 \times 10^{-8}$  M); 6) **4.2** ( $1 \times 10^{-8}$  M). Scale bar is 10  $\mu$ m. Compound structures are shown in Figure 4.2.

**Table 4.2. Con A toxicity in PC12 and SW837 cells.**

Cell Line	Conditions				Viability <sup>d</sup>	± SE
	Ligand	Concentration (Mannose Eq.) <sup>a</sup>	Concentration Ligand (M) <sup>b</sup>	Con A <sup>c</sup>		
PC12	-	-	-	+	100	10
PC12	<b>4.3</b>	40 eq.	$4 \times 10^{-6}$	-	90	26
PC12	<b>4.3</b>	40 eq.	$4 \times 10^{-6}$	+	99	18
PC12	<b>4.1</b>	40 eq.	$6 \times 10^{-8}$	-	97	1
PC12	<b>4.1</b>	40 eq.	$6 \times 10^{-8}$	+	70	1
PC12	<b>4.2</b>	40 eq.	$3 \times 10^{-8}$	-	98	9
PC12	<b>4.2</b>	3.3 eq. <sup>e</sup>	$2 \times 10^{-9}$	+	73	2
SW837	-	-	-	+	100	3
SW837	<b>4.3</b>	64 eq.	$6 \times 10^{-6}$	-	111	12
SW837	<b>4.3</b>	64 eq.	$6 \times 10^{-6}$	+	101	16
SW837	<b>4.1</b>	64 eq.	$1 \times 10^{-7}$	-	97	5
SW837	<b>4.1</b>	64 eq.	$1 \times 10^{-7}$	+	51	5
SW837	<b>4.2</b>	64 eq.	$4 \times 10^{-8}$	-	109	9
SW837	<b>4.2</b>	64 eq.	$4 \times 10^{-8}$	+	61	6
HCT15	-	-	-	+	100	13
HCT15	<b>4.3</b>	64 eq.	$6 \times 10^{-6}$	-	114	4
HCT15	<b>4.3</b>	64 eq.	$6 \times 10^{-6}$	+	111	9
HCT15	<b>4.1</b>	64 eq.	$1 \times 10^{-7}$	-	89	9
HCT15	<b>4.1</b>	64 eq.	$1 \times 10^{-7}$	+	60	8
HCT15	<b>4.2</b>	64 eq.	$4 \times 10^{-8}$	-	83	7
HCT15	<b>4.2</b>	64 eq.	$4 \times 10^{-8}$	+	67	9

<sup>a</sup> Concentrations are given as mannose equivalents relative to Con A monomer.

<sup>b</sup> Concentrations are given as molar concentration of the ligand or polymer.

<sup>c</sup> For experiments in which Con A is added (+), the concentration was  $1 \times 10^{-7}$  M (1 eq.)

<sup>d</sup> Viability is given as the mean of 6 replicates, error is the standard error of the mean.

<sup>e</sup> Ligand **4.2** had an effective concentration lower than **4.1**; the concentration that showed the greatest toxicity is shown for comparison.

#### **4.4.1. Synthetic multivalent ligands are effective tools for controlling receptor clustering.**

We found that multivalent ligands can be used to control the extent of clustering of Con A at the cell surface and therefore the toxicity of this lectin. In the presence of mannose-substituted polymers, Con A can assemble into higher order complexes in solution. It is these complexes that presumably cluster target cell-surface glycoproteins. It is this crosslinking of cell-surface lectin-binding glycoproteins that leads ultimately to apoptosis. This study provides a general and selective strategy for potentiation of signal transduction events that rely on the clustering of a target receptor.

Cell viability assays were used to quantitate the ability of Con A to induce apoptosis in the presence of multivalent mannose-substituted polymers. Based on previous studies of Con A binding to mannose-substituted polymers in solution, we expected the multivalent ligands could control the extent of clustering of the lectin at the cell surface (Gestwicki *et al.*, 2002c). Our results demonstrate that multivalent polymers can potentiate the toxicity of Con A are consistent with such a model (Gestwicki and Kiessling, 2002). The multivalent mannose-substituted scaffolds are active at nanomolar concentrations in the presence of Con A. Moreover, they are able to induce Con A toxicity at concentrations 40-fold below the LC<sub>50</sub> value for Con A alone. These data suggest that scaffolded Con A complexes are more efficient at clustering the target cell-surface proteins.

Comparison of our results across cell types suggests that specific cell types can respond differently to clustering of Con A. For example, PC12 cells respond to treatment with Con A in the presence of **4.2** with an EC<sub>50</sub> of 1.3 mannose equivalents, this is as much as 14-fold more potent than the response observed in SW837 cells and 6-fold more potent than the response in HCT15 cells. Therefore, potentiation of Con A toxicity can target different cell

types more effectively than others. Interestingly, we only observe this effect in the case of the longer polymer, **4.2**, but not in the case of the shorter polymer, **4.1**. These data suggest that potentiation of Con A toxicity is dependent both on cell type and the ability of the multivalent ligand to bring a sufficient number of lectins into close proximity (Gestwicki *et al.*, 2000b; Gestwicki *et al.*, 2002c; Gestwicki *et al.*, 2002b).

Our finding that the assembly of multiple copies of Con A on mannose-substituted polymers potentiates the toxicity of this lectin illustrate a versatile strategy for controlling signal transduction. Although the clustering of cell surface receptors by multivalent antibodies or lectins is well known, we have used multivalent ligands, which are traditionally considered inhibitors (Lundquist and Toone, 2002; Page *et al.*, 1996a; Woller and Cloninger, 2002), as effectors of lectin toxicity. In our initial studies of multivalent polymers, we observed that polymers similar to the ones used in this study can be effective inhibitors of Con A mediated hemagglutination (Kanai *et al.*, 1997; Mortell *et al.*, 1996; Strong and Kiessling, 1999). However, multivalent ligands can also serve as scaffolds for the assembly of Con A – complexes (Burke *et al.*, 2000; Cairo *et al.*, 2002; Gestwicki *et al.*, 2002c). Here, we demonstrate that multivalent ligands can be used to tune a biological response. Specifically, at low concentrations that favor the formation of Con A oligomers (i.e. low molar ratio of multivalent ligand epitopes to Con A binding sites), the ligand acts as a template to assemble highly toxic Con A complexes. When the multivalent ligand concentration is high (i.e. high molar ratio of mannose epitopes to Con A binding sites), the Con A binding sites are occupied. As a result, the multivalent ligand now acts as an inhibitor of lectin toxicity. This change in activity can be observed when PC12 cells are treated with Con A in the presence of multivalent ligand **4.2** (Figure 4.3). The polymer acts as an effector of lectin toxicity at low

molar ratios (in the range of 0.2-2 mannose equivalents); however, at higher molar ratios (10-20 mannose equivalents) oligomer formation is less favored and cell viability returns to control levels. These observations are consistent with quantitative precipitation and FRET studies of multivalent ligand binding to Con A (Burke *et al.*, 2000; Gestwicki *et al.*, 2002c).

The clustering of cell-surface receptors is a general process by which signal transduction cascades are initiated (Heldin, 1995). Oligomeric lectins have been used to activate signaling. Mammalian lectins, such as the galectins, are structurally homologous to Con A and have been shown to activate T cell apoptosis by clustering target cell-surface glycoproteins (Bouckaert *et al.*, 1999; Pace *et al.*, 1999; Perillo *et al.*, 1998). The activity of the galectins can be modulated by antibodies that mediate dimerization (Liu *et al.*, 1996). Antibody-mediated dimerization of lectins cannot be used to investigate the consequences of higher order clustering. Our strategy however, provides a simple method to modulate the clustering and therefore the activity of lectins. Thus, the activity of a lectin can be influenced specifically and varied systematically.

Our data suggest that multivalent ligand structure could be optimized to provide selective targeting of specific cell types. In our studies of Con A toxicity in PC12 cells, we observe that the higher valency polymer **4.2** is 20-fold more effective than the lower valency polymer **4.1**. Moreover, the effective concentration of polymer **4.2** in SW837 cells is different from that of the PC12 cells. These data suggest that lectin toxicity can be selectively modulated for particular cell types. Moreover, in our studies the valency of the multivalent ligand used can affect the potentiation of lectin toxicity.

The use of multivalent ligands as effectors is emerging as a general strategy for investigating and manipulating signaling events (Kiessling *et al.*, 2000a). Synthetic



multivalent ligands have served as valuable tools for the study of bacterial chemotaxis, apoptosis, T cell activation, and L-selectin shedding (Belshaw *et al.*, 1996; Cochran and Stern, 2000; Gestwicki and Kiessling, 2002; Gordon *et al.*, 1998; Portoghese, 2001). Our studies of Con A toxicity demonstrate that glycoprotein oligomerization state can have a profound effect on lectin-initiated apoptosis in vitro. Moreover, our results suggest strategies to control this and other lectin-mediated processes.

The clustering of multivalent lectins could provide a means for improved lectin specificity. The lectin FRIL is structurally similar to Con A, and is able to regulate the proliferation of cells (Colucci *et al.*, 1999). It has been proposed that the oligomerization of this and other lectins could provide improved selectivity when complexed by a native multivalent ligand (Dam and Brewer, 2002; Hamelryck *et al.*, 2000). Our model studies with Con A provide a concrete demonstration that receptor clustering can modulate signal output. We have observed that Con A activity is regulated by clustering the protein onto a multivalent ligand. Additionally, we find that the structure of the ligand is able to provide selective effects in different cell types. Therefore, multivalent ligands similar to those used here may provide useful reagents for the selective control of biologically relevant lectins in other systems.

#### **4.5.1. Specific cell receptors for inducing apoptosis.**

Our studies of lectin-induced toxicity relied on the non-covalent interaction of three species: the polymer backbone, the soluble receptor (Con A), and its putative cell-surface binding partner (PZR). The advantages of this strategy are three-fold: 1) The combinatorial nature of the interaction allows the system to explore many degenerate states capable of activating signal transduction; 2) the multivalent ligand is synthesized from small molecule

precursors, such as monosaccharides; 3) the combination of two separate binding events results in a concentration *range* of activity (for example our results using **4.2** in PC12 cells, Figure 4.3.2). Below this range, there is insufficient binding of the multivalent ligand to form soluble clusters; above this range there is excess ligand that saturates the receptor. Thus, there is a region of effector activity (clustered) and inhibitor activity (saturation) for the ligand.

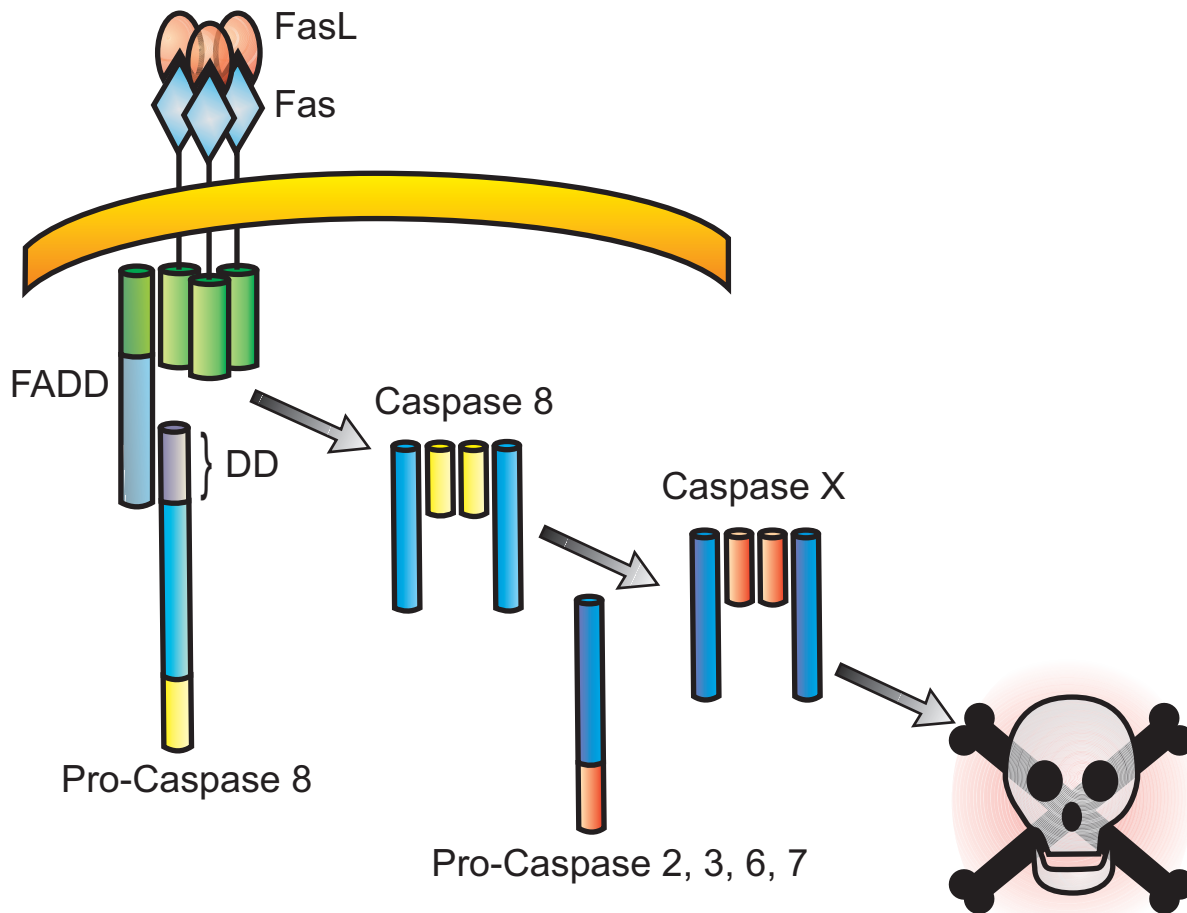
An alternative approach could simplify this system by removing one of these non-covalent interactions. Multivalent ligands with a covalently linked group able to bind to the target receptor directly would eliminate the intermediary binding step required for generating a multivalent display of a protein of interest. Additionally, ligands in which binding epitopes are presented through covalent linkage to the backbone are more structurally defined. We therefore identified a well-characterized receptor system known to cause signal transduction upon crosslinking with known binding partners available.

Candidate receptors must provide a simple means of assessing signal transduction upon clustering. Therefore, we considered receptors known to induce apoptosis of cells upon clustering, because cell viability assays could be used to quantitate the effects of the multivalent ligands. One of the most characterized receptors in the apoptotic pathway is CD95/Fas/APO-1. The Fas receptor is a member of the tumor necrosis factor (TNF) receptor family and is activated by the soluble Fas ligand (FasL) (Wallach *et al.*, 1999). FasL oligomerizes upon binding to Fas, resulting in crosslinking of the receptor (Bajorath, 1999b; Orlinick *et al.*, 1997b; Orlinick *et al.*, 1997a; Schneider *et al.*, 1997). This interaction has been studied by fluorescence microscopy and SDS-PAGE (Bajorath, 1999a; Medema *et al.*, 1997; Weber and Vincenz, 2001). Some evidence suggests that Fas may exist as a trimer before ligand binding (Chan *et al.*, 2000; Siegel *et al.*, 2000). However, crosslinking of the

receptor with multivalent antibodies (*vide infra*) induces apoptosis. The response to antibodies suggests that higher-order assemblies of Fas may be required for effective signaling.

Initiation of apoptosis by Fas clustering is believed to involve the formation of a death-inducing signaling complex (DISC). The complex is believed to include oligomerized Fas, cytotoxicity-dependent APO-1-associated proteins (CAPs), FADD, and pro-caspase 8 (Blatt and Glick, 2001; Kischkel *et al.*, 1995). Within the complex, the pro-caspase is converted to an active caspase, leading to initiation of the apoptotic cascade and ultimately cell death (Figure 4.7) (Blatt and Glick, 2001; Crowe *et al.*, 1998; Martin *et al.*, 1998; Wallach *et al.*, 1999).

Although it is clear that the Fas receptor requires oligomerization for activation, structural information related to this organization is sparse. Several models of Fas oligomerization in the cell membrane have been described based on crystal structures of fragments and mutagenesis studies (Bajorath, 1999a; Orlinick *et al.*, 1997a; Weber and Vincenz, 2001). Multivalent ligands could provide a unique method to study the structural requirements of this membrane bound assembly. For example, polymers with defined distances between binding sites could be used to determine the effect of receptor proximity within the complex. Alternatively ligands with different numbers of binding sites could report on the optimal size of the active complex. Therefore, we designed polyvalent ligands capable of crosslinking Fas receptor in order to establish that this strategy would be effective.



#### Figure 4.7. Fas-initiated apoptotic signalling

Binding of FasL to Fas oligomerizes the receptors. The oligomer is generally thought to be a trimer as observed in crystal structures of FasL and native SDS-PAGE, (Kischkel *et al.*, 1995) although higher order structures have been proposed. (Weber and Vincenz, 2001) The death domains (DD) of these receptors recruit FADD, which activates pro-caspase-8 to caspase-8. The caspase then initiates the apoptotic cascade beginning with caspases-2,3,6, and 7. (Blatt and Glick, 2001; Wallach *et al.*, 1999)

#### 4.5.2. Strategies for crosslinking Fas.

Several strategies for initiating crosslinking of the Fas receptor have been reported in the literature. Soluble FasL (sFasL) has been used *in vitro* and *in vivo* to cause crosslinking of Fas (Kawaguchi *et al.*, 2000; Schneider *et al.*, 1997). Native FasL is a 40 kDa membrane protein. Truncated forms of the protein are also known (~25-29 kDa), and these have been shown to require two *N*-glycosylated sites for activity (Schneider *et al.*, 1997). FasL appears to function as a trimeric structure, and this is considered to be part of the mechanism of Fas clustering (Bajorath, 1999b). Although FasL has not been crystallized, the structure is thought to be similar to that of other TNF family members (Bajorath, 1999b). Therefore, several model structures have been proposed (Bajorath, 1999a; Weber and Vincenz, 2001). Use of sFasL as an agent for clustering Fas is complicated by limitations on the production of the glycoprotein from cell culture (Roth *et al.*, 1999).

Strategies using chemical inducers of dimerization (CID) have also been employed to cluster Fas receptors fused to cyclophilin domains could be crosslinked using dimeric cyclosporin ligands (Belshaw *et al.*, 1996). Importantly, several studies using IgG and IgM antibodies have shown that antibody crosslinking is sufficient to cause apoptotic signaling in a variety of cell types; interestingly, IgM molecules appear to be more active than IgG (Frei *et al.*, 1998; Komada *et al.*, 1999; Meterissian *et al.*, 1997). Ichikawa *et al.* demonstrated that  $\alpha$ -Fas antibodies were more active when treated with secondary antibodies to enhance clustering (Ichikawa *et al.*, 2000). Engineered and non-specifically crosslinked whole antibodies have been used with varied success (Holler *et al.*, 2000; Todorovska *et al.*, 2001). Finally, multivalent fusion proteins have been constructed with multiple FasL regions and self associating protein domains (Holler *et al.*, 2000).

Each of these strategies has inherent disadvantages. FasL is difficult to produce in large quantities and is, therefore, difficult to study (Roth *et al.*, 1999). CID strategies are useful for *in vitro* study, but by design they require the generation of a cell line with the appropriate fusion protein (Belshaw *et al.*, 1996). Antibody strategies are also restricted to *in vitro* work; due to their large molecular weights and high immunogenicity. Engineered antibody constructs are extremely inefficient to produce due to statistical factors (Kroesen *et al.*, 1998). Multivalent fusion proteins suffer from the disadvantage of being extremely large (FasL ~ 40kD, trimeric constructs ~ 400 kD) (Holler *et al.*, 2000; Schneider *et al.*, 1997). We propose that synthetic and semi-synthetic methods will allow the construction of more efficient and more active compounds. The resulting reagents are anticipated to be effective crosslinking agents for Fas and useful for both *in vitro* and *in vivo* studies.

The most promising studies to date have been reported by Willuda *et al.* using “miniantibodies” (Willuda *et al.*, 2001). These authors were able to engineer tetrameric scFv regions of  $\alpha$ -Fas antibodies. These constructs are of medium molecular weight (~ 130 kD) and valency (3-4 binding sites). Moreover, these materials are capable of penetrating tumor tissues, and are stable in plasma. These artificial constructs are limited however, in their valency and in the orientation of their binding sites. Synthetic approaches to macromolecular species that allow control of both valency and density of binding epitopes could allow better optimized ligands than are currently available.

#### **4.5.3. Therapeutic utility of Fas selective ligands.**

Methods to selectively control apoptotic signaling could give rise to new anticancer strategies. Compounds that target several receptors in the apoptosis pathway are currently under investigation. Receptors must be carefully chosen to affect only cancerous tissue, and

exclude non-cancerous tissue. Many cell types are Fas(+) and therefore Fas targeting strategies are limited to regions where tissue is generally Fas(-) but harbors cancerous tissue that is Fas(+). Several forms of malignant glioma are known to be Fas-sensitive. Importantly, brain epithelial tissue is not sensitive to Fas crosslinking, making Fas targeting strategies potentially feasible for treating malignant glioma.

Weller *et al.* have studied the feasibility of using Fas clustering as a selective apoptosis signal in malignant glioma (Roth and Weller, 1999; Weller *et al.*, 1998). These authors and others have shown that FasL is able to induce apoptosis in cultured cells as well as *ex vivo* tumors (Frei *et al.*, 1998; Kawaguchi *et al.*, 2000). Antibodies that crosslink Fas have also been described (Decaudin *et al.*, 2001; Roth and Weller, 1999). Combination strategies are also emerging which employ treatment of resistant tumors with chemotherapeutic agents and FasL. These strategies have shown synergistic effects; combined therapy is often far more effective than either therapy alone would predict (Hueber *et al.*, 1998).

Although all of these strategies are under development, more versatile approaches may prove to be superior for studies of this system. As we have observed in model systems (Gestwicki *et al.*, 2002b), there may be an optimal architectural configuration of multivalent ligands for Fas. Antibody strategies, while effective, are limited with regard to structural parameters. Additionally, these materials are of high molecular weight and may not penetrate tumor tissue well (Figure 4.10). Willuda *et al.* showed that multivalent “miniantibodies”, truncated scFv fragments with self-associating fusion sequences attached (tetramers ~ 130 kD), were of small enough molecular weight to penetrate tumors (Willuda *et al.*, 2001). These constructs were also stable and active against tumors. These results suggest that antibody

fragments arranged into a multivalent presentation could provide potent compounds for tumor therapy. To initiate our studies, we developed a general strategy to synthesize multivalent conjugates containing  $\alpha$ -Fas antibody fragments.

#### **4.5.4. Antibody conjugates for clustering apoptosis receptors.**

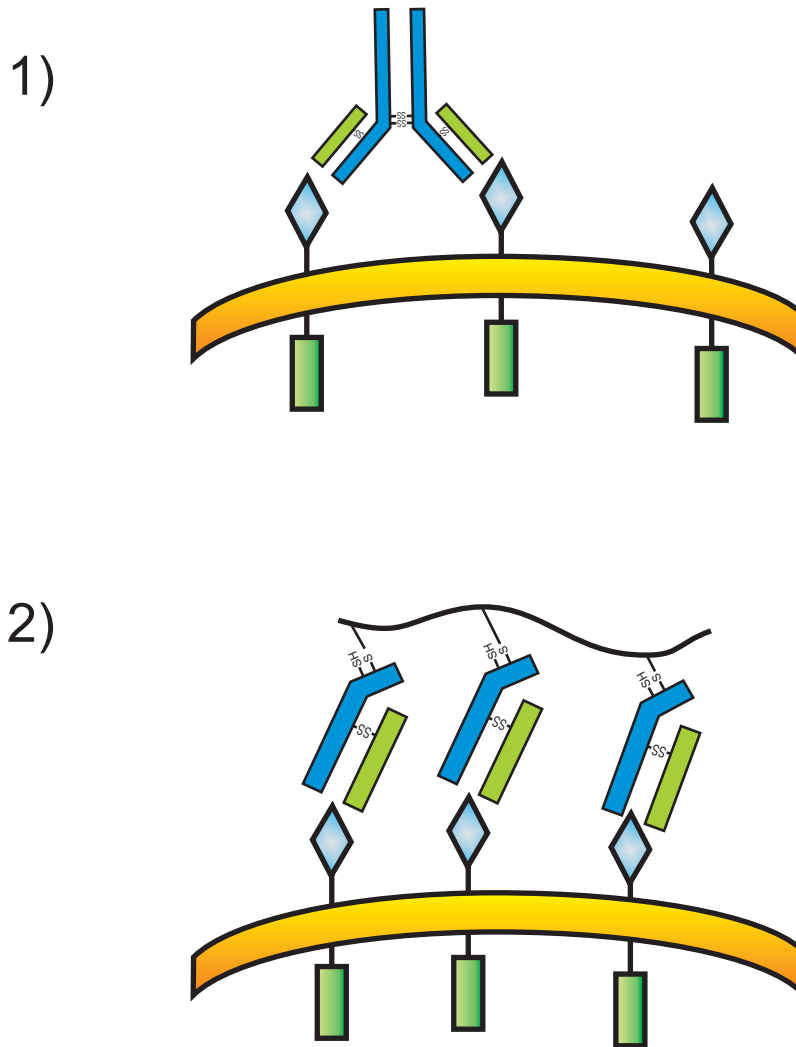
An ideal reagent for selective Fas crosslinking would be of high valency and low molecular weight. Additionally, the conjugate should have limited immunogenicity and should be stable to proteolysis. Our model studies of multivalent ligand architecture using Con A suggested that linear polymers can be one of the most efficient presentations of multivalent binding sites to cluster large numbers of receptors (Cairo *et al.*, 2002; Gestwicki *et al.*, 2002b). We reasoned that a synthetic polymer could serve as an efficient backbone for the presentation of Fab' fragments specific for Fas (Figure 4.8). Synthetic polymers also provide a great deal of structural variation. In this way, medium-sized molecular weight conjugates of different valencies may prove effective. The use of a single backbone to present antibody binding sites should provide ligands of significantly lower molecular weight than are possible with native antibodies (Figure 4.10). The Fc portions of whole antibodies impart excess molecular weight and are not required for the desired interactions. Therefore, synthetic conjugates of Fab' should provide higher valencies for the same molecular weight.

We used ATRP-derived backbones for our conjugation strategies. The ATRP reaction involves a radical initiator that reacts to afford a living polymerization of  $\alpha$ - $\beta$  unsaturated carbonyl compounds (Liang *et al.*, 1999; Matyjaszewski and Xia, 2001; Patten and Matyjaszewski, 1998). The resulting polymers of ethylacrylate monomer units are of low



polydispersity and can be easily modified for introduction of new functional groups. We envisioned that conjugation of ATRP polymers to antibody fragments would provide compounds with the desired properties. Therefore, we synthesized ATRP polymers containing maleimide groups, which can react selectively with a cysteine side-chain in the antibody fragment (4.4, Figure 4.2). This strategy avoids undesired side reactions of the lysine residues in the antibody which would be expected with an amide bond-forming strategy, providing a polymer with consistent and oriented binding sites.

Several antibodies capable of crosslinking Fas are available (Komada *et al.*, 1999). We employed the IgG producing clone DX2. This antibody had been previously shown to cause apoptosis in cultured malignant glioma (T98G) (Kawaguchi *et al.*, 2000). Antibody Fab' was prepared by standard methods using pepsin digestion to remove the Fc portion of the antibody. Subsequent reduction of the inter-chain disulfide bonds in the F(ab')<sub>2</sub> (Figure 4.9.1)(Hermanson, G. T., 1996) resulted in fragments containing free sulfhydryl residues that undergo reaction with the maleimide-functionalized polymer to yield the desired conjugate (Figure 4.9.2). We prepared sufficient quantities of this material to perform preliminary experiments and characterize the ability of these ligands to induce apoptosis in Fas-sensitive cells in vitro.



**Figure 4.8. Crosslinking of Fas using antibodies or antibody conjugates.**

(1) Fas can be crosslinked at the cell surface using multivalent antibodies. (2) Synthetic conjugates containing antibody fragments that bind Fas may provide a more efficient display of binding sites.

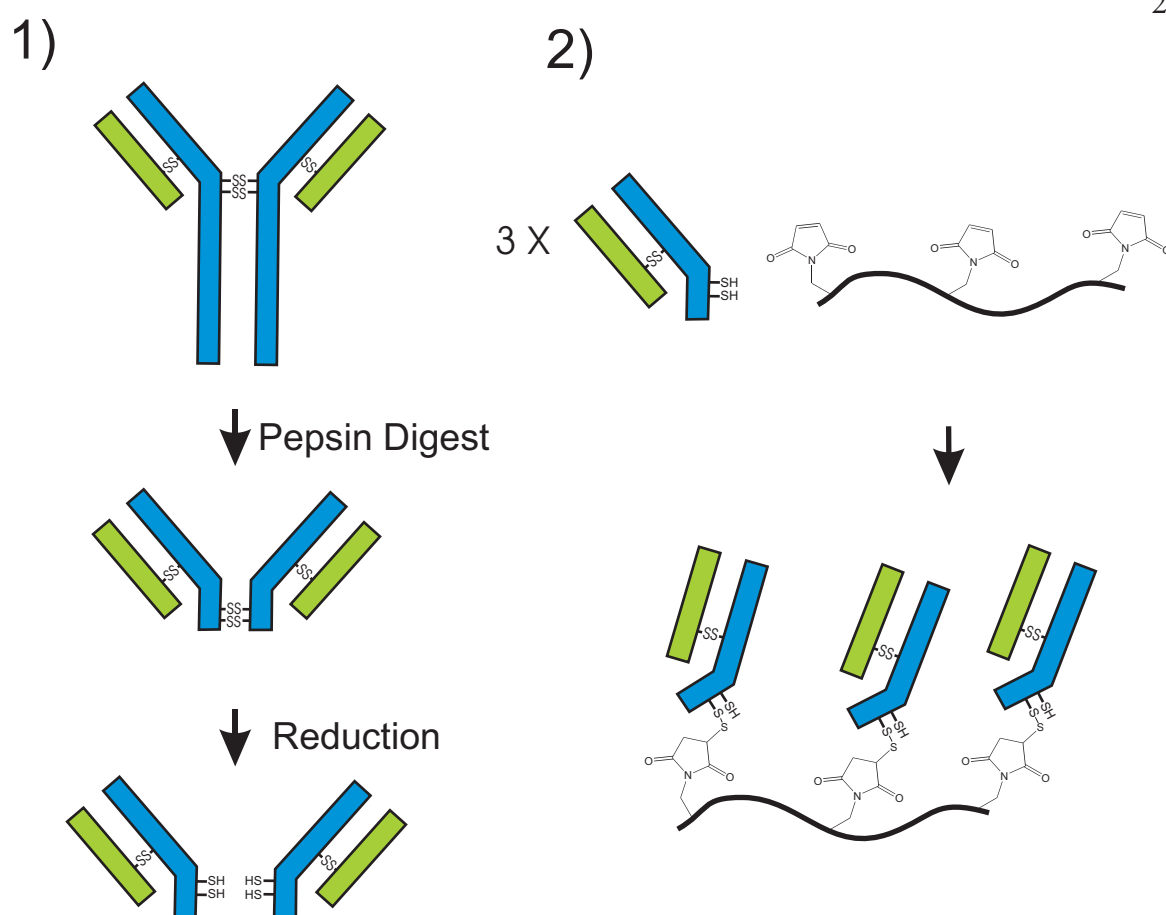
#### 4.5.5. Toxicity of multivalent Fab' conjugates.

We employed cell viability assays with a human malignant glioma line, T98G, for determining the activity of our antibody conjugates (Kawaguchi *et al.*, 2000). We first confirmed that the polymer backbone alone and the whole antibody alone were not cytotoxic (Figure 4.11.1). The IgG (clone DX2) was not toxic to cells at low concentrations (3  $\mu\text{g/mL}$ ). Higher valency IgM antibodies (clone CH-11) were toxic to cells with an  $\text{LC}_{50}$  of approximately 25  $\mu\text{g/mL}$  (Figure 4.11.3). As expected, cells treated with synthetic antibody conjugates showed dramatic reductions in cell viability at concentrations of 5  $\mu\text{g/mL}$  (Figure 4.11.1). These data suggest that the synthetic antibody conjugates are effective reagents for killing Fas(+) cells. Ongoing work will compare the activities of semi-synthetic conjugates to antibodies and provide more detailed characterization.

To more accurately compare enhancements of activity, more extensive characterization of the antibody conjugates will be required. We have analyzed the conjugates used by SDS-PAGE, and we observe the MW of the ligands to be approximately 210 kD. This mass suggests the conjugation of three separate Fab' fragments to the backbone. However, larger scale experiments are required to confirm the presence or absence of lower molecular weight species of lower abundance. Additionally, a range of concentrations for each conjugate will be required to establish the actual  $\text{LC}_{50}$  of each conjugate for comparison to the parent IgG.

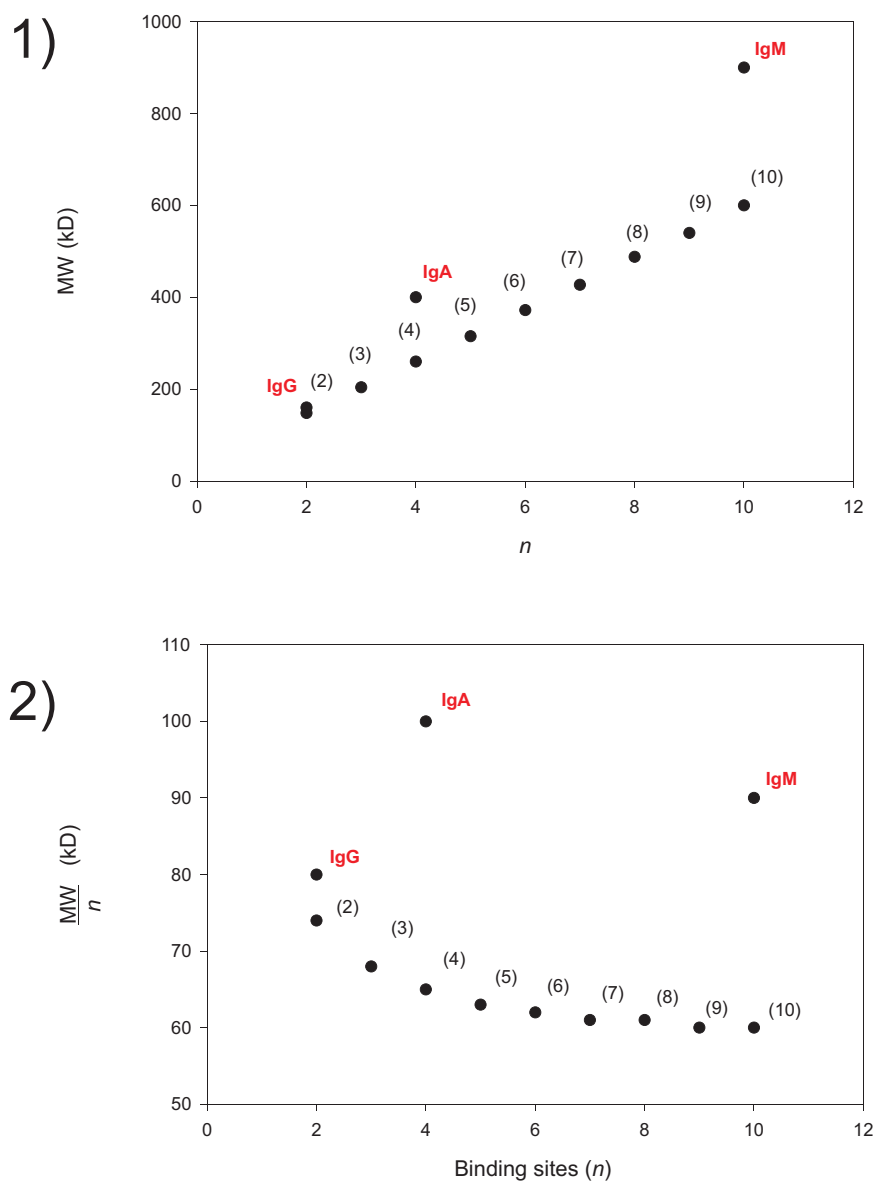
Considering these results, we propose that future studies using multivalent ligands with different structural features will provide new insights into membrane oligomerization of Fas. Analogous to our previous studies in solution, we would predict that determinations of

ligand avidity, binding stoichiometry, binding kinetics, and signaling will test structural hypotheses regarding Fas oligomerization. All of these parameters, particularly ligand avidity and stoichiometry can be characterized using cytometry methods (Owen *et al.*, 2002). Additionally, FRET methods may provide a method for *in situ* determination of receptor proximity.



**Figure 4.9. Preparation of multivalent antibody conjugates.**

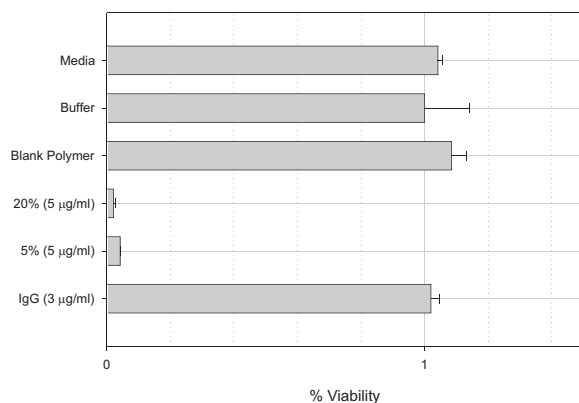
IgG is treated with pepsin in order to cleave the Fc portion of the antibody. The remaining  $F(ab')_2$  can then be selectively reduced using cysteamine to form the Fab' fragment with two thiol groups available for reaction with maleimide polymers. The resulting conjugate has uniform orientation of the Fab' binding sites away from the polymer.



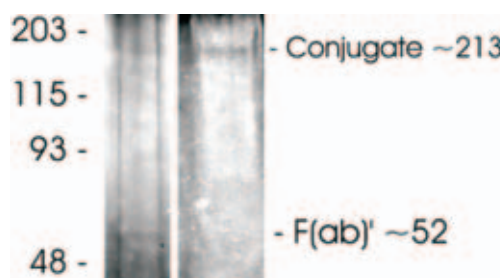
**Figure 4.10. Theoretical properties of antibody conjugates.**

Multivalent antibodies are well known crosslinking reagents. However, a large portion of the MW of these proteins is not required for binding (Fc). Therefore, conjugates constructed with Fab' fragments should have a considerably smaller MW per binding site. The theoretical MW of conjugates of **4.4** and Fab' fragments are plotted versus their valency (1). IgG, IgA, and IgM are also included for comparison. The ratio of MW to valency shows that the efficiency of the binding site presentation is significantly improved using conjugates (2).

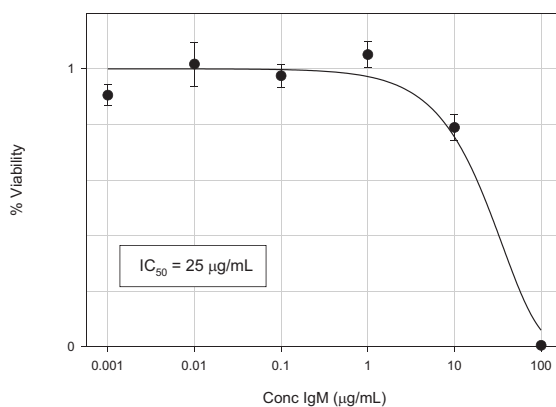
1)



2)



3)



**Figure 4.11. Activity of  $\alpha$ -Fas conjugates.**

1) Cell viability experiments using antibody conjugates were performed using a cultured human malignant glioma line (T98G). Viability measurements represent at least five replicates per point, and the error represents the standard deviation. Concentrations were determined by  $A_{280}$  (see: Experimental Methods.) Both conjugates are highly toxic at 5  $\mu\text{g/mL}$ , however the parent IgG is not toxic at this concentration. Treatment of the cells with an unconjugated polymer did not show any change in viability. 2) Characterization of the conjugates by SDS-PAGE gel with silver staining shows conversion of the Fab' to a higher molecular weight conjugate ( $\sim 210$  kD). 3)  $LC_{50}$  determination of IgM (clone CH-11) in T98G cells. The measured  $LC_{50}$  is approximately 25  $\mu\text{g/mL}$ . Compound structures are shown in Figure 4.2.

#### 4.6. Conclusions.

The use of multivalent ligands as effectors is emerging as a general strategy for the study of signaling events (Kiessling *et al.*, 2000a). Researchers from these and other laboratories have used multivalent ligands for the study of bacterial chemotaxis, T cell activation, and L-selectin shedding (Cochran and Stern, 2000; Gestwicki and Kiessling, 2002; Gordon *et al.*, 1998; Kiessling *et al.*, 2000a). Our studies of Con A- and Fas-crosslinking demonstrate that receptor oligomerization state can have a profound effect on apoptotic signaling *in vitro*, a finding that suggests strategies to control multivalent binding events. The applications demonstrated here suggest an essential role for synthetic macromolecular chemistry in the manipulation and study of biological systems.

The specific strategies used here employed two separate approaches to receptor crosslinking at the cell surface. Using multivalent saccharide polymers, we were able to alter the proximity of cell surface receptors that bound to Con A. The complexes formed in these experiments consisted of three components: the multivalent ligand (polymer), the soluble receptor (Con A), and the cell surface receptor (PZR). These studies provided a direct application of our model studies of receptor crosslinking in solution from Chapter 3. We observed that ligands generated by ROMP were able to crosslink Con A in solution and were able to scaffold lectins that potentiated Con A cell toxicity. The putative glycoprotein ligand for Con A, PZR, was therefore presumably clustered in at the membrane *via* scaffolded Con A complexes in solution.

We also employed a more direct crosslinking strategy using receptor-binding antibody fragments covalently-linked to the polymer backbone. These compounds were able to directly bind and crosslink target cell surface receptors. Synthetic conjugates of intermediate MW (~



210 kD) were shown to induce apoptosis in cultured glioma cell lines. We anticipate our results will lead to effective methods for the activation of apoptosis in malignant Fas(+) cells.

We have hypothesized that multivalent ligands could provide tools for “outside-in” signal transduction. Using two disparate systems, we have observed potent changes in apoptotic signaling. These strategies used both direct binding (polymer-Fas) and scaffolded receptor binding (polymer-Con A-PZR) to alter signaling. The activities of the macromolecular complexes are strikingly consistent with those predicted from solution-phase studies previously conducted with multivalent lectins. Therefore, we have established a panel of solution techniques for high throughput identification of active ligands, and the activity identified in this way was predictive of the cellular response. This paradigm of multivalent ligand design should provide a robust framework for the development of synthetic agents that cluster cell-surface receptors and elicit desired activities.

#### 4.7. Experimental Methods.

##### *Reagents:*

All cell culture media, serum, and reagents were obtained from GIBCO BRL (Rockville, MD) unless otherwise noted. MTT (3-(4,5-dimethylthiazol-2-yl)-2,5-diphenyltetrazolium bromide) was obtained from Sigma-Aldrich Chemical Co. (Milwaukee, WI). Tissue culture flasks used were culture treated with vented caps (Cell<sup>+</sup>, Sarstedt, Norton, NC). Multivalent mannose-substituted polymers were prepared using the ROMP and the post-polymerization modification strategy, and they were characterized as described (Strong and Kiessling, 1999). Polymer lengths (*n*) were determined by <sup>1</sup>H NMR integration of internal olefin resonances and terminal phenyl resonances.

##### *Cell Culture of PC12, SW837, and HCT15 cells:*

All cells were grown in a humidified incubator at 37 °C and 5% CO<sub>2</sub>. PC12 cells (ATCC: CRL-1721) were grown in media containing 84% RPMI 1640 (with L-glutamine), 5% heat inactivated fetal bovine serum, 10% heat inactivated horse serum, and 1% penicillin/streptomycin (10,000 units/mL). Low serum media for viability assays contained 97.5% RPMI 1640, 0.5% heat inactivated fetal bovine serum, 1.0% heat inactivated horse serum, and 1% penicillin/streptomycin. SW837 (ATCC: CCL-235) and HCT15 cells (ATCC: CCL-225) were grown in 88% MEM (with Earl's salts and L-glutamine), 10% heat inactivated fetal bovine serum, 1% penicillin/streptomycin. Low serum media for viability assays contained 98% MEM, 1% heat inactivated fetal bovine serum, and 1% penicillin/streptomycin. Cells were harvested at confluence by treatment with trypsin (0.25% trypsin and 0.4 mM EDTA) followed by quenching with fresh medium. Cells were centrifuged to a pellet (2100 rpm for 10 minutes), aspirated, then re-suspended in fresh

medium. The population was determined by haemocytometer, cells were then transferred to 96-well plates (tissue culture treated, CoStar, Corning NY) in media at 10,000 cells/well. Plates were then incubated for 24 h to allow cells to adhere. Before the addition of samples, media was removed and replaced with fresh low serum media.

*Viability Assays using PC12, SW837 and HCT15 cells:*

Concanavalin A (Con A) and fluorescein-labeled succinyl-Con A (Fl-sCon A) was obtained from Vector Labs (Burlingham, CA) and was prepared fresh for all experiments. The concentration of the Con A stock solutions were determined using  $A_{280}^{1\%} = 13.7$  (assuming Con A monomers with a molecular mass of 26,000 Da) (Liener, I. E., 1976). All samples were prepared in HBS buffer (HEPES 10 mM, NaCl 150 mM, and  $\text{CaCl}_2$  1 mM, pH = 7.4) at 5x the final concentration to allow dilution with media. Samples and controls in HBS (20  $\mu\text{L}$ ) were then added to a fresh plate of cells in fresh low serum media (80  $\mu\text{L}$ ) 24 h after plating. The samples were then incubated for 48 h at 37 °C. After incubation, 10  $\mu\text{L}$  of a 5 mg/mL solution of MTT in low serum media was added to each well. After 4 h, 100  $\mu\text{L}$  of lysis buffer (50% dimethyl formamide / 20% sodium dodecyl sulfate, pH = 4.7) was added. Control samples for each experiment contained buffer, Con A in buffer, and the highest concentration of ligand in buffer without Con A. Background controls were prepared by lysis of cells prior to addition of MTT. The cells were incubated overnight, and the resulting absorbance was read on a Biostar plate reader at 570 nm. Percent cell viability was determined by the following equation:

$$\%V = \frac{G_1 - G_0}{G_{con} - G_0} \quad \text{eq. 4.1}$$

where  $G_0$  is the signal derived from lysed cell control,  $G_{con}$  is the signal from control cells treated with Con A and buffer, and  $G_1$  is the signal from a sample in buffer.

Viability data were fit to a standard  $IC_{50}$  equation:

$$\%V = \frac{a - d}{1 + \left(\frac{x}{c}\right)^b} + d \quad \text{eq. 4.2}$$

where  $x$  is the concentration of polymer,  $\%V$  is the measured viability,  $a$  is the maximum of the curve,  $b$  is the slope of the curve,  $c$  is the  $IC_{50}$ , and  $d$  is the minimum of the curve. Error in reported values is the standard error of the fit.

#### *Microscopy Procedure:*

Cells were grown until confluent, harvested, and counted as above. The cells were added to 6 well plates containing 1.5 ml of fresh media and flame-sterilized glass coverslips ( $25 \times 10^3$  cells per well). Coverslips for PC12 culture were first treated with collagen (50  $\mu\text{g/mL}$  rat tail collagen I, in 0.02 M acetic acid) and washed. Cells were allowed to adhere for 48 h. The media was removed and replaced with samples (0.2 mL sample in HBS, 0.8 mL low serum media). Samples contained Con A ( $1 \times 10^{-7}$  M) or polymers **4.1** (10 mannose equivalents for PC12 cells; 20 mannose equivalents for SW837 cells) or **4.2** (10 mannose equivalents PC12; 20 mannose equivalents SW837) and Con A ( $1 \times 10^{-7}$  M). The cells were then incubated for 48 h. The plate was removed to 4 °C and washed 2X with HBS, and then fixed with 2% paraformaldehyde for 60 minutes (2% paraformaldehyde, HEPES 50 mM, NaCl 150

mM, CaCl<sub>2</sub> 5 mM, pH = 7.4). After fixing, the cells were washed with fresh HBS 2X, and the coverslips were mounted on glass slides with Vectashield preservative (Vector Labs, Burlingame CA). Images were acquired at 400x magnification on a Zeiss Axioscope.

#### *Fluorescent Microscopy:*

Cells were grown until confluent and harvested as above. The cells were added to 6 well plates containing 1.5ml of fresh media and flame-sterilized glass coverslips (25e<sup>3</sup> cells per well). Coverslips for PC12 cell culture were first treated with collagen as above. Cells were allowed to adhere for 48 h. The media was removed and replaced with samples in HBS (0.5 mL). Samples contained Fl-sCon A (1 x 10<sup>-6</sup> M, determined using  $A_{280}^{1\%} = 13.7$ ), polymer samples contained either **4.1** or **4.2** (200 mannose eq.) and Fl-sCon A (1 x 10<sup>-6</sup> M). The cells were then incubated for 2 h at 37 °C, and removed to 4 °C and washed 2X with HBS. The cells were then fixed with paraformaldehyde for 60 minutes (2% paraformaldehyde, HEPES 50 mM, NaCl 150, CaCl<sub>2</sub> 5mM, pH = 7.4). After fixing, the cells were washed again with fresh HBS 2X, and the coverslips were mounted on glass slides with Vectashield preservative (Vector Labs, Burlingame, CA). Images were acquired at 400x magnification on a Zeiss Axioscope with a FITC filter set. Images were false colored from black and white.

#### *Culture of T98G cells.*

All cells were grown in a humidified incubator at 37 °C and 5% CO<sub>2</sub>. T98G cells (ATCC: CRL-1690) were grown in media containing 89% MEM (with Eagle's salts), 10% heat inactivated fetal bovine serum, and 1% penicillin/streptomycin (10,000 units/mL). Cells were harvested at confluence by treatment with trypsin (0.25% trypsin and 0.4 mM EDTA)

followed by quenching with fresh medium. Cells were centrifuged to a pellet (2100 rpm for 10 minutes), aspirated, then re-suspended in fresh medium. The population was determined by haemocytometer, cells were then transferred to 96-well plates (tissue culture treated, CoStar, Corning NY) in media at 10,000 cells/well. Plates were then incubated for 24 h to allow cells to adhere.

*Viability assays using T98G cells.*

Viability experiments for T98G cells were similar to above. All experiments were conducted using culture medium. Briefly, cells were harvested at confluence and plated at a density of 10,000 cells per well. Cells were allowed to adhere for 24 h. Samples were added as 20  $\mu$ L ea. into wells already containing 80  $\mu$ L of fresh media. Cells with samples were incubated for 48 h at 37 °C in 5% CO<sub>2</sub>. Viability was then assessed using MTT reduction over 4 h, followed by lysis and measurement of A<sub>570</sub>.

*Isolation of Fab' fragments.*

Antibody fragments were prepared according to standard methods (Hermanson, G. T., 1996). Purified mouse (monoclonal) anti-human Apo-1/Fas/CD95 antibody (clone DX2, lot# 0201, cat# AHS9544, Biosource Int., Camarillo, CA) was obtained in 0.5 ml PBS at 1 mg/mL antibody. The antibody was diluted to 0.1 mg/mL in sodium acetate buffer (20 mM NaOAc, pH 4.5) and added to a slurry of immobilized pepsin resin (0.25 mL, Pierce). The slurry was agitated at 37 °C for 24 h to digest the IgG into F(ab')<sub>2</sub>. The digestion was quenched by the addition of high pH buffer (3 mL, 10 mM Tris-HCl, pH 8.0). The gel was removed by centrifugation and washed with buffer. The digestion was purified over a column of immobilized protein A (equilibrated with 10 mM Tris-HCl, pH 8.0) to remove resulting Fc

fragments. The eluent was observed using  $A_{280}$  and BCA assay (Pierce), and the first major peak was isolated and concentrated to  $\sim 1$  mg/mL. Remaining undigested IgG and Fc fragments were eluted from the column using low pH buffer (0.1 M glycine, pH 2.8).

The  $F(ab')_2$  fragment was dialyzed into PBS (0.1 M sodium phosphate, 0.15M NaCl, 10 mM EDTA, pH 7.2) at 1 mg/mL. The fragment was reduced by the addition of 6 mg of 2-mercaptoethylamine (2-aminoethanethiol hydrochloride, Aldrich) per 1 mL of protein solution. The solution was incubated for 90 min at 37 °C in a sealed tube. To remove excess reductant, the solution was passed over a flow-through column containing Sephadex G-25 resin equilibrated in PBS (0.1 M sodium phosphate, 0.15M NaCl, 10mM EDTA, pH=7.2). The column was monitored by  $A_{280}$  and BCA assay (Pierce). Fractions containing protein free of reductant were pooled and immediately reacted with maleimide containing polymer (4.4).

Products of each step were monitored by SDS-PAGE (samples were boiled, but free of DTT in order to observe whole IgG and Fab'). Observed bands were found at the following ranges: IgG1  $\sim 150$ -160 kD,  $F(ab')_2 \sim 105$  kD, Fab'  $\sim 52$  kD, conjugates  $\sim 213$  kD. Concentrations of fragments were determined using extinction coefficients of:  $\epsilon_{280}$  IgG =  $7.5 \times 10^4 \text{ M}^{-1}\text{cm}^{-1}$ ,  $\epsilon_{280}$  Fab' =  $22.1 \times 10^4 \text{ M}^{-1}\text{cm}^{-1}$ .

#### *Synthesis of multivalent conjugates.*

Maleimide polymer 4.4 was dissolved in PBS at 100  $\mu\text{g/mL}$  and combined with a solution of freshly reduced Fab' in PBS. The final molar ratio was 4:1 Fab' to polymer. The solution was incubated at ambient temperature for 12 h. The sample was then concentrated and dialyzed into fresh PBS. Analysis by SDS PAGE showed appearance of a new band at  $\sim$

210 kD and disappearance of the Fab' band at ~ 52 kD. Concentrations of the conjugates were calculated using the extinction coefficient of Fab'.



## Appendix. Surface Immobilization of Multivalent Ligands and Receptors.

Portions of this work are published in:

“Selective Immobilization of Multivalent Ligands for Surface Plasmon Resonance and Fluorescence Microscopy.” Gestwicki, J. E., Cairo, C. W., Mann, D. A., Owen, D. E., and Kiessling, L. L., *Analytical Biochemistry*, **2002**, 305, 149-155.

Contributions:

Compounds **A.1** and **A.2** were contributed by R.M. Owen.

Compounds **A.3** and **A.4** were contributed by F.J. Boehm.

Compound **A.5** was contributed by L.E. Strong.

GGBP was contributed by J.E. Gestwicki.

P- and L-selectin were contributed by D.A. Mann.

## **A.1. Immobilization of end-labeled ROMP-derived polymers.**

### **A.1.1. Introduction.**

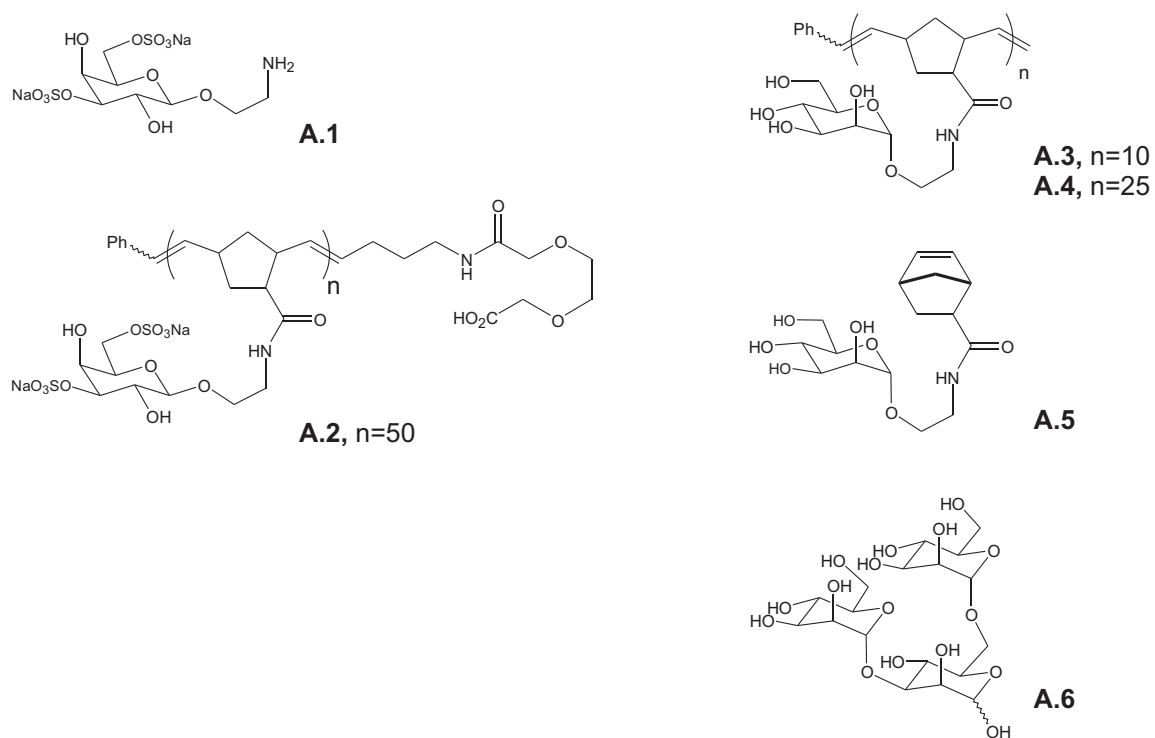
Several biological systems exploit multivalent presentation of ligands for the enhancement of specificity and affinity (Kiessling and Pohl, 1996; Mammen *et al.*, 1998a). The precise mechanisms of these enhancements are difficult to study due to the lack of homogeneous multivalent substrates. Using methods for the preparation of end labeled multivalent saccharide polymers, we prepared substrates for surface plasmon resonance (SPR) studies. These materials present uniformly oriented multivalent ligands with low polydispersity and can therefore be used as model systems for studying these interactions. We examined the effect of changing the presentation of 3,6-disulfogalactose using these ligands immobilized on an SPR biosensor. Using a similar molar quantity of sites on two surfaces, one with 3,6-disulfogalactose presented on a polymer backbone and one presented with an even distribution on the surface, the measured affinity of proteins that recognize these substrates is altered. We find that presentation of the monosaccharide on a polymer backbone results in an apparent 5-6 fold increase in affinity.

### **A.1.2. SPR studies of selectin binding.**

SPR biosensors provide an exceptionally sensitive means to study binding interactions. These experiments are extremely versatile and can be used for the derivation of kinetic and thermodynamic binding parameters. We reasoned that SPR could provide a useful means to study multivalent binding interactions, however we required a method for the selective and homogeneous immobilization of either a multivalent ligand or its receptor. Ring opening metathesis polymerization (ROMP) has been used to prepare multivalent

presentations of saccharides with low polydispersity for a number of different systems (Gestwicki and Kiessling, 2002; Kanai *et al.*, 1997; Maynard *et al.*, 2001; Sanders *et al.*, 1999). Recent work has developed selective end-capping strategies for this method that provide a single site on each polymer for reaction (Gordon *et al.*, 2000; Owen *et al.*, 2002). Using this strategy we employed end-capped polymers produced by ROMP to synthesize surfaces for studies of the binding of receptors to immobilized multivalent ligands (compound **A.2**, Figure A.1).

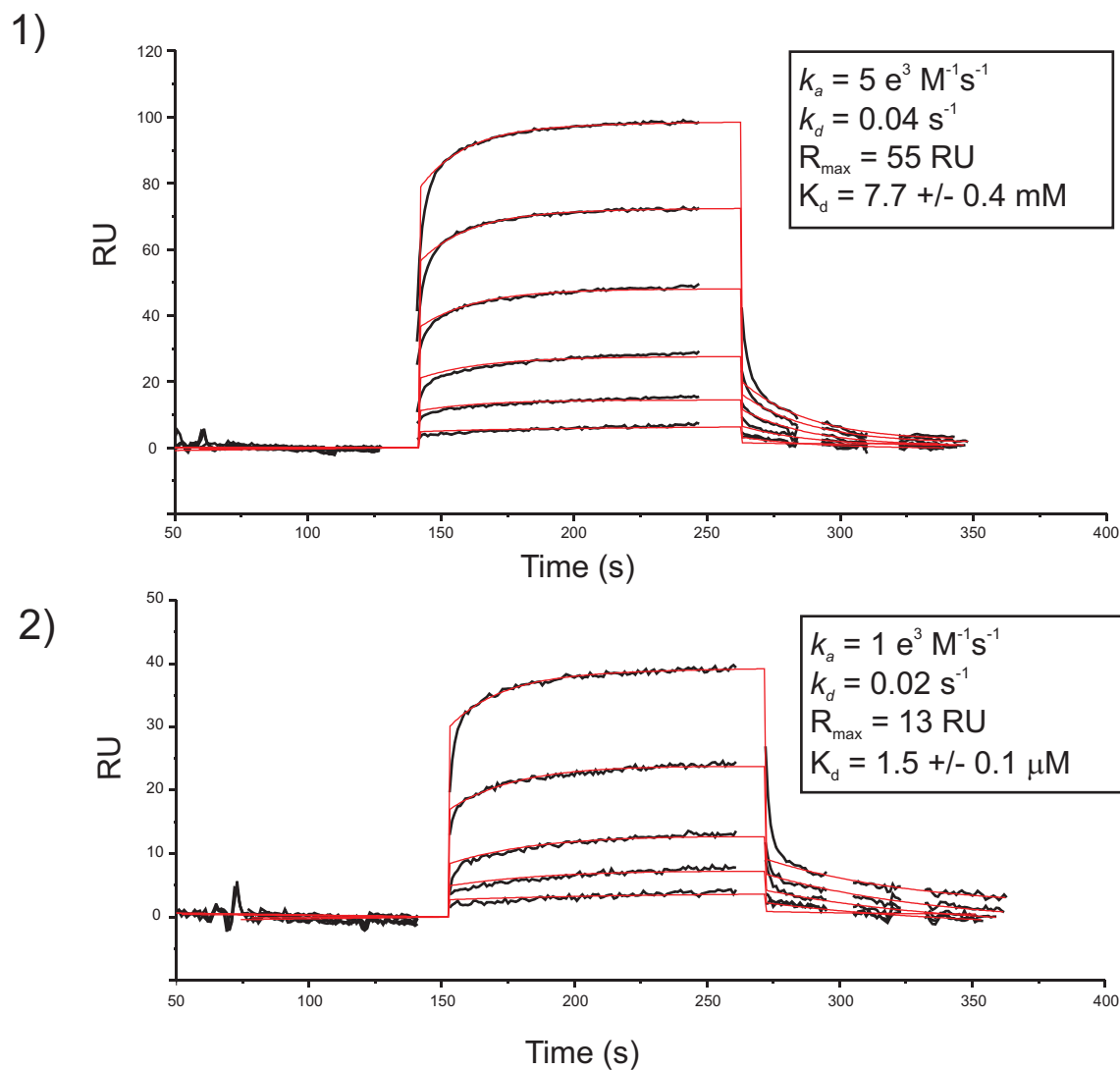
We selected an end-capping strategy that was compatible with the standard amine-coupling chemistry used for carboxymethyl dextran surfaces (CMD) in SPR studies. The carboxylate-substituted surface was first activated by treatment with EDC/NHS and then reacted with ethylene diamine according to standard protocols (O'Shannessy *et al.*, 1992). The amine-bearing surface could then be reacted with the carboxylate-capped ROMP-derived ligand **A.2** to provide a polymer derivatized surface (82 RU,  $\sim 0.2$  fmol/mm<sup>2</sup>). Additionally, we used the amine-bearing monosaccharide **A.1** to provide a control surface (175 RU,  $\sim 0.4$  fmol/mm<sup>2</sup>). Both surfaces were matched to have similar quantities of sites on each surface based on the change in response units on immobilization. Therefore, each surface should have a similar quantity of binding sites and should only differ in the presentation of those sites. The polymer surface was designed to mimic the presentation of multivalent proteins such as mucins that present multiple saccharide sites in close proximity. The monomer derivatized surface should present a control with randomly distributed sites that are relatively isolated. Comparison of the activity of these two surfaces should provide an indication of the influence of saccharide presentation on binding affinity.



**Figure A.1. Compounds used for SPR studies.**

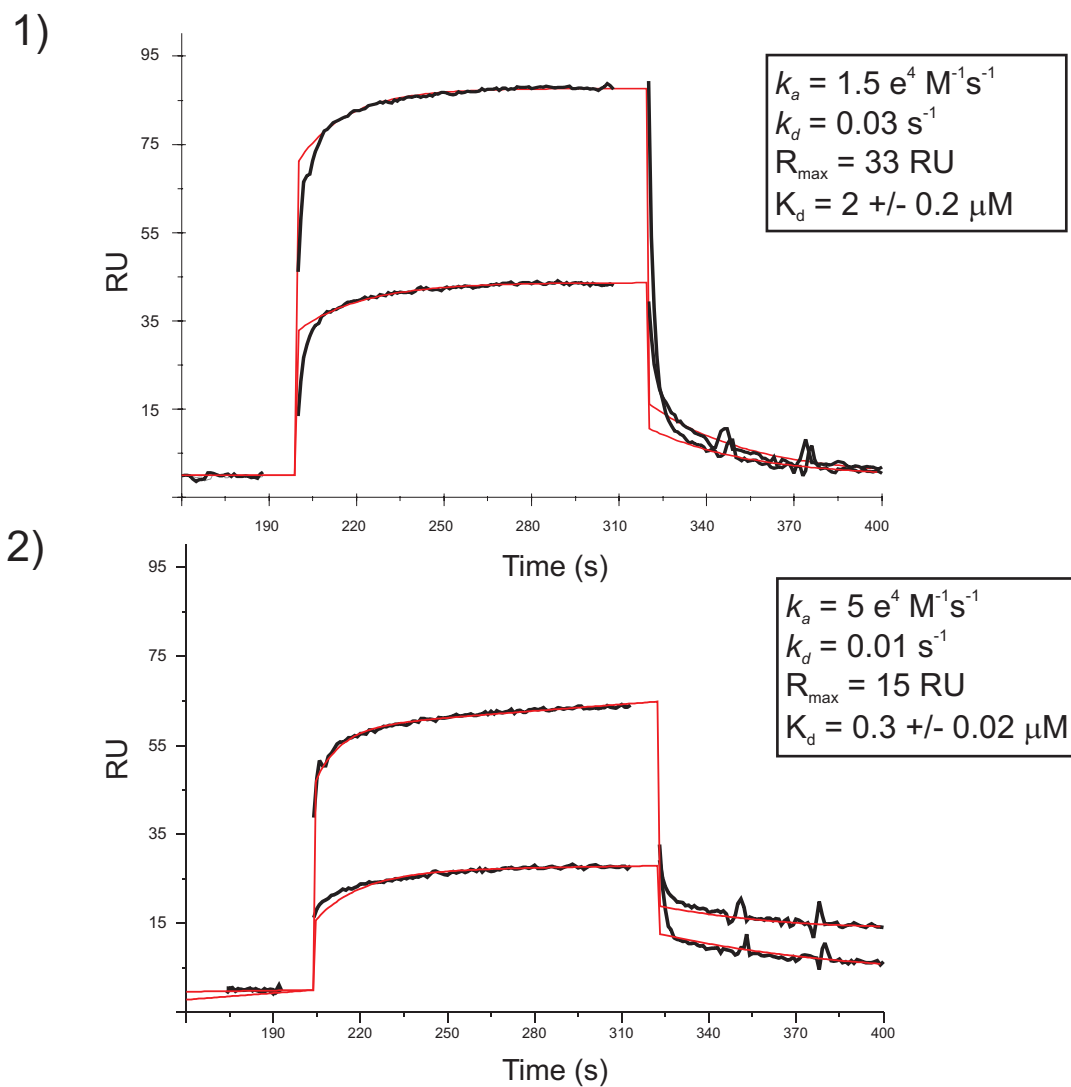
The saccharide ligand used in these studies, 3,6-disulfogalactose, is expected to be a weak binding ligand for the P- and L-selectin. Multivalent presentation of 3,6-disulfogalactose is known to provide tight binding inhibitors of selectin mediated rolling (Sanders *et al.*, 1996; Sanders *et al.*, 1999). Therefore, we predicted that P- and L-selectin could have different binding interactions with the two synthetic surfaces we prepared. Injections of P-selectin at 4, 3, 2, 1, 0.5, and 0.1  $\mu\text{M}$  protein are shown for both surfaces after reference subtraction in Figure A.2. Injections of L-selectin at 2 and 1  $\mu\text{M}$  are shown in Figure A.3. Each of these series of injections were analyzed using a 1:1 kinetic model (Morton and Myszka, 1998; Myszka, 2000; Schuck, 1997). The results of the fits are shown in red in both figures, and the parameters are given.

These experiments found that the affinity of the monomer *versus* the polymer surfaces is significantly different for both P- and L-selectin. In the case of P-selectin we observe a 5-fold increase in affinity for the polymer from the monomer surface. In the case of L-selectin we observe a 6-fold increase of affinity between these two surfaces. The effects of multivalent presentation appear to manifest predominately in the association rates, but the dissociation rates vary in each case as well. This is a significant result as it suggests a physical mechanism by which proteins could enhance their specificity for appropriate multivalent ligands.



**Figure A.2. P-selectin binding to immobilized monomer and polymer surfaces.**

SPR binding experiments were performed using P-selectin at a range of concentrations (4, 3, 2, 1, 0.5, and 0.1  $\mu\text{M}$ ) on the monomer surface (A.1, top) and the polymer surface (A.2, bottom). These curves were fit using a 1:1 binding model (red). The parameters of the fit are shown for each set of traces.



**Figure A.3. L-selectin binding to immobilized monomer and polymer surfaces.**

SPR binding experiments were performed using L-selectin at a range of concentrations (2 and 1  $\mu\text{M}$ ) on the monomer surface (A.1, top) and the polymer surface (A.2, bottom). These curves were fit using a 1:1 binding model (red). The parameters of the fit are shown for each set of traces.

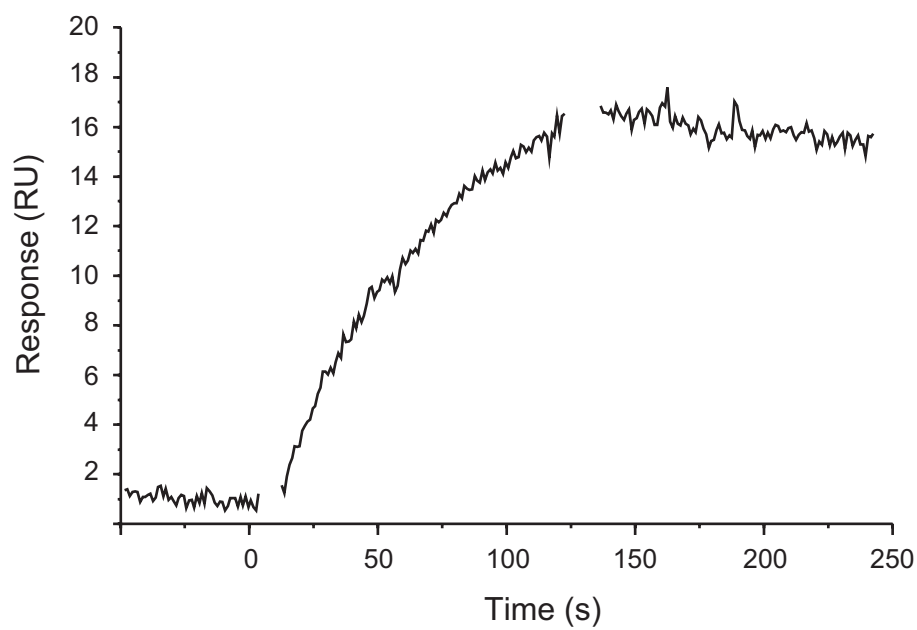
### **A.1.3. SPR studies of cell binding.**

With a synthetic surface capable of binding P- and L-selectin, we hypothesized that we could also examine the binding of L-selectin-expressing cells to these surfaces. Therefore, we exposed Jurkat cells (human leukocyte) to the polymer surface and examined the SPR response (Figure A.5). Although the response is relatively small, we expect that the cells are unable to penetrate the matrix, and therefore only a small portion of the cells can contribute to changes in the signal. Additional experiments were also conducted using fluorescence microscopy to confirm that Jurkat cells bound specifically to the polymer derivatized lane (Gestwicki *et al.*, 2002a).

### **A.1.4. Conclusion.**

Using end-capped ROMP-derived ligands we were able to synthesize uniform surface presentations of multivalent saccharide polymers. These ligands have an enhanced apparent affinity due to their multivalent presentation when compared to randomly distributed monosaccharides. These enhancements were on the order of 5-6 fold for the binding of P- and L-selectin to these surfaces. These studies provide an indication of the mechanisms responsible for the enhanced affinity and specificity generally observed for multivalent ligands in biological systems. The methodology described here should be general and could provide useful materials for more detailed studies of a variety of receptors for multivalent ligands.





**Figure A.4. Jurkat cell binding to immobilized polymer A.2.**

Jurkat cells (10,000 cells/mL) were injected over the polymer surface (A.2) and the SPR response was monitored.

## **A.2. Density-dependent multivalent binding of Con A.**

### **A.2.1. Introduction.**

Multivalent binding interactions are complicated by the presence of multiple simultaneous binding modes, as discussed in Chapter 2. As a result, it is often difficult to determine the contributions of particular binding modes to activity. General methods to study these interactions in the presence or absence of contributing binding modes are needed to understand multivalent binding in solution. We recognized that certain binding modes, such as receptor clustering, are dependent on the proximity of the receptors involved. The surface immobilization of receptors could provide site isolation of the binding sites, and therefore prevent receptor clustering events. Comparison of these measurements to those with mobile receptors could provide an indication of the energetic contribution of receptor clustering.

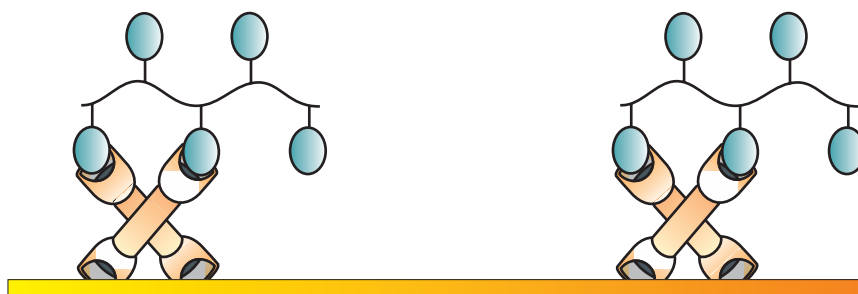
We immobilized high and low density surfaces of the multivalent lectin Concanavalin A (ConA). Due to the range of quantities immobilized, these surfaces should allow the measurement of multivalent binding events under conditions impossible to achieve in solution. Specifically, on a low density surface a small multivalent analyte may not be able to access an intermolecular binding mode due to site isolation; however, a high density surface with reduced spacing between receptors should have access to this additional binding mode (Figure A.5). Using appropriate variations in both the analyte valency and ligand density it should be possible to measure kinetic and thermodynamic parameters of interactions which *lack* particular features such as crosslinking (not present on a low density surface with small ligands), chelate effects (a low density surface with a sufficiently large ligand), and statistical effects (all surfaces with multivalent ligands). We describe here initial studies to determine the feasibility of this approach. We found that the surface density of receptors does influence

the apparent affinity of multivalent ligands. Additionally, we observe differences in the dissociation kinetics due to changes in surface density.

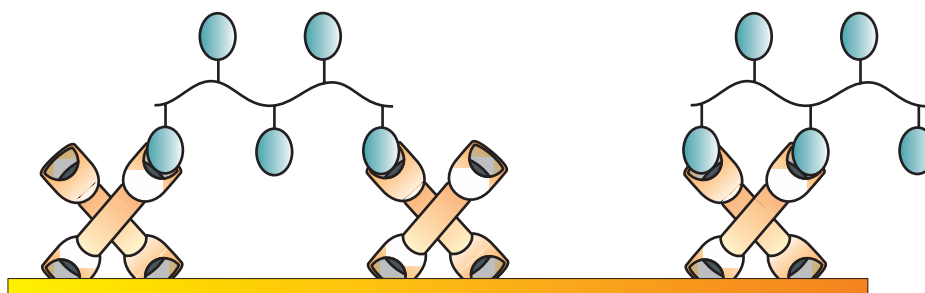
1)



2)



3)



**Figure A.5. Site isolation of multivalent receptors.**

Immobilization of a multivalent receptor (Con A) at low density could allow the study of interactions that eliminate potential binding modes. In the case of a low density surface (2) multivalent ligands are able to interact with only one Con A complex at a time, therefore measured interactions lack contributions from crosslinked binding modes. At high density (3) multivalent ligands of sufficient length can span multiple Con A complexes. Measurements on these surfaces should be similar to those in solution.

### A.2.2. Preparation of SPR surfaces with Con A.

We prepared two sets of surfaces using either C1 or CM5 chips (BIAcore). CM5 chips (also described in Chapter 1) contain a CMD matrix that provides a negatively charged surface. The C1 chip is a short monolayer with terminal carboxylates. This surface lacks a dextran matrix, however it does present a more hydrophobic surface of lower site capacity as a result. This chip has ~10% of the binding capacity of a typical CM5 dextran surface.

Con A was immobilized on these surfaces (pH=7.4 in HBS buffer using standard amide bond forming conditions, i.e. NHS/EDC protocols). The amount of Con A on each surface was varied to provide a range of Con A site density for study (Table A.1). Underivatized carboxylates on these surfaces were deactivated by treatment with ethanolamine. Running buffer was TBS at pH = 8.0 (Tris-HCl 10mM, NaCl 150 mM, CaCl<sub>2</sub> 2 mM, TWEEN20 0.005% v/v and BSA 0.02 mg/mL). Flow rate was 10  $\mu$ L/min and no mass transport effects were observed in control experiments using higher flow rates. Control surfaces were either blank lanes blocked with ethanolamine or lanes coupled to BSA. Regeneration buffers for these experiments were running buffer containing 100 mM  $\alpha$ -methyl-mannose.

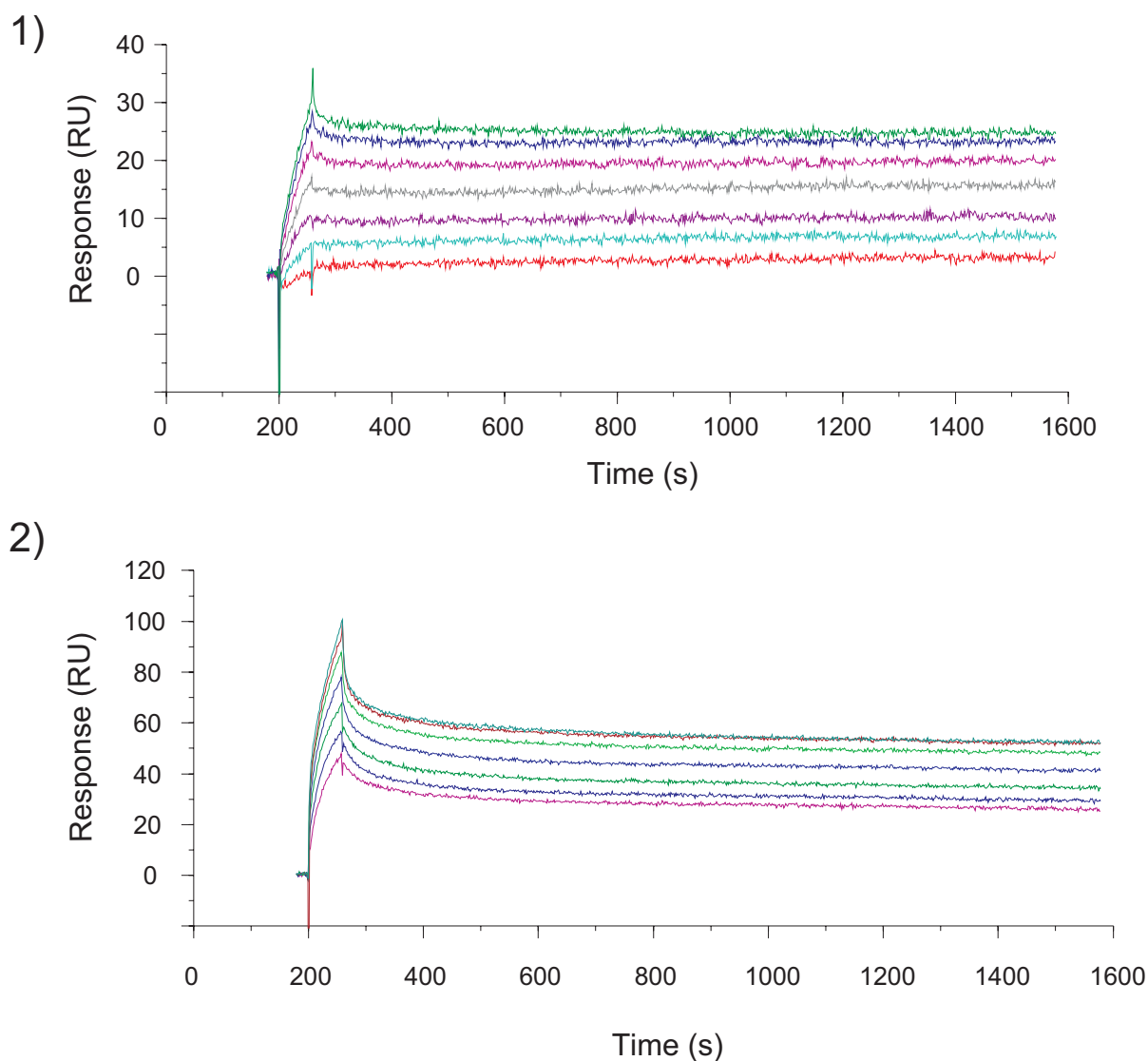
**Table A.1. Variable density Con A surfaces.**

<i>Lane</i>	<i>Chip I – C1</i>	<i>Chip II – CM5</i>
Fc 1	Blank	Ethanolamine blocked
Fc 2	2-4 kRU Con A (inactive)	2.5 kRU Con A HD
Fc 3	0.5 kRU Con A LD	1.4 kRU Con A LD
Fc 4	1.5 kRU Con A HD	0.6 kRU Con A VLD

Ligands for these studies were mannose-substituted ROMP-derived polymers. We used two different length polymers, **A.3** had a DP of 10 and **A.4** had a DP of 25. All polymer concentrations were reported on a saccharide residue basis and solutions were prepared in running buffer. Equilibrium responses were determined by subtraction of the response in the underivatized lane from the response in the sample lane to correct for bulk refractive index.

### **A.2.3. Kinetic studies of multivalent ligand binding to Con A.**

Seven concentrations of **A.3** and **A.4** were injected over the C1 surfaces described above (Chip I, 5000, 2500, 1250, 625, 312, 157, and 78  $\mu$ M)(Figure A.6). Mannose-substituted monomer **A.5** gave insufficient response levels, even at 5 mM concentration on all surfaces. Mannose-substituted 10mer **A.3** gave usable responses ( $> 10$  RU) in the low density (LD) and high density (HD) lanes of the C1 surface. Figure A.6.1 shows injections of seven concentrations of **A.3** over the LD Con A surface. Under these conditions the association phase does not appear to reach equilibrium in the contact time given and the dissociation phase shows an extremely slow off-rate. These experiments were also performed on the HD surface (Figure A.6.2), both the association and dissociation kinetics appear more complex. Again the association phase does not reach equilibrium and here the dissociation appears to be second order. Fits of the linear portion of the dissociation phase of the curve give observed rates that vary by almost 600 fold (Table A.2).



**Figure A.6. Injections of A.3 and A.4 over Con A immobilized surfaces.**

1) Injections of mannose polymer A.3 over a low density C1 surface are shown. Concentrations are 5000, 2500, 1250, 625, 312, 157, and 78  $\mu\text{M}$  in running buffer.

2) Injections of mannose polymer A.3 over a high density C1 surface are shown. Concentrations are 5000, 2500, 1250, 625, 312, 157, and 78  $\mu\text{M}$  in running buffer.

**Table A.2. Linear fits for dissociation phase of compound A.3.**

<i>Surface</i>	<i>k<sub>obs</sub> (RU/sec)</i>
LD	-1.57 x 10 <sup>-4</sup>
A.3 5000 μM	
HD	-3.88 x 10 <sup>-3</sup>
A.3 5000 μM	

Although the proposed experiments rely on the spatial immobilization of receptors, an analysis on the flexible CM5 matrix was also attempted. The matrix of the CM5 chip is potentially flexible and therefore may allow for a system that can engage in intermolecular binding modes even at low density. This could be advantageous in assessing thermodynamic differences between the two surfaces. Mannose-substituted polymers **A.3** and **A.4** were run on this surface at seven concentrations each and their apparent affinities were determined.

#### **A.2.4. Saturable binding of ligands to Con A surface.**

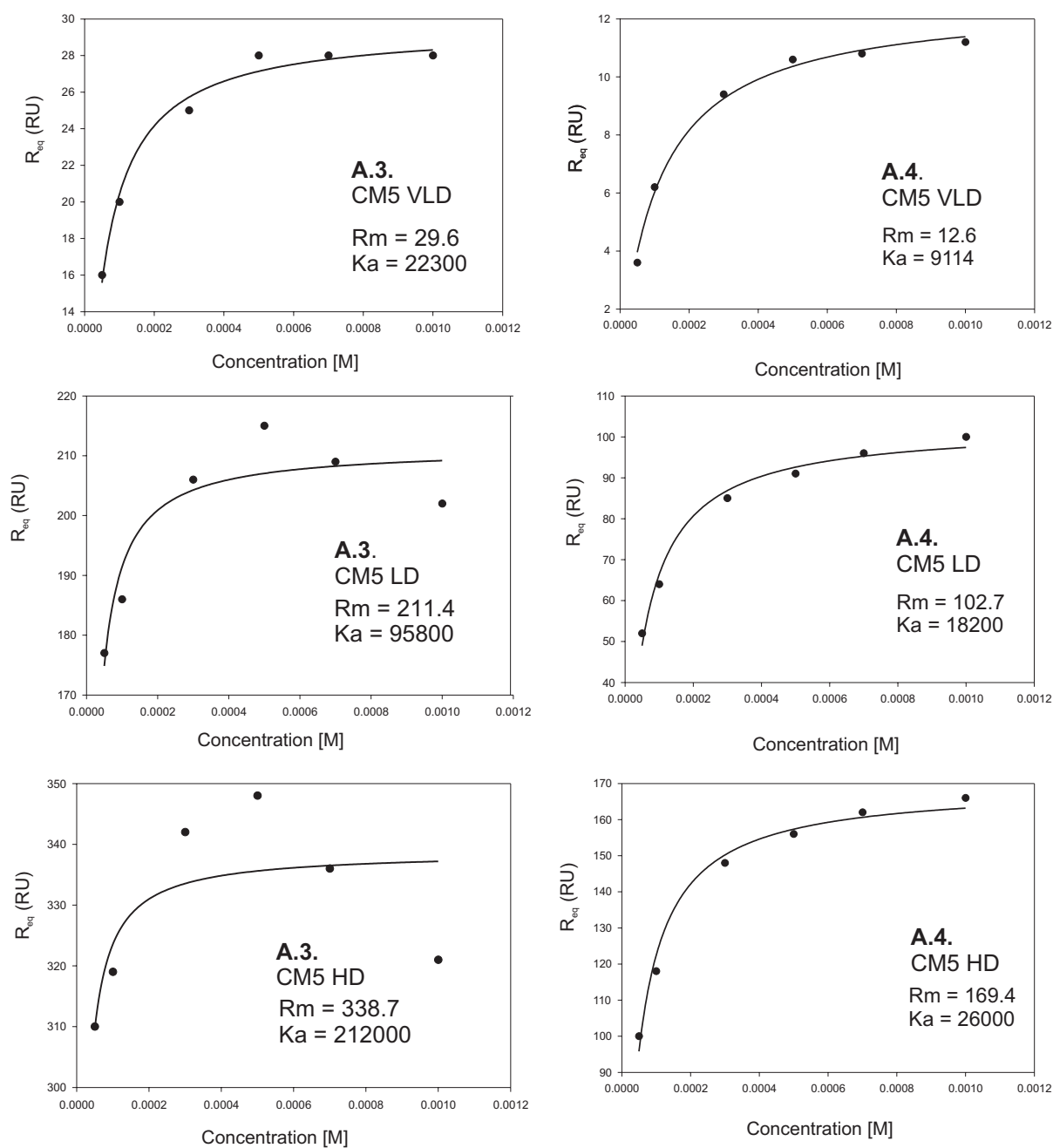
To analyze the data thermodynamically the equilibrium RU values can be used to fit a multivalent Scatchard plot (Kalinin *et al.*, 1995). This data can be fit to a standard binding curve to determine the apparent association constant. Representative raw binding data for compounds **A.3** and **A.4** are shown on both HD and LD CM5 surfaces in Figure A.7. We expect that variation of the number of Con A sites on the surface will result in changes in the apparent affinity at high enough levels of immobilization. Steric crowding could result in decreased apparent affinity. However, intermolecular interactions could result in increased apparent binding affinity. Using assumptions of the surface area of a typical CM5 surface and the volume of the cell, the average distance between Con A binding sites can be approximated (Howell *et al.*, 1998). The results of these theoretical calculations are shown in Figure A.8.



From these calculations and the estimated length of the ligands (Kanai *et al.*, 1997), we would predict to see changes in apparent affinity near 100 and 1000 RU for ligands **A.3** and **A.4**.

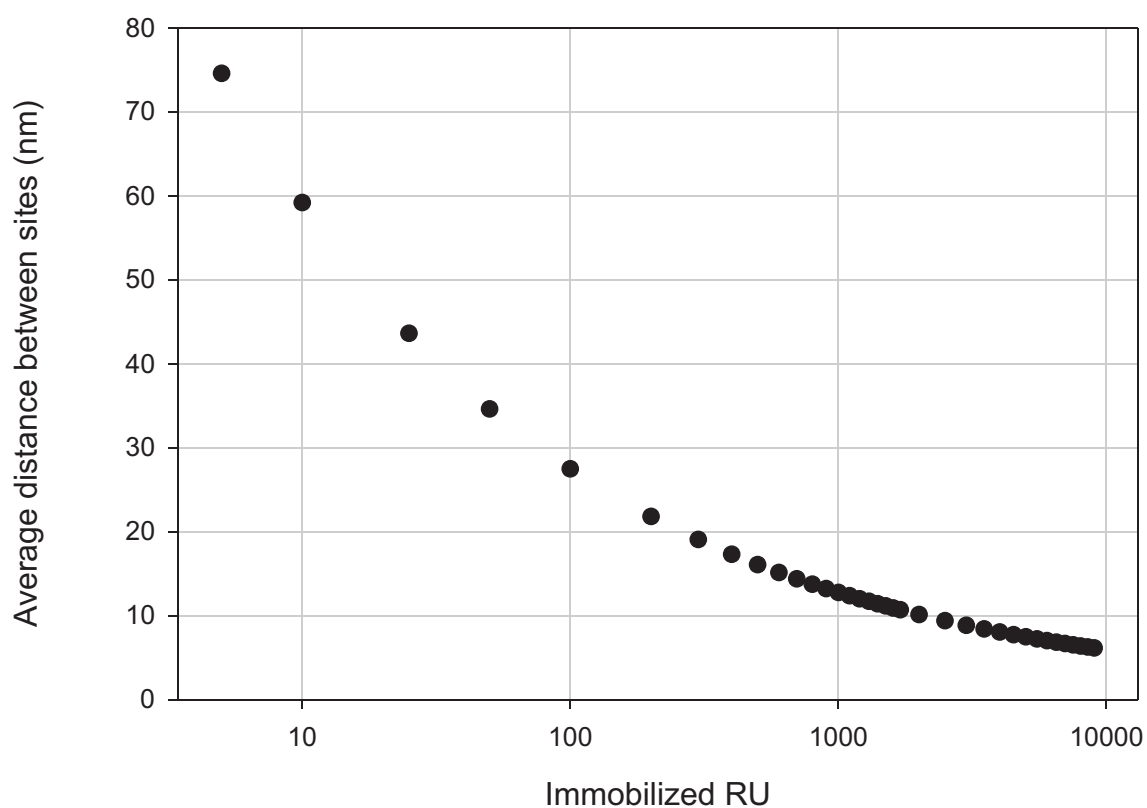
Therefore, we obtained apparent affinity measurements of various Con A surface densities on C1 and CM5 surfaces (Figure A.9 and A.10). Data obtained for C1 surfaces using compound **A.3** and a high affinity monovalent ligand for Con A, trimannoside **A.6**, are shown in Figure A.9. These experiments suggest that the apparent affinity of the monovalent ligand is invariant with density. However, the apparent affinity of ligand **A.3** begins to increase above ~1100 RU. Unfortunately, the limited capacity of the C1 surface prevented the immobilization of more than ~1350 RU on this surface.

To examine the effect of higher Con A densities on the apparent affinity of compounds **A.3** and **A.4**, CM5 chips were used. Two chips were used to prepare six different densities of Con A immobilized under the same conditions as above. The apparent affinities of these surfaces for compounds **A.3** and **A.4** are plotted versus the density of Con A on each surface (Figure A.10). Both polymers show significant increases in their apparent affinity for Con A in these experiments. Interestingly, at high density polymer **A.3** shows a 2-fold increase in apparent affinity and polymer **A.4** shows a 4-fold increase.



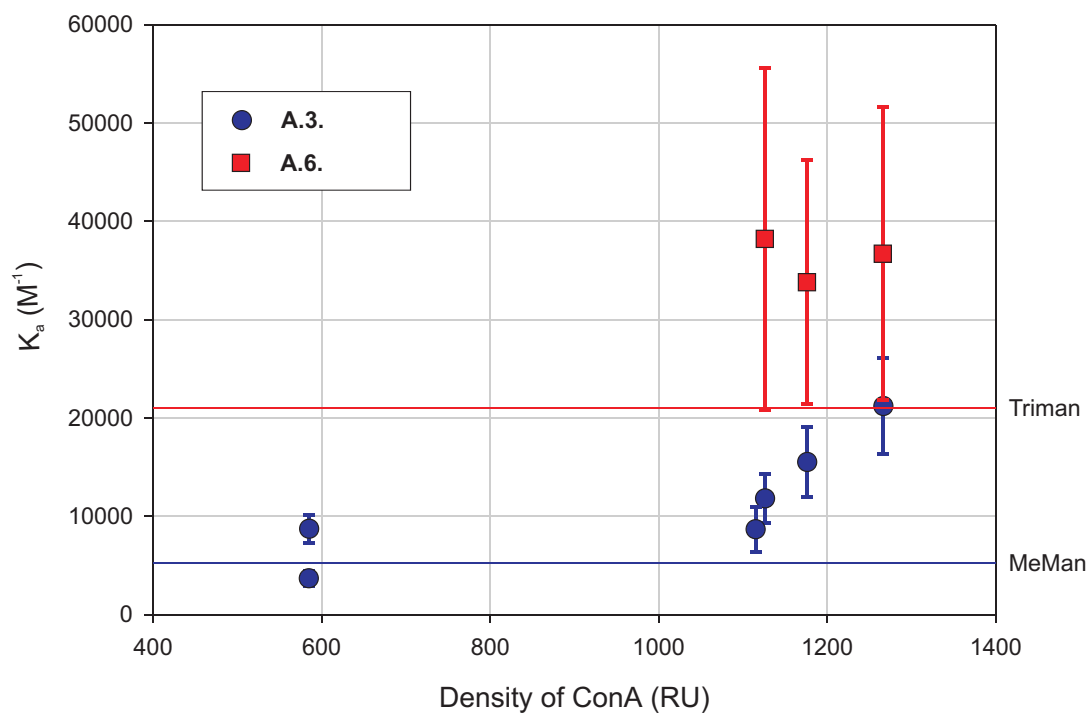
**Figure A.7. Apparent affinity measurements of A.3 and A.4 on CM5 surfaces.**

Equilibrium responses for injections of A.3 and A.4 over HD and LD surfaces of Con A (CM5) are shown. This representative set shows that both polymer give an apparent increase in affinity as the amount of immobilized Con A is increased. Additionally, the two polymers have significantly different apparent affinities.



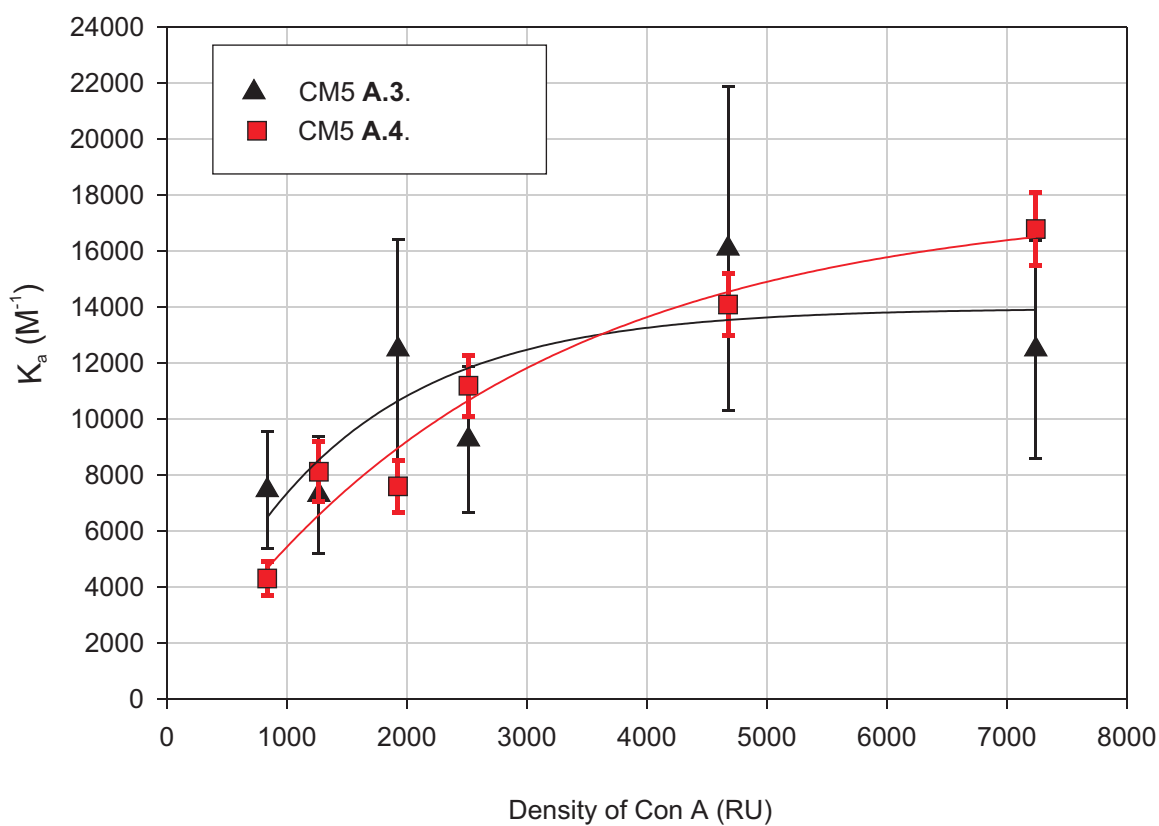
**Figure A.8. Theoretical inter-site distance for immobilized Con A.**

Using the size of the flow cell and assumptions described by Howell *et al.*, the average inter-site distance for Con A binding sites was calculated and plotted for different levels of immobilization.(Howell *et al.*, 1998)



**Figure A.9. Variation of apparent affinity on C1 surfaces.**

Various levels of Con A were immobilized on a C1 surface and the apparent affinity of A.3 was measured from an equilibrium binding experiment. A high affinity ligand for Con A, trimannoside A.6 was also used to confirm that multivalency of the ligand was required for changes in the apparent affinity. The expected affinity of mannose and the trimannoside is plotted for reference. (Williams *et al.*, 1992)



**Figure A.10. Variation of apparent affinity on CM5 surfaces.**

Various levels of Con A were immobilized on a CM5 surface and the apparent affinity of compounds **A.3** and **A.4** were measured by equilibrium binding. Both compounds experience an increase in apparent affinity between 1000-3000 RU.

### **A.2.5. Conclusions.**

Our experiments using variable surface densities of Con A provide an interesting example of surface avidity effects. We found that the apparent affinity of multivalent ligands in solution can be strongly influenced by the amount of immobilized receptor used to measure its affinity. Surface avidity effects are not entirely unknown, however they are not often quantitated (Bamdad, 1998; Shinohara *et al.*, 1997). In this system, we propose that experiments such as these could provide useful indications of the relative contributions of avidity effects for solution binding events. For example, surface densities that are low enough to approximate site isolation could be used to measure the affinity of a ligand in the total absence of avidity effects. Therefore, low-density surfaces could provide a measure of interactions in the absence of clustering. Alternatively, high-density surfaces should approach solution-based experiments where all potential binding modes are accessible. These measurements are currently difficult to achieve in solution-based assays. These experiments provide an initial example of methods to quantitate these effects, however, full characterization of these interactions will require detailed thermodynamic and kinetic analysis. Additionally, direct comparison of these interactions between immobilized and solution assays such as isothermal titration calorimetry (ITC) will be necessary to quantitate the differences between these two configurations.

### **A.3. Experimental methods.**

Sensor chips (CM5 and C1) were purchased from BIAcore (Uppsala, Sweden). SPR experiments were performed on a BIAcore 2000 instrument. Reagents for immobilization (*N*-ethyl-*N'*-(diethylaminopropyl)-carbodiimide (EDC), *N*-hydroxysuccinimide (NHS), and

ethanolamine) were purchased from Aldrich (Milwaukee, WI). Running buffer for SPR was HEPES-buffered saline (HBS, 10 mM HEPES, 150 mM NaCl, pH 7.4) for selectin experiments and Tris-buffered saline (Tris-HCl 10 mM, NaCl 150 mM, 2 mM CaCl<sub>2</sub>, TWEEN20 0.005% v/v and BSA 0.02 mg/mL, pH 8.0) for Con A experiments. Regeneration buffers were TBS (10 mM Tris, 1 mM EDTA, 150 mM NaCl pH 8.5) for selectin experiments and TBS with mannose (100 mM  $\alpha$ -methyl-mannose, 10 mM Tris, 150 mM NaCl, pH 8.0) for Con A experiments. Buffers were filtered (0.25  $\mu$ m) prior to use. The control protein, glucose/galactose binding protein (GGBP), was produced by osmotic shock, as described previously (Gestwicki *et al.*, 2000a). The carbohydrate recognition domain and first EGF-like domain of P- and L-selectin were produced in baculovirus (Mann, 2000). The molecular weight of GGBP is 35 kDa and those of P- and L-selectin are approximately 65 kDa. Protein concentrations were determined by UV-visible spectroscopy at 280 nm. Jurkat cells were maintained as described previously (Gordon *et al.*, 2000). The trimannoside, compound **A.6**, was obtained from Vector Labs, Reading UK, and used as provided.

The surface was prepared for conjugation to polymer as follows. The carboxymethyl dextran (CMD) matrix of a CM5 chip was activated by injection of a solution of EDC and NHS (70  $\mu$ L, 200 mM EDC, 50 mM NHS) at a flow rate of 5  $\mu$ L/min (O'Shannessy *et al.*, 1992). The resulting surface was treated with a solution of ethylene diamine (50  $\mu$ L, 1 M, pH 8.5) to generate a surface bearing free amine groups.

The synthesis of a multivalent ligand with a terminal protected acid was performed as described previously (Gordon *et al.*, 2000). From the acid-bearing polymer **A.2**, an activated ester was generated by treatment with NHS/EDC (50 mM NHS, 200 mM EDC) for 15 minutes at 23 °C in HBS. The resulting polymer bearing a single NHS-ester was purified by

G-50 size exclusion chromatography and immediately injected (0.04  $\mu$ M in HBS) over the amine-bearing CMD surface described above. The SPR response obtained from polymer conjugation to the surface was used to monitor the reaction. The control lane was prepared by analogous treatment without addition of polymer. The monomer-derivatized lane was generated by injection of 30  $\mu$ L of **A.1** (2 mM in HBS pH 7.4) over an NHS-activated CMD surface. The coupling of the monomer was less efficient at pH 4.5 or 8.5.

To measure protein binding by SPR, solutions of P- or L-selectin or GGBP in HBS were injected over the derivatized and control lanes of the modified CM5 surface at a flowrate of 5  $\mu$ L/min. P-Selectin was injected at 4  $\mu$ M, 3  $\mu$ M, 2  $\mu$ M, 1  $\mu$ M, 0.5  $\mu$ M, and 0.1  $\mu$ M. L-Selectin was injected at 2  $\mu$ M and 1  $\mu$ M. GGBP was injected at 4  $\mu$ M. The theoretical  $R_{\max}$  for selectin binding to a surface bearing 82 RU of polymer **A.1** is approximately 140. Global fits to determine the dissociation constants were performed in BIAevaluation software using a 1:1 binding model (Morton and Myszka, 1998).

For cell binding experiments, Jurkat cells were washed 3x with ice-cold HBS and then injected at a concentration of 10,000 cells/mL. Three injections of 10  $\mu$ L were performed. A representative sensorgram is shown (Fig. A.4).



## References

- Acheson, D. W. K., Kane, A. V., and Keusch, G. T. (2000) Shiga Toxins. In Holst, O. (ed.), *Bacterial Toxins: Methods and Protocols*. Humana Press, Totowa, New Jersey, pp. 41-63.
- Adler, J., Hazelbauer, G. L., and Dahl, M. M. (1973) Chemotaxis toward sugars in *Escherichia Coli*. *J. Bacteriol.*, **115**, 824-847.
- Alouf, J. E. (2000) Bacterial Protein Toxins: An Overview. In Holst, O. (ed.), *Bacterial Toxins: Methods and Protocols*. Humana Press, Totowa, New Jersey, pp. 1-26.
- Ames, P., Studdert, C. A., Reiser, R. H., and Parkinson, J. S. (2002) Collaborative signaling by mixed chemoreceptor teams in *Escherichia coli*. *Proc. Natl. Acad. Sci. U. S. A.*, **99**, 7060-7065.
- Anderson, J. and Melchers, F. (1976) Lymphocyte Stimulation by Concanavalin A. In Bittiger, H. and Schnebli, H. P. (eds.), *Concanavalin A as a Tool*. John Wiley & Sons, New York, pp. 505-522.
- Annaert, W. and De Strooper, B. (2000) Neuronal models to study amyloid precursor protein expression and processing in vitro. *Biochim. Biophys. Acta-Molecular Basis of Disease*, **1502**, 53-62.
- Antzutkin, O. N., Balbach, J. J., Leapman, R. D., Rizzo, N. W., Reed, J., and Tycko, R. (2000) Multiple quantum solid-state NMR indicates a parallel, not antiparallel, organization of beta-sheets in Alzheimer's beta- amyloid fibrils. *Proc. Natl. Acad. Sci. U. S. A.*, **97**, 13045-13050.
- Ashwell, A. G. and Morell, G. (1974) The role of surface carbohydrates in the hepatic recognition and transport of circulating glycoproteins. *Adv. Enzymol.*, **41**, 99-128.
- Attie, A. D. and Raines, R. T. (1995) Analysis of Receptor-Ligand Interactions. *J. Chem. Educ.*, **72**, 119-124.
- Bajorath, J. (1999a) Analysis of Fas-ligand interactions using a molecular model of the receptor-ligand interface. *J. Comput. Aided Mol. Des.*, **13**, 409-418.

- Bajorath, J. (1999b) Identification of the ligand binding site in Fas (CD95) and analysis of Fas-ligand interactions. *Proteins: Struct. , Funct. , Genet.*, **35**, 475-482.
- Balbach, J. J., Ishii, Y., Antzutkin, O. N., Leapman, R. D., Rizzo, N. W., Dyda, F., Reed, J., and Tycko, R. (2000) Amyloid fibril formation by A beta(16-22), a seven-residue fragment of the Alzheimer's beta-amyloid peptide, and structural characterization by solid state NMR. *Biochemistry*, **39**, 13748-13759.
- Ballerstadt, R. and Schultz, J. S. (1997) Competitive-binding assay method based on fluorescence quenching of ligands held in close proximity by a multivalent receptor. *Anal. Chim. Acta*, **345**, 203-212.
- Bamdad, C. (1998) The use of variable density self-assembled monolayers to probe the structure of a target molecule. *Biophys. J.*, **75**, 1989-1996.
- Bard, F., Cannon, C., Barbour, R., Burke, R. L., Games, D., Grajeda, H., Guido, T., Hu, K., Huang, J. P., Johnson-Wood, K., Khan, K., Kholodenko, D., Lee, M., Lieberburg, I., Motter, R., Nguyen, M., Soriano, F., Vasquez, N., Weiss, K., Welch, B., Seubert, P., Schenk, D., and Yednock, T. (2000) Peripherally administered antibodies against amyloid beta- peptide enter the central nervous system and reduce pathology in a mouse model of Alzheimer disease. *Nat. Med.*, **6**, 916-919.
- Barondes, S. H., Castronovo, V., Cooper, D. N. W., Cummings, R. D., Drickamer, K., Feizi, T., Gitt, M. A., Hirabayashi, J., Hughes, C., Kasai, K., Leffler, H., Liu, F. T., Lotan, R., Mercurio, A. M., Monsigny, M., Pillai, S., Poirer, F., Raz, A., Rigby, P. W. J., Rini, J. M., and Wang, J. L. (1994) Galectins - A Family of Animal Beta-Galactoside-Binding Lectins. *Cell*, **76**, 597-598.
- Becker, J. W., Cunningham, B. A., Reeke, G. N. Jr., Wang, J. L., and Edelman, G. M. (1976) The Molecular Structure of Concanavalin A. In Bittiger, H. and Schnebli, H. P. (eds.), *Concanavalin A as a Tool*. John Wiley & Sons, New York, pp. 33-54.
- Belshaw, P. J., Spencer, D. M., Crabtree, G. R., and Schreiber, S. L. (1996) Controlling programmed cell death with a cyclophilin-cyclosporin-based chemical inducer of dimerization. *Chem. Biol.*, **3**, 731-738.
- Benzinger, T. L. S., Gregory, D. M., Burkoth, T. S., Miller-Auer, H., Lynn, D. G., Botto, R. E., and Meredith, S. C. (1998) Propagating structure of Alzheimer's beta-amyloid((10-35)) is parallel beta-sheet with residues in exact register. *Proc. Natl. Acad. Sci. U. S. A.*, **95**, 13407-13412.

- Benzinger, T. L. S., Gregory, D. M., Burkoth, T. S., Miller-Auer, H., Lynn, D. G., Botto, R. E., and Meredith, S. C. (2000) Two-dimensional structure of beta-amyloid(10-35) fibrils. *Biochemistry*, **39**, 3491-3499.
- Bernardi, A., Checchia, A., Brocca, P., Sonnino, S., and Zuccotto, F. (1999) Sugar mimics: An artificial receptor for cholera toxin. *J. Am. Chem. Soc.*, **121**, 2032-2036.
- Bertozzi, C. R. and Kiessling, L. L. (2001) Chemical glycobiology. *Science*, **291**, 2357-2364.
- Blatt, N. B. and Glick, G. D. (2001) Signaling pathways and effector mechanisms pre-programmed cell death. *Bioorg. Med. Chem.*, **9**, 1371-1384.
- Boos, W., Gordon, A. S., Hall, R. E., and Price, H. D. (1972) Transport Properties of the Galactose-binding Protein of *Escherichia coli*. *J. Biol. Chem.*, **247**, 917-924.
- Bouckaert, J., Hamelryck, T., Wyns, L., and Loris, R. (1999) Novel structures of plant lectins and their complexes with carbohydrates. *Curr. Opin. Struct. Biol.*, **9**, 572-577.
- Bray, D., Levin, M. D., and Morton-Firth, C. J. (1998) Receptor clustering as a cellular mechanism to control sensitivity. *Nature*, **393**, 85-88.
- Burke, S. D., Zhao, Q., Schuster, M. C., and Kiessling, L. L. (2000) Synergistic formation of soluble lectin clusters by a templated multivalent saccharide ligand. *J. Am. Chem. Soc.*, **122**, 4518-4519.
- Cairo, C. W., Gestwicki, J. E., Kanai, M., and Kiessling, L. L. (2002) Control of Multivalent Interactions by Binding Epitope Density. *J. Am. Chem. Soc.*, **124**, 1615-1619.
- Chan, F. K. M., Chun, H. J., Zheng, L. X., Siegel, R. M., Bui, K. L., and Lenardo, M. J. (2000) A domain in TNF receptors that mediates ligand-independent receptor assembly and signaling. *Science*, **288**, 2351-2354.
- Chorev, M. and Goodman, M. (1993) A Dozen Years of Retro-Inverso Peptidomimetics. *Acc. Chem. Res.*, **26**, 266-273.
- Cochran, J. R., Cameron, T. O., and Stern, L. J. (2000) The relationship of MHC-peptide binding and T cell activation probed using chemically defined MHC class II oligomers. *Immunity*, **12**, 241-250.
- Cochran, J. R. and Stern, L. J. (2000) A diverse set of oligomeric class II MHC-peptide complexes for probing T-cell receptor interactions. *Chem. Biol.*, **7**, 683-696.

- Colucci, G., Moore, J. G., Feldman, M., and Chrispeels, M. J. (1999) cDNA cloning of FRIL, a lectin from *Dolichos lablab*, that preserves hematopoietic progenitors in suspension culture. *Proc. Natl. Acad. Sci. U. S. A.*, **96**, 646-650.
- Cooper, A. and Johnson, C. M. (1994a) Introduction to Microcalorimetry and Biomolecular Energetics. In Jones, C., Mulloy, B., and Thomas, A. H. (eds.), *Microscopy, Optical Spectroscopy, and Macroscopic Techniques*. Humana Press, Totowa, New Jersey, pp. 109-124.
- Cooper, A. and Johnson, C. M. (1994b) Isothermal Titration Microcalorimetry. In Jones, C., Mulloy, B., and Thomas, A. H. (eds.), *Microscopy, Optical Spectroscopy, and Macroscopic Techniques*. Humana Press, Totowa, New Jersey, pp. 137-150.
- Corbell, J. B., Lundquist, J. J., and Toone, E. J. (2000) A comparison of biological and calorimetric analyses of multivalent glycodendrimer ligands for concanavalin A. *Tetrahedron-Asymmetry*, **11**, 95-111.
- Cribbs, D. H., Kreng, V. M., Anderson, A. J., and Cotman, C. W. (1996) Cross-linking of concanavalin A receptors on cortical neurons induces programmed cell death. *Neuroscience*, **75**, 173-185.
- Crowcroft, N. S. (1994) Cholera: current epidemiology. *Commun. Dis. Rep. CDR Rev.*, **4**, R157-R164.
- Crowe, D. L., Boardman, M. L., and Fong, K. S. (1998) Anti-Fas antibody differentially regulates apoptosis in Fas ligand resistant carcinoma lines via the caspase 3 family of cell death proteases but independently of bcl2 expression. *Anticancer Res.*, **18**, 3163-3170.
- Dam, T. K. and Brewer, C. F. (2002) Thermodynamic studies of lectin-carbohydrate interactions by isothermal titration calorimetry. *Chem. Rev.*, **102**, 387-429.
- Dam, T. K., Roy, R., Das, S. K., Oscarson, S., and Brewer, C. F. (2000) Binding of multivalent carbohydrates to concanavalin A and Dioclea grandiflora lectin - Thermodynamic analysis of the "multivalency effect". *J. Biol. Chem.*, **275**, 14223-14230.
- Dam, T. K., Roy, R., Page, D., and Brewer, C. F. (2002a) Negative cooperativity associated with binding of multivalent carbohydrates to lectins. thermodynamic analysis of the "multivalency effect". *Biochemistry*, **41**, 1351-1358.
- Dam, T. K., Roy, R., Page, D., and Brewer, C. F. (2002b) Thermodynamic binding parameters of individual epitopes of multivalent carbohydrates to concanavalin a as

- determined by "reverse" isothermal titration microcalorimetry. *Biochemistry*, **41**, 1359-1363.
- Decaudin, D., Beurdeley-Thomas, A., Nemati, F., Miccoli, L., Pouillart, P., Bourgeois, Y., Goncalves, R. B., Rouillard, D., and Poupon, M. F. (2001) Distinct experimental efficacy of anti-Fas/APO-1/CD95 receptor antibody in human tumors. *Exp. Cell Res.*, **268**, 162-168.
- Dimick, S. M., Powell, S. C., McMahon, S. A., Moothoo, D. N., Naismith, J. H., and Toone, E. J. (1999) On the meaning of affinity: Cluster glycoside effects and concanavalin A. *J. Am. Chem. Soc.*, **121**, 10286-10296.
- Dohi, H., Nishida, Y., Furuta, Y., Uzawa, H., Yokoyama, S., Ito, S., Mori, H., and Kobayashi, K. (2002) Molecular design and biological potential of galacto-type trehalose as a nonnatural ligand of Shiga toxins. *Org. Lett.*, **4**, 355-357.
- Dubois, M., Gilles, K. A., Hamilton, J. K., Rebers, P. A., and Smith, F. (1956) Colorimetric Method for Determination of Sugars and Related Substances. *Anal. Chem.*, **28**, 350-356.
- Easterbrook-Smith, S. B. (1993) A Light-Scattering Method for Measuring the Sizes of Insoluble Immune-Complexes. *Mol. Immunol.*, **30**, 637-640.
- Egnaczyk, G. F., Greis, K. D., Stimson, E. R., and Maggio, J. E. (2001) Photoaffinity cross-linking of Alzheimer's disease amyloid fibrils reveals interstrand contact regions between assembled beta-amyloid peptide subunits. *Biochemistry*, **40**, 11706-11714.
- Esfand, R. and Tomalia, D. A. (2001) Poly(amidoamine) (PAMAM) dendrimers: from biomimicry to drug delivery and biomedical applications. *Drug Discovery Today*, **6**, 427-436.
- Esler, W. P., Stimson, E. R., Ghilardi, J. R., Felix, A. M., Lu, Y. A., Vinters, H. V., Mantyh, P. W., and Maggio, J. E. (1997) A beta deposition inhibitor screen using synthetic amyloid. *Nat. Biotechnol.*, **15**, 258-263.
- Esler, W. P., Stimson, E. R., Ghilardi, J. R., Lu, Y. A., Felix, A. M., Vinters, H. V., Mantyh, P. W., Lee, J. P., and Maggio, J. E. (1996) Point substitution in the central hydrophobic cluster of a human beta-amyloid congener disrupts peptide folding and abolishes plaque competence. *Biochemistry*, **35**, 13914-13921.
- Evans, D. A., Funkenstein, H., Albert, M. S., Scherr, P. A., Cook, N. R., Chown, M. J., Hebert, L. E., Hennekens, C. H., and Taylor, J. O. (1989) Prevalence of Alzheimers-

- Disease in a Community Population of Older Persons - Higher Than Previously Reported. *Jama-Journal of the American Medical Association*, **262**, 2551-2556.
- Falnes, P. O. and Sandvig, K. (2000) Penetration of protein toxins into cells. *Curr. Opin. Cell Biol.*, **12**, 407-413.
- Fan, E. K., Merritt, E. A., Verlinde, C. L. M. J., and Hol, W. G. J. (2000a) AB(5) toxins: structures and inhibitor design. *Curr. Opin. Struct. Biol.*, **10**, 680-686.
- Fan, E. K., Zhang, Z. S., Minke, W. E., Hou, Z., Verlinde, C. L. M. J., and Hol, W. G. J. (2000b) High-affinity pentavalent ligands of Escherichia coli heat-labile enterotoxin by modular structure-based design. *J. Am. Chem. Soc.*, **122**, 2663-2664.
- Findeis, M. A., Musso, G. M., Arico-Muendel, C. C., Benjamin, H. W., Hundal, A. M., Lee, J. J., Chin, J., Kelley, M., Wakefield, J., Hayward, N. J., and Molineaux, S. M. (1999) Modified-peptide inhibitors of amyloid beta-peptide polymerization. *Biochemistry*, **38**, 6791-6800.
- Fisher, H. F. and Singh, N. (1995) Calorimetric methods for interpreting protein-ligand interactions. *Energetics of Biological Macromolecules*, **259**, 194-221.
- Fletcher, M. D. and Campbell, M. M. (1998) Partially modified retro-inverso peptides: Development, synthesis, and conformational behavior. *Chem. Rev.*, **98**, 763-795.
- Fox, J. D. and Robyt, J. F. (1991) Miniaturization of Three Carbohydrate Analysis Using a Microsample Plate Reader. *Anal. Biochem.*, **195**, 93-96.
- Fraser, C. and Grubbs, R. H. (1995) Synthesis of Glycopolymers of Controlled Molecular-Weight by Ring-Opening Metathesis Polymerization Using Well-Defined Functional-Group Tolerant Ruthenium Carbene Catalysts. *Macromolecules*, **28**, 7248-7255.
- Frei, K., Ambar, B., Adachi, N., Yonekawa, Y., and Fontana, A. (1998) Ex vivo malignant glioma cells are sensitive to Fas (CD95/APO-1) ligand-mediated apoptosis. *J. Neuroimmunol.*, **87**, 105-113.
- Frostell-Karlsson, A., Remaeus, A., Roos, H., Andersson, K., Borg, P., Hamalainen, M., and Karlsson, R. (2000) Biosensor analysis of the interaction between immobilized human serum albumin and drug compounds for prediction of human serum albumin binding levels. *J. Med. Chem.*, **43**, 1986-1992.

- Games, D., Adams, D., Alessandrini, R., Barbour, R., Berthelette, P., Blackwell, C., Carr, T., Clemens, J., Donaldson, T., Gillespie, F., Guido, T., Hagopian, S., JohnsonWood, K., Khan, K., Lee, M., Leibowitz, P., Lieberburg, I., Little, S., Masliah, E., McConlogue, L., Montoyazavala, M., Mucke, L., Paganini, L., Penniman, E., Power, M., Schenk, D., Seubert, P., Snyder, B., Soriano, F., Tan, H., Vitale, J., Wadsworth, S., Wolozin, B., and Zhao, J. (1995) Alzheimer-Type Neuropathology in Transgenic Mice Overexpressing V717f Beta-Amyloid Precursor Protein. *Nature*, **373**, 523-527.
- Gargano, J. M., Ngo, T., Kim, J. Y., Acheson, D. W. K., and Lees, W. J. (2001) Multivalent inhibition of AB(5) toxins. *J. Am. Chem. Soc.*, **123**, 12909-12910.
- Gazit, E. (2002) A possible role for pi-stacking in the self-assembly of amyloid fibrils. *FASEB J.*, **16**, 77-83.
- Gerken, T. A., Owens, C. L., and Pasumathy, M. (1998) Site-specific core 1 O-glycosylation pattern of the porcine submaxillary gland mucin tandem repeat - Evidence for the modulation of glycan length by peptide sequence. *J. Biol. Chem.*, **273**, 26580-26588.
- Gestwicki, J. E., Cairo, C. W., Mann, D. A., Owen, D. E., and Kiessling, L. L. (2002a) Selective Immobilization of Multivalent Ligands for Surface Plasmon Resonance and Fluorescence Microscopy. *Anal. Biochem.*, **305**, 149-155.
- Gestwicki, J. E., Cairo, C. W., Strong, L. E., Oetjen, K. A., and Kiessling, L. L. (2002b) Influencing Receptor-Ligand Binding Mechanisms with Multivalent Ligand Architecture. *J. Am. Chem. Soc.*, submitted for publication.
- Gestwicki, J. E. and Kiessling, L. L. (2002) Inter-receptor communication through arrays of bacterial chemoreceptors. *Nature*, **415**, 81-84.
- Gestwicki, J. E., Strong, L. E., Borchardt, S. L., Cairo, C. W., Schnoes, A. M., and Kiessling, L. L. (2001) Designed potent multivalent chemoattractants for Escherichia coli. *Bioorg. Med. Chem.*, **9**, 2387-2393.
- Gestwicki, J. E., Strong, L. E., Cairo, C. W., Boehm, F. J., and Kiessling, L. L. (2002c) Cell Aggregation by Scaffolded Receptor Clusters. *Chem. Biol.*, **9**, 163-169.
- Gestwicki, J. E., Strong, L. E., and Kiessling, L. L. (2000a) Tuning chemotactic responses with synthetic multivalent ligands. *Chem. Biol.*, **7**, 583-591.

- Gestwicki, J. E., Strong, L. E., and Kiessling, L. L. (2000b) Visualization of single multivalent receptor-ligand complexes by transmission electron microscopy. *Angew. Chem., Int. Ed. Engl.*, **39**, 4567-4570.
- Ghanta, J., Shen, C. L., Kiessling, L. L., and Murphy, R. M. (1996) A strategy for designing inhibitors of beta-amyloid toxicity. *J. Biol. Chem.*, **271**, 29525-29528.
- Ghosh, A. K., Shin, D. W., Downs, D., Koelsch, G., Lin, X. L., Ermolieff, J., and Tang, J. (2000) Design of potent inhibitors for human brain memapsin 2 (beta- secretase). *J. Am. Chem. Soc.*, **122**, 3522-3523.
- Gieni, R. S., Li, Y., and Hayglass, T. (1995) Comparison of [H-3] Thymidine Incorporation with MTT-and MTS- Based Bioassays for Human and Murine Il-2 and Il4 Analysis - Tetrazolium Assays Provide Markedly Enhanced Sensitivity. *J. Immunol. Methods*, **187**, 85-93.
- Glick, G. D., Toogood, P. L., Wiley, D. C., Skehel, J. J., and Knowles, J. R. (1991) Ligand Recognition by Influenza-Virus - the Binding of Bivalent Sialosides. *J. Biol. Chem.*, **266**, 23660-23669.
- Goldstein, I. J. (1976) Carbohydrate Binding Specificity of Concanavalin A. In Bittiger, H. and Schnebli, H. P. (eds.), *Concanavalin A as a Tool*. John Wiley & Sons, New York, pp. 55-65.
- Goodsell, D. S., Morris, G. M., and Olson, A. J. (1996) Automated docking of flexible ligands: Applications of AutoDock. *J. Mol. Recognit.*, **9**, 1-5.
- Goodsell, D. S. and Olson, A. J. (1990) Automated Docking of Substrates to Proteins by Simulated Annealing. *Proteins: Struct. , Funct. , Genet.*, **8**, 195-202.
- Gordon, D. J., Sciarretta, K. L., and Meredith, S. C. (2001) Inhibition of beta-amyloid(40) fibrillogenesis and disassembly of beta-amyloid(40) fibrils by short beta-amyloid congeners containing N-methyl amino acids at alternate residues. *Biochemistry*, **40**, 8237-8245.
- Gordon, E. J., Gestwicki, J. E., Strong, L. E., and Kiessling, L. L. (2000) Synthesis of end-labeled multivalent ligands for exploring cell-surface-receptor-ligand interactions. *Chem. Biol.*, **7**, 9-16.
- Gordon, E. J., Sanders, W. J., and Kiessling, L. L. (1998) Synthetic ligands point to cell surface strategies. *Nature*, **392**, 30-31.



- Gorelik, E. (1998) Cytotoxic Effects of Lectins. In Rhodes, J. M. and Milton, J. D. (eds.), *Lectin Methods and Protocols*. Humana Press, Totowa, NJ, pp. 453-459.
- Grebe, T. W. and Stock, J. (1998) Bacterial chemotaxis: The five sensors of a bacterium. *Curr. Biol.*, **8**, R154-R157.
- Hacker, G. (2000) The morphology of apoptosis. *Cell Tissue Res.*, **301**, 5-17.
- Hamelryck, T. W., Moore, J. G., Chrispeels, M. J., Loris, R., and Wyns, L. (2000) The role of weak protein-protein interactions in multivalent lectin-carbohydrate binding: Crystal structure of cross-linked FRIL. *J. Mol. Biol.*, **299**, 875-883.
- Han, H., Cho, C. G., and Lansbury, P. T., Jr. (1996) Technetium complexes for the quantitation of brain amyloid. *J. Am. Chem. Soc.*, **118**, 4506-4507.
- Harkany, T., Abraham, I., Konya, C., Nyakas, C., Zarandi, M., Penke, B., and Luiten, P. G. M. (2000) Mechanisms of beta-amyloid neurotoxicity: Perspectives of pharmacotherapy. *Rev. Neurosci.*, **11**, 329-382.
- Harper, J. D., Wong, S. S., Lieber, C. M., and Lansbury, P. T. (1997) Observation of metastable A beta amyloid protofibrils by atomic force microscopy. *Chem. Biol.*, **4**, 119-125.
- Haseley, S. R., Talaga, P., Kamerling, J. P., and Vliegenthart, J. F. G. (1999) Characterization of the carbohydrate binding specificity and kinetic parameters of lectins by using surface plasmon resonance. *Anal. Biochem.*, **274**, 203-210.
- Hazelbauer, G. L., Berg, H. C., and Matsumura, P. (1993) Bacterial Motility and Signal Transduction. *Cell*, **73**, 15-22.
- Heldin, C. H. (1995) Dimerization of Cell-Surface Receptors in Signal-Transduction. *Cell*, **80**, 213-223.
- Hermanson, G. T. (1996) Antibody Modification and Conjugation. *Bioconjugate Techniques*. Academic Press, San Diego, CA, pp. 456-527.
- Hester, G. and Wright, C. S. (1996) The Mannose-specific bulb lectin from *Galanthus nivalis* (snowdrop) binds mono- and dimannosides at distinct sites. Structure analysis of refined complexes at 2.3 angstrom and 3.0 angstrom resolution. *J. Mol. Biol.*, **262**, 516-531.

- Higuchi, K., Hosokawa, M., and Takeda, T. (1999) Senescence-accelerated mouse. *Methods Enzymol.*, **309**, 674-686.
- Hilbich, C., Kisterswoike, B., Reed, J., Masters, C. L., and Beyreuther, K. (1992) Substitutions of Hydrophobic Amino-Acids Reduce the Amyloidogenicity of Alzheimers-Disease Beta-A4 Peptides. *J. Mol. Biol.*, **228**, 460-473.
- Holler, N., Kataoka, T., Bodmer, J. L., Romero, P., Romero, J., Deperthes, D., Engel, J., Tschopp, J., and Schneider, P. (2000) Development of improved soluble inhibitors of FasL and CD40L based on oligomerized receptors. *J. Immunol. Methods*, **237**, 159-173.
- Horan, N., Yan, L., Isobe, H., Whitesides, G. M., and Kahne, D. (1999) Nonstatistical binding of a protein to clustered carbohydrates. *Proc. Natl. Acad. Sci. U. S. A.*, **96**, 11782-11786.
- Howell, S., Kenmore, M., Kirkland, M., and Badley, R. A. (1998) High-density immobilization of an antibody fragment to a carboxymethylated dextran-linked biosensor surface. *J. Mol. Recognit.*, **11**, 200-203.
- Howlett, D. R., George, A. R., Owen, D. E., Ward, R. V., and Markwell, R. E. (1999a) Common structural features determine the effectiveness of carvedilol, daunomycin and rolitetracycline as inhibitors of Alzheimer beta-amyloid fibril formation. *Biochem. J.*, **343**, 419-423.
- Howlett, D. R., Perry, A. E., Godfrey, F., Swatton, J. E., Jennings, K. H., Spitzfaden, C., Wadsworth, H., Wood, S. J., and Markwell, R. E. (1999b) Inhibition of fibril formation in beta-amyloid peptide by a novel series of benzofurans. *Biochem. J.*, **340**, 283-289.
- Hueber, A., Winter, S., and Weller, M. (1998) Chemotherapy primes malignant glioma cells for CD95 ligand- induced apoptosis up-stream of caspase 3 activation. *Eur. J. Pharmacol.*, **352**, 111-115.
- Ichikawa, K., Yoshida-Kato, H., Ohtsuki, M., Ohsumi, J., Yamaguchi, J., Takahashi, S., Tani, Y., Watanabe, M., Shiraishi, A., Nishioka, K., Yonehara, S., and Serizawa, N. (2000) A novel murine anti-human Fas mAb which mitigates lymphadenopathy without hepatotoxicity. *Int. Immunol.*, **12**, 555-562.
- Ivanoff, B. and Robertson, S. E. (1997) Pertussis: a worldwide problem. *Dev. Biol. Stand.*, **89**, 3-13.

- Janek, K., Rothmund, S., Gast, K., Beyermann, M., Zipper, J., Fabian, H., Bienert, M., and Krause, E. (2001) Study of the conformational transition of A beta(1-42) using D- amino acid replacement analogues. *Biochemistry*, **40**, 5457-5463.
- Janus, C., Chishti, M. A., and Westaway, D. (2000) Transgenic mouse models of Alzheimer's disease. *Biochim. Biophys. Acta-Molecular Basis of Disease*, **1502**, 63-75.
- Jencks, W. P. (1981) On the Attribution and Additivity of Binding Energies. *Proc. Natl. Acad. Sci. U. S. A.*, **78**, 4046-4050.
- Kalinin, N. L., Ward, L. D., and Winzor, D. J. (1995) Effects of Solute Multivalence on the Evaluation of Binding Constants by Biosensor Technology - Studies with Concanavalin-A and Interleukin-6 As Partitioning Proteins. *Anal. Biochem.*, **228**, 238-244.
- Kanai, M. and Kiessling, L. L. (2002) Controlled Synthesis of Water Soluble Materials Through Living Ring Opening Metathesis Polymerization. *in preparation*,
- Kanai, M., Mortell, K. H., and Kiessling, L. L. (1997) Varying the size of multivalent ligands: The dependence of concanavalin A binding on neoglycopolymer length. *J. Am. Chem. Soc.*, **119**, 9931-9932.
- Karlsson, R. and Stahlberg, R. (1995) Surface-Plasmon Resonance Detection and Multispot Sensing for Direct Monitoring of Interactions Involving Low-Molecular- Weight Analytes and for Determination of Low Affinities. *Anal. Biochem.*, **228**, 274-280.
- Kawaguchi, S., Mineta, T., Ichinose, M., Masuoka, J., Shiraishi, T., and Tabuchi, K. (2000) Induction of apoptosis in glioma cells by recombinant human Fas ligand. *Neurosurgery*, **46**, 431-438.
- Khan, M. I., Mandal, D. K., and Brewer, C. F. (1991) Interactions of Concanavalin-A with Glycoproteins - A Quantitative Precipitation Study of Concanavalin-A with the Soybean Agglutinin. *Carbohydr. Res.*, **213**, 69-77.
- Kiessling, L. L., Gestwicki, J. E., and Strong, L. E. (2000a) Synthetic multivalent ligands in the exploration of cell-surface interactions. *Curr. Opin. Chem. Biol.*, **4**, 696-703.
- Kiessling, L. L. and Mann, D. A. (2001) The Chemistry and Biology of Multivalent Saccharide Displays. In Wang, P. G. and Bertozzi, C. R. (eds.), *Glycochemistry: Principles, Synthesis and Applications*. Marcel Dekker, Inc., New York, NY.

- Kiessling, L. L. and Pohl, N. L. (1996) Strength in numbers: Non-natural polyvalent carbohydrate derivatives. *Chem. Biol.*, **3**, 71-77.
- Kiessling, L. L., Strong, L. E., and Gestwicki, J. E. (2000b) Principles for multivalent ligand design. *Ann. Rep. Med. Chem.*, **35**, 321-330.
- Kilpatrick, D. C. (1999) Mechanisms and assessment of lectin-mediated mitogenesis. *Mol. Biotechnol.*, **11**, 55-65.
- Kim, M., Rao, M. V., Tweardy, D. J., Prakash, M., Galili, U., and Gorelik, E. (1993) Lectin-Induced Apoptosis of Tumor-Cells. *Glycobiology*, **3**, 447-453.
- Kim, Y. J. and Varki, A. (1997) Perspectives on the significance of altered glycosylation of glycoproteins in cancer. *Glycoconj. J.*, **14**, 569-576.
- Kischkel, F. C., Hellbardt, S., Behrmann, I., Germer, M., Pawlita, M., Krammer, P. H., and Peter, M. E. (1995) Cytotoxicity-Dependent Apo-1 (Fas/Cd95)-Associated Proteins Form a Death-Inducing Signaling Complex (Disc) with the Receptor. *EMBO J.*, **14**, 5579-5588.
- Kiss, R., Camby, I., Duckworth, C., DeDecker, R., Salmon, I., Pasteels, J. L., Danguy, A., and Yeaton, P. (1997) In vitro influence of Phaseolus vulgaris, Griffonia simplicifolia, concanavalin A, wheat germ, and peanut agglutinins on HCT-15, LoVo, and SW837 human colorectal cancer cell growth. *Gut*, **40**, 253-261.
- Kitano, H., Sumi, Y., and Tagawa, K. (2001) Recognition of novel lipopolypeptides with many pendent sugar residues by lectin. *Bioconjugate Chem.*, **12**, 56-61.
- Kitov, P. I., Sadowska, J. M., Mulvey, G., Armstrong, G. D., Ling, H., Pannu, N. S., Read, R. J., and Bundle, D. R. (2000) Shiga-like toxins are neutralized by tailored multivalent carbohydrate ligands. *Nature*, **403**, 669-672.
- Klein, W. L., Krafft, G. A., and Finch, C. E. (2001) Targeting small A beta oligomers: the solution to an Alzheimer's disease conundrum? *Trends Neurosci.*, **24**, 219-224.
- Klemm, J. D., Schreiber, S. L., and Crabtree, G. R. (1998) Dimerization as a regulatory mechanism in signal transduction. *Annu. Rev. Immunol.*, **16**, 569-592.
- Klotz, I. M. and Urquhart, J. M. (1948) The binding of organic ions by proteins: Buffer effects. *J. Phys. Chem.*, **53**, 100-114.

- Klunk, W. E., Debnath, M. L., Koros, A. M. C., and Pettegrew, J. W. (1998) Chrysamine-G, a lipophilic analogue of Congo red, inhibits A beta-induced toxicity in PC12 cells. *Life Sci.*, **63**, 1807-1814.
- Kogelberg, H. and Feizi, T. (2001) New structural insights into lectin-type proteins of the immune system. *Curr. Opin. Struct. Biol.*, **11**, 635-643.
- Komada, Y., Inaba, H., Li, Q. S., Azuma, E., Zhou, Y. W., Yamamoto, H., and Sakurai, M. (1999) Epitopes and functional responses defined by a panel of anti- Fas (CD95) monoclonal antibodies. *Hybridoma*, **18**, 391-398.
- Koo, E. H., Lansbury, P. T., and Kelly, J. W. (1999) Amyloid diseases: Abnormal protein aggregation in neurodegeneration. *Proc. Natl. Acad. Sci. U. S. A.*, **96**, 9989-9990.
- Kotloff, K. L., Winickoff, J. P., Ivanoff, B., Clemens, J. D., Swerdlow, D. L., Sansonetti, P. J., Adak, G. K., and Levine, M. M. (1999) Global burden of Shigella infections: implications for vaccine development and implementation of control strategies. *Bull. World Health Organ*, **77**, 651-666.
- Krantz, M. J., Holtzman, N. A., Stowell, C. P., and Lee, Y. C. (1976) Attachment of thioglycosides to proteins: enhancement of liver membrane binding. *Biochemistry*, **15**, 3963-3968.
- Kroesen, B. J., Helfrich, W., Molema, G., and de Leij, L. (1998) Bispecific antibodies for treatment of cancer in experimental animal models and man. *Adv. Drug Delivery Rev.*, **31**, 105-129.
- Kulkarni, G. V., Lee, W., Seth, A., and Mcculloch, C. A. G. (1998) Role of mitochondrial membrane potential in concanavalin A- induced apoptosis in human fibroblasts. *Exp. Cell Res.*, **245**, 170-178.
- Kulkarni, G. V. and Mcculloch, C. A. G. (1995) Concanavalin-A Induced Apoptosis in Fibroblasts - the Role of Cell-Surface Carbohydrates in Lectin Mediated Cytotoxicity. *J. Cell. Physiol.*, **165**, 119-133.
- Kuner, P., Bohrmann, B., Tjernberg, L. O., Naslund, J., Huber, G., Celenk, S., Gruninger-Leitch, F., Richards, J. G., Jakob-Roetne, R., Kemp, J. A., and Nordstedt, C. (2000) Controlling polymerization of beta-amyloid and prion-derived peptides with synthetic small molecule ligands. *J. Biol. Chem.*, **275**, 1673-1678.

- Ladbury, J. E. and Chowdhry, B. Z. (1996) Sensing the heat: The application of isothermal titration calorimetry to thermodynamic studies of biomolecular interactions. *Chem. Biol.*, **3**, 791-801.
- Lansbury, P. T., Jr. (1997) Inhibition of amyloid formation: a strategy to delay the onset of Alzheimer's disease. *Curr. Opin. Chem. Biol.*, **1**, 260-267.
- Lawrence, L. J., Kortt, A. A., Iliades, P., Tulloch, P. A., and Hudson, P. J. (1998) Orientation of antigen binding sites in dimeric and trimeric single chain Fv antibody fragments. *FEBS Lett.*, **425**, 479-484.
- Lee, R. T. and Lee, Y. C. (2000) Affinity enhancement by multivalent lectin-carbohydrate interaction. *Glycoconj. J.*, **17**, 543-551.
- Li, Y. P., Bushnell, A. F., Lee, C. M., Perlmutter, L. S., and Wong, S. K. F. (1996) beta-Amyloid induces apoptosis in human-derived neurotypic SH- SY5Y cells. *Brain Res.*, **738**, 196-204.
- Liang, Y. Z., Li, Z. C., Chen, G. Q., and Li, F. M. (1999) Synthesis of well-defined poly[(2-beta-D- glucopyranosyloxy)ethyl acrylate] by atom transfer radical polymerization. *Polymer International*, **48**, 739-742.
- Lichtenbelt, J. W., Ras, J. M. C., and Wilson, G. S. (1974) Turbidity of coagulating lyophobic sols. *J. Colloid Interface Sci.*, **46**, 522-527.
- Liener, I. E. (1976) Isolation and Properties of Concanavalin A. In Bittiger, H. and Schnebli, H. P. (eds.), *Concanavalin A as a Tool*. John Wiley & Sons, New York, pp. 17-31.
- Lindhahl, U., Kusche-Gullberg, M., and Kjellen, L. (1998) Regulated diversity of heparan sulfate. *J. Biol. Chem.*, **273**, 24979-24982.
- Lindhorst, T. K. and Kieburg, C. (1996) Glycocoating of oligovalent amines: Synthesis of thiourea-bridged cluster glycosides from glycosyl isothiocyanates. *Angew. Chem. ,Int. Ed. Engl.*, **35**, 1953-1956.
- Ling, H., Boodhoo, A., Hazes, B., Cummings, M. D., Armstrong, G. D., Brunton, J. L., and Read, R. J. (1998) Structure of the Shiga-like toxin I B-pentamer complexed with an analogue of its receptor Gb(3). *Biochemistry*, **37**, 1777-1788.
- Lis, H. and Sharon, N. (1998) Lectins: Carbohydrate-specific proteins that mediate cellular recognition. *Chem. Rev.*, **98**, 637-674.

- Liu, F. T., Hsu, D. K., Zuberi, R. I., Hill, P. N., Shenhav, A., Kuwabara, I., and Chen, S. S. (1996) Modulation of functional properties of galectin-3 by monoclonal antibodies binding to the non-lectin domains. *Biochemistry*, **35**, 6073-6079.
- Livnah, O., Stura, E. A., Middleton, S. A., Johnson, D. L., Jolliffe, L. K., and Wilson, L. A. (1999) Crystallographic evidence for preformed dimers of erythropoietin receptor before ligand activation. *Science*, **283**, 987-990.
- Lorea, P., Goldschmidt, D., Darro, F., Salmon, I., Bovin, N., Gabius, H. J., Kiss, R., and Danguy, A. (1997) In vitro characterization of lectin-induced alterations on the proliferative activity of three human melanoma cell lines. *Melanoma Res.*, **7**, 353-363.
- Lowe, T. L., Strzelec, A., Kiessling, L. L., and Murphy, R. M. (2001) Structure-function relationships for inhibitors of beta-amyloid toxicity containing the recognition sequence KLVFF. *Biochemistry*, **40**, 7882-7889.
- Lu, B. and Chung, T. C. (2000) Synthesis of maleic anhydride grafted polyethylene and polypropylene, with controlled molecular structures. *J. Polym. Sci. , Part A: Polym. Chem.*, **38**, 1337-1343.
- Lundquist, J. J., Debenham, S. D., and Toone, E. J. (2000) Multivalency effects in protein-carbohydrate interaction: The binding of the Shiga-like toxin 1 binding subunit to multivalent C-linked glycopeptides. *J. Org. Chem.*, **65**, 8245-8250.
- Lundquist, J. J. and Toone, E. J. (2002) The cluster glycoside effect. *Chem. Rev.*, **102**, 555-578.
- Mallucci, L. (1976) Preparation and Use of Fluorescent Concanavalin A Derivatives. In Bittiger, H. and Schnebli, H. P. (eds.), *Concanavalin A as a Tool*. John Wiley & Sons, New York, pp. 69-78.
- Mammen, M., Choi, S. K., and Whitesides, G. M. (1998a) Polyvalent interactions in biological systems: Implications for design and use of multivalent ligands and inhibitors. *Angew. Chem. ,Int. Ed. Engl.*, **37**, 2755-2794.
- Mammen, M., Dahmann, G., and Whitesides, G. M. (1995) Effective Inhibitors of Hemagglutination by Influenza-Virus Synthesized from Polymers Having Active Ester Groups - Insight Into Mechanism of Inhibition. *J. Med. Chem.*, **38**, 4179-4190.

- Mammen, M., Helmersen, K., Kishore, R., Choi, S. K., Phillips, W. D., and Whitesides, G. M. (1996) Optically controlled collisions of biological objects to evaluate potent polyvalent inhibitors of virus-cell adhesion. *Chem. Biol.*, **3**, 757-763.
- Mammen, M., Shakhnovich, E. I., Deutch, J. M., and Whitesides, G. M. (1998b) Estimating the entropic cost of self-assembly of multiparticle hydrogen-bonded aggregates based on the cyanuric acid center dot melamine lattice. *J. Org. Chem.*, **63**, 3821-3830.
- Mandal, D. K. and Brewer, C. F. (1992) Interactions of Concanavalin-A with Glycoproteins - Formation of Homogeneous Glycoprotein Lectin Cross-Linked Complexes in Mixed Precipitation Systems. *Biochemistry*, **31**, 12602-12609.
- Mann, D. A. (2000), "Identifying inhibitors of protein-carbohydrate interactions: From novel glycomimetics to polymeric multivalent neoglycoligands", Thesis, University of Wisconsin-Madison.
- Mann, D. A., Kanai, M., Maly, D. J., and Kiessling, L. L. (1998) Probing low affinity and multivalent interactions with surface plasmon resonance: Ligands for concanavalin A. *J. Am. Chem. Soc.*, **120**, 10575-10582.
- Manning, D. D., Hu, X., Beck, P., and Kiessling, L. L. (1997) Synthesis of sulfated neoglycopolymers: Selective P-selectin inhibitors. *J. Am. Chem. Soc.*, **119**, 3161-3162.
- Mannino, R. J., Ballmer, K., and Burger, M. M. (1978) Growth inhibition of transformed cells with succinylated concanavalin A. *Science*, **201**, 824.
- Martin, D. A., Siegel, R. M., Zheng, L. X., and Lenardo, M. J. (1998) Membrane oligomerization and cleavage activates the caspase-8 (FLICE/MACH alpha 1) death signal. *J. Biol. Chem.*, **273**, 4345-4349.
- Matko, J. and Edidin, M. (1997) Energy transfer methods for detecting molecular clusters on cell surfaces. *Methods Enzymol.*, **278**, 444-462.
- Matyjaszewski, K. and Xia, J. H. (2001) Atom transfer radical polymerization. *Chem. Rev.*, **101**, 2921-2990.
- Maynard, H. D., Okada, S. Y., and Grubbs, R. H. (2001) Inhibition of cell adhesion to fibronectin by oligopeptide- substituted polynorbornenes. *J. Am. Chem. Soc.*, **123**, 1275-1279.



- McGaughey, G. B., Gagne, M., and Rappe, A. K. (1998) pi-stacking interactions - Alive and well in proteins. *J. Biol. Chem.*, **273**, 15458-15463.
- Medema, J. P., Scaffidi, C., Kischkel, F. C., Shevchenko, A., Mann, M., Krammer, P. H., and Peter, M. E. (1997) FLICE is activated by association with the CD95 death-inducing signaling complex (DISC). *EMBO J.*, **16**, 2794-2804.
- Merritt, E. A. and Hol, W. G. J. (1995) Ab(5) Toxins. *Curr. Opin. Struct. Biol.*, **5**, 165-171.
- Meterissian, S. H., Kontogiannia, M., Po, J., Jensen, G., and Ferdinand, B. (1997) Apoptosis induced in human colorectal carcinoma by anti-Fas antibody. *Ann. Surg. Oncol.*, **4**, 169-175.
- Mi, Z. B., Mai, J., Lu, X. L., and Robbins, P. D. (2000) Characterization of a class of cationic peptides able to facilitate efficient protein transduction in vitro and in vivo. *Molecular Therapy*, **2**, 339-347.
- Minke, W. E., Hong, F., Verlinde, C. L. M. J., Hol, W. G. J., and Fan, E. (1999a) Using a galactose library for exploration of a novel hydrophobic pocket in the receptor binding site of the Escherichia coli heat-labile enterotoxin. *J. Biol. Chem.*, **274**, 33469-33473.
- Minke, W. E., Roach, C., Hol, W. G. J., and Verlinde, C. L. M. J. (1999b) Structure-based exploration of the ganglioside GM1 binding sites of Escherichia coli heat-labile enterotoxin and cholera toxin for the discovery of receptor antagonists. *Biochemistry*, **38**, 5684-5692.
- Moore, C. L. and Wolfe, M. S. (1999) Inhibition of beta-amyloid formation as a therapeutic strategy. *Expert Opinion on Therapeutic Patents*, **9**, 135-146.
- Morris, G. M., Goodsell, D. S., Huey, R., and Olson, A. J. (1996) Distributed automated docking of flexible ligands to proteins: Parallel applications of AutoDock 2.4. *J. Comput. Aided Mol. Des.*, **10**, 293-304.
- Mortell, K. H., Weatherman, R. V., and Kiessling, L. L. (1996) Recognition specificity of neoglycopolymers prepared by ring-opening metathesis polymerization. *J. Am. Chem. Soc.*, **118**, 2297-2298.
- Morton, T. A. and Myszka, D. G. (1998) Kinetic analysis of macromolecular interactions using surface plasmon resonance biosensors. *Methods Enzymol.*, **295**, 268-294.

- Murphy, R. M., Slayter, H., Schurtenberger, P., Chamberlin, R. A., Colton, C. K., and Yarmush, M. L. (1988) Size and Structure of Antigen-Antibody Complexes - Electron-Microscopy and Light-Scattering Studies. *Biophys. J.*, **54**, 45-56.
- Myszka, D. G. (2000) Kinetic, equilibrium, and thermodynamic analysis of macromolecular interactions with BIACORE. *Methods Enzymol.*, **323**, 325-340.
- Myszka, D. G., Wood, S. J., and Biere, A. L. (1999) Analysis of fibril elongation using surface plasmon resonance biosensors. *Methods Enzymol.*, **309**, 386-402.
- Nagase, F., Abo, T., Hiramatsu, K., Suzuki, S., Du, J., and Nakashima, I. (1998) Induction of apoptosis and tyrosine phosphorylation of cellular proteins in T cells and non-T cells by stimulation with concanavalin A. *Microbiol. Immunol.*, **42**, 567-574.
- Naslund, J., Haroutunian, V., Mohs, R., Davis, K. L., Davies, P., Greengard, P., and Buxbaum, J. D. (2000) Correlation between elevated levels of amyloid beta-peptide in the brain and cognitive decline. *Jama-Journal of the American Medical Association*, **283**, 1571-1577.
- Nicolson, G. L. (1976) Concanavalin A: The Tool, the Techniques and the Problems. In Bittiger, H. and Schnebli, H. P. (eds.), *Concanavalin A as a Tool*. John Wiley & Sons, New York, pp. 3-15.
- O'Shannessy, D. J., Brighamburke, M., and Peck, K. (1992) Immobilization Chemistries Suitable for Use in the Biacore Surface-Plasmon Resonance Detector. *Anal. Biochem.*, **205**, 132-136.
- Olsen, L. R., Dessen, A., Gupta, D., Sabesan, S., Sacchettini, J. C., and Brewer, C. F. (1997) X-ray crystallographic studies of unique cross-linked lattices between four isomeric biantennary oligosaccharides and soybean agglutinin. *Biochemistry*, **36**, 15073-15080.
- Orlinick, J. R., Elkon, K. B., and Chao, M. V. (1997a) Separate domains of the human Fas ligand dictate self- association and receptor binding. *J. Biol. Chem.*, **272**, 32221-32229.
- Orlinick, J. R., Vaishnaw, A., Elkon, K. B., and Chao, M. V. (1997b) Requirement of cysteine-rich repeats of the Fas receptor for binding by the Fas ligand. *J. Biol. Chem.*, **272**, 28889-28894.
- Owen, R. M., Gestwicki, J. E., Young, T., and Kiessling, L. L. (2002) Synthesis and Applications of End-labeled Neoglycopolymers. *Org. Lett.*, **in press**,

- Pace, K. E., Lee, C., Stewart, P. L., and Baum, L. G. (1999) Restricted receptor segregation into membrane microdomains occurs on human T cells during apoptosis induced by galectin-1. *J. Immunol.*, **163**, 3801-3811.
- Page, D., Aravind, S., and Roy, R. (1996a) Synthesis and lectin binding properties of dendritic mannopyranoside. *Chem. Commun.*, 1913-1914.
- Page, D. and Roy, R. (1997) Synthesis and biological properties of mannosylated starburst poly(amidoamine) dendrimers. *Bioconjugate Chem.*, **8**, 714-723.
- Page, D., Zanini, D., and Roy, R. (1996b) Macromolecular recognition: Effect of multivalency in the inhibition of binding of yeast mannan to concanavalin A and pea lectins by mannosylated dendrimers. *Bioorg. Med. Chem.*, **4**, 1949-1961.
- Page, M. I. and Jencks, W. P. (1971) Entropic Contributions to Rate Accelerations in Enzymic and Intramolecular Reactions and the Chelate Effect. *Proc. Natl. Acad. Sci. U. S. A.*, **68**, 1678-1683.
- Pallitto, M. M., Ghanta, J., Heinzelman, P., Kiessling, L. L., and Murphy, R. M. (1999) Recognition sequence design for peptidyl modulators of beta- amyloid aggregation and toxicity. *Biochemistry*, **38**, 3570-3578.
- Pallitto, M. M. and Murphy, R. M. (2001) A mathematical model of the kinetics of beta-amyloid fibril growth from the denatured state. *Biophys. J.*, **81**, 1805-1822.
- Patten, T. E. and Matyjaszewski, K. (1998) Atom transfer radical polymerization and the synthesis of polymeric materials. *Adv. Mater.*, **10**, 901-915.
- Perillo, N. L., Marcus, M. E., and Baum, L. G. (1998) Galectins: versatile modulators of cell adhesion, cell proliferation, and cell death. *J. Mol. Med.*, **76**, 402-412.
- Perrimon, N. and Bernfield, M. (2000) Specificities of heparan sulphate proteoglycans in developmental processes. *Nature*, **404**, 725-728.
- Petrie, R. J., Schnetkamp, P. P. M., Patel, K. D., Awasthi-Kalia, M., and Deans, J. P. (2000) Transient translocation of the B cell receptor and Src homology 2 domain-containing inositol phosphatase to lipid rafts: Evidence toward a role in calcium regulation. *J. Immunol.*, **165**, 1220-1227.

- Pike, C. J., Walencewicz, A. J., Glabe, C. G., and Cotman, C. W. (1991) Invitro Aging of Beta-Amyloid Protein Causes Peptide Aggregation and Neurotoxicity. *Brain Res.*, **563**, 311-314.
- Podlisny, M. B., Walsh, D. M., Amarante, P., Ostaszewski, B. L., Stimson, E. R., Maggio, J. E., Teplow, D. B., and Selkoe, D. J. (1998) Oligomerization of endogenous and synthetic amyloid beta- protein at nanomolar levels in cell culture and stabilization of monomer by congo red. *Biochemistry*, **37**, 3602-3611.
- Portoghese, P. S. (2001) From models to molecules: Opioid receptor dimers, bivalent ligands, and selective opioid receptor probes. *J. Med. Chem.*, **44**, 2259-2269.
- Puertas, A., Maroto, J. A., and las Nieves, F. J. (1998) Theoretical description of the absorbance versus time curve in a homocoagulation process. *Colloids Surf. , A*, **140**, 23-31.
- Puertas, A. M. and delasNieves, F. J. (1997) A new method for calculating kinetic constants within the Rayleigh-Gans-Debye approximation from turbidity measurements. *J. Phys. :Condens. Matter*, **9**, 3313-3320.
- Quesenberry, M. S., Lee, R. T., and Lee, Y. C. (1997) Difference in the binding mode of two mannose-binding proteins: Demonstration of a selective minicluster effect. *Biochemistry*, **36**, 2724-2732.
- Rao, J. H., Lahiri, J., Isaacs, L., Weis, R. M., and Whitesides, G. M. (1998) A trivalent system from vancomycin center dot D-Ala-D-Ala with higher affinity than avidin center dot biotin. *Science*, **280**, 708-711.
- Rao, J. H., Yan, L., Xu, B., and Whitesides, G. M. (1999) Using surface plasmon resonance to study the binding of vancomycin and its dimer to self-assembled monolayers presenting D-Ala-D-Ala. *J. Am. Chem. Soc.*, **121**, 2629-2630.
- Reuter, J. D., Myc, A., Hayes, M. M., Gan, Z., Roy, R., Qin, D., Yin, R., Pichler, L. T., Esfand, R., Tomalia, D. A., and Baker, J. R., Jr. (1999) Inhibition of viral adhesion and infection by sialic-acid-cojugated dendritic polymers. *Bioconjugate Chem.*, **10**, 271-278.
- Rich, R. L. and Myszka, D. G. (2000) Advances in surface plasmon resonance biosensor analysis. *Curr. Opin. Biotechnol.*, **11**, 54-61.
- Rochet, J. C. and Lansbury, P. T. (2000) Amyloid fibrillogenesis: themes and variations. *Curr. Opin. Struct. Biol.*, **10**, 60-68.

- Roseman, D. S. and Baenziger, J. U. (2001) The mannose/N-acetylgalactosamine-4-SO<sub>4</sub> receptor displays greater specificity for multivalent than monovalent ligands. *J. Biol. Chem.*, **276**, 17052-17057.
- Roth, W., Isenmann, S., Naumann, U., Kugler, S., Bahr, M., Dichgans, J., Ashkenazi, A., and Weller, M. (1999) Locoregional Apo2L/TRAIL eradicates intracranial human malignant glioma xenografts in athymic mice in the absence of neurotoxicity. *Biochem. Biophys. Res. Commun.*, **265**, 479-483.
- Roth, W. and Weller, M. (1999) Chemotherapy and immunotherapy of malignant glioma: molecular mechanisms and clinical perspectives. *Cell. Mol. Life Sci.*, **56**, 481-506.
- Roy, R., Page, D., Perez, S. F., and Bencomo, V. V. (1998) Effect of shape, size, and valency of multivalent mannosides on their binding properties to phytohemagglutinins. *Glycoconj. J.*, **15**, 251-263.
- Ryder, S. D., Jacyna, M. R., Levi, A. J., Rizzi, P. M., and Rhodes, J. M. (1998) Peanut ingestion increases rectal proliferation in individuals with mucosal expression of peanut lectin receptor. *Gastroenterology*, **114**, 44-49.
- Ryder, S. D., Smith, J. A., Rhodes, E. G. H., Parker, N., and Rhodes, J. M. (1994) Proliferative Responses of Ht29 and Caco2 Human Colorectal- Cancer Cells to a Panel of Lectins. *Gastroenterology*, **106**, 85-93.
- Sacchettini, J. C., Baum, L. G., and Brewer, C. F. (2001) Multivalent protein-carbohydrate interactions. A new paradigm for supermolecular assembly and signal transduction. *Biochemistry*, **40**, 3009-3015.
- Sanders, W. J., Gordon, E. J., Dwir, O., Beck, P. J., Alon, R., and Kiessling, L. L. (1999) Inhibition of L-selectin-mediated leukocyte rolling by synthetic glycoprotein mimics. *J. Biol. Chem.*, **274**, 5271-5278.
- Sanders, W. J., Katsumoto, T. R., Bertozzi, C. R., Rosen, S. D., and Kiessling, L. L. (1996) L-selectin-carbohydrate interactions: Relevant modifications of the Lewis x trisaccharide. *Biochemistry*, **35**, 14862-14867.
- Schenk, D., Barbour, R., Dunn, W., Gordon, G., Grajeda, H., Guido, T., Hu, K., Huang, J. P., Johnson-Wood, K., Khan, K., Kholodenko, D., Lee, M., Liao, Z. M., Lieberburg, I., Motter, R., Mutter, L., Soriano, F., Shopp, G., Vasquez, N., Vandevent, C., Walker, S., Wogulis, M., Yednock, T., Games, D., and Seubert, P. (1999) Immunization with amyloid-beta attenuates Alzheimer disease- like pathology in the PDAPP mouse. *Nature*, **400**, 173-177.

- Schnebli, H. P. (1976) A Microhaemagglutination Inhibition Assay for Concanavalin A. In Bittiger, H. and Schnebli, H. P. (eds.), *Concanavalin A as a Tool*. John Wiley & Sons, New York, pp. 279-284.
- Schneider, P., Bodmer, J. L., Holler, N., Mattmann, C., Scuderi, P., Terskikh, A., Peitsch, M. C., and Tschopp, J. (1997) Characterization of Fas (Apo-1, CD95)-Fas ligand interaction. *J. Biol. Chem.*, **272**, 18827-18833.
- Schrock, R. R., Lee, J. K., Odell, R., and Oskam, J. H. (1995) Exploring Factors That Determine Cis/Trans Structure and Tacticity in Polymers Prepared by Ring-Opening Metathesis Polymerization with Initiators of the Type Syn- and Anti-Mo(NAr)(CHCMe(2)Ph)(OR)(2) - Observation of A Temperature-Dependent Cis/Trans Ratio. *Macromolecules*, **28**, 5933-5940.
- Schuck, P. (1997) Use of surface plasmon resonance to probe the equilibrium and dynamic aspects of interactions between biological macromolecules. *Annu. Rev. Biophys. Biomol. Struct.*, **26**, 541-566.
- Schuster, M. C., Mortell, K. H., Hegeman, A. D., and Kiessling, L. L. (1997) Neoglycopolymers produced by aqueous ring-opening metathesis polymerization: Decreasing saccharide density increases activity. *J. Mol. Cat. A: Chemical*, **116**, 209-216.
- Schwarz, R. E., Wojciechowicz, D. C., Picon, A. I., Schwarz, M. A., and Paty, P. B. (1999) Wheatgerm agglutinin mediated toxicity in pancreatic cancer cells. *Br. J. Cancer*, **80**, 1754-1762.
- Schwarze, S. R., Ho, A., Vocero-Akbani, A., and Dowdy, S. F. (1999) In vivo protein transduction: Delivery of a biologically active protein into the mouse. *Science*, **285**, 1569-1572.
- Scrutton, N. S. and Raine, A. R. C. (1996) Cation-pi bonding and amino-aromatic interactions in the biomolecular recognition of substituted ammonium ligands. *Biochem. J.*, **319**, 1-8.
- Selkoe, D. J. (1997) Neuroscience - Alzheimer's disease: Genotypes, phenotype, and treatments. *Science*, **275**, 630-631.
- Selkoe, D. J. (1999) Translating cell biology into therapeutic advances in Alzheimer's disease. *Nature*, **399**, A23-A31.
- Serpell, L. C. (2000) Alzheimer's amyloid fibrils: structure and assembly. *Biochim. Biophys. Acta-Molecular Basis of Disease*, **1502**, 16-30.

- Shearman, M. S. (1999) Toxicity of protein aggregates in PC 12 cells: 3-(4, 5-dimethylthiazol-2-yl)-2,5-diphenyltetrazolium bromide assay. *Methods Enzymol.*, **309**, 716-723.
- Shearman, M. S., Beher, D., Clarke, E. E., Lewis, H. D., Harrison, T., Hunt, P., Nadin, A., Smith, A. L., Stevenson, G., and Castro, J. L. (2000) L-685,458, an aspartyl protease transition state mimic, is a potent inhibitor of amyloid beta-protein precursor gamma-secretase activity. *Biochemistry*, **39**, 8698-8704.
- Shearman, M. S., Ragan, C. I., and Iversen, L. L. (1994) Inhibition of Pc12 Cell Redox Activity Is A Specific, Early Indicator of the Mechanism of Beta-Amyloid-Mediated Cell-Death. *Proc. Natl. Acad. Sci. U. S. A.*, **91**, 1470-1474.
- Shen, C. L. and Murphy, R. M. (1995) Solvent Effects on Self-Assembly of Beta-Amyloid Peptide. *Biophys. J.*, **69**, 640-651.
- Shen, C. L., Scott, G. L., Merchant, F., and Murphy, R. M. (1993) Light-Scattering Analysis of Fibril Growth from the Amino- Terminal Fragment Beta(1-28) of Beta-Amyloid Peptide. *Biophys. J.*, **65**, 2383-2395.
- Shilton, B. H., Flocco, M. M., Nilsson, M., and Mowbray, S. L. (1996) Conformational changes of three periplasmic receptors for bacterial chemotaxis and transport: The maltose-, glucose/galactose- and ribose-binding proteins. *J. Mol. Biol.*, **264**, 350-363.
- Shimizu, T. S., Le Novere, N., Levin, M. D., Beavil, A. J., Sutton, B. J., and Bray, D. (2000) Molecular model of a lattice of signalling proteins involved in bacterial chemotaxis. *Nature Cell Biology*, **2**, 792-796.
- Shinohara, Y., Hasegawa, Y., Kaku, H., and Shibuya, N. (1997) Elucidation of the mechanism enhancing the avidity of lectin with oligosaccharides on the solid phase surface. *Glycobiology*, **7**, 1201-1208.
- Shinohara, Y., Kim, F., Shimizu, M., Goto, M., Tosu, M., and Hasegawa, Y. (1994) Kinetic Measurement of the Interaction Between An Oligosaccharide and Lectins by A Biosensor Based on Surface- Plasmon Resonance. *Eur. J. Biochem.*, **223**, 189-194.
- Shohan, J., Inbar, M., and Sachs, L. (1970) Differential toxicity on normal and transformed cells in vitro and inhibition of tumour development in vivo by concanavalin a. *Nature*, **227**, 1244.

- Siegel, R. M., Frederiksen, J. K., Zacharias, D. A., Chan, F. K. M., Johnson, M., Lynch, D., Tsien, R. Y., and Lenardo, M. J. (2000) Fas preassociation required for apoptosis signaling and dominant inhibition by pathogenic mutations. *Science*, **288**, 2354-2357.
- Sigal, G. B., Mammen, M., Dahmann, G., and Whitesides, G. M. (1996) Polyacrylamides bearing pendant alpha-sialoside groups strongly inhibit agglutination of erythrocytes by influenza virus: The strong inhibition reflects enhanced binding through cooperative polyvalent interactions. *J. Am. Chem. Soc.*, **118**, 3789-3800.
- Sipe, J. D. (1992) Amyloidosis. *Annu. Rev. Biochem.*, **61**, 947-975.
- Sittampalam, G. and Wilson, G. S. (1984) Experimental-Observations of Transient Light-Scattering Complexes Formed During Immunoprecipitin Reactions. *Anal. Chem.*, **56**, 2170-2175.
- Smith, C. K. and Regan, L. (1995) Guidelines for Protein Design - the Energetics of Beta-Sheet Side-Chain Interactions. *Science*, **270**, 980-982.
- Smith, E. A., Wanat, M. J., Cheng, Y. F., Barreira, S. V. P., Frutos, A. G., and Corn, R. M. (2001) Formation, spectroscopic characterization, and application of sulfhydryl-terminated alkanethiol monolayers for the chemical attachment of DNA onto gold surfaces. *Langmuir*, **17**, 2502-2507.
- Soto, C. (1999) beta-amyloid disrupting drugs - Potential in the treatment of Alzheimer's disease. *Cns Drugs*, **12**, 347-356.
- Soto, C., Kindy, M. S., Baumann, M., and Frangione, B. (1996) Inhibition of Alzheimer's amyloidosis by peptides that prevent beta-sheet conformation. *Biochem. Biophys. Res. Commun.*, **226**, 672-680.
- Soto, C., Sigurdsson, E. M., Morelli, L., Kumar, R. A., Castano, E. M., and Frangione, B. (1998) beta-sheet breaker peptides inhibit fibrillogenesis in a rat brain model of amyloidosis: Implications for Alzheimer's therapy. *Nat. Med.*, **4**, 822-826.
- Stone, J. D., Cochran, J. R., and Stern, L. J. (2001) T-cell activation by soluble MHC oligomers can be described by a two-parameter binding model. *Biophys. J.*, **81**, 2547-2557.
- Strong, L. E. and Kiessling, L. L. (1999) A general synthetic route to defined, biologically active multivalent arrays. *J. Am. Chem. Soc.*, **121**, 6193-6196.



- Sugiyama, J. E., Glass, D. J., Yancopoulos, G. D., and Hall, Z. W. (1997) Laminin-induced acetylcholine receptor clustering: An alternative pathway. *J. Cell Biol.*, **139**, 181-191.
- Symons, A., Cooper, D. N., and Barclay, A. N. (2000) Characterization of the interaction between galectin-1 and lymphocyte glycoproteins CD45 and Thy-1. *Glycobiology*, **10**, 559-63.
- Thompson, J. P. and Schengrund, C. L. (1997) Oligosaccharide-derivatized dendrimers: defined multivalent inhibitors of the adherence of the cholera toxin B subunit and the heat labile enterotoxin of E-coli GM1. *Glycoconj. J.*, **14**, 837-845.
- Thorsett, E. D. and Latimer, L. H. (2000) Therapeutic approaches to Alzheimer's disease. *Curr. Opin. Chem. Biol.*, **4**, 377-382.
- Tjernberg, L. O., Lilliehook, C., Callaway, D. J. E., Naslund, J., Hahne, S., Thyberg, J., Terenius, L., and Nordstedt, C. (1997) Controlling amyloid beta-peptide fibril formation with protease-stable ligands. *J. Biol. Chem.*, **272**, 12601-12605.
- Tjernberg, L. O., Naslund, J., Lindqvist, F., Johansson, J., Karlstrom, A. R., Thyberg, J., Terenius, L., and Nordstedt, C. (1996) Arrest of beta-amyloid fibril formation by a pentapeptide ligand. *J. Biol. Chem.*, **271**, 8545-8548.
- Todorovska, A., Roovers, R. C., Dolezal, O., Kortt, A. A., Hoogenboom, H. R., and Hudson, P. J. (2001) Design and application of diabodies, triabodies and tetrabodies for cancer targeting. *J. Immunol. Methods*, **248**, 47-66.
- Toone, E. J. (1994) Structure and Energetics of Protein Carbohydrate Complexes. *Curr. Opin. Struct. Biol.*, **4**, 719-728.
- Trnka, T. M. and Grubbs, R. H. (2001) The development of L2X2Ru = CHR olefin metathesis catalysts: An organometallic success story. *Acc. Chem. Res.*, **34**, 18-29.
- Tseng, B. P., Esler, W. P., Clish, C. B., Stimson, E. R., Ghilardi, J. R., Vinters, H. V., Mantyh, P. W., Lee, J. P., and Maggio, J. E. (1999) Deposition of monomeric, not oligomeric, A beta mediates growth of Alzheimer's disease amyloid plaques in human brain preparations. *Biochemistry*, **38**, 10424-10431.
- Ueno, T., Tanaka, S., and Umeda, M. (1997) Liposome turbidimetric assay (LTA). *Adv. Drug Delivery Rev.*, **24**, 293-299.
- Vijayan, M. and Chandra, N. (1999) Lectins. *Curr. Opin. Struct. Biol.*, **9**, 707-714.

- Vrasidas, I., de Mol, N. J., Liskamp, R. M. J., and Pieters, R. J. (2001) Synthesis of lactose dendrimers and multivalency effects in binding to the cholera toxin B subunit. *Eur. J. Org. Chem.*, 4685-4692.
- Vyas, M. N., Vyas, N. K., and Quioco, F. A. (1994) Crystallographic Analysis of the Epimeric and Anomeric Specificity of the Periplasmic Transport Chemosensory Protein-Receptor for D-Glucose and D-Galactose. *Biochemistry*, **33**, 4762-4768.
- Vyas, N. K., Vyas, M. N., and Quioco, F. A. (1987) A Novel Calcium-Binding Site in the Galactose-Binding Protein of Bacterial Transport and Chemotaxis. *Nature*, **327**, 635-638.
- Vyas, N. K., Vyas, M. N., and Quioco, F. A. (1988) Sugar and Signal-Transducer Binding-Sites of the Escherichia- Coli Galactose Chemoreceptor Protein. *Science*, **242**, 1290-1295.
- Wallach, D., Varfolomeev, E. E., Malinin, N. L., Goltsev, Y. V., Kovalenko, A. V., and Boldin, M. P. (1999) Tumor necrosis factor receptor and Fas signaling mechanisms. *Annu. Rev. Immunol.*, **17**, 331-367.
- Walsh, D. M., Klyubin, I., Fadeeva, J. V., Cullen, W. K., Anwyl, R., Wolfe, M. S., Rowan, M. J., and Selkoe, D. J. (2002) Naturally secreted oligomers of amyloid  $\beta$  protein potently inhibit hippocampal long-term potentiation in vivo. *Nature*, **416**, 535-539.
- Walsh, D. M., Lomakin, A., Benedek, G. B., Condron, M. M., and Teplow, D. B. (1997) Amyloid beta-protein fibrillogenesis - Detection of a protofibrillar intermediate. *J. Biol. Chem.*, **272**, 22364-22372.
- Wang, H. X., Ng, T. B., Ooi, V. E. C., and Liu, W. K. (2000) Effects of lectins with different carbohydrate-binding specificities on hepatoma, choriocarcinoma, melanoma and osteosarcoma cell lines. *International Journal of Biochemistry & Cell Biology*, **32**, 365-372.
- Wang, J. L., Gunther, G. R., and Edelman, G. M. (1976) Chemical and Biological Properties of Dimeric Concanavalin A Derivatives. In Bittiger, H. and Schnebli, H. P. (eds.), *Concanavalin A as a Tool*. John Wiley & Sons, New York, pp. 585-598.
- Ward, R. V., Jennings, K. H., Jepras, R., Neville, W., Owen, D. E., Hawkins, J., Christie, G., Davis, J. B., George, A., Karran, E. H., and Howlett, D. R. (2000) Fractionation and characterization of oligomeric, protofibrillar and fibrillar forms of beta-amyloid peptide. *Biochem. J.*, **348**, 137-144.

- Weatherman, R. V., Mortell, K. I., Chervenak, M., Kiessling, L. L., and Toone, E. J. (1996) Specificity of C-glycoside complexation by mannose glucose specific lectins. *Biochemistry*, **35**, 3619-3624.
- Weber, C. H. and Vincenz, C. (2001) A docking model of key components of the DISC complex: death domain superfamily interactions redefined. *FEBS Lett.*, **492**, 171-176.
- Weigel, P. H., Schnaar, R. L., Kuhlenschmidt, M. S., Schmell, E., Lee, R. T., Lee, Y. C., and Roseman, S. (1979) Adhesion of hepatocytes to immobilized sugars. *J. Biol. Chem.*, **254**, 10830-10838.
- Weiner, S. J., Kollman, P. A., Case, D. A., Singh, U. C., Ghio, C., Alagona, G., Profeta, S., and Weiner, P. (1984) A New Force-Field for Molecular Mechanical Simulation of Nucleic-Acids and Proteins. *J. Am. Chem. Soc.*, **106**, 765-784.
- Weller, M., Kleihues, P., Dichgans, J., and Ohgaki, H. (1998) CD95 ligand: Lethal weapon against malignant glioma? *Brain Pathol.*, **8**, 285-293.
- Williams, B. A., Chervenak, M. C., and Toone, E. J. (1992) Energetics of Lectin-Carbohydrate Binding - A Microcalorimetric Investigation of Concanavalin A-Oligomannoside Complexation. *J. Biol. Chem.*, **267**, 22907-22911.
- Willuda, J., Kubetzko, S., Waibel, R., Schubiger, P. A., Zangemeister-Wittke, U., and Pluckthun, A. (2001) Tumor targeting of mono-, di-, and tetravalent Anti-p185(HER-2) miniantibodies multimerized by self-associating peptides. *J. Biol. Chem.*, **276**, 14385-14392.
- Wiseman, T., Williston, S., Brandts, J. F., and Lin, L. N. (1989) Rapid Measurement of Binding Constants and Heats of Binding Using A New Titration Calorimeter. *Anal. Biochem.*, **179**, 131-137.
- Woller, E. K. and Cloninger, M. J. (2001) Mannose functionalization of a sixth generation dendrimer. *Biomacromolecules*, **2**, 1052-1054.
- Woller, E. K. and Cloninger, M. J. (2002) The lectin-binding properties of six generations of mannose-functionalized dendrimers. *Org. Lett.*, **4**, 7-10.
- Wu, P. G. and Brand, L. (1994) Resonance Energy-Transfer - Methods and Applications. *Anal. Biochem.*, **218**, 1-13.

- Yi, D., Lee, R. T., Longo, P., Boger, E. T., Lee, Y. C., Petri, W. A., and Schnaar, R. L. (1998) Substructural specificity and polyvalent carbohydrate recognition by the *Entamoeba histolytica* and rat hepatic N- acetylgalactosamine/galactose lectins. *Glycobiology*, **8**, 1037-1043.
- Zagorski, M. G., Yang, J., Shao, H. Y., Ma, K., Zeng, H., and Hong, A. (1999) Methodological and chemical factors affecting amyloid beta peptide amyloidogenicity. *Methods Enzymol.*, **309**, 189-204.
- Zhao, R., Guerrah, A., Tang, H., and Zhao, Z. J. (2002) Cell Surface Glycoprotein PZR Is a Major Mediator of Concanavalin A-Induced Cell Signaling. *J. Biol. Chem.*, **277**, 7882-7888.